2018

The Separation of the Polar Constituents of Petroleum

Robson, William

The Separation of the Polar Constituents of Petroleum

by

William James Robson

A thesis submitted to Plymouth University

in partial fulfilment for the degree of

DOCTOR OF PHILOSOPHY

School of Geography, Earth and Environmental Sciences

January 2018

Acknowledgements

I would like to express my sincere thanks to my supervisors Prof Steve Rowland, Dr Paul Sutton and Dr Anthony Lewis for their excellent supervision and continuous guidance, support and friendship. I would also like to acknowledge the intellectual and financial support provided by Dr Neil Chilcott and the team at Kernow Analytical Technology. Without their support, I would not have had the freedom to explore new ideas and travel as I have.

In addition to working with Steve, Paul, Anthony and Neil, I have been exceptionally fortunate to work with a fantastic group scientists, all of whom I would like to thank for making the last three years an enlightening and enjoyable experience. In particular, I would like to thank Dr Paul McCormack for sharing his LC-MS wisdom and for our daily discussions over coffee, and Drs Yann Aminot and Mike Wilde for their continuing friendship and advice.

I am also grateful to Andrew Tonkin, Andy Arnold, Claire Williams, Louise Argent, Jeremy Clark, Ian Doidge and all the technical staff for always making time to help.

A big thanks goes to my friends and colleagues at Plymouth University including Patri, Katie, Maurizio, Kate, Lukas, Lara, Antony, Kat, Anita, Deniz, Maya and the team at the Fortescue for filling the past three years with good times and laughs. I would also like to extend my sincere thanks to Hayley, Dan and Lyra for their friendship and for giving me a home for the past 12 months.

Finally, I would like to thank my parents, sister and girlfriend Francesca for their continuing love and support. Thanks for putting up with me!

Authors Declaration

At no time during the registration for the degree of Doctor of Philosophy has the author been registered for any other University award without prior agreement of the Graduate Sub-Committee.

Work submitted for this research degree at Plymouth University has not formed part of any other degree either at Plymouth University or at another establishment.

This study was financed as a full studentship (3 years) by Plymouth University with additional funding provided by Kernow Analytical Technology (KAT, Ltd.).

Relevant scientific conferences and workshops were regularly attended at which work was often presented and several papers prepared for publication.

Word count of main body of thesis: 64,000

Signed:

Date:

SEPARATION OF THE POLAR CONSTITUENTS OF CRUDE OIL

William James Robson

Abstract

Identification of the heteroatom (nitrogen, sulphur, and oxygen; NSO)-containing compounds of petroleum is of key importance when considering industrial and environmental issues associated with crude oil production. The inherent molecular complexity of petroleum is such that detailed compositional investigations must ideally be preceded by some form of pre-fractionation. However, the more commonly performed methods of crude oil fractionation are often insufficient in the extent to which they separate oils, not allowing defined "molecular" fractions to be obtained and thus hindering more detailed investigations. The following work therefore focused on the development of chromatographic methods to aid in the characterisation of NSO compounds present within crude oils.

A novel solid phase extraction (SPE) procedure was developed utilising both ion exchange and adsorption chromatography. The method enabled fractions broadly defined as 'saturated' hydrocarbons; 'aromatic' hydrocarbons; basic nitrogen compounds; naphthenic acids; phenols and other oxygen-containing species; carbazoles; sulfoxides; and thiophenes, to be isolated reproducibly and quantitatively from relatively small crude oil samples (~ 0.5 g). Assessment of method selectivity with a suite of 'model' compounds showed that the resulting fractions were quite well defined, with classes of 'model' compounds being isolated within discrete fractions. Application to five crude oils of widely varying properties and origins, such as API gravity (12.1−38.3°), demonstrated the potential for the wide-ranging use of the method. Sample recoveries were high (77−98%) with simple evaporative losses accounting for the majority of sample loss. Repeatability was also high, demonstrated by triplicate analyses of 'model' compound mixtures, oils spiked with 'model' compounds and oils alone.

Subsequent, more detailed, analysis of the fractions using multidimensional gas chromatography-mass spectrometry (GC×GC-MS) and liquid chromatography-high-resolution accurate mass-mass spectrometry (LC-HRAM-MS) showed the advantages of the new isolation method. For example, alkylated series ($C_{1\text{-}5}$) of quinolines, carbazoles, fluorenones, dibenzothiophenes and xanthones were identified within their predicted fractions. Furthermore, comparison of mass spectra obtained from GC×GC-MS analyses with reference spectra resulted in the tentative identification of compounds hitherto not previously reported in crude oils, again illustrating the advantage of the isolation method. Novel series of thioxanthones, tocopherols (E vitamins) and terpenoidal sulfoxides and ketones were assigned within the isolated fractions.

Following the successful evaluation of the method, the scheme was subsequently employed to investigate the effects of changing geochemical parameters on the composition of isolated NSO-containing compounds. For example, studies of NSO fractions from series of crude oils at different stages of thermal maturity or of biodegradation, led to the identification of a number of potential new molecular markers within the basic-nitrogen and ketone fractions. This work shows clear potential for the developed NSO isolation method to be used in further compositional studies as a tool to aid in geochemical investigations.

Table of Contents

List of Tables

List of Figures

Abbreviations

AE- anion exchange

ANS- Alaska North Slope

APCI- atmospheric pressure chemical ionisation

API- American Petroleum Institute

APPI- atmospheric pressure photoionisation

BSTFA- N,O-Bis(trimethylsilyl)trifluoroacetamide

CE- collision energy or cation exchange

CID- collision induced dissociation

Da- Dalton

DEE- diethyl ether

DCM- dichloromethane

DOP-diisooctyl phthalate

DSC- Discovery

EI- electron ionisation

EIC- extracted ion chromatogram

ENR- ethyl naphthalene ratio

ESI- electrospray ionisation

FT-IR- Fourier transform-infrared spectroscopy

FT-ICR- Fourier transform-ion cyclotron resonance

FA- formic acid

GC- gas chromatography

GC×GC- multidimensional gas chromatography

HCD- higher-energy collisional dissociation

HPLC- high-pressure liquid chromatograph

HRAM- high resolution accurate mass

IEC- ion exchange chromatography

IPA- isopropyl alcohol

KOH- potassium hydroxide

MeOH- methanol

MNR- methyl naphthalene ratio

MPI- methyl phenanthrene index

MPLC- medium pressure liquid chromatography

MS- mass spectrometry

m/z- mass to charge ration

NA- naphthenic acid

NH_3- ammonia

NIST- National Institute of Standards and Technology

NSO- Nitrogen, Sulphur and Oxygen

OSPW- oil sands process water

PAH- polycyclic aromatic hydrocarbon

PIN- paraffins, *iso*-paraffins and naphthalenes

PW- produced water

RI- refractive index

S- sulphur or silica

SARA- saturates, aromatics, resins and asphaltenes

SAX- strong anion exchange

SCD- sulphur chemiluminescence detector

SCX- strong cation exchange

SPE- solid phase extraction

TAN- total acid number

TBN- total base number

THF- tetrahydrofuran

TIC- total ion chromatogram

TJP- Tia Juana Pesado

TLC-FID- thin layer chromatography- flame ionisation detector

TOC- total organic carbon

TOF- time of flight

UCM- unresolved complex mixture

uHRMS- ultrahigh resolution mass spectrometry

UV- ultraviolet

VRE- vitrinite reflectance equivalence

Chapter 1. Introduction

Petroleum is defined by the American Petroleum Institute (API) thus: "…a complex combination of hydrocarbons. It consists predominantly of aliphatic, alicyclic and aromatic hydrocarbons. It may also contain certain amounts of nitrogen, oxygen and sulphur compounds. This category encompasses light, medium, and heavy petroleums, as well as the oils extracted from tar sands" (API, 2011). The term petroleum therefore refers to a broad category including both crude oil and the products acquired through the processing of crude oils.

Petroleum is arguably the most compositionally complex organic mixture in Nature and significant variations in this composition result in a great variety of physical and chemical properties. As a result, the qualitative and quantitative study of crude oil composition is of great importance in the exploration, extraction and refining of petroleum. Information pertaining to the molecular composition of crude oils is essential when determining refining conditions and allows for the prediction and management of flow assurance issues. Of particular importance when conducting these evaluations is determining the abundance and speciation of the heteroatomic, nitrogen, sulphur and oxygen (NSO)-containing compounds. Certainly, these so called "polar compounds" can have damaging effects on production, causing significant downtime and greatly affecting the economic viability of crude oils (Marshall and Rodgers, 2004). As production of unconventional crude oils increases, so does the occurrence of such issues. Thus, the current study aimed to improve on the current knowledge of these polar, NSO-compounds.

1.1 Origins of crude oil

The formation, accumulation and preservation of undegraded organic matter are prerequisites for the existence of petroleum source rocks. In this instance, the term organic matter refers solely to material comprised of organic molecules in monomeric or polymeric forms, derived directly or from the organic part of organisms (Tissot and Welte, 1984). Primary sources of organic matter for petroleum production include marine phytoplankton and bacteria, with some contribution from benthic algae and zooplankton. Sources for crude oils formed later than the Devonian period (~400 million years ago) also include terrestrial organic matter derived from land plants. Following phytoplankton and bacteria, higher land plants are the third most important contributor to organic matter in sediments (Tissot and Welte, 1984).

The majority of evidence indicates that the sedimentation and burial of organic matter make up the initial stages of petroleum formation (Killops and Killops, 2005). In the early stages of deposition, under conditions of low temperature (up to 50 ºC) and pressure (up to ~300 bars), organic matter undergoes the process of diagenesis. During diagenesis, the burial depth of sediments increases, resulting in their consolidation, de-watering and compaction. Diagenesis of the organic matter results in the degradation of biopolymers such as proteins and carbohydrates, which either are preserved or recombined by polycondensation and polymerisation, resulting in the formation of a poorly characterised macromolecular material known as kerogen (Tissot and Welte, 1984; Sinninghe Damsté *et al.*, 1995). Kerogen is most often described by its lack of solubility in alkaline inorganic solvents or common organic solvents and compositionally is described as "a macromolecule comprising condensed cyclic nuclei linked by heteroatomic bonds or aliphatic chains" (Tissot and Welte, 1984).

Increasing temperature and decreasing amounts of water limit biological activity, ultimately leading to the breaking of chemical bonds and the process of catagenesis (Killops and Killops, 2005). Catagenesis, first proposed by Vassoevich (1957), involves the thermal breakdown of kerogen, ultimately resulting in oil formation. The catagenesis of sediments occurs at burial depths of ~1100 m to ~3000m, with associated temperature increases from 50 ºC up to 150 ºC and increasing pressures from 300 bars up to 1500 bars (Tissot and Welte, 1984). During catagenesis, medium to low molecular weight hydrocarbons begin to form and dominate and at the point at which metagenesis is reached; methane is the only remaining hydrocarbon.

1.2 The composition of crude oil

The elemental composition of all crude oils is dominated by carbon and hydrogen. However, all oils also contain a certain percentage of nitrogen, oxygen and sulphur, as well as an assortment of metals (primarily nickel and vanadium). A typical crude oil would be expected to have an atomic ratio of 1600-2200 hydrogen atoms for every 1000 carbon atoms and up to 25 sulphur atoms, 40 oxygen atoms and 15 nitrogen atoms (Killops and Killops, 2005). Figure 1-1 highlights some common hydrocarbon classes found in crude oil and shows examples of heteroatom-containing molecules.

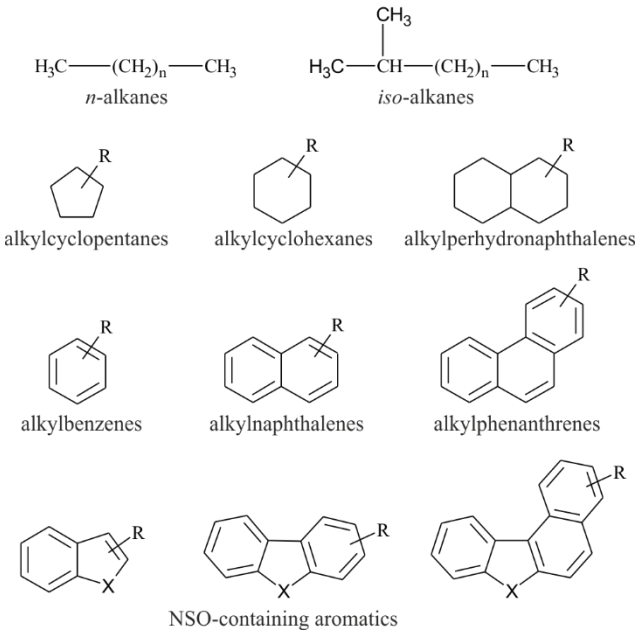

Figure 1-1. Major hydrocarbons and simple heteroatomic compounds found in crude oils (X denotes the presence of nitrogen, sulphur or oxygen atoms)

The origins of many of the heteroatomic compounds within crude oils are not wholly understood. Certainly, the deposited organic matter contains a wide variety of heterocompounds, of which some are biogenic and some are formed during diagenesis. However, many of these biogenic compounds are likely converted to hydrocarbons during diagenesis and catagenesis (Nagy and Colombo, 1967). It is therefore likely that large numbers of NSO-containing compounds are not related to any particular biogenic precursor and as such they vary greatly in molecular weight, structure and aromaticity. A fraction of many crude oils is thought to be composed of molecules demonstrating high aromaticity and substantial heteroatom content (often referred to as asphaltenes) and similarities can be observed between these high molecular weight molecules and the kerogen itself (Killops and Killops, 2005).

1.2.1 Oxygen-containing compounds

Among the heteroatom-containing components of petroleum, naphthenic acids and phenols are the most common oxygen containing compound classes. Naphthenic acids

(NA) are traditionally defined as mono-carboxylic acids, which include chain compounds and compounds with one or more alicyclic ring structures. However, the elucidation of aromatic and heteroatom containing acid structures required the definition be updated to include "non-naphthenic" acids (Knotnerus, 1957). Crude oil-derived carboxylic acids are thought to have a number of different origins: they may result from preservation of original biological products unaffected by catagenesis or be due to bacterial degradation of hydrocarbons following catagenesis (Tissot and Welte, 1984). The concentrations of NAs in petroleum samples vary greatly and range from undetectable up to 3% by mass (Lochte and Littman, 1955). Acid concentrations within petroleum are often referred to by the Total Acid Number (TAN), which reflects the mass of potassium hydroxide (KOH) in milligrams (mg) required to neutralise 1 g of oil.

Naphthenic acids are responsible for a number of issues throughout oil extraction and refining processes. As a result, there has been a growing interest in the characterisation of NA in recent years. The corrosion of production equipment during refining, transportation and storage by NA is an issue that has long affected "downstream" operations (Derungs, 1956). Studies have shown NA corrosion to be dependent on a number of factors including temperature, sulphur content, fluid velocity and acid concentration and composition (Derungs, 1956; Turnbull *et al.*, 1998; Slavcheva *et al.*, 1999; Alvisi and Lins, 2011; Jin *et al.*, 2015). Experiments have shown corrosion to reach a maximum between operating temperatures of 220-400 °C, corresponding to the boiling points of many of the more abundant acid species (Turnbull *et al.*, 1998). Whilst a general correlation between TAN and corrosivity exists, the composition of individual acids within the bulk NA has been suggested to have a significant impact on corrosion (Slavcheva *et al.*, 1999). Thus, the structural characterisation of NA is of importance, potentially yielding valuable information regarding the mechanisms of corrosion.

The deposition of so called ‘calcium naphthenates’ during production is another well-recognised problem and one that has grown significantly in recent years (Juyal *et al.*, 2015). Interaction of NA with divalent cations (Ca^{2+} and Mg^{2+}) present in formation or injected waters, can result in formation of a sticky deposit which, when exposed to air hardens, leading to pipeline and equipment blockages and hence flow assurance issues (Dyer *et al.*, 2003). Investigation into the composition of these naphthenate deposits has led to the identification of series of high molecular weight C_{80-82}, 4-8 ringed acids with four carboxylic acid groups (Figure 1-2) (Lutnaes *et al.*, 2006; Lutnaes *et al.*, 2007; Smith *et al.*, 2007; Sutton *et al.*, 2010). Characterisation of these structures is of interest for both the mitigation of deposition issues and in conducting geochemical studies on crude oils.

Organic acids are also a major constituent of the waters generated during the production of oil and gas from onshore and offshore wells; these are commonly termed “Produced Waters” (PW). The majority of these acids have been shown to be a mixture of low molecular weight carboxylic acids, the most abundant of which are usually formic (methanoic) or acetic (ethanoic) acids (Neff *et al.*, 2011). Samples of PW from the North Sea, Gulf of Mexico and California have been reported to contain between 60 and 7,100 mg L^{-1} of low molecular weight organic acids (MacGowan and Surdam, 1988; Jacobs *et al.*, 1992; Flynn *et al.*, 1996). Crude oils that have been subjected to bacterial alteration are often enriched in NA. As such, their associated PWs typically contain high concentrations of NA, usually each with about 8-30 carbon atoms. Studies on PW from the Troll C platform on the Norwegian shelf showed significant variations in NA composition and concentrations, which was linked to the different degrees of anaerobic biodegradation of crude oil in different parts of the reservoir (Barman Skaare *et al.*, 2007). The vast accumulations of oil sands process affected waters (OSPW) generated from the production of the Athabasca oil sands deposits have also been shown to contain high

concentrations of NA (40 and 120 mg L^{-1}) (Holowenko *et al.*, 2002) and these are responsible for much of the inherent toxicity of OSPW (Li *et al.*, 2017).

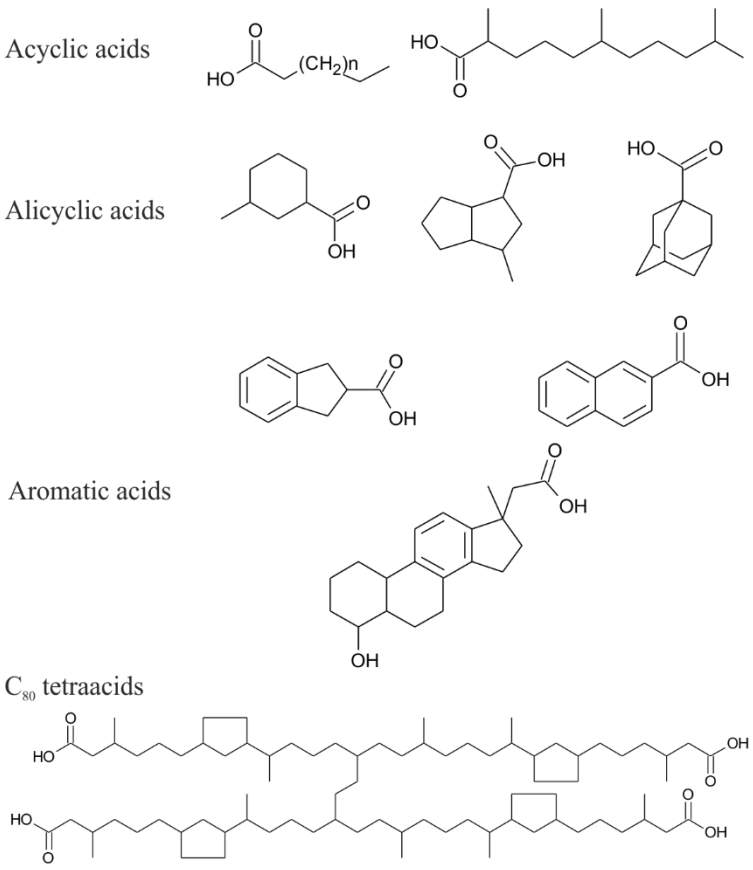

Figure 1-2. Examples of identified acyclic, cyclic, aromatic and C_{80} crude oil derived NA (Smith *et al.*, 2007; Rowland *et al.*, 2011a; Rowland *et al.*, 2011d; Bowman *et al.*, 2014; Wilde *et al.*, 2015).

The characterisation and structural identification of NA has received much attention over the past fifty years and had been thoroughly reviewed in recent works (Wilde, 2015; Headley *et al.*, 2016). Recent approaches to NA characterisation often employ ultra-high resolution mass spectrometry (uHRMS), allowing the unequivocal assignment of molecular formulae. For example, Qian *et al.* (2001) identified the molecular formulae of over 3000 acids in a single sample of a South American heavy crude. However, although these analyses are able to show the broader molecular distribution of compounds, rarely are they able to provide any information on the structures of individual acids. Recent

works have addressed the lack of structural knowledge, successfully employing the use of multidimensional gas chromatography to identify the structures of numerous NA in OSPW and crude oils (e.g. Rowland *et al.*, 2011a; Rowland *et al.*, 2011c; Rowland *et al.*, 2011d; West *et al.*, 2013; Wilde *et al.*, 2015). Examples of identified NA structures identified in crude oils and OSPW are shown in Figure 1-2.

Low molecular weight alkylphenols also occur widely in crude oils however, these have received comparatively little attention compared to NAs (MacCrehan and Brown-Thomas, 1987; Bennett *et al.*, 1996; Bennett *et al.*, 2007b). Alkylphenols are thought to be formed *via* the hydroxylation of alkyl benzenes (Bastow *et al.*, 2005) and have been used as geochemical markers of secondary crude oil migration (Bennett *et al.*, 2007a) because of their sensitivity to fluid-rock interactions. Additionally, due to their solubility in water, alkylphenols are also significant constituents of PW, typically present at concentrations no greater than 20 mg L^{-1} (Neff *et al.*, 2011). Examples of phenols identified in crude oils and PW are shown below in Figure 1-3.

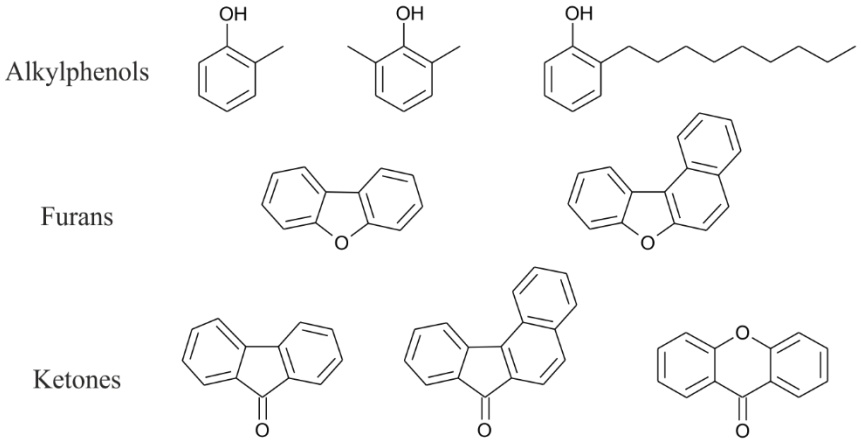

Figure 1-3. Examples of alkylphenols, furans and aromatic ketones identified in crude oils (Bennett *et al.*, 1996; Bennett and Larter, 2000; Oldenburg *et al.*, 2002; Neff *et al.*, 2011; Li and Ellis, 2015).

The less commonly studied lower abundance oxygen-containing compounds include furans and ketones. A series of dibenzofurans and benzonaphthofurans (Figure 1-3) have been reported in both crude oils and source rocks (Li and Ellis, 2015; Yang *et al.*, 2017), and have been suggested as potential markers of original depositional environment and oil maturity. The first aromatic ketones reported in crude oils were the fluorenones (Figure 1-3), which were identified in Wilmington Petroleum (Latham *et al.*, 1962). Bennett *et al.* (2000) later developed a method for the isolation of fluorenones and benzofluorenones and suggested that post-sampling oxidation could be an important factor affecting fluorenone concentrations. Another ketone series identified within crude oils is the xanthones (Figure 1-3) and alkylated homologues, the concentrations of which have been reported to correlate closely with crude oil maturity (Oldenburg *et al.*, 2002).

1.2.2 Nitrogen-containing compounds

In general, nitrogen compounds found in petroleum can be divided into two major groups: basic pyridinic and non-basic pyrrolic compounds. The basic nitrogen compounds include amines, anilines, pyridines, quinolines, benzoquinolines and their alkylated and hydrogenated derivatives (Singh *et al.*, 2011). Non-basic nitrogen compounds include pyrroles (including petroleum metalloporphyrins), indoles, carbazoles and their alkylated derivatives (Li *et al.*, 2010). Tissot and Welte (1984) reported that around 90% of crude oils contain less than 0.2 wt% nitrogen and this nitrogen is found predominantly as non-basic pyrrolic aromatics (Larter *et al.*, 1996; Li *et al.*, 1997). Little is known on the origin of nitrogen compounds in crude oils. Historically, they have been thought to be skeletal fragments of plant alkaloids (Tissot and Welte, 1984; Baxby *et al.*, 1994). However, more recent work by Oldenburg *et al.* (2007), identified significant differences in nitrogen isotope ratios between the non-basic and basic nitrogen fractions, suggesting a different origin.

Generally, geochemical interest in nitrogen compounds has been focused on the non-basic pyrrolics. Larter *et al.* (1996) were the first to identify the geochemical potential of these, employing the alkylcarbazoles as markers of secondary crude oil migration. Carbazoles and benzocarbazoles (Figure 1-4) have also been regularly employed as markers of thermal maturity (Bennett *et al.*, 2002; Bakr, 2009; Faboya *et al.*, 2014). The geochemical relevance of these compounds has fuelled further characterisation of nitrogen fractions leading to the identification of numerous alkyl-indoles, carbazole and benzocarbazoles (Adam *et al.*, 2007; von Mühlen *et al.*, 2007).

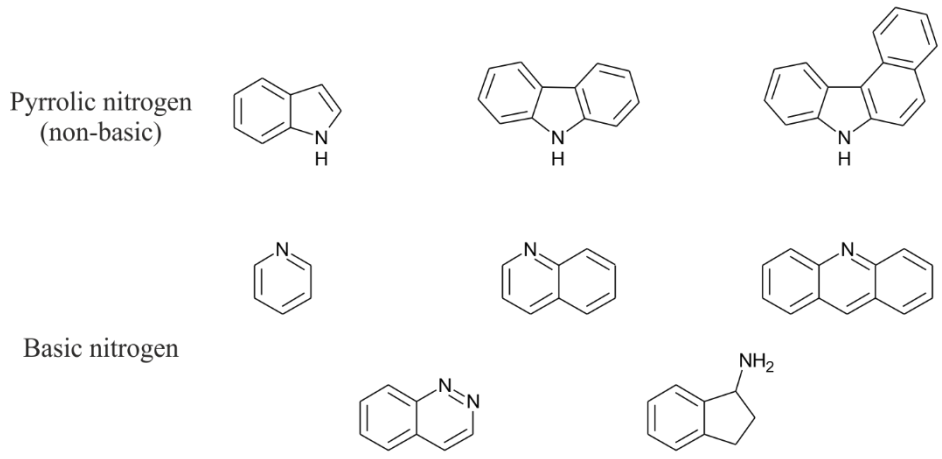

Figure 1-4. Examples of non-basic and basic nitrogen compounds identified in crude oils (Frolov *et al.*, 1989; Yamamoto *et al.*, 1991; von Mühlen *et al.*, 2007; Faboya *et al.*, 2014)

Basic nitrogen compounds are known to be responsible for the poisoning of acidic sites in catalytic fluid processes and hydrocracking zeolite catalysts (Scherzer and Mcarthur, 1986). Mills *et al.* (1950) identified that quinoline-type (aromatic nitrogen) structures absorb irreversibly to catalyst surfaces, reducing catalytic activity. Yamamoto and co-workers (1991) conducted the first large scale characterisation of basic nitrogen crude oil components, identifying series of quinoline and benzoquinoline type compounds (Figure 1-4). More recent studies utilising ultrahigh resolution mass spectrometry (uHRMS) have

enabled the distribution of basic nitrogen species to be studied (Xiaobo *et al.*, 2014; Kong *et al.*, 2015; Vasconcelos *et al.*, 2017) and by employing multidimensional chromatographic techniques other authors have been able to identify numerous low molecular weight basic nitrogen compounds (Dijkmans *et al.*, 2015; Cappelli Fontanive *et al.*, 2016).

Organic nitrogen compounds are also responsible for causing instability in middle distillate fuels, causing the formation and deposition of sediment during storage and in engines (Worstell *et al.*, 1981). Results from investigations on the effect of nitrogen speciation on sediment formation suggested alkylated non-basic nitrogen compounds to be largely responsible for gum formation (Batts and Fathoni, 1991). However, more recent work by Bauserman *et al.* (2008) has shown deposition to not be specific to either basic or non-basic nitrogen species. The study concludes that gum formation occurs due to an imbalance in the ratios of basic and non-basic species.

1.2.3 Sulphur-containing compounds

Sulphur is the most abundant element (on average) in crude oil, after carbon and hydrogen, with an average content of ~0.65% by weight (Tissot and Welte, 1984). The major known sulphur-containing compounds in crude oils are thiophenes and sulphides; minor groups include elemental sulphur, thiols, sulfoxides, and hydrogen sulphide (the latter in 'sour' crudes). Interestingly, in modern organisms oxygen and nitrogen are far more abundant than sulphur. Therefore, it is generally accepted that sulphur is introduced into organic matter after sedimentation and prior to petroleum generation (Payzant *et al.*, 1986).

More often than not, the sulphur originates from the environmental conditions at the time of source rock deposition. On deposition of fine muds (i.e. shales or carbonates), a closed environment is quickly formed in which interstitial waters are separated from the seawater

above. Microbial action quickly exhausts the available oxygen, resulting in an anoxic environment in which sulphate-reducing bacteria reduce sulphate to hydrogen sulphide (Chester, 1993). In iron rich environments (i.e. clay muds), the majority of the sulphur is likely present as iron sulfides and when iron is less abundant (i.e. carbonate muds), the sulphur remains as free sulphur which can progressively combine with organic matter during diagenesis. The large-scale incorporation of sulphur into organic matter in these environments likely results in the formation of high-sulphur petroleums, such as those in the Middle East and South Aquitaine Basins (Tissot and Welte, 1984).

Sulphur compounds have been studied quite extensively in recent years due to their high abundance and industrial, environmental and geochemical relevance. Thiophenic (aromatic sulphur; Figure 1-5) compounds are typically the most abundant form of organosulphur in crude oils (Tissot and Welte, 1984). Despite being non-corrosive, high concentrations of thiophenic sulphur require removal *via* hydrosulphurisation to meet regulations on the sulphur content of fuels (Lobodin *et al.*, 2015). The characterisation of thiophenic structures in crude oils has improved understanding of the mechanisms and kinetics of the conversion processes, assisting in the development of superior catalysts (Breysse *et al.*, 2003). As such, many researchers have conducted structural characterisations focused on thiophenes. Recent studies typically employ multidimensional chromatographic separations with mass spectrometric and sulphur chemiluminescence detection (SCD) to investigate the composition of sulphur compounds and have resulted in numerous structural identifications (e.g., Avila *et al.*, 2014; Dijkmans *et al.*, 2015; Cappelli Fontanive *et al.*, 2016; Gieleciak *et al.*, 2016).

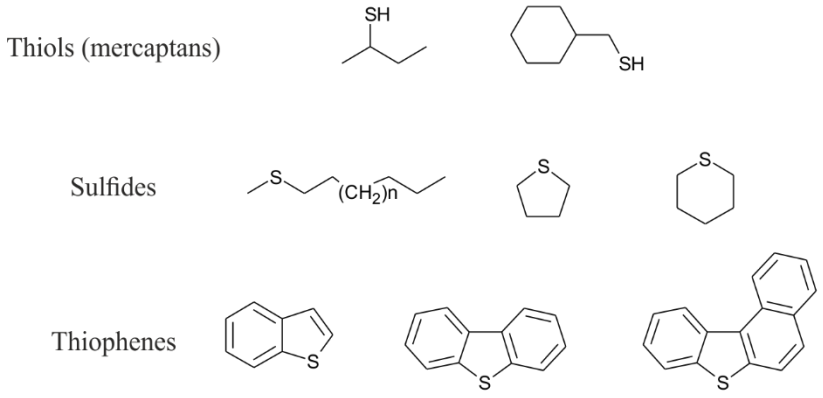

Figure 1-5. Examples of thiols, sulfides and thiophenes identified in crude oils (Tissot and Welte, 1984; Niu *et al.*, 2014; Dijkmans *et al.*, 2015; Gieleciak *et al.*, 2016).

As well as being of industrial interest, a number of studies have ascribed a geochemical relevance to the thiophenes. Only recently, Li and co-workers suggested that dibenzothiophenes and benzonaphthothiophenes could be used as measures of both crude oil maturity (Li *et al.*, 2014a) and migration distances (Li *et al.*, 2014b). Fang *et al.* (2016) further demonstrated this potential, employing dibenzothiophene and benzonaphthothiophene as markers of secondary crude oil migration and reservoir filling pathways in the carbonate reservoir of the Tarim Basin, NW China.

Two other types of organosulphur: sulfides and thiols (mercaptans; Figure 1-5), are responsible for corrosion in refining operations and are often termed ‘reactive’ or “corrosive”. Approaches to the analysis of sulfides and thiols often involve derivatisation to increase stability of the analytes (Thomson *et al.*, 1997). Indeed, the reactivity of the sulfides is such that they are often oxidised to sulfoxides on exposure of crude oil samples to air, a reaction that is often encouraged to increase the ease of analysis (Payzant *et al.*, 1983; Somogyvari *et al.*, 1988; Liu *et al.*, 2010b). Results from these studies have enabled the identification of individual sulfide (often as sulfoxide or derivatised analogues) and thiols.

Procedures for the qualitative and quantitative separation of sulphur species in crude oils often struggle to obtain sufficient chromatographic resolution due to overlap of groups in adsorption phase chromatography (Snyder, 1961b; Rodgers *et al.*, 1998). Whilst uHRMS techniques do allow various sulphur species to be identified (e.g., Purcell *et al.*, 2007; Liu *et al.*, 2010a), ionisation efficiencies are not uniform across compound classes so concentrations can rarely be measured. Recent studies have reported some progress in resolving sulphur species (Lobodin *et al.*, 2015); however, they remain largely uncharacterised.

1.2.4 Compounds possessing multiple functionality

In addition to the aforementioned compound classes, individual compounds containing a mixture of nitrogen, sulphur and oxygen atoms have also been identified in crude oils. Compounds containing multiple heteroatoms are typically larger in size, found in the 500-100 $gmol^{-1}$ range (Chacón-Patiño *et al.*, 2018) and as a consequence, have only been characterised on a molecular level. Indeed, these compounds are most commonly observed during mass spectrometric studies of asphaltene-type fractions (e.g. Pereira *et al.*, 2014b; Giraldo-Davila *et al.*, 2016; Witt *et al.*, 2018) and the nature of the analyses is such that functionality of the heteroatom components can only be predicted.

1.3 Separation of crude oil

To facilitate chemical compositional laboratory investigations, crude oils are routinely fractionated into bulk classes. These separations aim to reduce the overall complexity of crude oils, or related geochemical samples, by concentrating compounds of interest into fractions. The last fifty years have seen the development of a significant number of crude oil fractionation procedures, covering a wide area of applications. These procedures can be broadly placed into one of three categories: (1) the so-called SARA (saturates, aromatics, resins and asphaltenes) type separations, (2) targeted separations (i.e.

separations designed to isolate a bulk fraction with specific properties or a specific compound or compound class) and (3) class type separations, extensively separating whole crude oils into specific fractions based on compound class or desired chemical and physical properties.

1.3.1 SARA methods

Of the three method types, SARA type methods are the most commonly performed. The original SARA method was developed by Jewell *et al.* (1974) and utilises gravimetric adsorption chromatography to provide a group type separation of crude oil components. The method was first developed to assist in qualitative and quantitative investigations into so-called "residuals" (atmospheric and vacuum residues obtained from crude oil distillation). However, in recent years it has also been employed to evaluate asphaltene stability and as a measure of crude oil quality (Kharrat *et al.*, 2007). SARA separations yield four fractions: the 'saturates', containing the non-polar hydrocarbons (i.e. paraffins, iso-paraffins and naphthenes; PIN), the 'aromatics', containing compounds with one or more aromatic rings (i.e. polycyclic aromatic hydrocarbons; PAHs) and thiophenes, the 'resins', comprising the bulk of the non-hydrocarbons or NSO-containing compounds and finally the 'asphaltenes' traditionally a solubility class (i.e. those crude oil components that are insoluble in C_{5-7} *n*-alkane solvents).

The four SARA fractions are generated based on the solubility of crude oil components in a sequence of solvents of increasing polarity and on their affinity for a series of chromatographic phases (e.g., silica, alumina, ion exchange resins and natural clays). The original SARA method required the sequential elution of samples through two hand-packed chromatographic columns, the first containing a mixture of natural clay and ion exchange resins and the second based on adsorption chromatography (silica or alumina). Saturates fractions were first eluted in an *n*-alkane solvent (*n*-pentane or hexane),

followed by the aromatics in a chloroform/methanol gradient and the resins in chloroform. Asphaltenes were isolated prior to column chromatography to avoid their irreversible adsorption to the silica/alumina phases (Jewell *et al.*, 1974).

After the publication of the initial method in 1974, SARA methods were widely adopted as the method of choice for crude oil separations. The following twenty years saw the development of many iterations of the SARA method, with the most significant development being the use of high-pressure liquid chromatography (HPLC), which greatly decreased the time required per separation and improved method reproducibility. Some of the more significant developments in SARA methodologies include work by Suatoni *et al.* (1975; 1980) who were the first to employ HPLC to generate fractions. Later work by Bollet *et al*. (1981) saw the development of a SARA method focused on the fractionation of heavy petroleums, utilising HPLC with alkylamine- and alkylnitrile-bonded silica columns and refractive index (RI) and ultraviolet (UV) detection. Work by Grizzle and Sablotny (1986) sought to reduce analysis times further, developing another HPLC-based method utilising aminopropyl columns. Hayes and Anderson (1986) were the first to publish a SARA method utilising only one chromatographic column, developing a purpose built "olefin-selective" phase. However, the majority of these methods were largely unpopular, with common complaints concerning long column re-equilibration and reactivation times and the considerable sample preparation times required (Bissada *et al.*, 2016a).

The American Society for Testing and Materials has previously recommended a number of SARA variants (ASTM, 2008; ASTM, 2009). However, these methods were widely criticised for reasons including the large volumes of both sample and solvents required; poor precision; difficulties in automating the procedure and the long analysis times (Karlsen and Larter, 1991; Fan *et al.*, 2002). In an effort to improve reproducibility, Karlsen and Larter (1996) developed a SARA method utilising thin layer chromatography

with flame ionisation detection (TLC-FID). The method employed silica rods as the stationary phase, followed by subsequent elution with a solvent series of increasing polarity. The use of TLC-FID over the traditional column chromatography or HPLC methods offered a number of advantages: sample preparation time was greatly reduced as deasphalting was no longer required, sample volumes required for analyses were reduced significantly and reproducibility was greatly improved. Indeed, in 2001 this method was adopted by the Energy Institute (EI) as a standard IP test method (EI, 2001). However, TLC-FID methods are destructive and it has been suggested that differences in detector response for apolar and polar fractions could affect quantitative results (Bissada *et al.*, 2016a). Furthermore, as SARA fractions cannot be further studied, TLC-FID methods are more routinely employed in industry evaluations than for research applications.

Modern developments in SARA methodologies tend to employ HPLC systems rather than TLC to perform separations. To remove the need for the deasphalting of oils before separations, recently developed (SAR-AD) methods have employed the use of Teflon packed columns to precipitate asphaltenes prior to separation (Boysen and Schabron, 2013; Adams *et al.*, 2015). Subsequent elution with benzene or toluene allows collection of the asphaltene fractions. Recently Kim *et al*. (2016) developed a preparative SARA type separation, generating five fractions (saturates, aromatics1, aromatics2, polars1 and polars2) using a flash chromatography system. Bissada *et al.* (2016a) developed a heavily automated, high throughput SARA method utilising a novel automated multi-dimensional (AMD-) HPLC. Whilst these methods are certainly improvements on previous SARA methodologies, they are only reproducible if they are conducted using the same instrumentation. Thus, a significant investment must be made by laboratories in order to adopt these procedures. Additionally, given that compositional investigations are

typically focused on the analysis of the fractions themselves, as opposed to their method of generation, there is no evidence that these SARA methods will be widely adopted.

There have been extensive investigations into the effectiveness of many SARA methodologies and these have identified a number of serious inadequacies (Fan *et al.*, 2002; Kharrat *et al.*, 2007; Adams *et al.*, 2015; Bissada *et al.*, 2016a). Inter-comparison studies in which multiple laboratories perform the same SARA procedure on the same samples have shown significant inconsistencies, including differences in fraction composition and poor analytical precision (~7-8% deviation for fractions) (Kharrat *et al.*, 2007; Bissada *et al.*, 2016a). Additionally, the large number of SARA methodologies available can create confusion amongst users, where datasets generated from different methods are assumed to be interchangeable. SARA methods almost always utilise adsorption chromatography and as such are often reported to suffer from poor recovery, owing to the irreversible adsorption of the more polar compounds to the stationary phase (Fan *et al.*, 2002; Boysen and Schabron, 2013).

Historically, compositional investigations employed SARA methodologies to isolate fractions for chemical and physical characterisations. Initial investigations focused primarily on saturates (e.g., Peters *et al.*, 1986; Netzel and Guffey, 1989; Horstad *et al.*, 1990; Philp *et al.*, 1990) and aromatics fractions (e.g., Azogu, 1981, Kolesnikov et al., 1988, Jarm et al., 1990). Indeed, the saturates fraction typically contains many critical biomarkers which are routinely used to determine crude oil origin, maturity, biodegradation and deposition environment (Peters *et al.*, 2005), thus enabling this single fraction to provide information on many geochemical parameters.

Investigations into the composition of the resin and asphaltene fractions have long been hindered by instrumental limitations. The high polarity, complexity and molecular weight of these fractions makes them inherently challenging to study. The advent of uHRMS

Fourier transform-ion cyclotron resonance-mass spectrometers; (FT-ICR-MS; Comisarow and Marshall, 1974) and later, orbitrap mass spectrometers (Makarov *et al.*, 2006) has led to the establishment of the field of petroleomics and aided significantly towards an improved understanding of the heteroatom containing components of crude oils (Marshall and Rodgers, 2004). With resolving powers in excess of 100,000 these instruments enable the mass spectral resolution of species differing in mass by 0.0034 Da. Additionally, accurate mass measurements allow for molecular formula to be assigned confidently to ionised species across mass ranges far exceeding those accessible by traditional gas chromatography (GC) instruments (e.g. 200-2000 *m/z*). The application of these techniques to petroleum samples has enabled the assignment of 20,000 distinct elemental compositions ($C_cH_hN_nO_oS_s$) in petroleum samples (Marshall and Rodgers, 2004).

The widespread installation of these instruments has led to the publication of large numbers of uHRMS data sets, often focused on 'characterisation' of resin and asphaltene fractions. The simplicity of SARA separations is likely the reason for their regular use in these compositional investigations, where the resultant fractions are analysed by uHRMS instrumentation (e.g., Liu *et al.*, 2010a; Akmaz *et al.*, 2011; Cho *et al.*, 2012; Gaspar *et al.*, 2012; Ugochukwu *et al.*, 2013; Ghislain *et al.*, 2017). Increased attention is often paid to the asphaltene fraction, owing to industrial interest on account of deposition issues (Adams, 2014). The high average molecular weight (750 $gmol^{-1}$) and high polarity, combined with solubility issues, makes analysis of the asphaltenes a challenging problem (Subramanian *et al.*, 2016). Analysis by uHRMS techniques has enabled the molecular characterisation (Molnárné Guricza and Schrader, 2015b; Molnárné Guricza and Schrader, 2015a; Giraldo-Davila *et al.*, 2016; Silva *et al.*, 2016). However, the identification of individual asphaltenes is still yet to be made.

The lack of specificity associated with SARA fractions is such that any compound that falls within the 'polarity window' determined by the method (i.e. the conditions used to obtain the particular resins fraction) will be collected. As a result, a wide array of NSO-compounds possessing many different functionalities are collected within the resins and asphaltene fractions, which are often analysed without further separation. Recent work by Huba *et al.* (2016) drew attention to the significant effects of ion suppression and variations in ionisation efficiency in many commonly detected NSO functionalised compound classes. This suggests that the bulk analysis of resin and asphaltene fractions in this manner does not reflect the true concentrations of compound classes and significant data could be lost due to the effects of ion suppression. Additionally, while data visualization techniques, such as the use of Kendrick plots, can provide information on the broader molecular distribution of compounds, without any form of chromatographic separation, information on individual structures is not available. For example, analysis of alkylated aromatics, such as the trimethylnaphthalenes, would produce only one peak (corresponding to the molecular mass), despite the presence of up to 14 structural isomers known to be present within crude oils (Mayer and Duswalt, 1973; Rowland *et al.*, 1984). As issues such as toxicity (Nelson, 2001), catalyst poisoning (Argyle and Bartholomew, 2015), and deposition (Sutton *et al.*, 2010) are often structurally dependent, analysis by uHRMS techniques alone is often inadequate.

1.3.2 Targeted separations

Investigations into crude oil composition often require the isolation of specific compounds or specific compounds classes. To measure these compounds quantitatively they must first be isolated from whole crude oil samples. In these cases, a targeted approach to separation is often selected to avoid unnecessary work and generation of unwanted fractions. Over the last several decades, many of these methods been presented. However, they are rarely reproduced.

Several methodologies for the isolation of crude oil acids have been developed in recent years. Foreseeing an increasing interest to study OSPW, Frank *et al.* (2006) developed a method for the clean-up of organic acids from PW. The method utilised a weak-anion exchanger (diethylaminoethyl-cellulose) to remove humic-like material from water samples. Sutton and Rowland (2014) also employed the use of anion exchange chromatography (a polymerically bonded quaternary amine) to isolate the so-called 'ARN' acids from petroleums and petroleum pipeline deposits. Rowland *et al.* (2014) developed a method for the isolation of organic acids from crude oils, employing aminopropyl functionalised silica to isolate acids. This particular method is thought likely to suffer very low selectivity towards acids due the high sample loading reported and retention and elution of addition polar material in such 'acidic' fractions.

Other oxygen-containing compounds in crude oil have also been targeted in separations. Thus, Bennett and Larter (2007b) developed a method for the isolation of phenols from crude oils. The method utilised C_{18} functionalised silica SPE cartridges and fractions were eluted in dichloromethane (DCM). However, whilst the resulting fractions were of sufficient purity for that particular study, they were also seen to contain high levels of both fluorenones and carbazoles. Therefore, the same procedure was used later to investigate the fluorenones in crude oils (Bennett and Larter, 2000; Bennett *et al.*, 2002).

A number of methods for the selective isolation of nitrogen compounds from crude oils have also been established. Li *et al.* (1992a) developed a HPLC-based method utilising an aminocyano column to isolate both basic and neutral nitrogen species. The authors later successfully employed this method to investigate correlations between pyrrolic nitrogen species and thermal maturity (Li *et al.*, 1997). Frolov and co-workers (1989; 1997) developed HPLC methods for the isolation of carbazoles, utilising a silica column and sequential elution with solvents of increasing polarity. Larter *et al.* (1996) and Bennett *et al.* (2002) both also developed methods for the isolation of carbazole and

benzocarbazoles from crude oils, employing sequential alumina and silica, and Florisil SPE cartridges respectively. Merdrignac *et al.* (1998) developed both a liquid-liquid separation and a HPLC based method (sulfonic acid functionalised column) for the isolation of basic nitrogen compounds from crude oils. More recently, Oliveira *et al.* (2004) successfully employed a number of ion exchange resins to isolate basic nitrogen compounds, demonstrating the potential for the use of ion exchange SPE for the isolation of basic species from crude oils.

Sulphur compounds have also been targeted for isolation in separation procedures. One of the first examples of the isolation of sulphur species appears to be work by Drushel and Sommers (1967) who developed a separation scheme based on silica column chromatography. Sequential elution of the silica columns with a solvent series of increasing polarity resulted in the reported separation and isolation of sulfides, thiophenes and sulfones. Nishioka (1988) also developed a column chromatography method utilising silica gel impregnated with palladium chloride to isolate aromatic sulphur (thiophenic) compounds from heavy crude oils. Mössner and Wise (1999) demonstrated the successful use of aminopropylsilane SPE cartridges to isolate thiophenic sulphur compounds from crude oils.

Recent years have seen the preferential use of multidimensional gas chromatography (GC×GC) with both sulphur chemiluminescence detection (SCD) and MS to analyse thiophenic sulphur compounds in petroleum samples (e.g., Avila *et al.*, 2014; Niu *et al.*, 2014; Dijkmans *et al.*, 2015; Cappelli Fontanive *et al.*, 2016; Gieleciak *et al.*, 2016). As in other recent investigations into thiophenic sulphur compounds (e.g., da Silveira *et al.*, 2016; Fang *et al.*, 2016), the abundance of the thiophenes is such that simple separations yielding just ‘saturates’ and ‘aromatics’ type fractions are often sufficient for analysis.

1.3.3 Class-type separations

Less commonly reported are the more extensive, class-type separations, in which whole crude oils are fractionated into several fractions. These fractions are typically based on adsorption of crude oil components to a number of sequentially employed chromatographic phases, followed by their elution in a series of solvents. These schemes can isolate fractions defined by a polarity range (i.e. medium/low polarity) or be designed to isolate fractions specific to compound classes present in crude oils (e.g. thiophenes, carbazoles, organic acids, etc.). Historically, these separations were laborious, generating large numbers of fractions and the many stages of separation resulted in significant losses due to irreversible adsorption (reviewed: Lundanes and Greibrokk, 1994). However, despite the drawbacks, this approach has many benefits. The most significant is the ability to collect fractions based on compound class. Despite the potential of such methods, only two of these methods have been discussed regularly.

The most comprehensive of these is that of Snyder and Buell (1968) who designed an extensive separation procedure based largely on the adsorption chromatography principles previously developed by Snyder (1961a). The method required up to 13 individual column separations, generating a total of 36 fractions and reportedly resulted in the collection of relatively specific fractions of furans, thiophenes, indoles, sulfoxides, carbazoles, quinolones, phenols, pyridines, quinolines and carboxylic acids. The separation proceeded with introduction of whole crude oil samples to a chromatographic column packed with anion exchange resin to facilitate isolation of organic acids. The neutral fraction from this separation was subsequently dried and re-introduced to an alumina packed chromatographic column. At this stage, the sample was separated into fractions defined as ‘non-polars’ (i.e. material not retained by alumina) and ‘polars’ (i.e. material retained and subsequently eluted off alumina). This ‘polar’ fraction was then subjected to an extensive series of separations; first on a cation exchange resin and then

on a series of alumina and silica columns. Fractions were eluted in specific binary mixtures of two of the following organic solvents: pentane, benzene, ethyl ether, isopropanol, methanol and acetonitrile.

Despite the claimed selectivity of the method of Snyder and Buell (1968), widely-published evidence of this method ever being reported or used by other authors could not be found. It is likely that the multiple separations and resource and time intensive nature of the procedures discouraged other authors from adopting the method.

Willsch *et al.* (1997) developed a fractionation procedure using medium pressure liquid chromatography (MPLC) and a series of functionalised silica columns to obtain seven fractions from petroleum samples. The authors also employed a series of 86 model compounds to evaluate the selectivity of the devised separation and to allow prediction of compound class location within the scheme. The procedure began with the separation of whole crude oils on an unbonded silica column, resulting in the retention of so-called 'high polarity NSO compounds'. The non-retained fraction was subsequently separated on acid and base functionalised silica, facilitating isolation of organic acids and bases. Finally, separation on a second unbonded silica column resulted in the collection of fractions of saturated and aromatic hydrocarbons and low- and medium- polarity NSO compounds.

Separation of the model compound series showed the method to have only a limited selectivity towards compound classes, with the majority of compounds eluting within the 'low polarity' NSO compounds fraction. Recoveries from the method were poor, ranging from 63.4-84.8% after being adjusted for evaporative losses. Whilst not widely adopted, the method of Willsch *et al*. (1997) has been employed in other studies. For example, Clegg *et al.* (1998) employed the method to investigate the effects of thermal maturity on

the composition of carbazoles. Later, Oldenburg *et al.* (2002) utilised the method to isolate and characterise the xanthones of crude oil.

1.4 Analytical approaches to crude oil analysis

Throughout the investigations reported in this work, a wide array of analytical techniques were employed to separate and characterise crude oil samples. The majority of these techniques are used routinely in the study of petroleum and will only be introduced briefly herein. By employing a variety of analytical strategies, a more comprehensive characterisation of petroleum components could be achieved. The modern era of petroleomics has seen research institutes invest in uHRMS instruments (primarily FT-ICR-MS), which are now regularly employed as the only point of analysis (e.g. Dalmaschio *et al.*, 2014; Kong *et al.*, 2015; Ghaste *et al.*, 2016; Giraldo-Davila *et al.*, 2016). However, whilst molecular characterisations are valuable, the more challenging structural elucidations are equally, if not more important. Thus, the value of a complementary combined approach enabling both molecular and structural characterisation is evident.

1.4.1 Solid Phase Extraction (SPE)

The use of solid phase extraction (SPE) has become commonplace in analytical laboratories over the last 20 years. The technicalities and use of SPE will not be discussed here in detail, but is reviewed comprehensively by Andrade-Eiroa *et.al.* (2016a; 2016b). Briefly, a typical SPE procedure (Figure 1-6) involves the loading of a sample onto a solid chromatographic phase and subsequent elution of unwanted compounds whilst the target analytes remain adsorbed to the phase. Target analytes are then eluted from the column/cartridge using a different solvent system and collected. The gravity elution of solvents is aided by the application of a positive or negative pressure, which also allows constant flow rates to be achieved.

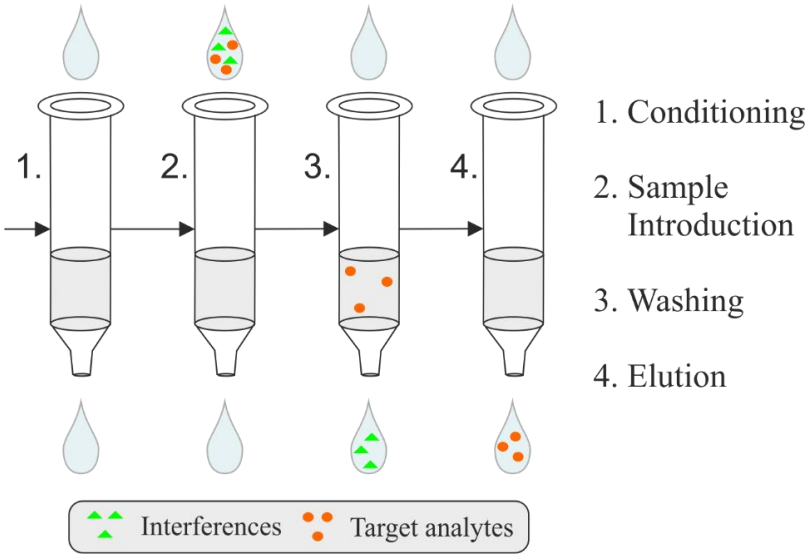

Figure 1-6. Schematic showing the step-wise procedure for a typical SPE separation.

SPE offers a number of distinct advantages over traditional column separations. Indeed, studies have shown SPE to significantly increase the efficiency (i.e. time, separation and cost) of organic compound separations (Andrade-Eiroa *et al.*, 2016a). Additionally, the use of disposable, pre-manufactured cartridges greatly reduces the time required to perform separations, as well as increasing separation reproducibility. Furthermore, the widespread use and low cost of SPE makes it an attractive option when developing new methodologies.

1.4.2 Multidimensional gas chromatography with mass spectrometry (GC×GC-MS)

GC×GC-MS has become a regularly employed technique for the analysis of environmental and petrochemical samples. The coupling of two GC columns of differing polarity enables complex crude oil derived mixtures to be separated by two ‘dimensions’, providing unparalleled chromatographic resolution and peak capacity. The principles of GC×GC (-MS) have been described in detail by many authors (e.g., Pursch *et al.*, 2002; Panic and Gorecki, 2006; Wilde, 2015).

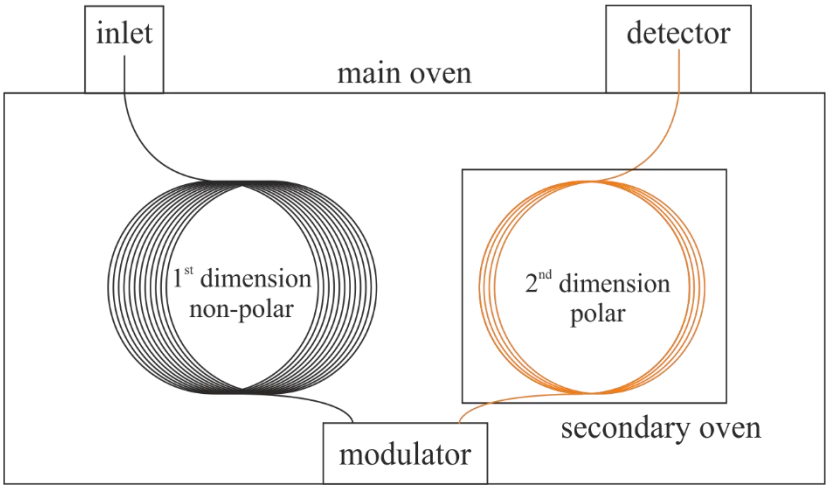

Figure 1-7. Schematic of generic GC×GC instrumentation

Briefly, comprehensive GC×GC involves the joining of two chromatographic columns of different selectivity with a modulator connecting the two columns together (Figure 1-7). A number of modulation strategies are available (reviewed: Edwards *et al.*, 2011; Franchina *et al.*, 2016), but in the present investigations, a two stage cooled loop-modulator was used. The modulator consists of perpendicular cold and hot jets, with a modulation loop (non-phase column) passing twice through the two jets. The cold jet constantly cools the modulation loop at two points, trapping analytes eluting off the 1st dimension column. The hot jet pulses at set periods (~1-10 secs) re-volatilising the trapped components, effectively 're-injecting' them onto the second column. This modulation process occurs constantly throughout the GC run and allows all components to be separated by both columns.

The inherent complexity of crude oil mixtures makes GC×GC a useful approach for analysis. This is highlighted in Figure 1-8, where both GC-MS and GC×GC-MS chromatograms obtained from the separation of a crude oil sample are presented. The complexity of the sample is such that analysis by GC-MS produces an unresolved chromatographic 'hump'. Separation of the same sample by GC×GC-MS affords vastly improved resolution, with several higher polarity compounds (e.g. cyclised, aromatic or

NSO-containing compounds) being successfully resolved in the 2nd dimension, albeit many hydrocarbons are still less well resolved.

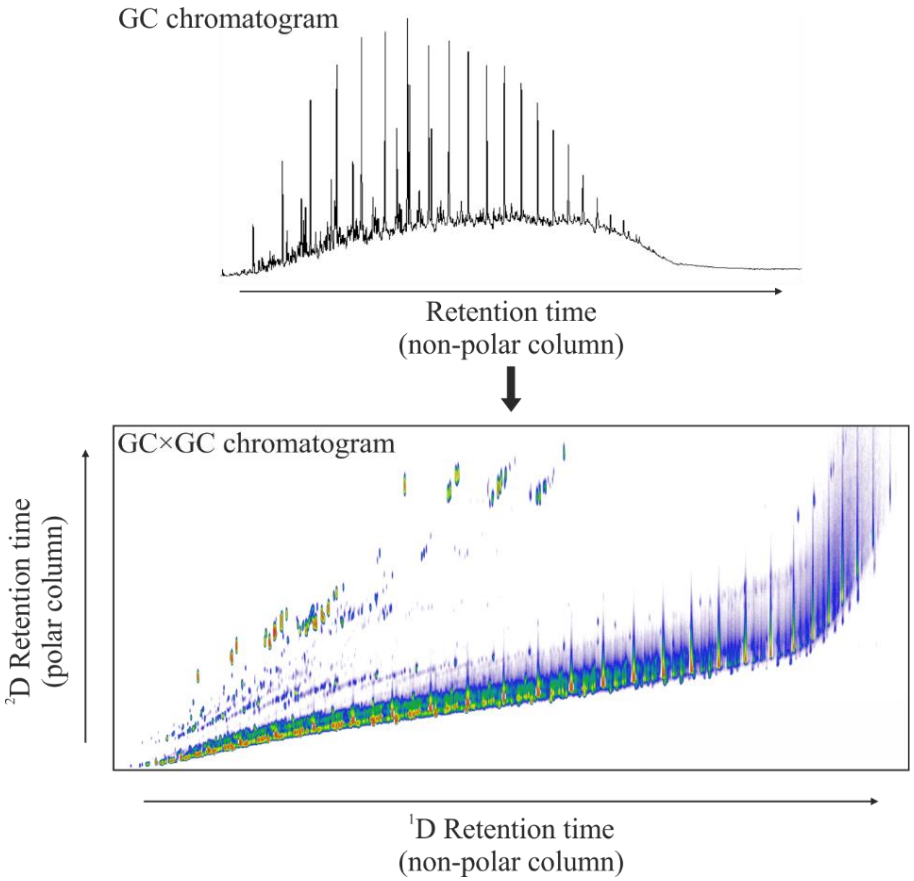

Figure 1-8. GC- and GC×GC-MS TICs from the analysis of a crude oil fraction showing improved chromatographic resolution because of the 2nd dimension in the GC×GC and the representation of the 2D chromatogram as a contour plot.

1.4.3 High and ultrahigh resolution mass spectrometry: orbitrap and ion cyclotron resonance mass spectrometers

High (>10,000) and ultrahigh (>100,000) resolution mass spectrometers (HRMS and uHRMS) are also exceptionally well suited to the analysis of petrochemical mixtures (Rodgers and Marshall, 2007). The mass resolution of a mass spectrometer is a measure of the ability to distinguish between two peaks of similar mass to charge ratios (*m/z)* at a given mass/charge. This is well illustrated in Figure 1-9, which shows the effects of increasing mass resolution on two ions differing by just *m/z* 0.0112 at mass/charge 222

Da. The complexity and huge number of distinct elemental compositions ($C_cH_hN_nO_oS_s$) existing within crude oil creates highly complex isotopic distributions, requiring high and ultrahigh mass resolution instruments.

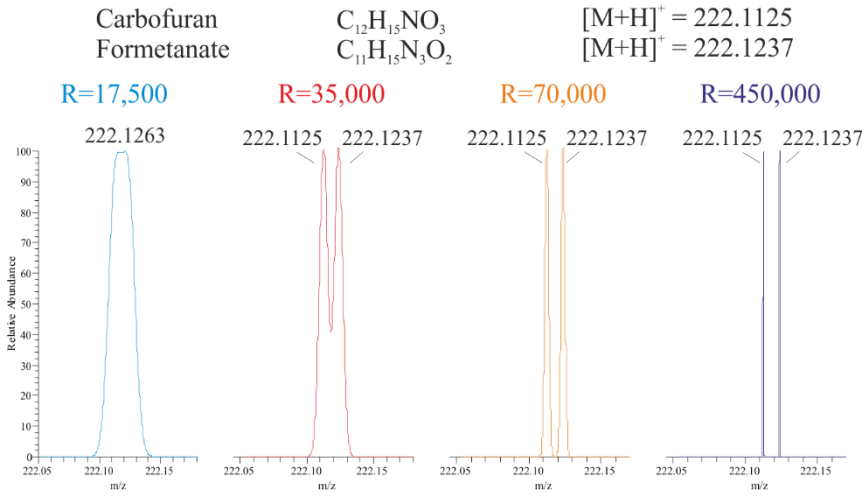

Figure 1-9. The effects of increasing mass spectral resolution on two pesticides (Carbofuran and Formetanate) of similar mass, showing unresolved peaks at resolutions of 17,500 and 35,000 and resolved peaks at 70,000 and 450,000 (modified from Thermo Fisher).

HRMS/uHRMS instruments include both orbitrap and Fourier transform-ion cyclotron resonance (FT-ICR) mass spectrometers, both of which were used in the present study. The ICR instruments determine the *m/z* of an ion by first trapping them in a magnetic field (Penning trap), where they are excited by an oscillating electric field, orthogonal to that of the magnetic field. Excitation of the ions to a larger cyclotron radius causes the ion packets to induce a charge on an electrode thus, enabling their detection. This signal is then subject to a Fourier transform, which yields the mass spectrum. The principles of FT-ICR-MS are described in detail by Marshall *et al* (1998).

Whilst unmatched in mass resolution and mass accuracy, FT-ICR-MS instruments suffer from slow acquisition rates (~1 Hz at a mass resolution of 100,000). As a result, the coupling of FT-ICR-MS to chromatographic instrumentation results in poor

chromatographic resolution, especially when MS/MS scans are also required (Ghaste *et al.*, 2016). With higher acquisition rates and the ability to perform both MS/MS and MS^n experiments, the Orbitrap mass spectrometers are ideal instruments for liquid chromatography (LC)-HRAM-MS analyses (Makarov *et al.*, 2006). The instrument used in the present study was the Q Exactive Focus Orbitrap mass spectrometer (Figure 1-10), with a mass resolution of 70,000 (at *m/z* 400) and capable of MS/MS experiments *via* a higher-energy collisional dissociation (HCD) cell. The orbitrap detector itself is an ion trap mass analyser in which ions are trapped by their inertia and their attraction to the central electrode. The current induced on the outer electrode by the ions allows their detection and subsequent Fourier transform yields the mass spectrum (Makarov, 2000; Hu *et al.*, 2005).

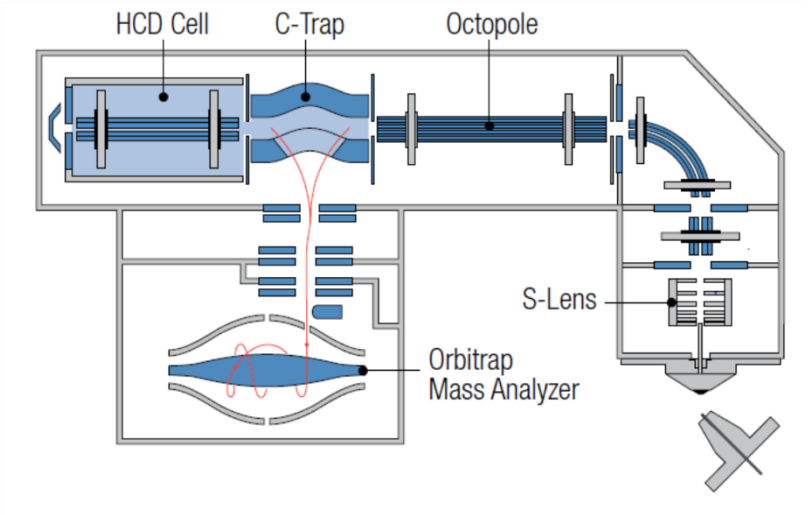

Figure 1-10. Schematic of a Q Exactive Focus Orbitrap mass spectrometer (reproduced from Thermo Fisher)

1.5 Present investigation

The above literature review discussed both the industrial and geochemical relevance of many of the NSO containing classes within crude oils and highlighted the need for more thorough characterisations to be conducted.

The overall aim of the present works was therefore to contribute to knowledge on the composition and concentrations of these much less known 'NSO-containing' (the so-called 'polar'), constituents of crude oils. The past fifty years have seen significant progress in the elucidation of the structural characteristics of the more abundant saturated and aromatic hydrocarbons (reviewed Peters *et al.*, 2005). However, the increased complexity and lower abundance of the many NSO-containing crude oil constituents, combined with previous instrumental limitations, has resulted in somewhat slower progress being made for the NSO compounds. As a result, significant developments have been more or less limited only to the past twenty years.

The first objective herein was to review the literature for existing methods and thus to select an appropriate chromatographic separation method to allow for the generation of chemically discrete NSO fractions from crude oils. Initial work focussed on the evaluation of the selected method. Assuming the designated criteria were satisfied, the method would then be to be employed to generate fractions from a variety of crude oil samples. These fractions would then be subject to analysis by a variety of advanced chromatographic and mass spectrometric techniques to allow for both molecular and structural characterisation.

Chapter 2. General Experimental and Analytical Procedures

All laboratory glassware and apparatus was cleaned in Decon 90 (liquid detergent, Fisher), rinsed with deionised water, dried in an oven at 110 °C and solvent rinsed prior to use.

Unless stated otherwise, all solvents used for experimental procedures were at least HPLC grade (Rathburn Chemicals, Scotland): *n*-hexane, dichloromethane (DCM), tetrahydrofuran (THF), methanol (MeOH) and toluene, except diethyl ether (DEE; reagent grade, Rathburn Chemicals, Scotland). Water (H_2O) was 18.2 MΩ · cm grade (Elga Maxima Analytical; Elga Ltd., U.K.). Acid-base modifiers were reagent grade; formic acid (FA, 95%; Sigma-Aldrich Company Ltd., U.K.) and ammonium hydroxide (aq; 35%; Fisher Scientific, U.K.).

2.1 Model Compounds

The model compound mixture was composed of 20 compounds (Table 2-1) which were carefully chosen to represent various polar compound *classes* known to be present in crude oils, rather than to represent the extraordinary *numbers* of compounds in crude oil (Tissot and Welte, 1984). Compounds from the following classes were chosen therefore: polycyclic aromatic hydrocarbons (PAHs), sulphides, sulfoxides, thiophenes, sulfones, furans, phenols, ketones, carbazoles, quinolines, nitro-, and naphthenic acids (including additionally functionalised acids).

All model compounds were purchased from suppliers at ≥ 97% purity, which was confirmed by GC-MS analysis. Compounds were obtained from the following suppliers: adamantane carboxylic acid, 5 β-cholanic acid, dibenzyl disulfide, dibenzyl sulfoxide, dibenzofuran, dibenzofuran-4-carboxylic acid, dibenzothiophene sulfone, fluorenone, 4-dibenzothiophene carboxylic acid, 5-nitroindol, 4-pentylbicyclo[2.2.2]octane-1-

carboxylic acid, 2-phenyl phenol, phenanthrene and xanthone from the Sigma-Aldrich (Poole, U.K.), benzo[h]quinoline, dibenzyl sulfoxide, dibenzothiophene, fluoranthene from Acros Organics (Belgium), and benzo[a]pyrene from Supelco Inc. (Bellefonte, USA).

2.1.1 Preparation of 'model' compound mixture

The model compound mixture was prepared in THF to a concentration of 0.2 mg mL^{-1} (per component). Each model compound was accurately weighed into a 7 mL glass vial and made up to a concentration of 8 mg mL^{-1} in THF. Each stock solution (100 μL) was then syringed into a pre-weighed 7 mL glass vial and a further 2 mL of THF added. The resulting stock solution was refrigerated and its integrity checked by gas chromatography-mass spectrometry (GC-MS) prior to use.

2.1.2 Quantification of 'model' compounds by gas chromatography-mass spectrometry (GC-MS)

Throughout method development, model compounds were tracked through the various chromatographic separations and quantified within the resultant fractions, by GC-MS. Fractions were collected in 22 mL glass vials and after drying would be weighed and diluted, in DCM, to appropriate concentrations prior to analysis by GC-MS. Quantification of compounds within fractions was made by comparison with a 5-point calibration series for each of the compounds in the mixture (1, 5, 10, 15 and 25 mg L^{-1}). Data were batch processed using the Mass Hunter quantitative analysis suite (version B.07.00; Agilent Technologies, UK). Acids were analysed as their trimethylsilyl esters (Section 2.4.2).

Table 2-1. Model compounds used to evaluate crude oil separation methods.

Model Compound	Structure	Molecular Weight (g mol^{-1})	Purity (%)	Melting/Boiling Point (°C)	Supplier
Phenanthrene	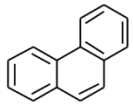	178.07825	99.5	99.24 340	Sigma-Aldrich Company Ltd., Poole, U.K.
Fluoranthene	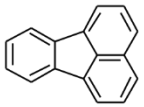	202.07825	99.6	110.19 384.0	Acros Organics, Belgium
Benzo[*a*]pyrene	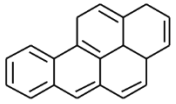	252.09390	99.9	181.1 nda	Supelco Inc., Bellefonte, USA
Dibenzothiophene	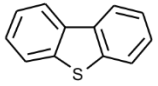	184.03467	99	98.2 332.5	Acros Organics, Belgium
Dibenzothiophene sulfone	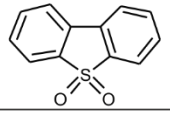	216.02450	97	231-233 nda	Sigma-Aldrich Company Ltd., Poole, U.K.
Dibenzyl disulphide	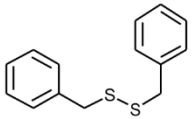	246.05369	98	71.5 nda	Sigma-Aldrich Company Ltd., Poole, U.K.
Dibenzyl sulfoxide	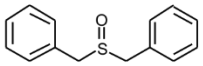	230.07654	98	134 210	Acros Organics, Belgium
Dibenzofuran	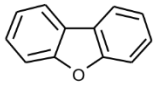	168.05752	99	86.5 287.0	Sigma-Aldrich Company Ltd., Poole, U.K.

Model Compound	Structure	Molecular Weight (g mol^{-1})	Purity (%)	Melting/Boiling Point (°C)	Supplier
2-Pheylphenol	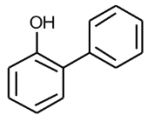	170.07317	99	57-59 280-284	Sigma-Aldrich Company Ltd., Poole, U.K.
Xanthone	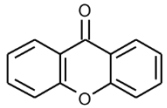	196.05243	97	174.0 351.0	Sigma-Aldrich Company Ltd., Poole, U.K.
Fluorenone	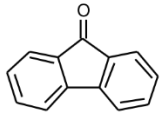	180.05752	98	83.5 342	Sigma-Aldrich Company Ltd., Poole, U.K.
Carbazole	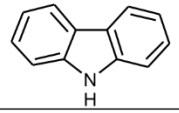	167.07350	95	246.3 354.7	Sigma-Aldrich Company Ltd., Poole, U.K.
Benzo(h)quinoline	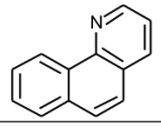	179.07350	97	52.0 339.0	Acros Organics, Belgium
5-Nitroindole	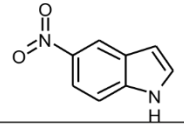	162.14544	96	205-207 nda	Sigma-Aldrich Company Ltd., Poole, U.K.
4-Pentylbicyclo [2.2.2] octane 1-carboxylic acid	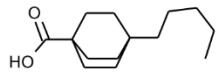	224.33916	99	160-162 nda	Sigma-Aldrich Company Ltd., Poole, U.K.
4-dibenzothiophene carboxylic acid	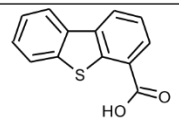	228.26642	99	nda nda	Sigma-Aldrich Company Ltd., Poole, U.K.

Model Compound	Structure	Molecular Weight (g mol^{-1})	Purity (%)	Melting/Boiling Point (°C)	Supplier
Dibenzofuran-4-carboxylic acid	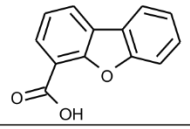	212.20082	97	211-215 nda	Sigma-Aldrich Company Ltd., Poole, U.K.
1-Adamantane carboxylic acid	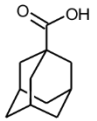	180.24354	99	172-174 nda	Sigma-Aldrich Company Ltd., Poole, U.K.
5β-Cholanic acid	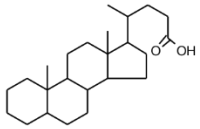	360.57320	95	165-167 nda	Sigma-Aldrich Company Ltd., Poole, U.K.

2.2 Methods of Crude Oil Separation

The following separation procedures were conducted using the solid phase extraction (SPE) apparatus detailed in Figure 2-1. All SPE separations were carried out using a Biotage® Vacmaster-10™ manifold (Biotage®, Hengoed, U.K.) equipped with 10× PTFE stopcock/needles (Biotage®, Hengoed, U.K.). Stopcocks were rinsed thoroughly with DCM prior to use and the manifold was cleaned between sample treatments. The SPE cartridges were conditioned sequentially immediately before use. All elutions were conducted under reduced pressure conditions at a constant flow rate of approximately 50 drops min^{-1} (1 mL approx. 60 drops). All samples were collected and stored in 22 mL glass vials. Solvent was removed from fractions at a constant temperature (solvent dependant) and under a steady stream of N_2. With the exception of fractions containing the saturated hydrocarbons, fractions were dried until a constant weight was attained.

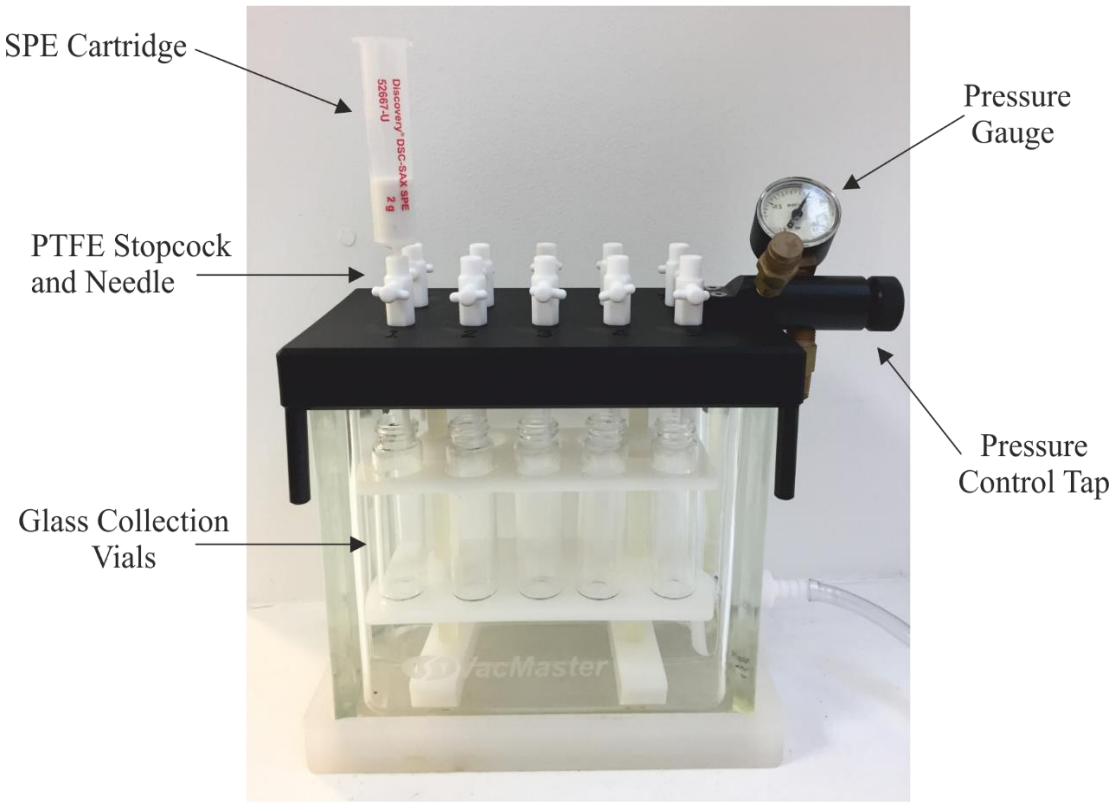

Figure 2-1. Labelled solid phase extraction (SPE) manifold with attached SPE cartridge used for crude oil separations.

2.2.1 General method for the separation of crude oils using a modernised iteration of the method of Snyder and Buell (1968)

The separation procedures are summarised in the flow diagram detailed in Figure 2-2. Crude oil was first homogenized (1 hr, Stuart SSL1 Orbital Shaker, 100 rpm) and ~0.3 g was weighed accurately into a 7 mL glass vial. The crude oil sample was then diluted in DEE/H_2O/NH_3 (7mL/0.1%/0.1%, v/v/v) and mixed (vortex, 30 s).

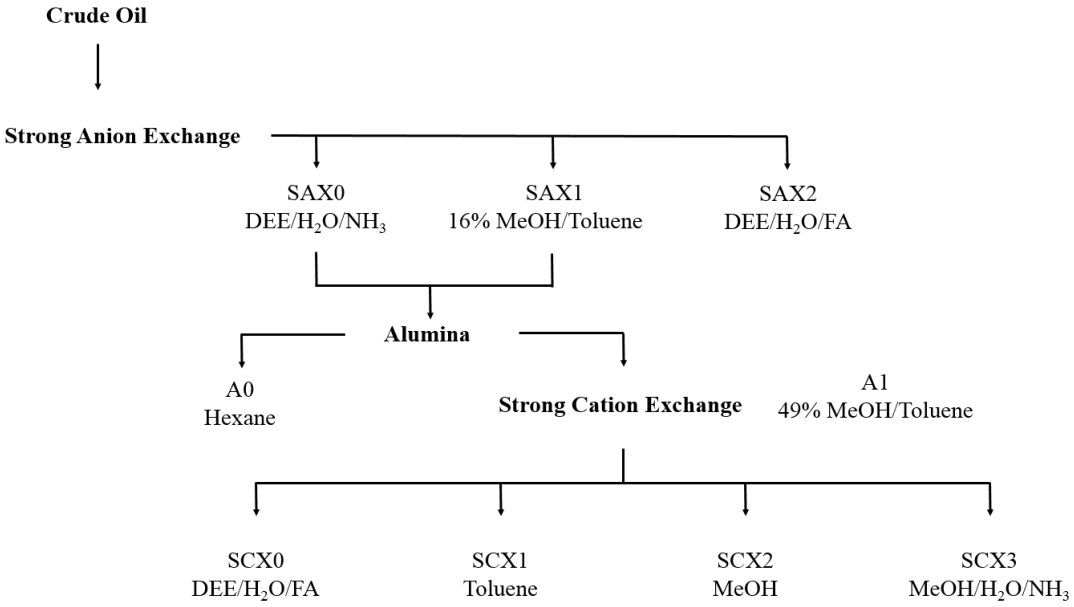

Figure 2-2. Flow diagram for the separation of crude oils following the method of Snyder and Buell (1968). Fraction numbers are related to solid phase extraction phase (e.g. SAX = strong anion exchange, SCX = strong cation exchange). Positive integers refer to the order of elution from SPE cartridges. Elution solvents are listed along with the fraction label.

The diluted sample was then applied to a sequentially pre-conditioned (NH_3 (aq) (1%, 20mL), H_2O (10 mL) and DEE (20 mL)) SAX (DSC-SAX, 12 mL, 2g; Sigma-Aldrich company Ltd., U.K., 0.14 mequiv g^{-1}), SPE cartridge. The cartridge was eluted under vacuum (-0.25 bar) with the following solvents: DEE/H_2O/NH_3 (20 mL/0.1%/0.1%,

v/v/v; SAX0) with washings (3x) of the sample vial, 16% methanol/toluene (20 mL; SAX1), and DEE/H_2O/FA (20 mL/0.1%/2%, v/v/v; SAX2). Fractions SAX0 and 1 were then dried partially (until approx. 1/3 of original sample volume remained) under a steady stream of N_2 at appropriate temperatures (DEE: 30 °C and methanol/toluene: 70 °C). These fractions were combined to form one composite fraction (SAX01) after which the remaining solvent was removed. Fraction SAX2 was dried under N_2 (30 °C).

Fraction SAX01 was reconstituted in *n*-hexane (1 mL), mixed (vortex, 30 s) and applied to an alumina (Isolute Al-N; 2 g, 6 mL; Biotage®, Hengoed, U.K.) SPE cartridge, previously conditioned with *n*-hexane (20 mL). The cartridge was eluted under vacuum (-0.25 bar) with *n*-hexane (10 mL; A0; "nonpolar fraction") with washings (3x) of the sample vial and with methanol/toluene (49:51%, 10 mL; A1; "polar fraction"). Fractions were dried under N_2 at appropriate temperatures (*n*-hexane: 30 °C and methanol/toluene: 70 °C).

Fraction A1 was reconstituted in DEE/H_2O/FA (7 mL/0.1%/0.1%, v/v/v), mixed (vortex, 30s), sonicated (10 mins), and applied to a sequentially pre-conditioned (20 mL, 0.1% FA (aq); 10 mL, H_2O; 10 mL, toluene; 20 mL, methanol; 20 mL, DEE; flush dried between eluents) SCX (DSC-SCX, 12 mL, 2 g; Sigma-Aldrich company Ltd., U.K., 0.8 mequiv g-1) SPE cartridge. The cartridge was eluted under vacuum (-0.25 bar) with DEE/H_2O/FA (19 mL/0.1%/0.1%, v/v/v; SCX0) with washings (3x) of the sample vial, toluene (20 mL; SCX1), methanol (20 mL; SCX2) and methanol/H_2O/NH_3 (20mL/0.1%/2%; SCX3). Fractions were subsequently blown down under a steady stream of N_2 at appropriate temperatures (DEE: 30 ºC, methanol and toluene: 70 ºC)

2.2.2 General method for the separation of crude oils using the SPE procedures developed herein (Robson *et al.*, 2017)

The separation procedures are summarised in the flow diagram detailed in Figure 2-3. Crude oil was first homogenized (1 hr, Stuart SSL1 Orbital Shaker, 100 rpm) and ~0.5 g was weighed accurately into a 7 mL glass vial. The crude oil was diluted in DEE/H_2O/FA (7 mL; 0.1%/0.1%; v/v/v) and mixed (vortex, 10s).

Subsequently the diluted sample was introduced onto a sequentially pre-conditioned (20 mL, 0.1% FA (aq); 10 mL, H_2O; 20 mL, THF; 20 mL, toluene; 20 mL, DEE; flush dried between eluents) SCX, SPE cartridge (DSC-SCX, 12 mL, 2g; Sigma-Aldrich Company Ltd., Poole, U.K.). Fractions were sequentially eluted from the SCX cartridge under vacuum (-0.1 bar) with the following solvents: DEE/H_2O/FA (20mL; 0.1%/0.1%; v/v/v; SCX0), toluene (20 mL; SCX1), THF (20mL; SCX2), THF/H_2O/ammonia (20 mL; 0.1%/2%; v/v/v; SCX3) and THF/H_2O/ammonia (20 mL; 0.1%/5%; v/v/v; SCX4), flush dried between eluents. Solvents were removed under nitrogen at suitable temperatures (DEE, THF: 30 ºC, toluene: 70 ºC).

After drying, fraction SCX0 was diluted with DEE/H_2O/ammonia (7 mL; 0.1%/0.1%; v/v/v) and applied to a pre-conditioned (20 mL, 1% ammonia (aq); 10mL H_2O; 20 mL THF; 20 mL toluene; 20 mL DEE) strong anion exchange (SAX) SPE cartridge (DSC-SAX, 12 mL, 2g, Sigma-Aldrich Company Ltd., Poole, U.K.). Fractions were eluted sequentially from the SAX cartridge under vacuum (-0.1 bar) in the following solvents: DEE/H_2O/ammonia (20 mL; 0.1%/0.1%; v/v/v; SAX0), toluene (20 mL; SAX1), THF (20 mL; SAX2), and THF/H_2O/FA (20 mL; 0.1%/2%; v/v/v; SAX3) flush dried between eluents. Fractions were dried under nitrogen (DEE, THF: 30 ºC, toluene: 70 ºC).

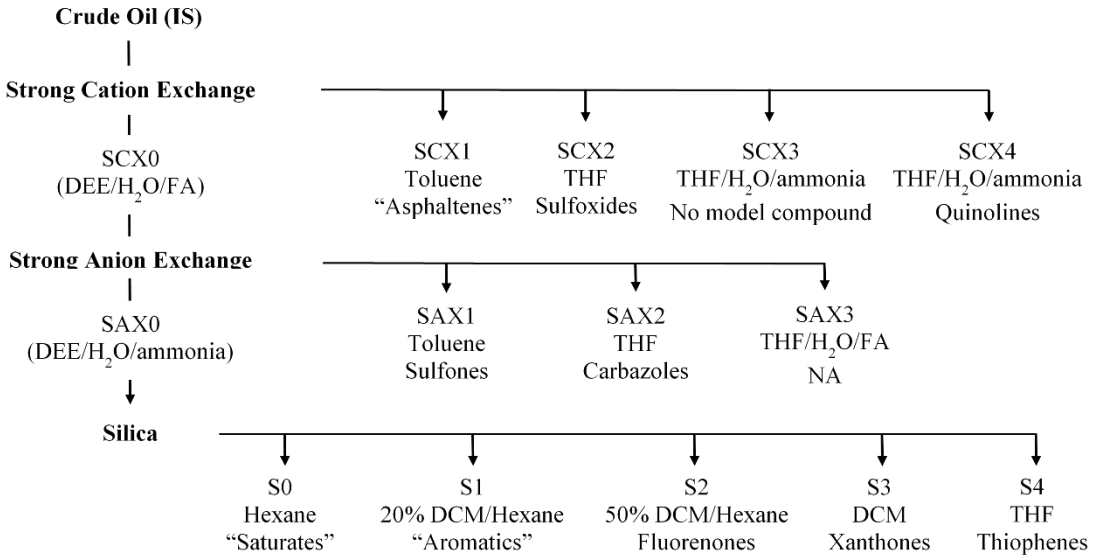

Figure 2-3. Flow diagram for the compound class separation of crude oils into discrete compound classes. Fraction numbers are related to solid phase extraction phase (e.g. SCX = strong cation exchange, SAX = strong anion exchange, S= silica); suffix 0 refers to non-retained fractions and positive integers to the order of elution from SPE cartridges. Elution solvents and location of model compound elutions are listed along with the fraction label.

Separation on silica was conducted using a sub-sample (~0.1g) of fraction SAX0 which was diluted in n-hexane (100 μL) and applied to a sequentially pre-conditioned (10mL, THF; 10mL, DCM; 10 mL, n-hexane) silica SPE cartridge (Isolute® SI, 1g, 6 mL, Biotage®, Hengoed, U.K.). Fractions were sequentially eluted from the silica cartridge under vacuum (-0.1 bar) with the following solvents: n-hexane (10 mL; S0), DCM/n-hexane (20%/80%, v/v; 10 mL; S1), DCM/hexane (50%/50%, v/v; 10 mL; S2), DCM (10 mL; S3), and THF (10 mL; S4). Solvent was removed under nitrogen at a suitable temperature (30 ºC).

2.3 Instrumentation

2.3.1 Fourier transform-infrared spectroscopy (FT-IR)

FT-IR analysis was performed using a Bruker Alpha FT-IR with a platinum ATR module equipped with a diamond window. Spectra were obtained at a resolution of 4 cm^{-1} using a DTGC detector, running 16 scans per spectrum, with a scanning range of 4000 to 375 cm^{-1} and run in absorbance mode.

When sample quantity was limited, samples were analysed using a Bruker IFS 66 spectrometer attached to a Hyperion FT-IR microscope.

2.3.2 Gas chromatography- mass spectrometry (GC-MS)

GC-MS analyses were conducted on an Agilent 7890A Gas Chromatograph (Agilent Technologies, Wilmington, DE) interfaced with a 7683 B autosampler and to a 5975 A quadrupole mass selective detector (MSD).

GC columns differed during the course of the investigation. Column A was an Rxi-1ms (Crossbond 100% dimethyl polysiloxane) fused silica column (30m × 0.25 mmID and 0.25 μm film thickness; Restek Corporation, USA). Column B was a (5% phenyl)-methylpolysiloxane HP5-MS (30 m × 0.25 mm × 0.25 μm).

Helium carrier gas was used at a constant flow rate of 1.0 mL min^{-1} and samples (1 μL) were injected into a 250 ºC splitless injector. The oven was programmed to 40 ºC (1 min hold), then heated to 300 ºC at 10 ºC min^{-1}. The MS transfer line temperature was 280 ºC. Data were collected and analysed with Agilent Chemstation software. Individual compounds were identified from mass spectra and retention positions in total ion current profile (TIC; m/z 50–500 mass range) with a constant ionisation potential (70 eV). System suitability was routinely checked using the internal calibration procedure and perfluorotributylamine (PFTBA).

2.3.3 Comprehensive multidimensional gas chromatography-time of flight mass spectrometry (GC×GC-MS)

Comprehensive multidimensional gas chromatography-mass spectrometry (GC×GC-MS) analyses were performed using a 7890A Gas Chromatograph (Agilent Technologies, UK) interfaced with a Zoex ZX2 GC×GC cryogenic modulator (Zoex, Houston, TX, USA) and a Markes/Almsco Bench Tof dx™ time of flight mass spectrometer (Markes International Limited, Llantrisant, Wales, UK).

Certain instrumental conditions were changed during the course of the investigation to optimise the analysis of the various fractions analysed:

Instrument set up **A**: the first dimension column was a 100% dimethyl polysiloxane (60 m × 0.25 mm × 0.25 μm) Rxi®-1ms (Restek, Bellefonte, USA), followed by a 1.5 m × 0.25 mm deactivated fused silica modulation loop. The second-dimension column was a 50% phenyl polysilphenylene siloxane (2.5 m × 0.25 mm × 0.25 μm) BPX50 (SGE, Melbourne, Australia). The oven was programmed from 35 ºC (1 min hold), then to 150 ºC at 5 ºC min^{-1}, then to 350 ºC at 1.7 ºC min^{-1} (10 min hold). The hot jet was programmed to a temperature of 115 ºC (1 min hold), heated to 230 ºC at 5 ºC min^{-1}, then to 400 ºC at 1.8 ºC min^{-1}. The secondary oven was heated from 95 ºC (1 min hold) to 210 ºC at 5 ºC min^{-1}, and finally to 350 ºC at 1.6 ºC min^{-1}. The modulation time was 4, 8 and 9 s with a 350 ms pulse length. The MS transfer line temperature was maintained at 330 ºC.

Instrument set up **B**: the first dimension column was a (5% phenyl)-methylpolysiloxane (60 m × 0.25 mm × 0.25 μm) Rxi®-5ms (Restek, Bellefonte, USA), followed by a 1.5 m × 0.25 mm deactivated fused silica modulation loop. The second-dimension column was a 50% phenyl polysilphenylene siloxane (2.5 m × 0.25 mm × 0.25 μm) BPX50 (SGE, Melbourne, Australia). The oven was programmed from 100 ºC (1 min hold), to 190 ºC at 3 ºC min^{-1}, then to 250 ºC at 0.7 ºC min^{-1}, and finally to 330 ºC at 6 ºC min^{-1} (10 min

hold). The hot jet was programmed to a temperature of 105 ºC (1 min hold), heated to 210 ºC at 3 ºC min^{-1}, then to 285 ºC at 0.9 ºC min^{-1}, and finally to 340 ºC at 5 ºC min^{-1}. The secondary oven was heated from 150 ºC (1 min hold) to 230 ºC at 3 ºC min^{-1}, and finally to 350 ºC at 1.2 ºC min^{-1}. The modulation times were 6 and 8 s with a 350 ms pulse length. The MS transfer line temperature was maintained at 330 ºC.

Helium carrier gas was used (constant flow; 1.0 mL min^{-1}) and samples (1 μL) were injected into a split/splitless injector (splitless; 275 °C). Mass spectrometric parameters were as follows: ionisation energy -70 eV, scan speed 50 Hz, recorded mass range *m/z* 50-550. Data were collected in ProtoTof (Markes International, Llantrisant, Wales, U.K.). System suitability was routinely checked using the internal calibration procedure and perfluorotributylamine (PFTBA.

Software/Data processing

ChromSpace (Markes International Limited, Llantrisant, Wales, U.K.) was employed for the processing and presentation of GC × GC data.

The software allows presentation of chromatograms as two-dimensional colour contour plots, with the ability to: create personalised colour schemes, generate extracted ion chromatograms (EICs), compare mass spectra to library spectra and generate 3D images. Additionally the software has a feature called parametric filtering. This feature allows creation enhanced EICs by applying additional constraints such as retention time windows and relative or absolute abundances of specific ions within the chromatograms.

2.3.4 High temperature gas chromatography-flame ionization detection (HTGC-FID)

HTGC-FID analyses were conducted on an Agilent 6890 Series GC system (Agilent Technologies, Wilmington, DE) equipped with a cool on column (COC) inlet and an

Agilent 6850 FID detector. The inlet was programmed to track the over temperature and the FID was set to a constant temperature of 435 ºC. The installed column was an Agilent Vf-5HT Ultimetal (15 m x 0.25 mmID x 0.1 μm; Agilent Technologies, Wilmington, DE). The oven was heated from 40 ºC to 430 ºC at a rate of 15 ºC min^{-1}. Sample injections (0.5 μL) were performed manually and with a syringe/sample temperature of 70 ºC. A helium carrier gas was used at a constant flow rate of 1 mL min^{-1}.

2.3.5 Ultra high performance liquid chromatography high-resolution accurate mass-mass spectrometry (uHPLC-HRAM-MS)

uHPLC/HRAM-MS was carried out using a U3000 uHPLC liquid chromatography system (Thermo Fisher Scientific, UK) interfaced to a Q Exactive Focus mass spectrometer (Thermo Fisher Scientific, UK) fitted with a heated electrospray ionisation source (HESI II).

Certain instrumental conditions were altered throughout the course of this study in order to optimise analysis of fractions and model compounds:

Instrument set up **A**: the column was a Waters XBridge BEH C18 (50 × 2.1 mm, 3.5 μm) column (Waters, U.K.). The solvent gradient was as follows: 0.1% formic acid (FA) (aq)/ 0.1% FA acetonitrile (100:0 to 0:100, 10-minute runtime).

Instrument set up **B**: the column was an ACE Excel 3 SuperC18 (100 × 2.1 mm, 2.5 μm) column (Advanced Chromatography Technologies Ltd, UK). The solvent gradient for the analysis of basic fractions was as follows: 0.1% FA (aq)/ 0.1% FA in acetonitrile/ 0.1% FA in IPA (90:10:0 to 15:85:0 to 0:10:90; 30-minute runtime). All solvents were LC-MS grade (Sigma-Aldrich Company Ltd., U.K)

Separations were carried out at 50 °C with an eluent flow rate of 500 μL min^{-1}. Injection volume was 10 μL with a needle wash of methanol (MeOH). The mass spectrometer

conditions for full scan experiments were as follows: nitrogen sheath, auxiliary, and sweep gas (53, 14, and 3 arbitrary units, respectively), vaporiser temperature (300 °C), polarity (positive or negative ion), spray voltage (+3500/ -2500 V), capillary temperature (270°C) and S-lens RF level (50). The resolution was set at 70,000 at *m/z* 200 with a full scan (*m/z* 100-1000), AGC target ($1e^6$, automatic gain control) and micro scans (1). MS/MS fragmentation experiments were conducted in the higher-energy collision dissociation (HCD) cell. Mass spectrometer conditions were as follows: Resolution 35,000 at *m/z* 200, MS^2 isolation width 1 *m/z* and collision energy (CE) was set at 30, 40 and 50 eV.

External mass calibration (≤3 ppm) was used with auto-calibration using Pierce LTQ Velos ESI positive ion calibration solution (n-butylamine, caffeine, MRFA, and Ultramark 1621 (Thermo Fisher Scientific, UK)) and Pierce LTQ Velos ESI negative ion calibration solution (sodium dodecylsulfate, sodium taurocholate and Ultramark 1621 (Thermo Fisher Scientific, U.K.).

Software/Data processing

Data were acquired in Xcalibur 3.0.63 (Thermo Fisher Scientific, U.K.). Simple data processing, such as obtaining mass spectra, generating EICs and creating chromatographic figures, was conducted in Xcalibur. However, more advanced manipulations were conducted using the freeware platform MZmine 2 v2.24 (Pluskal *et al.*, 2010). Designed primarily for use in proteomics, MZmine is a modular, open source data processing toolbox for visualising and analysing mass spectrometry based molecular profile data. MZmine provides a free alternative for processing of mass spectrometry data in which the operator must choose the most appropriate algorithm when applying each module to their data set. The modules and parameters employed to process datasets presented herein are highlighted below:

- Data Import- LC-MS data files were directly imported into MZmine as .raw files.
- Mass Detection Module- used to generate a list of masses (ions) for each scan within the chromatographic run. The exact mass algorithm was used to create a mass list for each sample with a set noise level of 2.0E4.
- Chromatogram Builder- used the previously generated mass lists to build a chromatogram for each mass which could be detected continuously across scans. Chromatograms were built across the entire chromatographic run at an MS level of one and in positive ion mode. The minimum peak width was set to 0.1 minutes and the minimum intensity for the apex of a chromatographic peak set at 2.5E4. Minimum *m/z* tolerance for data points between scans was set at 5 ppm.
- Adduct Search- sodium and potassium adducts were searched for across entire peak tables.
- Molecular Formula Assignment- Molecular formula were predicted using the following constraints: number of C = 150, H = 300, N = 10, S = 10, O = 10, and an *m/z* tolerance of 5 ppm.
- Peak List Alignment- aligned peaks in peak lists of multiple samples, allowing the removal of ions present in procedural blanks, identifying model compounds within samples and highlighting the differences in sample composition. The algorithm aligned detected peaks through a match score based on the mass and retention time of each peak. The following parameters were used to align peak tables: *m/z* tolerance at 5 ppm, maximum retention time (absolute) difference at 0.2 minutes, RT time weight at 1 and *m/z* weight at 5. A successful match also required peaks to have been assigned the same molecular formula.

2.3.6 Fourier transform-ion cyclotron resonance-mass spectrometry (FT-ICR-MS)

FT-ICR-MS data was performed externally by Dr. Steven M. Rowland at Maglab, Florida State University. Data were collected using custom-built FT-ICR mass spectrometer equipped with a 9.4 T horizontal 220 mm bore diameter superconducting solenoid magnet operated at room temperature with a micro ESI emitter. Samples were analysed at a concentration of 50 ug mL^{-1} in 50/50 toluene:methanol with 1% formic acid, the flow rate was 50 uL min^{-1}, and ESI voltage was 2.5 kV. Data were processed using PetroOrg-N v13.3 (Florida State University, Tallahassee, FL).

2.4 Additional Procedures

2.4.1 Sub-sampling of crude oils

Sub-samples of crude oils were taken from the larger containers in which the oil samples were provided. The larger containers were agitated (3 hr, Stuart SSL1 Orbital Shaker, 100 rpm) prior to transfer of a small ~20 mL sample to a 22 mL glass vial. All separation and experimental procedures were conducted using these sub-samples.

2.4.2 Derivatisation using N,O-Bis(trimethylsilyl)trifluoroacetamide (BSTFA)

Prior to analysis by GC, acidic compounds were derivatised with BSFTA. An excess of the silylating reagent was added to samples, which were then sealed and heated for ~1h (70 °C). Excess BSTFA was then removed under N_2 (30 °C) and samples were reconstituted in an appropriate solvent. Derivatised samples were analysed immediately and disposed of within 7 days.

Chapter 3. Modification and evaluation of the method of Snyder and Buell (1968)

Chapter 2 described the implementation and evaluation of a previously published method for the class type separation of crude oil. To satisfy the initial project brief it was necessary to develop a method capable of generating fractions of the various NSO compounds present in crude oils. The method of Snyder and Buell (1968) was selected to generate fractions for analysis. Prior to separation of crude oil samples, the method was evaluated to test method selectivity, recovery and practicality. A series of 19 model compounds, selected to represent 13 functional groups occurring in compounds known to exist in crude oils, were employed to evaluate method selectivity. Model compounds were separated from a mixture of all 19, in triplicate experiments, both alone and when spiked into a crude oil, by a modified variant of the Snyder and Buell fractionation procedure. Compounds were then tracked throughout the separation and were quantified within each fraction by gas chromatography-mass spectrometry (GC-MS). Further evaluation of the method involved the separation of two crude oils, Alaska North Slope (ANS) and a Kuwait Blend. Fractions obtained from the separations were analysed by GC and GC×GC-MS, allowing fraction quality to be assessed.

3.1 Introduction

The large number of methods currently available for crude oil fractionations were reviewed in Chapter 1. A particular emphasis was placed on methods providing a "class type" separation and specifically highlighted was the extensive, class type, separation method of Snyder and Buell (1968). This particular method describes an extensive fractionation in which crude oils are separated into ~40 fractions (method schematic: Figure 3-1).

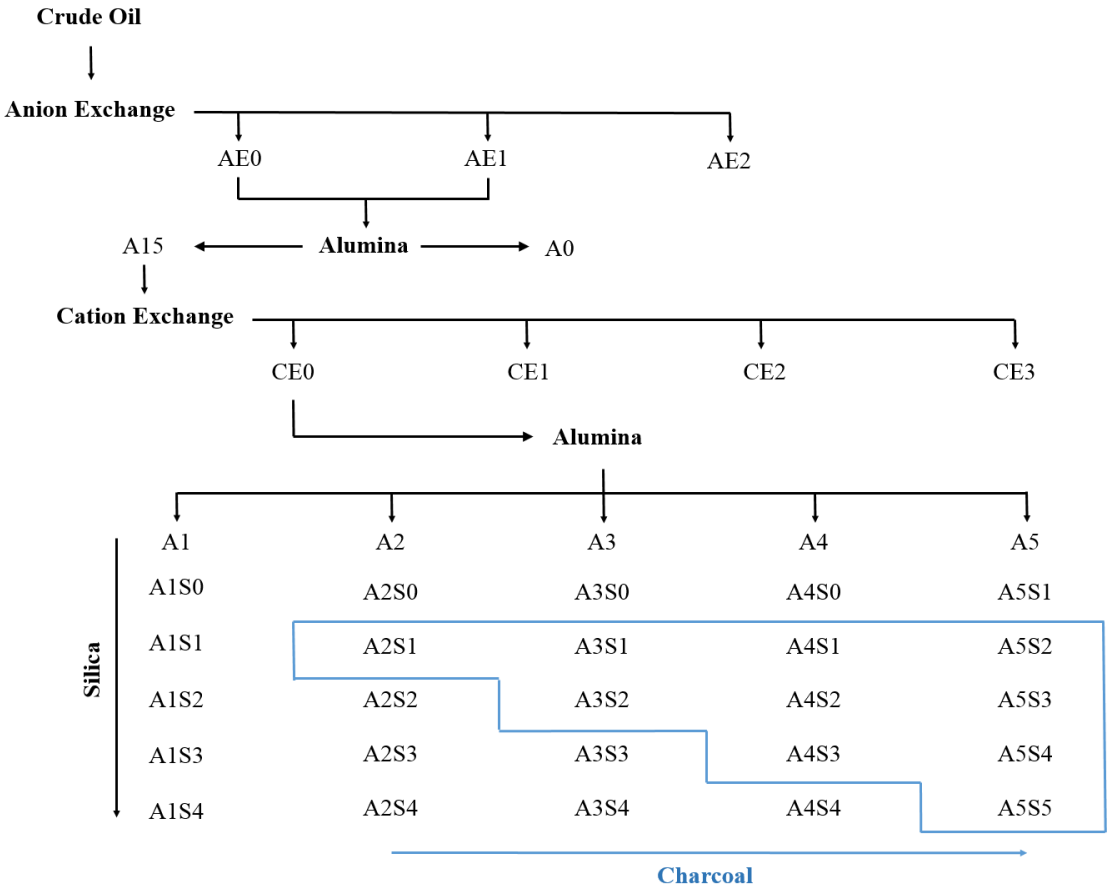

Figure 3-1. Flow diagram for separation of crude oil samples following the method of Snyder and Buell (1968), fractions within the blue grid are subject to further separation on a charcoal solid phase. Fraction numbers are related to the solid phase used in each step of the separation (e.g., CE = cation exchange, AE = anion exchange, S = silica, A = Alumina; integers to the order of elution from SPE cartridges).

In this particular scheme, separation of crude oil samples is achieved by employing a sequence of ion exchange and normal chromatographic phases, with fractions being eluted by a solvent system based on a polarity gradient. Extensive in its approach, the method reportedly allows the isolation of many heteroatomic compound classes known to be present in crude oils. For example, compounds such as dibenzothiophenes, dibenzofurans, pyridines and carbazoles can each be isolated within one or two fractions. Fractions such as this are desirable when conducting investigations focused on the elucidation of NSO-containing compounds in crude oils. By concentrating the compounds of interest into discrete fractions, sample complexity is greatly reduced and molecular charactersiation can proceed with greater ease.

The scheme commences with the isolation of crude oil acids by anion exchange chromatography. This particular step results in the generation of three fractions of which two, AE0 and AE1 (Figure 3-1), are recombined after collection to yield, in theory, a crude oil from which only the acids have been removed. The crude oil acids are isolated in fraction AE2. The second stage in the scheme is the separation of a combined AE01 fraction on alumina, generating just two fractions. It is at this stage that the boundary between ‘non-polar’ and ‘polar’ compounds is operationally defined, based on compound retention on alumina. Simply, any material retained on the alumina column can be considered ‘polar’, and the resulting fraction (A1) is then subject to the more extensive fractionation scheme. This reveals the logic of acid isolation prior to sample separation on alumina. Due to the high polarity of the alumina, the acidic components would adsorb irreversibly to the phase on introduction of a whole crude oil. It was therefore necessary to isolate the acids prior to this step. The remaining steps of the scheme focus on the fractionation of the ‘polar’ A1 fraction. First conducted is a separation by cation exchange chromatography in which compounds such as pyridines, sulfoxides and indoles are isolated. The non-ionic material is then subject to extensive separation on a series of

normal phases (silica and alumina; Figure 3-1). The result of these normal phase separations is the generation of 25 fractions of incrementally increasing polarity, each containing a small number of compound classes. Whilst the separation is described by the authors as a “class type” separation, this is not strictly the case since in practice many classes elute in multiple fractions.

Nevertheless, it was considered to be worthy further implementation of the Snyder method framework, a modified iteration had first to be developed and evaluated. The following work describes the development and evaluation of the method, testing the selectivity towards various compounds classes with a suite of model compounds and evaluation of performance when crude oil samples were separated.

3.2 Methods

3.2.1 Experimental Details

The general procedures for the separation of crude oil samples by the modernised method of Snyder and Buell (1968) are described in Chapter 2. Separations of both the model compound mixture, the model compound mixture spiked into crude oil and use of the method for the separation of 'polars' from an ANS crude oil were carried out in triplicate.

3.2.2 Crude Oil

The two crude oils separated were ANS crude oil and a Kuwait blend crude oil, both obtained from British Petroleum. The ANS crude oil was first subjected to a routine crude oil assay by Intertek (Sunbury, UK). The resulting data are shown in Table 3-1. Also performed on the ANS crude was the industry standard IP-469 SARA separation, the results of which are presented in Table 3-2.

Table 3-1. General characteristics of ANS and Kuwait blend crude oils.

Crude Oil	Region	API Gravity (°)	Sulphur (%)	TAN (mg KOH)	% Asphaltene
Alaska North Slope	North America	30.3[1]	0.96[1]	0.1[1]	2.10[1]
Kuwait Blend	Middle East	31.4[2]	2.52[2]	0.15[2]	3.00[2]

1. Data obtained from an externally conducted crude oil assay (Intertek, Sunbury, UK)
2. AlHumaidan, F.S., A. Hauser, M.S. Rana, and H.M.S. Lababidi. Energy Fuels. 2016, 30, 2892-2903.

Table 3-2. Results from the IP469 SARA separation of ANS crude oil.

	Initial Sample	Saturates	Aromatics	Resins A	Resins B
% mass	100	43.50	46.90	6.60	3.00

1. Data obtained from an externally conducted crude oil assay (Intertek, Sunbury, UK)

3.2.3 Analytical Procedures

The instrumentation used for the quantification of model compounds within fractions is detailed in Chapter 2. The GC-MS analyses were performed using an Rxi-1ms

(Crossbond 100% dimethyl polysiloxane) fused silica column (30m × 0.25 mmID and 0.25 μm film thickness; Restek Corporation, USA) with the following temperature program: 40 ºC (1 min hold), then heated to 300 ºC at 10 ºC min^{-1}. GC×GC-MS analyses were performed using conditions A, in which the oven was programmed from 35 ºC (1 min hold), then to 150 ºC at 5 ºC min^{-1}, then to 350 ºC at 1.7 ºC min^{-1} (10 min hold). The hot jet was programmed to a temperature of 115 ºC (1 min hold), heated to 230 ºC at 5 ºC min^{-1}, then to 400 ºC at 1.8 ºC min^{-1}. The secondary oven was heated from 95 ºC (1 min hold) to 210 ºC at 5 ºC min^{-1}, and finally to 350 ºC at 1.6 ºC min^{-1}. The modulation times were 8 and 9 s (sample dependent) with a 350 ms pulse length. Instrumental conditions were selected following significant method development conducted on the obtained fractions.

3.3 Results and Discussion

The major focus of the present work was to evaluate the selectivity of the separation method developed by Snyder and Buell (1968). Method evaluation was conducted in three stages. First, a mixture of 19 model compounds was subjected to the modified separation scheme and the amount of each compound quantified in each fraction. This allowed the original fraction assignments of Snyder and Buell to be assessed and for method selectivity and the potential effects of the method modifications to be investigated. Secondly, the model compound mixture was solubilised into a crude oil and once again compounds quantified in each fraction. This second stage was designed to investigate the potential solvating effect of the crude oil on compound elution and to identify any potential practical limitations of the method when working with real crude oil samples. Finally, two crude oils were separated by the method and the composition of the obtained fractions were investigated using GC techniques.

The suite of model compounds used in this evaluation comprised standards selected to investigate the claims (Snyder and Buell, 1968) of a "class type" separation. Representative compounds for each class ostensibly isolated by the method were sourced, as well as a number of additional compounds, the behaviours of which were not studied in the original method. Unfortunately, model compound choice was limited to those purchasable, or easily isolated from crude oils and/or crude oil deposits. Compounds included in the mixture typically only included a single representative for each chosen compound class in order to minimise complexity to a practical level. In most cases, only the parent compound was available for purchase. Model compounds included representatives for PAHs, sulfides, sulfoxides, thiophenes, sulfones, furans, phenols, ketones, carbazoles, quinolines, nitro compounds, and naphthenic acids (including additionally functionalized acids).

These ‘model’ compound separations allowed the prediction of compound class locations within fractions isolated by the scheme, observation of the potential interactions of different compound classes and, in this instance, the assessment of the original authors’ fraction designation. However, such data are necessarily limited by the number of available model compounds and do not represent the immense complexity of crude oils and should not be over-interpreted. Certainly, degree of alkylation and additional aromatic rings will affect chromatographic separation greatly, and it cannot be assumed that these compounds will behave as the model compounds chosen to represent them. Therefore, in this study, model compound elution can only be used to predict compound class location. Only when methods are subject to actual crude oil samples can the true efficacy of the separation be evaluated.

3.4 Modification of the method of Snyder and Buell (1968)

Prior to evaluation of the fractionation scheme, certain modifications to the original method were necessary in order to address a number of practical and safety concerns. The past 50 years have seen substantial changes in both analytical techniques and in safe laboratory practice. The result of these changes is that certain aspects of previously published work are no longer considered safe, and/or the techniques and methods used have been surpassed.

The original separation scheme of Snyder and Buell (1968) is extremely resource and labour intensive, and it was deemed impractical to conduct the entire method for the purpose of this evaluation. Therefore, it was decided to first evaluate the performance of the initial method steps before conducting the entire separation. Fractionation proceeded only as far as separation by cation exchange chromatography (Figure 3-1), generating data for nine fractions from which the method could be evaluated.

The most significant change made to the original method was to replace the traditional, hand-packed columns with commercially available pre-packed solid phase extraction (SPE) cartridges. First used for the separation of petroleum hydrocarbons by Theobald (1988), the use of SPE as a tool in crude oil fractionations has become widespread. Ease of use, combined with the diversity of solid phases available, has seen SPE employed for a wide array of applications within crude oil research. A number of examples include the extraction of acids (Rowland *et al.*, 2014; Sutton and Rowland, 2014), aromatic hydrocarbons (Sorensen *et al.*, 2016), sulphur compounds (Yang *et al.*, 2013b; Niu *et al.*, 2014) and for crude oil fingerprinting (Yang *et al.*, 2011). Use of an SPE system in this instance was therefore easily justified. By utilising pre-packed cartridges, both method reproducibility and the efficiency of extraction could be greatly improved. Significant time is also saved as activation of phases and the hand packing of columns is no longer necessary. For example, the cumulative preparation time for sorbents used in the original publication totalled 48 hours, which is effectively reduced to zero when hand-packed columns are substituted with SPE cartridges.

The cation exchange resin used in the original method of Snyder and Buell was substituted with the Discovery DSC-SCX strong cation exchange SPE cartridge (Sigma-Aldrich Company Ltd., U.K.) herein. Both the resin used in the original method and the Discovery cartridges utilise the same functional group, a highly acidic sulfonic acid (Figure 3-2A). The anion exchange resin was replaced with the Discovery DSC-SAX strong anion exchange SPE cartridge (Sigma-Aldrich Company Ltd., U.K.). Once again both the resin and the Discovery cartridge utilise the same functional group, a strongly basic quaternary amine (Figure 3-2B). The efficacy of both the Discovery SCX and SAX cartridges to separate basic and acidic compounds has been shown previously (Sutton and Rowland, 2014). Alumina separations were conducted on Isolute Al-N neutral alumina SPE cartridges (Biotage®, Hengoed, U.K.).

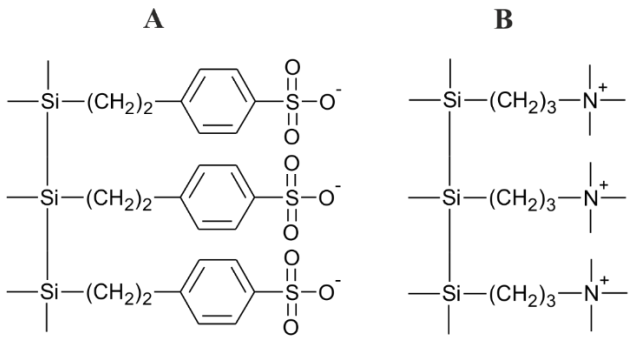

Figure 3-2. Structures for the Discovery SCX strong cation exchange phase; benzene sulfonic acid (**A**) and the Discovery SAX strong anion exchange phase; quaternary amine (**B).**

Whilst the mode of separation is essentially the same for both the resins and SPE cartridges, there are some important differences. Discovery ion exchange cartridges are silica supported, whereas the historically used ion exchange resins typically utilise a polystyrene support with a particle size approximately 10 times that of the modern phase. Using the silica-based ion exchange sorbents instead of the polymer-based resins offers several advantages. For example, silica-supported phases can be eluted with highly organic solvents without phase shrinking or phase swelling. The presence of the benzene ring in the structure of the phase (Figure 3-2A) offers some mixed mode capability to the cation exchange sorbent on account of hydrophobic interactions, which is of interest when separating highly aromatic systems. However, silica supports also have their limitations; they can begin to degrade at extreme pH and cost significantly more than the bulk resins.

Dramatic advances in chromatographic and mass-spectrometric techniques in the last fifty years have seen a remarkable increase in instrumental limits of detection and in the resolving power of chromatographic instruments (reviewed in Chapter 1). A direct consequence of the increased limits of detection and chromatographic separation is a corresponding decrease in the quantity of sample required for analysis. As such, it was

possible to separate far smaller quantities of crude oil than those described in the initial method by Snyder and Buell (Snyder and Buell, 1968).

Interestingly, whilst the original method described the ratios of sample to sorbent for alumina and silica chromatography, bed weights for ion exchange separations were not discussed (Snyder and Buell, 1968). In fact, despite the logic behind removing ionic/highly-polar material prior to normal phase separations, there are surprisingly few reported examples to draw from. Typically, column loadings for ion exchange separations can be calculated from column capacity values, given in milliequivalents. However, these values are not necessarily applicable to non-aqueous separations and the results from these calculations must be applied with caution. This approach has been used successfully by Sutton and Rowland (2014) who calculated column loadings for cation and anion exchange cartridges and by Loboden *et al.* (2015) who calculated column loadings for sulphur separations on Ag^+ SCX. Sutton and Rowland (2014) separated 1g of crude oil on 2g cation and anion exchange cartridges. Whilst this loading might appear rather high, around 80% of crude oils are thought to have nitrogen contents of less than 0.2 wt% (Tissot and Welte, 1984) and the concentrations of naphthenic acids rarely exceed 3 wt% (Lochte and Littman, 1955). Column loading with regard to acid and base content is therefore within acceptable limits (SCX ~1.6 mmol analyte; SAX ~0.28 mmol analyte), as only a small percentage of the bulk crude oil will interact with the ionic phases.

Publications describing normal phase separations vary quite substantially in their approach to column loading and sorbent bed weights. For example, the original Snyder and Buell (1968) method describes using 200-300 times more sorbent than sample, whereas Li *et al.*, (1997) describe successful separations with only a 20:1 ratio of sorbent to sample. Recent publications tend to favour these lower ratios. Moustafa and Andersson (2008) successfully isolated aromatic hydrocarbons from crude oil, separating 100 mg of crude oil with only 3g of silica and Rowland *et al.*, (2014) successfully applied a 0.5 g

sample to a 2 g column, isolating acids from crude oils. The sorbent masses described by Snyder and Buell (1968) therefore, seem unnecessary and rather impractical. Indeed, this was clear in later publications (Snyder *et al.*, 1968) in which separation of a 50 g sample required over 16 kg of alumina per separation and solvent elutions of 50 L per fraction. Clearly, this would be considered impractical, expensive and wasteful in today's laboratories.

Overall therefore, initial separations herein employed the sample and bed weights described by Sutton and Rowland (2014). Typically, a 1 g crude oil sample was introduced to a 2 g SAX cartridge. The non-retained material was re-introduced to a 2 g alumina cartridge followed by subsequent introduction onto a 2 g SCX cartridge. However, early experiments showed significant carry-over to be occurring during both SAX and alumina separations, resulting in sample sizes being reduced until adequate resolution was achieved. It was then observed however, that whilst a 0.5 g sample could be separated on a 2 g SAX cartridge, subsequent overloading of the 2 g alumina cartridge would occur when the SAX non-adsorbed eluent was re-introduced. Consequently, the initial sample size was further reduced to a ~0.3 g crude oil sample to minimize such issues.

Also of consequence with regard to crude oil recovery, is the vacuum applied in order to elute samples. As explained in Chapter 1, SPE systems utilise either a positive or a negative pressure in order to 'push' or 'draw' samples through the cartridges. Initial experiments herein used a vacuum of 0.6 bar with flow rate controlled by Teflon taps. However, substantial losses of both crude oil volatiles and of lower molecular weight 'model' compounds was observed. To minimize volatile losses, the applied vacuum was reduced to 0.1 bar, after which recovery was significantly improved. However, certain circumstances do require an increased vacuum in order to maintain flow rates. For example, particularly asphaltenic or waxy crude oil were observed to deposit material on

cartridge frits, creating blockages. In these cases, a larger pressure differential must be applied in order to maintain a constant flow rate.

The method of Snyder and Buell (1968) was designed around a solvent strength index developed by Snyder (1968). Relative solvent proportions used in the method were determined by calculation utilising the index of the solvents. However, a number of safety and practical concerns required alteration of the solvent system.

Snyder and Buell (1968) employed cyclohexane to introduce samples and to elute non-ionic material from ion exchange cartridges. However, the use of cyclohexane presents a number of issues that can be resolved by using another solvent system. Primarily, the boiling point of cyclohexane is significantly higher than potential alternatives. As solvents must be removed from each fraction, a solvent with minimal boiling point is desirable in order to minimize sample losses due to evaporation. Also of importance when conducting IEX separations, is the ability to modify the solvent by addition of aqueous acid and base to encourage formation of the appropriate ions in samples. Finally, for the purposes of this study, the solvent had to be capable of solubilising the selection of model compounds employed to evaluate method selectivity. Diethyl ether was ultimately selected to replace cyclohexane. With a boiling point some 46 °C lower than that of cyclohexane (cyclohexane, 80.74 °C; diethyl ether, 34.60 °C (Haynes, 2016)), a significantly higher capacity to solubilise water (cyclohexane, 0.345%; diethyl ether, 1.19-2.66% (Rowley and Reed, 1951; Roddy and Coleman, 1968)) and the ability to solubilise all model compounds, diethyl ether was considered a good replacement.

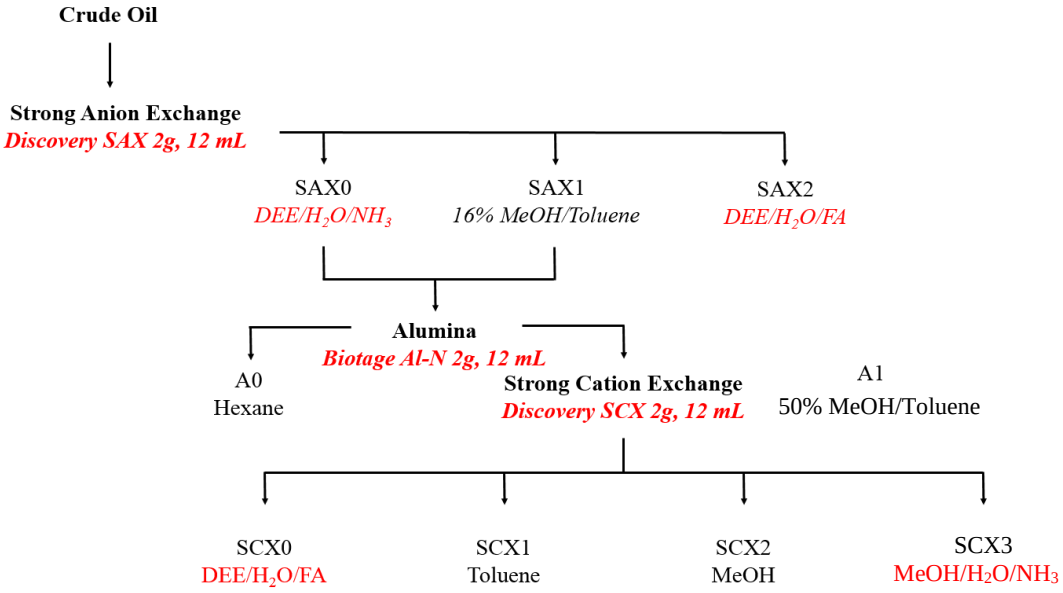

Figure 3-3. Flow diagram for the separation of crude oils following the modified method of Snyder and Buell (1968). Alterations to the original scheme have been highlighted in red. Fraction numbers are related to solid phase extraction phase; e.g. SAX = strong anion exchange, SCX = strong cation exchange; positive integers refer to the order of elution from SPE cartridges. Elution solvents are listed along with the fraction label. DEE; diethyl ether, FA; formic acid, NH_3; ammonia

To address safety concerns, the solvents benzene and pentane were substituted with toluene and hexane respectively. The solvents chosen to replace those previously used presented a negligible difference with regard to the polarity index, when compared with the original solvents (pentane and hexane = 0; benzene = 0.11 and toluene = 0.10), thus, providing an almost identical elution strength. A schematic for the modernised separation is shown in Figure 3-3.

3.4.1 The modified Snyder method: separation of 'model' compounds

Separation of the 19-component mixture of model compounds was conducted in triplicate by the modified method of Snyder and Buell. Analysis of each fraction and subsequent quantification of model compounds by GC-MS allowed the masses and recoveries of each compound to be obtained. Gravimetric data presented below in Figure 3-4 show the mass balances for each individual model compound; be it isolated completely within a single fraction, or split between multiple fractions.

Primary separation by anion exchange chromatography was designed to isolate naphthenic acids from crude oil samples. Given that all compounds eluting into both SAX0 and SAX1 would be subsequently combined and re-introduced to alumina, any acids eluting in SAX1 would be lost to irreversible adsorption. Initial tests identified the presence of the model acids in SAX1 and so for the purpose of this particular study, it was decided not to combine SAX1 and 2 fractions, but to treat them separately.

The 'splitting' of the model acids between SAX1 and 2 was confirmed by the quantification study (Figure 3-4D). Whilst the separation of acids between the two fractions is only minor for the majority of model acids, it is nonetheless undesirable. Early elution of the standards into fraction SAX1 is likely an issue either with the applied eluent volume (i.e. over-elution) or else with solvent strength. The additional functionality possessed by the furan- and thiophene- acids does not appear to have any effect on the activity of the carboxylic acid group; both acids were strongly retained and eluted primarily in the acidic fraction. Also present in fraction SAX2 was nitroindole, implying ionic interactions between the nitro- functional group and the quaternary amine phase.

Polycyclic aromatic hydrocarbon (PAH) distributions, presented in Figure 3-4E show the three, four, and five ringed aromatics are all located in the non-polar fraction (A0). This is in contradiction to the work presented by Snyder and Buell, who observed the presence

of tri- and tetra aromatics within the 'polar' fractions. It is likely that the poor retention of PAHs on alumina is a consequence of over-elution with *n*-hexane. Also eluting in the non-polar (A0) fraction were the furan (Figure 3-4A) and sulfide (Figure 3-4B) standards. Snyder and Buell also observed the elution of dibenzofuran within the non-polar fraction, however, sulfides were observed to separate on later silica separations, indicating their retention and elution in the polar, A1 fraction. Further evidence for the over-elution of the alumina cartridge, is observed in the splitting of the carbazole model compound (Figure 3-4C).

Following separation on alumina, the polar A1 fraction was separated by cation exchange chromatography. The work of Snyder and Buell indicated the complete isolation of pyridinic nitrogen species in the cationic fractions. However, data shown in Figure 3-4C identified poor separation of benzoquinoline, showing 'splitting' between SCX0 and SCX3. Poor recovery of the quinoline standard (Appendix 1) could imply the elution solvent for the cationic fraction was of insufficient strength and that the standard was irreversibly adsorbed to the phase. The sulfoxide standard was also isolated by cation exchange chromatography, eluting in fraction SCX1. This supports the observations of Snyder and Buell who recorded retention of sulfoxides on the cation exchange resin.

The remaining standards eluted in the retained fraction, SCX0. Elution of ketone and phenol standards (Figure 3-1A) in the SCX0 fraction confirms their inclusion in the 'polar' fraction and agrees well with the observations of Snyder and Buell. Also eluting in fraction SCX0 were the thiophene, sulfone (Figure 3-4B) and carbazole (Figure 3-4C) model compounds. It is therefore evident that further fractionation of the SCX0 fraction would be necessary to separate these compound classes into individual fractions.

Recovery was acceptable for the majority of model compounds (Appendix 1). Whilst variation between compounds was considerable, values were reproducible (average RSD

3.6%) for the individual compounds. Common losses associated with SPE procedures are able to explain compound recovery; i.e. adsorption of model compounds to SPE tubes and evaporative losses occurring on solvent removal.

Recoveries of acids were notably higher than for other compound classes. This is likely the result of phthalate contamination originating from the SPE cartridges. Typically, ion exchange separations are conducted under aqueous conditions and as a result glass cartridges are not available for purchase. The polypropylene tubes have limited resistance to the stronger organic solvents and in this instance, elution with diethyl ether and toluene is likely to solubilise phthalates from the plastic. Subsequent concentration and elution of these compounds in the acidic fraction yields a higher mass. This increased mass creates a bias when calculating compound masses within the fractions.

A reproducibly low recovery (Appendix 1) was observed for the sulfide model compound on separation by the procedures used in the scheme. It was thought likely that oxidation of the sulfide standard to the sulfoxide was occurring and resulted in the low recovery. However, no evidence of the predicted oxidation products could be located in any of the fractions. As an additional experiment, benzyl disulfide was solubilised in 0.1% formic acid in diethyl ether and left for 24 hours. The solvent was subsequently removed followed by analysis by GC-MS. Once again, no evidence of oxidation could be observed.

Potential matrix effects of crude oils on the separation of model compounds were investigated by observing the difference in separation when the mixed standard was spiked into the oil. The immense complexity of crude oils is such that solvation effects and molecular interactions are likely to affect the elution of model compounds. These effects are likely to differ with varying significance depending on the nature of the oil being subject to the separation.

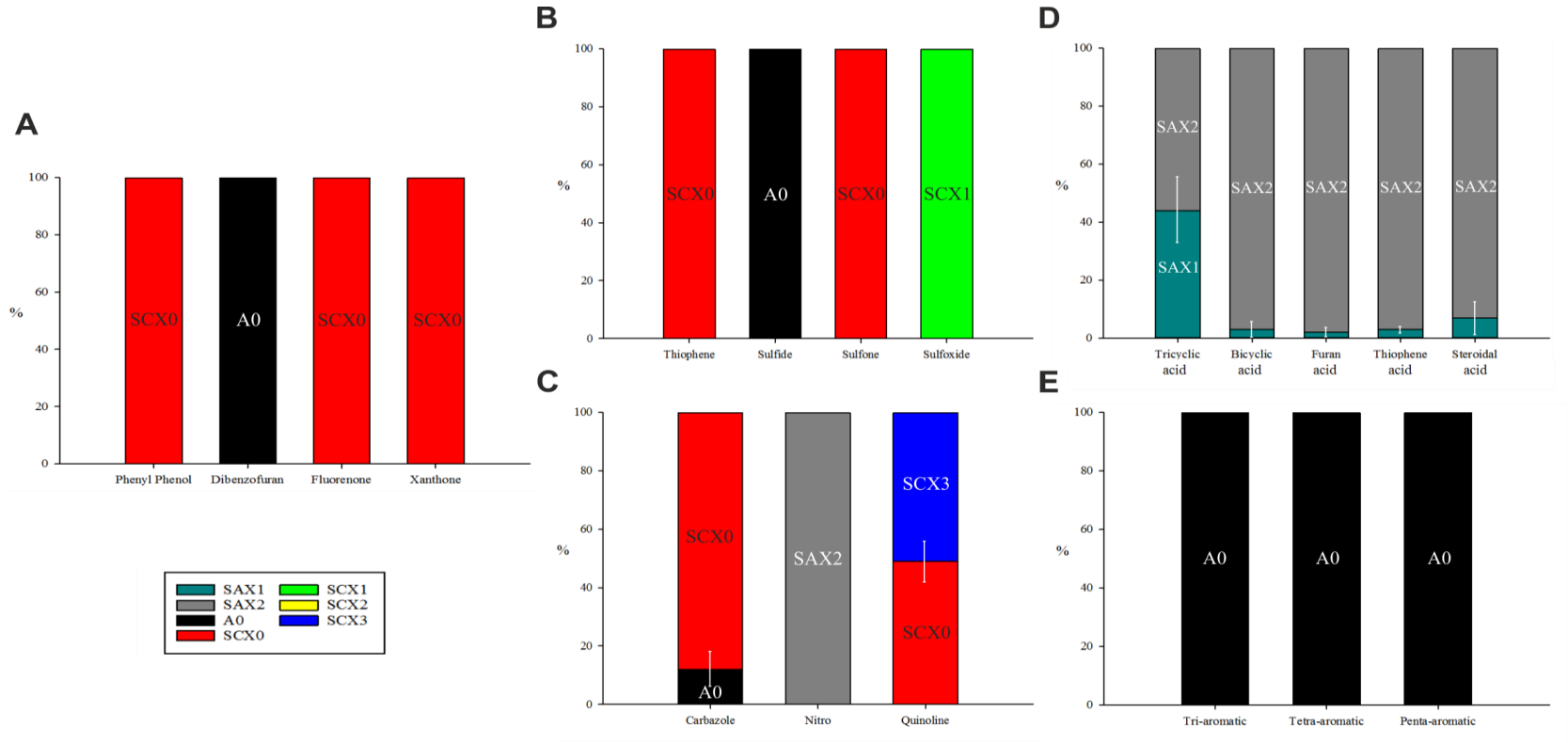

Figure 3-4. Averaged gravimetric data (n = 3; error bars represent separation of compounds between fractions) illustrating those chromatographic fractions which contained each of the model compounds. Compounds are arbitrarily grouped into charts of somewhat similar functionality: oxygen-containing (non-acid) compounds (A), sulphur-containing compounds (B), nitrogen-containing compounds (C), acids (D), and aromatic compounds (E). Single coloured bars indicate that a model compound was recovered in a single fraction.

The model compound mixture was spiked in triplicate into ~0.3g of ANS crude oil at a concentration of 0.2 mg mL^{-1}. The differences in model compound distribution after spiking and separation are presented below in Figure 3-5. No matrix effects were observed for the furan, fluorenone, xanthone, phenol, sulfone and nitro- model compounds, all of which eluted in the same fractions as when they were separated as a mixture without crude oil. Once again, acidic compounds were observed to 'split' between fractions SAX1 and SAX2 (Figure 3-5D). However, the distributions of individual model acids were different to that of the initial separation (Figure 3-4D). Dibenzothiophene no longer eluted within fraction SCX0, eluting in the non-polar fraction (A0; Figure 3-5B), agreeing with the observations of Snyder and Buell. Interestingly, the 4 and 5 ring PAHs showed the opposite behaviour, splitting between the A0 and SCX0 fractions (Figure 3-5E) and demonstrating an increase in retention to the alumina phase. Benzoquinoline also showed an increase in retention, now eluting completely within the basic SCX3 fraction (Figure 3-5C). Dibenzyl sulfoxide no longer eluted solely within fraction SCX 1, but was observed to elute within both fractions SXC1 and SCX2 (Figure 3-5). Differences in separation of the model compounds are likely due to the solvation effects of the crude oil itself and to the modification of the phase on adsorption of crude oil components.

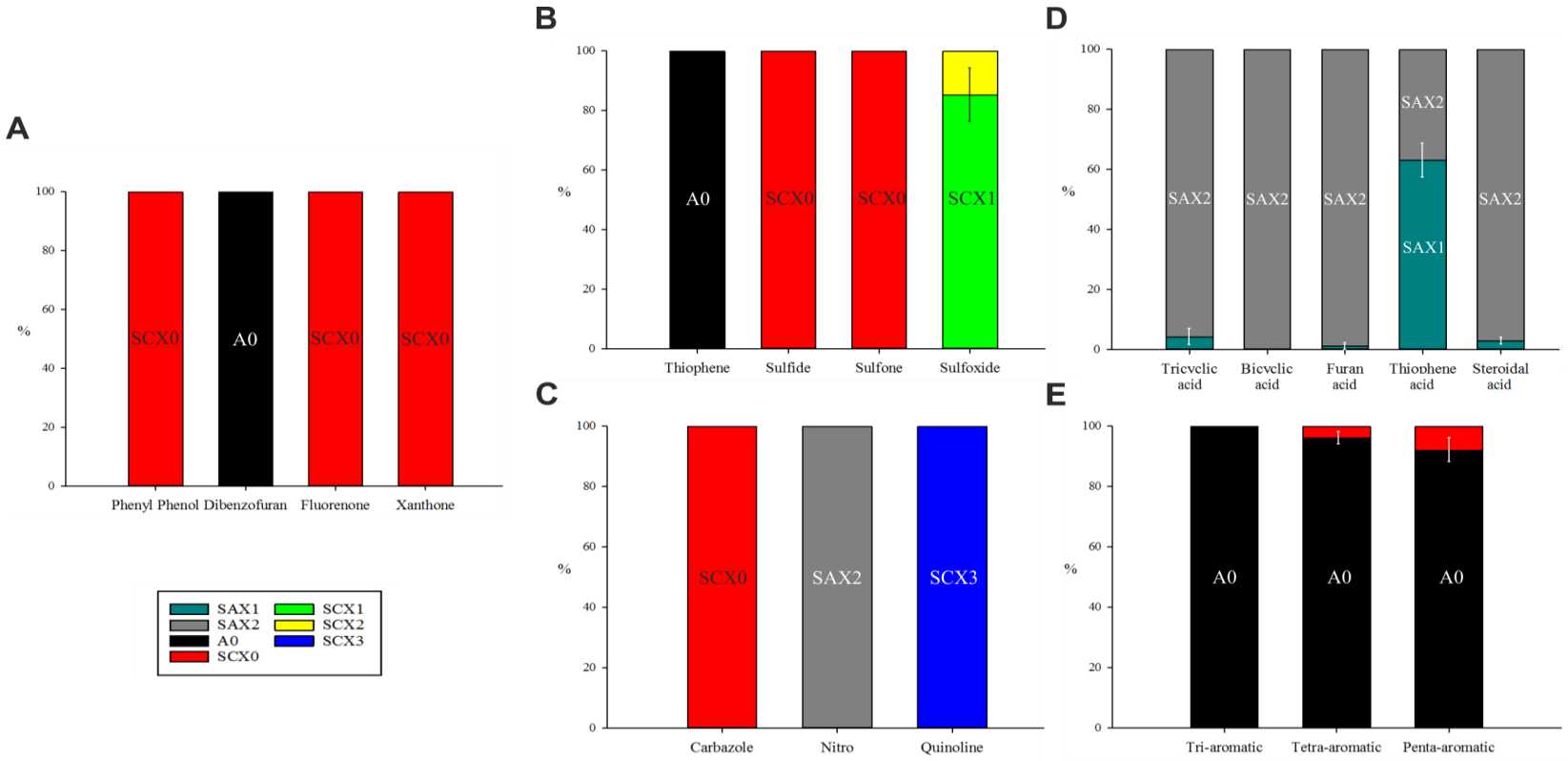

Figure 3-5. Averaged gravimetric data (*n* = 3; error bars represent separation of compounds between fractions) illustrating those chromatographic fractions which contained each of the model compounds when spiked into a crude oil. Compounds are arbitrarily grouped into charts of somewhat similar functionality: oxygen-containing (non-acid) compounds (A), sulphur-containing compounds (B), nitrogen-containing compounds (C), acids (D), and aromatic compounds (E). Single coloured bars indicate that a model compound was recovered in a single fraction.

3.5 The modified Snyder method: separation of crude oil samples

Whilst experimentation with model compounds mixtures can give insights into separation mechanisms and allow prediction of compound class locations, the separation of crude oil samples is necessary for a comprehensive evaluation of the scheme. Thus, two crude oils, an ANS and a Kuwait blend were separated by the modified Snyder method. Triplicate separation of the ANS crude oil was subsequently performed to investigate method reproducibility.

Mass distribution data from the SAX separations (Figure 3-6) showed only minor retention of sample, with 86.7% and 95.0% of the ANS and Kuwait blend samples eluting in the non-retained fraction respectively. Losses occurring during SAX separation varied quite substantially for the two crudes (ANS, 11.5%; Kuwait blend; 3.5%). Loss of volatile components from whole crude oil samples is inevitable when working under reduced pressures and during solvent removal procedures. Therefore, due to volatile losses, the initial stages of the separation are likely to incur the lowest sample recoveries.

Sample eluting in fraction SAX1 comprised only ~1% mass for both crude oil samples. The SAX cartridges remained heavily blackened after elution with 50% methanol/toluene. This suggested the mixture was of insufficient strength and not able to elute the deposited material. Subsequent investigations revealed elution with a stronger, higher polarity solvent (i.e. tetrahydrofuran) could remove the majority of this material. However, gravimetric data showed this material to be a relatively minor component, improving recovery an average of 0.7% from triplicate ANS SAX separations.

Fraction SAX2 comprises the acidic material removed from the crude oil samples. Neither crude used in this study were particularly acidic, having total acid numbers (TAN) of 0.1 and 0.15 (Table 3-1). As such, the low percentage masses observed in these fractions were expected. Certainly, to evaluate fully the efficacy of the acid isolation, a number of high

TAN crudes would need to be separated by the scheme and acid recoveries compared to those of other methods.

As discussed previously, separation of the combined SAX0 and SAX1 fractions on alumina was designed to isolate a 'polar' fraction from the crude oils. Introduction and elution of the combined fraction in *n*-hexane yielded the non-polar fraction. Elution of the retained material in 50% methanol/toluene gave the desired 'polar' fraction, which was then subject to the extensive fractionation scheme.

The distribution of masses between A0 and A1 eluted from the alumina are shown in Figure 3-6. For both the ANS and Kuwait blend, fraction A0 dominated, comprising 69.3% and 66.4% of the total sample mass. Interestingly, the mass of the A0 fractions was somewhat larger than expected when compared the results of the externally performed SARA analysis (IP469; Table 3-2), which for the ANS crude oil showed the saturated hydrocarbon fraction (comparable to the desired A0 non-polar fraction) to be 43.5%; some ~25% less than observed herein for the non-polar fraction. The previously observed presence of the PAH model compounds in fraction A0 suggests the breakthrough of the polyaromatics into fraction A0 to be the cause of the increased mass. The dark orange colour of the A0 fractions further supported this.

Significant losses, (17.1% and 28.2% for the ANS and Kuwait blend respectively), highlighted issues with the method. Heavily blackened SPE cartridges remained after elution with 50% methanol/toluene; indicating that a significant amount of material was still adsorbed to the phase. Irreversible adsorption of the more polar constituents of the crude oil samples, combined with insufficient solvent strength resulted in an inefficient separation.

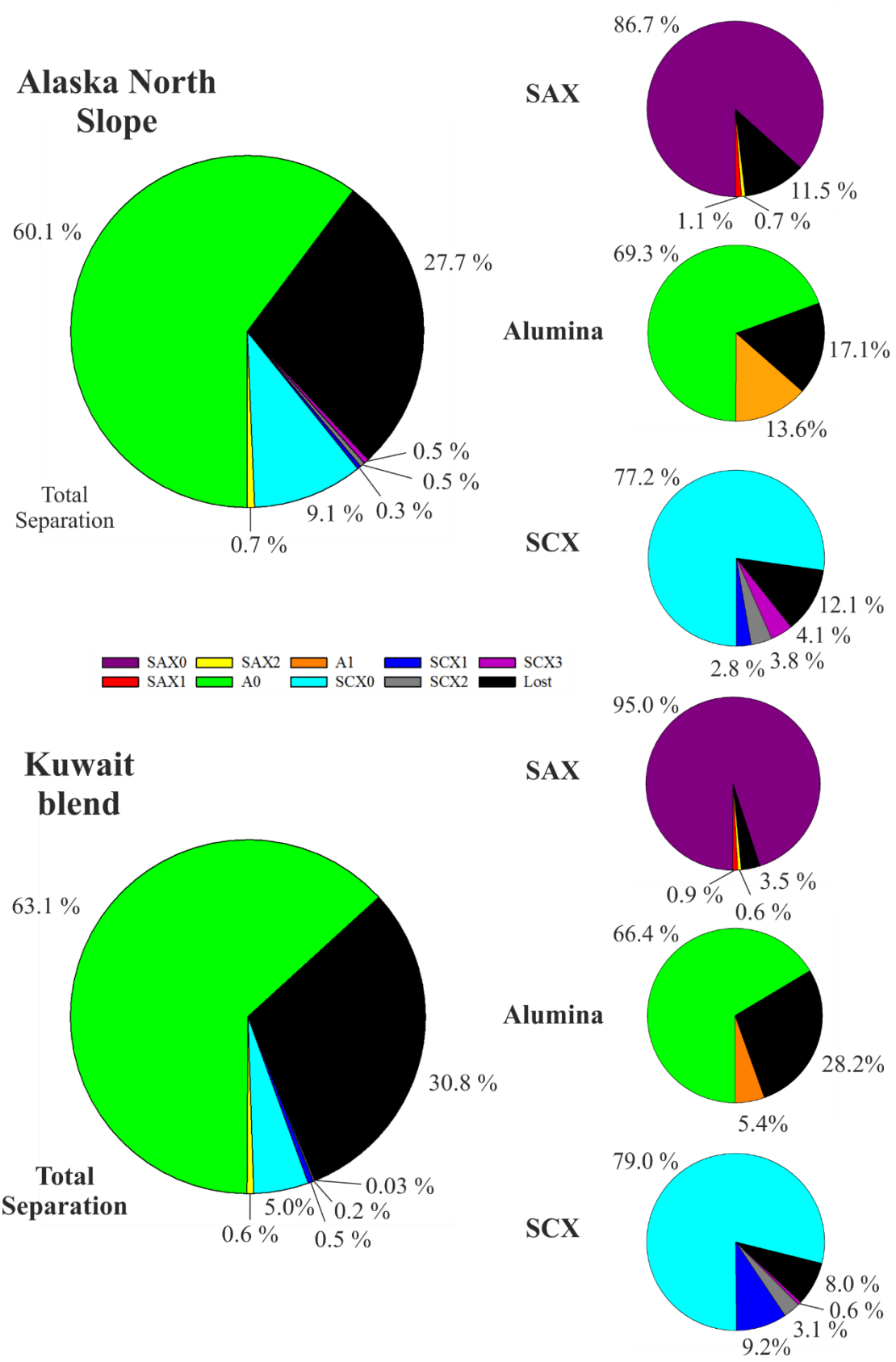

Figure 3-6. Mass distributions between fractions from the separation of ANS and Kuwait blend crude oils. Distributions from each individual columns separation are presented alongside the total distribution.

The mass distribution between fractions from separation by cation exchange chromatography (SCX) was also dominated by those components not adsorbing onto the stationary phase. The efficiency of the SCX was limited, only separating ~10% of the A1 fractions from non-interacting components. Losses were significant; 12.2% of the ANS and 8.0% of the Kuwait blend were lost. Low recoveries from the SCX separation can be largely attributed to the insufficient elution strength of the ammoniated methanol. After the final elution step, significant material appeared to remain adsorbed to the phase, indicated by the dark colour of the cartridges.

The total mass distributions for both the separation of the ANS and Kuwait blend (Figure 3-6) indicate a distinct lack of separation. Despite the application of 3 chromatographic phases and the collection of 9 fractions, approximately 70% of the sample mass eluted within 1 of 2 fractions. Certainly, the non-polar fraction, A0 is the larger of these two fractions, comprising 60.1% and 63.1% of the total sample for the ANS and the Kuwait blend respectively. Fraction SCX0, although significantly smaller than A0, encompassed the bulk of remaining recovered mass for both samples.

Losses for both samples were significant, with recoveries of 72.3% and 69.2% for the ANS and Kuwait blend respectively. Whilst the loss of volatile components is difficult to mitigate, a large percentage of the losses in this instance can be attributed to other deficiencies of the method. Primarily, insufficient solvent strength, combined with the order in which the stationary phases were employed, resulted in substantial losses to the irreversible adsorption of compounds. The poor elution strength of the 50% methanol/toluene, employed herein as the strongest eluent, likely contributed to the considerable losses during separation on alumina. Furthermore, the application of alumina, the most polar of normal phases, prior to cation exchange chromatography is illogical. Polar cationic compounds are likely lost on alumina before they can be isolated by SCX, further reducing recovery. Elution of the cationic fraction in 2% ammoniated

methanol also appeared to be inefficient in removing the cationic material, with substantial material remaining on the cartridge after elution.

Triplicate separation of the ANS crude gave an insight into method reproducibility. Average fraction masses, presented in Figure 3-7, showed again the extent to which the A0 and SCX0 fractions dominated after separation. Standard deviations for each fraction, in the form of error bars, show acceptable reproducibility (<± 10% variation) for the two major fractions. However, the other seven fractions present increased variances, with fractions SCX1 and SCX2 having particularly high errors. These errors suggest the method is unsuitable for use in quantitative studies.

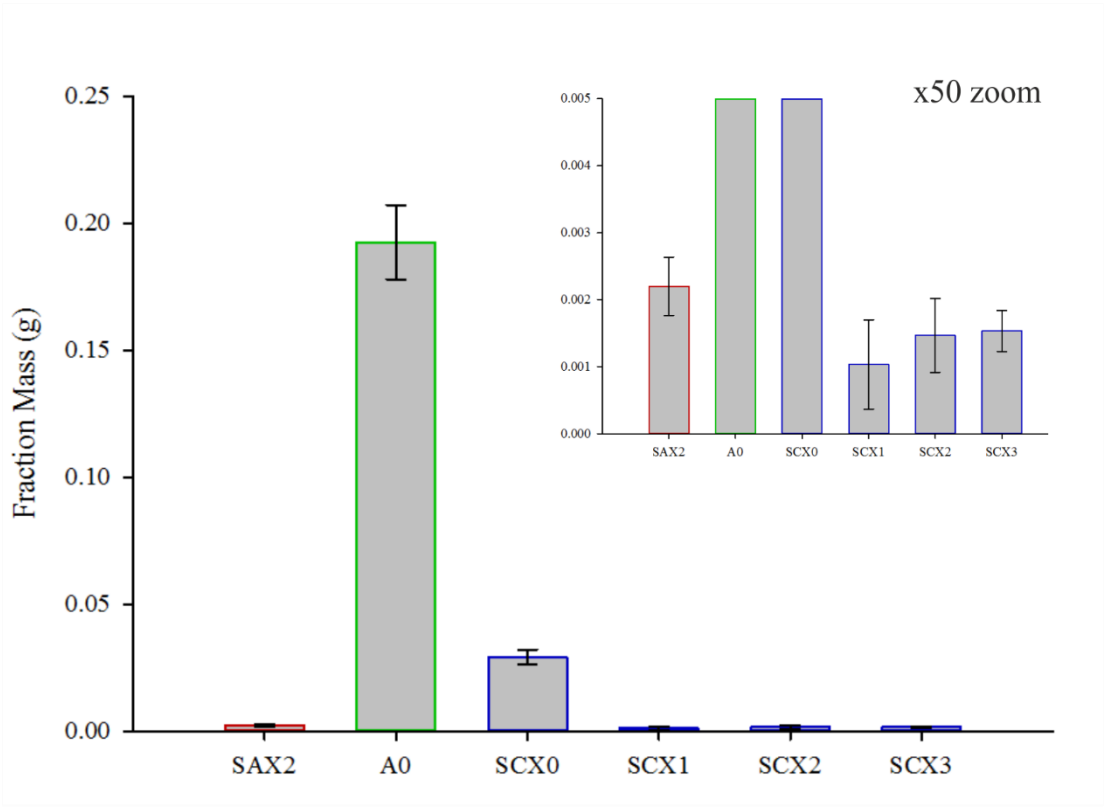

Figure 3-7. Average fraction mass from separations of ANS crude oil with standard deviations and a zoomed insert showing those fractions with lower masses. The border colours of each bar correspond to the mode of separation used (red; SAX, green; alumina, blue; SCX).

All fractions obtained from both the separation of the ANS and Kuwait blend crudes were subjected to analysis by GC-MS. The analysis of each fraction enabled further method evaluations to be conducted. Predictions of class locations, based on data from model compound elutions, were confirmed and effects of alkylation on separation selectivity were investigated. Chromatograms for all 14 fractions are presented in Figure 3-8. Many are largely characterised by the presence of unresolved chromatographic 'humps'. Such fractions were therefore additionally analysed by GC×GC-MS in an attempt to further reduce fraction complexity.

Analysis of SAX2 fractions by GC-MS produced chromatograms characterised by a number of dominant resolved peaks and unresolved complex mixtures (UCMs; Figure 3-9). Examination of the mass spectra of the three major chromatographic peaks (Figure 3-9 i,ii,iii) led to their identification (comparison with library spectra; NIST 2011) as hexadecanoic acid methyl ester (i), octadecanoic acid methyl ester (ii) and diisooctyl phthalate (DOP; iii; Figure 3-9). The C_{16} and C_{18} fatty acids are often observed to be more abundant in crude oils than the other *n*-fatty acids. The implication being the occurrence of microbial activity, potentially through incorrect storage of samples, resulting in microbe contamination (Peters *et al.*, 2005).

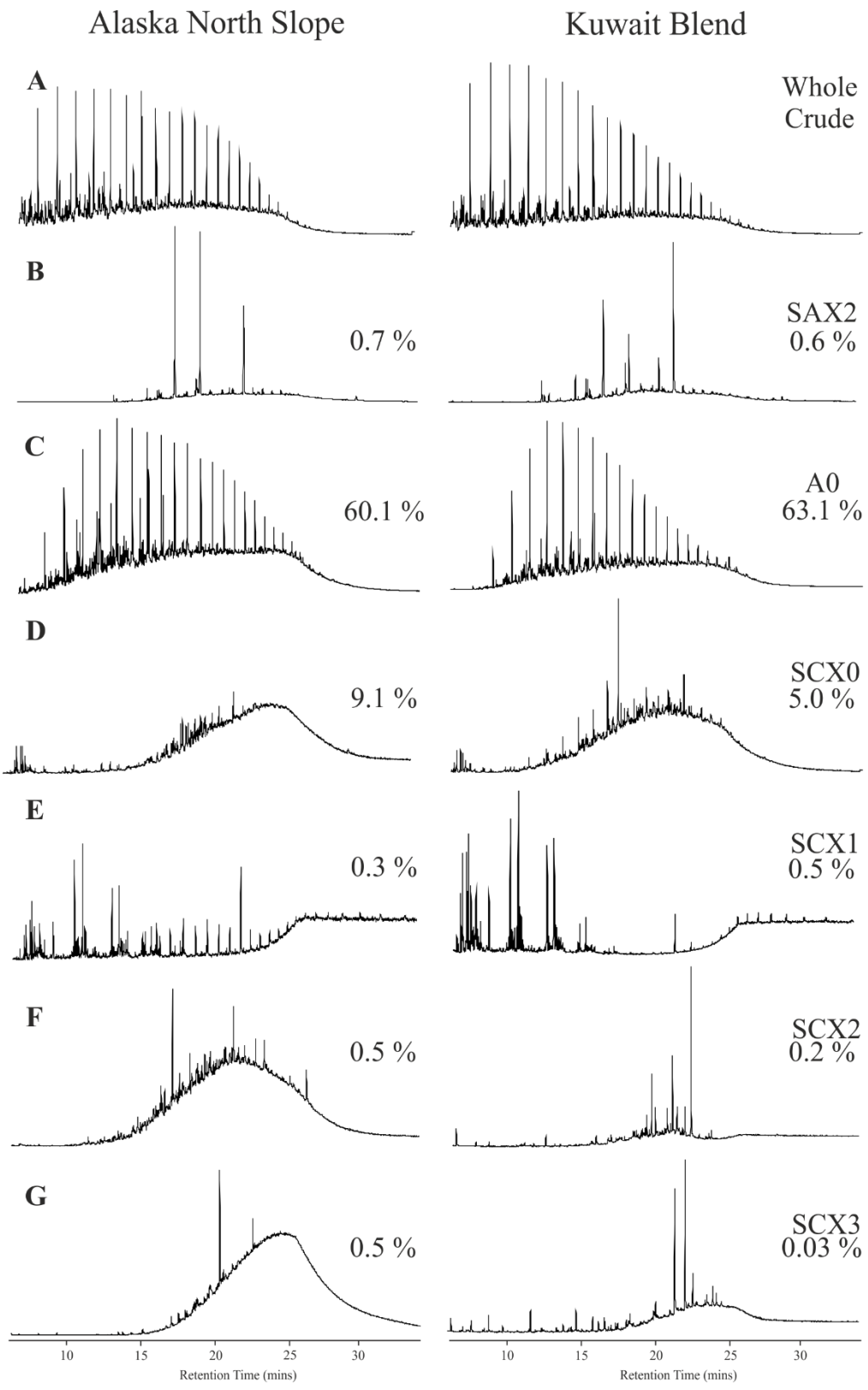

Figure 3-8. GC-MS TIC of ANS and Kuwait blend whole crude oils (A) and fractions obtained from SPE: fraction SAX2 (acids; B), fraction A0 (non-polars; C), fraction SCX0 (neutral polars; D), fraction SCX1 (E), fraction SCX2 (sulfoxides; F) and fraction SCX3 (bases; G). Weight percentages are shown for each fraction.

The presence of DOP within the SAX2, fraction was not unexpected. Phthalate contamination in analytical laborties is widespread, on account of their use as plastisicers (Reid *et al.*, 2007). The DOP was identified by comparison of the mass spectrum with that of the NIST library (RMatch 996). The mass spectrum (Figure 3-9C) shows a base peak at *m/z* 149, typical of phthalte compounds in general and a strong peak at *m/z* 167 which is characteristic of DOP. Strucutres for the two fragment ions are shown in Figure 3-9C. The fragmentation of phthalate compounds is discussed in detail in a number of studies (e.g. Jehuda, 1988; Yin *et al.*, 2014). The particularly high abundance of DOP in SAX2 compared to other fractions in this study, can be attributed to the concentration of the contaminant on the solid phase and subsequent elution within the acidic fraction.

Further investigations into the composition of the SAX2 fractions were not conducted as a part of this study. Recent studies have made substantial progress in the characterisation of petroleum acids and it was not the remit of the current work to conduct such investigations. For example, recent publications by Rowland and co-workers (2011a; 2011b; 2011d) demonstrate the application of GC techniques to identification of individual petroleum acids. More recent methods, such as those developed by Wilde *et al*., (2015) also highlight the complexity of petroleum acids and the additional steps necessary to elucidate petroleum acid structures.

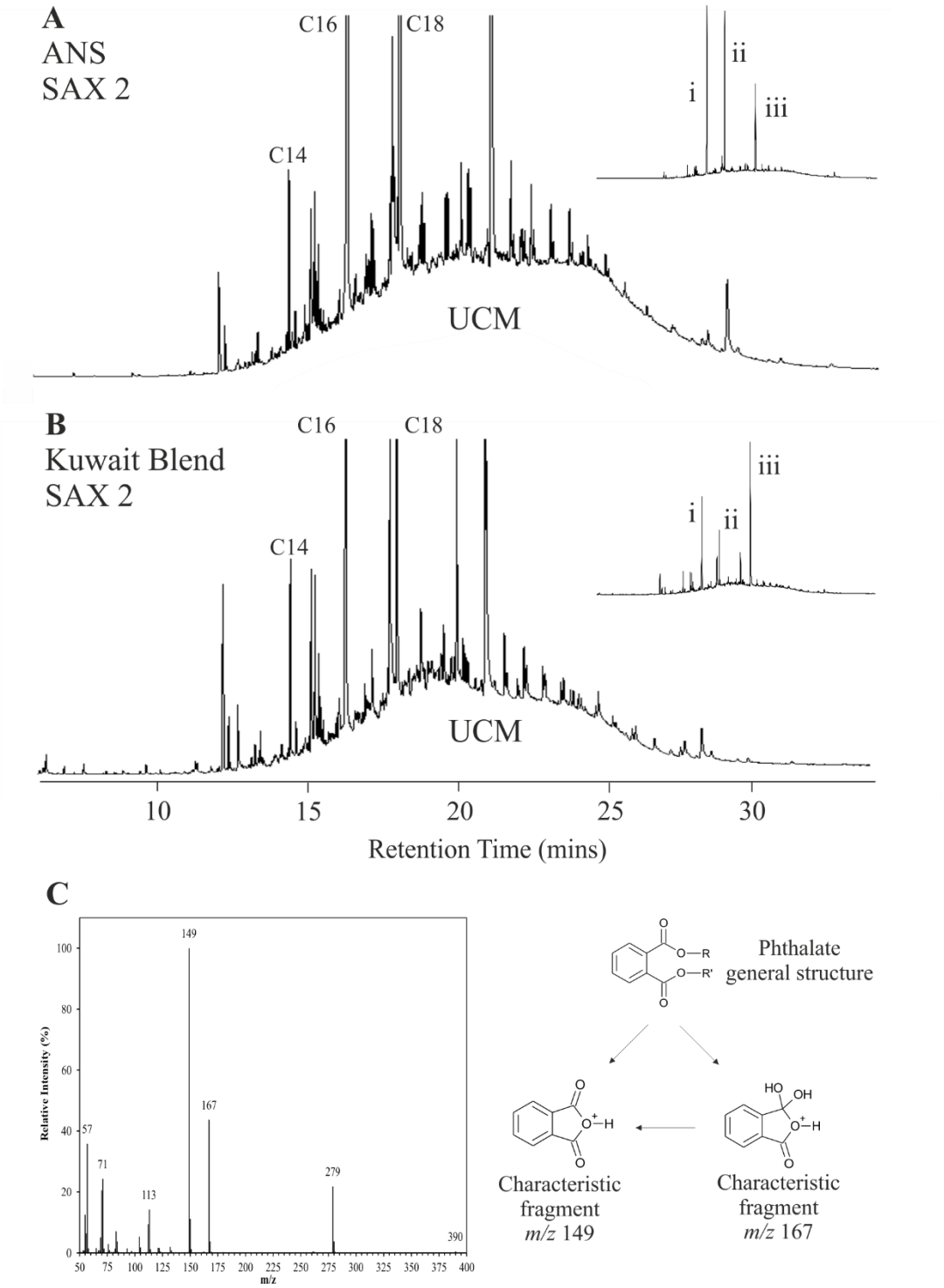

Figure 3-9. Expanded GC-MS TIC of ANS (**A**) and Kuwait blend (**B**) SAX2 (Acids) fractions, showing the presence of complex mixtures unresolved by GC-MS. C_{14}, C_{16} and C_{18} *n*-acids are labelled. Full chromatograms are presented in the top right corner in which the three major peaks have been labelled (i, ii, iii). Mass spectrum of diisooctyl phthalate (**C**) and structures of parent phthalate and the characteristic *m/z* 149 and 167 fragments.

Elution of the 5 model acids, combined with the data presented above, was sufficient to evaluate the efficiency of the method for isolation of acids from crude oil samples. A more comprehensive evaluation of the efficiency of acid extraction should probably be focused on the fractionation of high TAN crudes (>2.0). As presented in Table 3-1, both the ANS and Kuwait blend are low TAN crudes (0.1 and 0.15 respectively) and as such are not suitable for the full evaluation of the acid isolation technique.

Chromatograms from the GC-MS analysis of the A0 fractions displayed similar profiles to those of the whole crude oils (Figure 3-8; A and C). Both chromatograms displayed significant complexity, characterised by UCMs and *n*-alkanes. Losses of the more volatile components were highlighted on comparison of the A0 and whole crude oil chromatograms; losses of C_{10}-C_{14} *n*-alkanes were observed. Determining the efficiency of this separation step is particularly important for the evaluation of the method since inefficient retention of polar compounds at this point would obviously exclude them from the later stages of separation.

GC×GC-MS TIC chromatograms (Figure 3-10) showed the extent to which the larger aromatics and certain NSO compounds (Figure 3-10; iv and v) had eluted within the non-polar, A0 fraction. Predictions of class locations based on the elution of the model compounds fluorene, phenanthrene, dibenzothiophene and dibenzofurans, were all confirmed by their detection in the A0 fractions of both the ANS and Kuwait blend crude oils. Furthermore, the alkylated homologues for the aforementioned compounds (Figure 3-10; iv and v) were also found to elute within fraction A0. Certainly, the $C_{1\text{-}5}$ alkyl phenanthrenes and dibenzothiophenes are visible within the total ion chromatogram (TIC), indicating their high concentrations within the fraction.

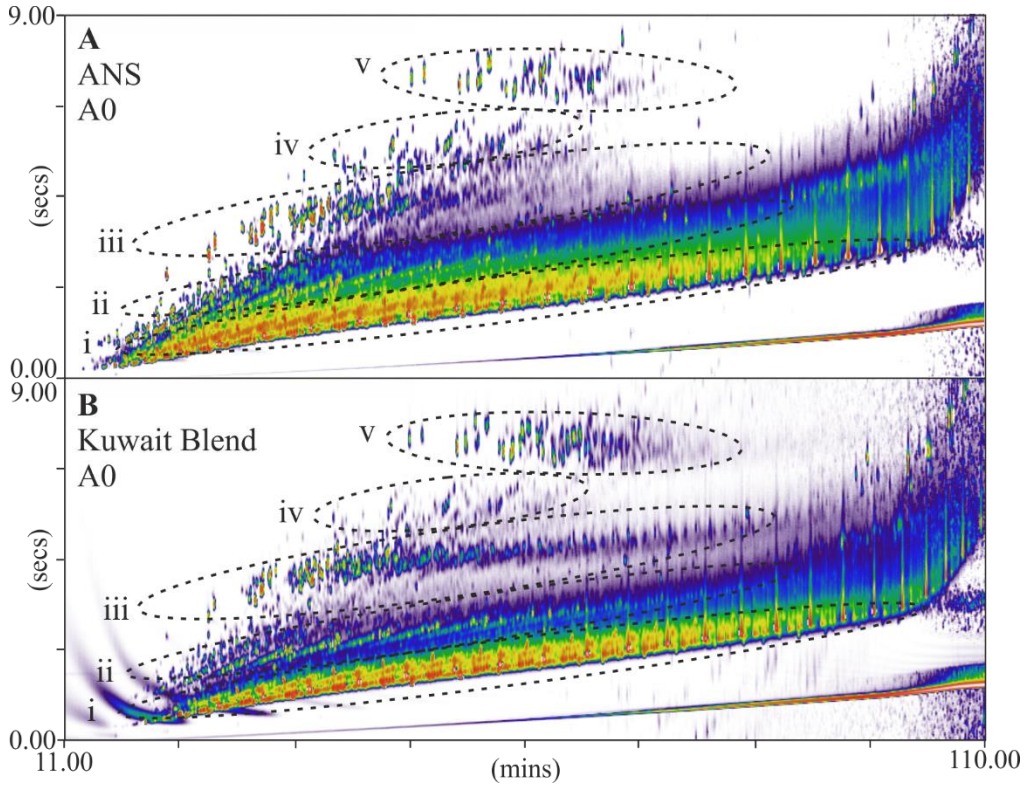

Figure 3-10. GC×GC-MS TICs of the A0 fractions obtained from the SPE separation of the ANS (**A**) and Kuwait blend (**B**) crude oils. Highlighted on each chromatogram are areas in which various compound classes elute: i; saturated hydrocarbons, ii; alkyl benzenes, iii; alkyl naphthalenes, iv; alkyl fluorenes and alky dibenzofurans, and v; alkyl phenanthrenes and alkyl dibenzothiophenes.

The separation of the 'polar' A1 fraction by strong cation exchange chromatography first yielded the non-adsorbed neutral fraction, SCX0. As evidenced by the model compound separations, this fraction comprised the bulk of the non-ionic polar material in the crude oil samples. Fraction complexity was highlighted by the UCMs obtained from analysis by GC-MS (Figure 3-8; D). Further analysis by GC×GC-MS allowed resolution of many UCM components and for fraction composition to be studied in more detail.

Comparison of the two chromatograms shown in Figure 3-11 highlighted the differences in composition. Examination of the ANS SCX0 chromatogram (Figure 3-11A) shows the UCM observed in the one-dimensional analysis (Figure 3-8D) to be largely composed of

two compound groups (i, ii). The SCX0 fraction obtained from the Kuwait blend was significantly more complex (Figure 3-11B); two additional major compound groups (iii, iv) were observed to be present at similar concentrations to that of the two groups also seen in the ANS analysis (i, ii). These observations highlight a substantial issue in the collection and analysis of bulk 'polar' fractions. In this instance, the absence of compound groups iii and iv in the ANS crude can be explained either by the fact they are indeed not present in the sample, or that they are simply below the limits of detection at this particular concentration. For example, it is possible that groups i and ii are significantly more abundant than other fraction components in the ANS sample; thus when both the ANS and Kuwait fractions are analysed at the same concentrations, the ANS analyses resulted in a chromatogram such as the one presented (Figure 3-11A) in which the less abundant groups were not detected. Unfortunately, this cannot always be resolved by simply increasing the concentration since then sample overloading is likely to damage instrumentation. Further SPE separations of fractions SCX0 are therefore necessary in order to allow isolation of the compound groups and separation/ isolation of higher molecular weight material.

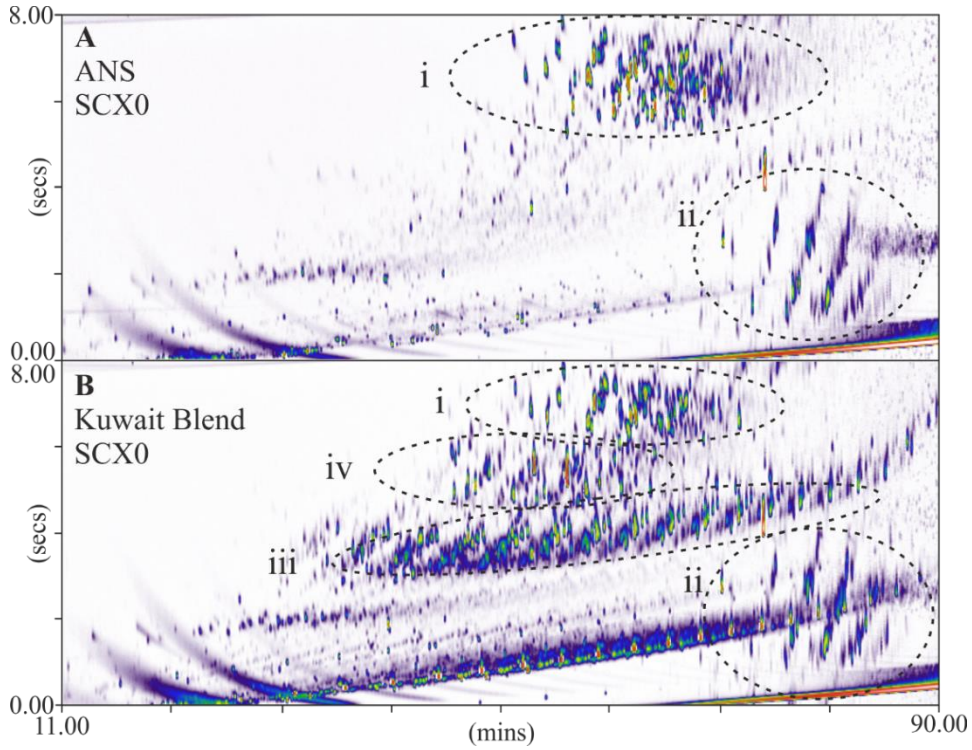

Figure 3-11. GC×GC-MS TICs of the SCX0 fractions obtained from the SPE separation of the ANS (**A**) and Kuwait blend (**B**) crude oils. The main compound groups are highlighted for each analyses; i and ii are observed in both the samples, whereas groups iii and iv are only present in the Kuwait blend.

Interpretation of mass spectra and comparison to spectral libraries allowed identification of compound groups i and ii as alkylated series of carbazoles and benzocarbazoles. Extraction of the appropriate molecular ions for the alkyl carbazoles and benzocarbazoles shows the extent of the two series within the fraction (Figure 3-12). As library spectra for the $C_{4\text{-}5}$ carbazoles were not available, identifications were made on the two-dimensional GC retention times, molecular masses and *ab inito* interpretation of spectra. The isolation of carbazoles within fraction SCX0 was predicted by the elution of the model compound and also agreed well with the observations of Snyder and Buell (1968). Whilst the carbazole appear to dominate in SCX0 fractions of both the ANS and Kuwait blend samples, the presence of other classes represented by model compounds were not as apparent.

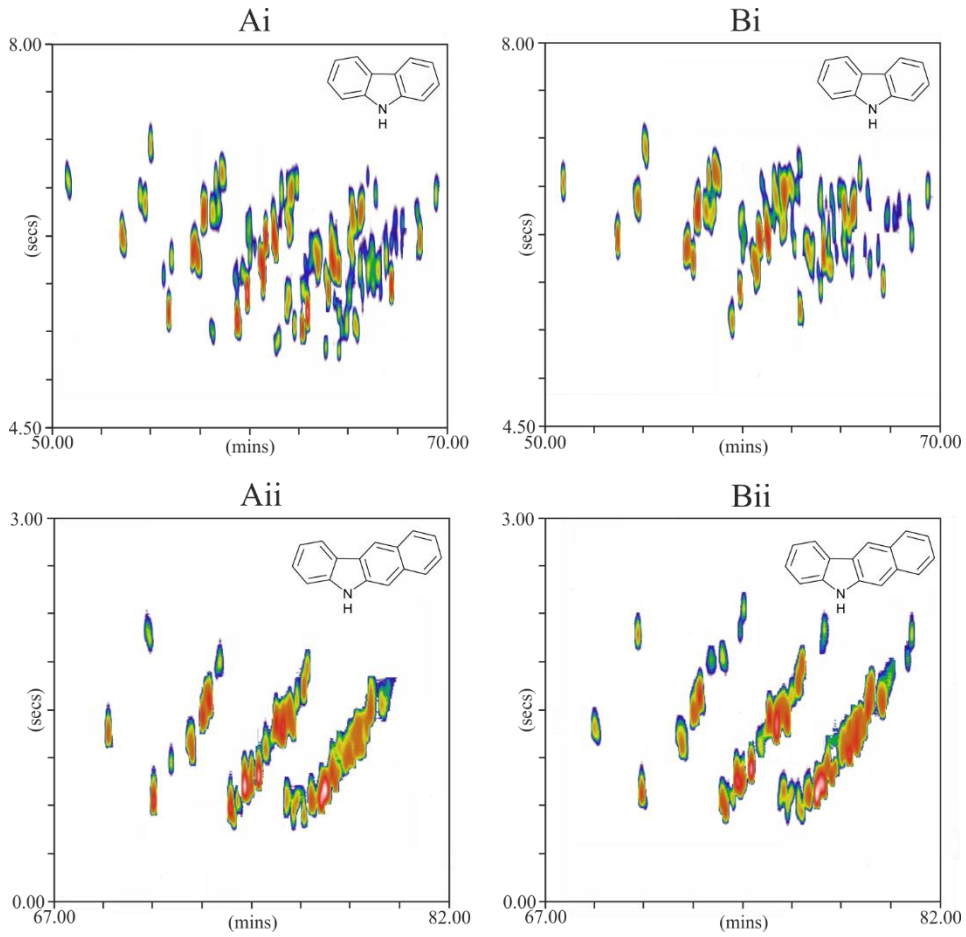

Figure 3-12. GC×GC-MS extracted ion chromatograms (EICs) of carbazole and $C_{1\text{-}5}$ homologues (*m/z* 167,181,195, 209, 223 and 237) and of benzocarbazole and $C_{1\text{-}3}$ homologues (*m/z* 217, 231, 245 and 259) from the analysis of fraction SCX0 from the separation of the ANS crude (Ai and Bi respectively) and the Kuwait blend crude (Aii and Bii respectively).

The composition of groups iii and iv observed in the analysis of the Kuwait blend SCX0 (Figure 3-11B) are largely unknown. None of the selected model compounds eluted within this region of the chromatogram. Library matches for a number of the earlier eluting compounds suggest series of saturated cyclic (iii) and bicyclic (iv) sulphur compounds. However, no library spectra were available for comparison of those with the more abundant later eluting peaks.

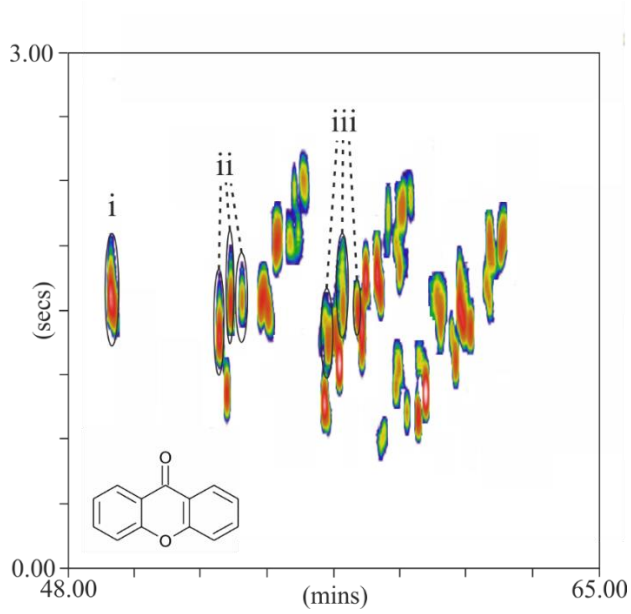

Figure 3-13. GC×GC/ MS EIC of xanthone (*m/*z196; i) and C_{1-2} alkyl homologues (*m/z* 210, 224; ii and iii respectively) from the analysis of fraction SCX0 from the separation of the ANS crude oil. Also visible because of chromatographic co-elution and common mass spectral ions, are the C_{2-4} alkyl carbazoles.

Extraction of the xanthone and alkylxanthone molecular ions led to their identification within the ANS crude only, but also highlighted an additional issue in the analysis of the bulk 'polar' fraction. The co-elution of the xanthone and carbazole alkyl-homologues is shown in Figure 3-13. The effects of this co-elution are worsened by the proximity of the molecular ions for the two groups of compounds, i.e. 209/210 (C_3 carbazole and C_1 xanthone) and 223/224 (C_4 carbazole and C_2 xanthone). As such, obtaining clean mass spectra for the higher xanthone homologues was not possible and the need for additional SPE separation is apparent.

Other compound classes predicted to elute in fraction SCX0, such as the fluorenones and sulfones, could not be identified within either the ANS or Kuwait blend crudes. A number of alkylated phenols were tentatively identified in the ANS SCX0 fraction; however, only at extremely low concentrations. The aggressive conditions (70 °C) previously employed

to remove the elution solvent for fraction A1 likely resulted in the loss of other lower molecular weight ‘polar’ compounds.

The study of fraction SCX1 did not proceed further than analysis by GC-MS (Figure 3-8E). The appearance of fractions SCX1 was very similar to that of the crude oil asphaltenes and it was thought that, because of the high molecular weight and aromaticity that it would not be amenable to GC techniques. Examination of the mass spectra for some of the GC-MS peaks suggested they were due to branched hydrocarbons, likely carried over from previous steps. Despite the elution of the sulfoxide standard within this fraction, no evidence of other members of this compound class could be found in the crude oil fractions.

Unfortunately, the SCX 2 fraction isolated from the Kuwait crude was of insufficient mass to analyse at the desired concentration. The resulting chromatogram (Figure 3-8F) showed peaks due to components which were also present in the procedural blanks. However, GC-MS analysis of the ANS SCX2 fraction yielded a UCM (Figure 3-8F) that was characterised by a series of cyclic sulfoxide compounds, such as those tentatively identified in Athabasca bitumen by Payzant *et al.* (1983). Snyder and Buell observed the elution of a number of compound classes within the second and third cation exchange fractions. These did not occur in crude oil separations conducted herein. No evidence of the presence of the indole, carbazole or benzocarbazole series was found in either SCX1 or SCX2.

Finally, GC-MS analysis of the basic SCX3 fraction also resulted in two UCMs (Figure 3-8G). Further GC×GC-MS analysis of the SCX3 fraction was attempted. However, chromatography was still poor and only a small number of peaks were resolved. The mass spectra of these peaks matched well with those of low carbons number alkyl benzoquinolines. This agrees with elution of the benzoquinoline standard within fractions

SCX3. Clearly, an alternative method of analysis (e.g. LC-HRAM-MS; Chapter 5) is required for better characterisation of such fractions.

3.6 Conclusions

The crude oil fractionation method of Snyder and Buell (1968) was modified and the modified procedures evaluated. Changes made to the original method reduced both the resources and the time required to conduct a single separation and complied with current health & safety regulations. Improved reproducibility was demonstrated by the triplicate separations of 19 model compounds and of an ANS crude oil, highlighting the benefits of substituting SPE cartridges for the traditional hand packed columns. Similarly, replacement anion and cation exchange phases performed well, with acid and basic compounds successfully retained by the respective columns. Changes to the applied solvent system appear to have few effects on the separations. However, the volumes of solvent applied during separation on alumina were likely excessive and resulted in rather poorly defined 'non-polar' (A0) and 'polar' (A1) fractions.

By employing a suite of model compounds representing some of the many NSO containing compounds known to be present in crude oils, compound class locations could be predicted within the scheme and the results compared to those reported by the original authors. In most cases, the results from the model compound separations agreed with those reported by Snyder and Buell (1968). The most notable differences occurred during separations on alumina. The cause of this was the previously mentioned, over elution with *n*-hexane, causing breakthrough of the poly-aromatics into the non-polar fraction. Moreover, isolation of 6 of the 19 investigated compound classes within a single fraction showed that additional separations of the SCX0 fraction would be required to generate more defined fractions. Separations of two crude oils by the method supported this further, with GCxGC-MS analysis of the SCX0 fractions revealing significant co-elution

of compound classes. Crude oil separations also highlighted the lack of separation afforded by the first three steps. Sample mass was largely concentrated in just 2 (A0 and SCX0) of the 9 fractions. Also of concern were the substantial losses occurring on the separation of crude oil samples. Recoveries of 72.3% and 69.2% were found for the ANS and Kuwait blend respectively. It was identified that many of these losses could be reduced if further alterations to the method were made. It was concluded that rather than continuing to apply the method by further separating fraction SCX0 the initial three separation steps could be restructured to yield a far superior separation, as described in the following chapter.

Chapter 4. Development of solid phase extraction (SPE) procedures

Chapter 4 describes the development of a novel solid phase extraction (SPE) procedure for the separation of crude oils into distinct fractions related to compound classes. From the work discussed in Chapter 3, it was concluded the method selected previously (Snyder and Buell, 1968) was not capable of providing the desired level of separation. The novel procedure developed herein addressed the limitations highlighted in the evaluation of the 'Snyder' methodology and resulted in the development of a reproducible, rapid and selective separation method. This method utilizes both ion exchange and adsorption chromatography to generate fractions of 'saturated' hydrocarbons, 'aromatic' hydrocarbons, basic compounds, naphthenic acids and other oxygen containing species, carbazoles, sulfones, and thiophenes from small crude oil samples (~0.5g). In all, using the optimised method, twelve fractions are obtained from a typical crude oil sample. The resultant fractions can then be examined in detail by suitable analytical-scale chromatographic and spectrometric methods. The method development and characterisation data for the resulting fractions has now been published: (Robson *et al.*, 2017).

4.1 Introduction

The inherent molecular complexity of crude petroleum is such that detailed compositional investigations must ideally be preceded by some form of pre-fractionation. A comprehensive literature review (Chapter 1) identified only a few methods capable of isolating fractions from crude oil based on compound class. These methods tended to be logistically demanding in their approach, and were both resource and time intensive. Such procedures often employed numerous separations using adsorption chromatography and, as a result, suffered from significant irreversible adsorption of the ionic and more polar crude oil species. These shortcomings were highlighted previously in Chapter 3, when the class-type separation of Snyder and Buell (1968) was evaluated.

Despite the drawbacks, the generation of broadly class-specific fractions is a significant advantage when conducting studies into crude oil composition. By concentrating individual compound classes into discrete fractions, analytical strategies can be more focused, and structural and molecular characterisation can be more easily achieved. It is likely that the complexity, high costs and poor recoveries associated with previously published methods has made them unattractive for routine use, rather than a reduced need for such fractions to be obtained. Certainly, when interest is focused on instrumental analysis and data collection, it is easy to see why complex pre-fractionation methods are often substituted for more efficient, but less effective, approaches. Indeed, this is reflected in how frequently the SARA methodologies are employed (Kharrat *et al.*, 2007) and how infrequently methods that are more comprehensive are cited and used for crude oil characterisations.

The present investigation aimed to develop a novel procedure for the comprehensive separation of crude oils, which separates oils into fractions based on the functionality of various compound classes in oils. By employing the use of authentic compounds

representative of many compound classes known to be present in crude oils, the scheme could be optimised and compound class location within the scheme could be reliably predicted for crude oil separations. Previous evaluation of the ‘Snyder’ methodology had highlighted several important factors that dramatically reduced sample recovery and separation efficiency and selectivity. In an attempt to address these issues, ideally the new method should provide high recovery, reproducibility and cost effectiveness for compound specific crude oil fractionations.

4.2 Methods

4.2.1 Experimental Detail

The general procedure for the separation of crude oil samples by the SPE procedure developed herein is described in Chapter 2. A comprehensive account of the development of the method is presented in Section 3.3. Separations of both the model compound mixture, the model compounds mixture spiked into a crude oil (Alaska North Slope; ANS) and the separation of the ANS crude oil were carried out in triplicate.

4.2.2 Crude Oil

An Alaska North Slope (ANS) crude oil (provided by British Petroleum) was employed to assist in the development of the following method. This oil was chosen in part because amounts available (~2.5 L) would subsequently allow sub-samples to be distributed to other laboratories for cross validation if necessary. General characteristics of the ANS crude oil have been previously presented in Chapter 3, Section 2.3.

4.2.3 Solvent Properties

Table 4-1. General properties of solvents considered for use in the separation scheme.

Solvent	Relative Polarity[1]	Boiling Point[1] (°C)	Miscible with Water
Hexane	0.009	68.0	No
Toluene	0.099	110.6	No
Diethyl ether	0.117	34.6	Very Slight
THF	0.207	66.0	Yes
DCM	0.309	39.6	No
Acetone	0.355	56.0	Yes
Methanol	0.762	64.7	Yes
Water	1.000	100.0	NA

1. Data obtained from Haynes, W.M. 2016. CRC Press.

4.2.4 Analytical Procedures

The instrumentation used for the quantification of model compounds and the analysis of crude oil fractions is detailed in Chapter 2. GC-MS analyses were performed using an Rxi-1ms (Crossbond 100% dimethyl polysiloxane) fused silica column (30m × 0.25 mmID and 0.25 μm film thickness; Restek Corporation, USA) with the following temperature program: 40 ºC (1 min hold), then heated to 300 ºC at 10 ºC min^{-1}. GC×GC-MS analysis were performed using set up A, in which the oven was programmed from 35 ºC (1 min hold), then to 150 ºC at 5 ºC min^{-1}, then to 350 ºC at 1.7 ºC min^{-1} (10 min hold). The hot jet was programmed to a temperature of 115 ºC (1 min hold), heated to 230 ºC at 5 ºC min^{-1}, then to 400 ºC at 1.8 ºC min^{-1}. The secondary oven was heated from 95 ºC (1 min hold) to 210 ºC at 5 ºC min^{-1}, and finally to 350 ºC at 1.6 ºC min^{-1}. The modulation time was 8 s (sample dependent) with a 350 ms pulse length.

4.3 Development of a SPE procedure for the isolation of 'polar' compound classes from crude oils

A thorough evaluation of the Snyder and Buell (1968) methodology (Chapter 3) identified significant capacity for improvements. Poor separation from the (Snyder and Buell, 1968) procedure, combined with low recovery of crude oil samples in experiments conducted herein, led to the design of a novel fractionation scheme. Whilst the previous implementation of a model compound mixture had allowed prediction of model compound 'locations' within fractions, it had become quickly apparent that this mixture could not be used to represent the behaviour of crude oil samples when fractionated. For example, issues such as solubility and flocculation of the higher molecular weight crude oil components were not exhibited by the model compound mixture during separation. The following procedures were therefore first developed using a whole crude oil. Specifically, the separation was designed to achieve maximum recovery of the ANS crude oil. This was then followed by refinement and evaluation of the method with the model compound mixture and using the model compound mixture spiked into the crude oil.

4.3.1 Development of ion exchange (IEX) separations

The work conducted in Chapter 3 highlighted the importance of the order in which the different modes of separation are applied. Certainly, by applying a polar phase such as alumina prior to ionic separations, a negative impact on the recovery of crude oil samples was observed. Without the prior removal of ionic compounds, they are likely to adsorb irreversibly to silica and alumina-based phases and, as a result, recovery of ionic materials from subsequent separations will likely be reduced. Such issues concerning the irreversible adsorption of crude oil components during adsorption chromatography have been well studied (Reviewed: Lundanes and Greibrokk, 1994). Removal/isolation of

higher polarity/ionic species results in substantially reduced losses and removes the need for de-asphalting steps, thus allowing whole crudes to be separated.

The method of Snyder and Buell (1968) is not alone in employing both normal phase and IEX to provide appropriate crude oil fractions. Separations utilising IEX more commonly follow the framework of Snyder and Buell (1968), applying anion exchange chromatography as the initial point of separation (Jewell *et al.*, 1972; McKay *et al.*, 1976; Boduszynski *et al.*, 1977; Jones *et al.*, 2001). More rarely observed are methods employing cation exchange chromatography as the initial point of separation (Conceição Oliveira *et al.*, 2004; Sutton and Rowland, 2014).

Despite the common implementation of a primary anion exchange step, there are significant benefits to performing the cation exchange separation first. As detailed in (Chapter 3), the cation exchange phase offers a mixed mode separation and, in this instance, π-π interactions can be employed to retain highly aromatic material. Isolation of the large conjugated aromatic, or asphaltenic, material at such an early stage would likely benefit later separations, reducing losses to irreversible adsorption as well as reducing matrix complexity.

Work conducted by Sutton and Rowland (2014) showed there to be no negative impacts on acid recovery when SCX separations were performed prior to SAX. Indeed, in the case of the C_{80} tetra acids, isolation was only possible when SCX had first been performed. To investigate the effects of IEX separation order on the recovery of ionic compounds, an experiment was designed herein, in which the order of SCX and SAX separations were reversed.

The experiment subjected ANS crude oil samples to three scenarios. The first involved the separation of a crude oil by SAX, re-introduction of the unretained fraction to an SCX cartridge and subsequent elution of fractions (Figure 4-1A). The second proceeded the

same as the first. However, much like in the separation of Snyder and Buell (1968) the neutral and deposited fractions eluted from the SAX cartridge were combined prior to introduction to the SCX cartridge (Figure 4-1B). The third involved the direct introduction of a crude oil sample to an SCX cartridge (Figure 4-1C) followed by separation of the neutral fraction on an SAX cartridge.

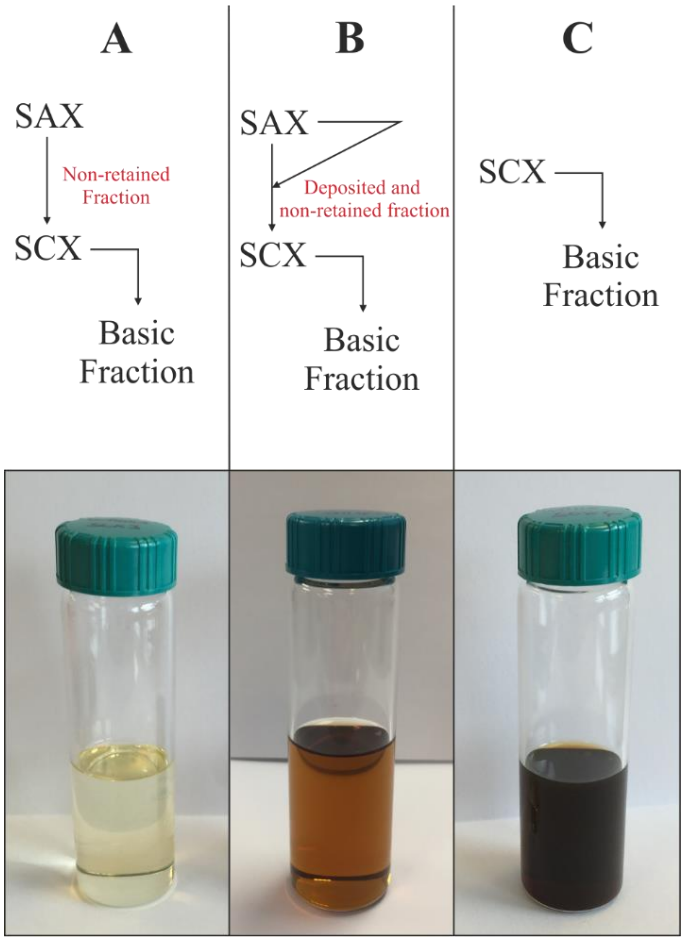

Figure 4-1.Flow diagram showing the SAX/SCX experimental procedures and illustrations of the contrasting colour and appearance of basic fractions from SCX SPE separation of ANS crude when (A) SAX is performed prior to SCX separation with no combination of neutral and deposited fractions, (B) when SAX is performed prior to SCX separation with combination of neutral and deposited fractions and (C) when SCX is performed first.

The results indicated substantial loss of basic material during SAX separations. Recovery of the basic fraction increased 10 times when samples were directly introduced to SCX cartridges. The improved recovery observed when neutral and deposited materials were combined, suggested that basic compounds are concentrated within that material which deposits during sample introduction to the SAX cartridge. No differences in the masses of the acidic fractions were observed in any of the three scenarios, agreeing well with the observations of Sutton and Rowland (2014). Therefore, separation procedures were designed around the following framework: SCX → SAX; in which the unretained fraction obtained from the SCX separation would be further separated by SAX.

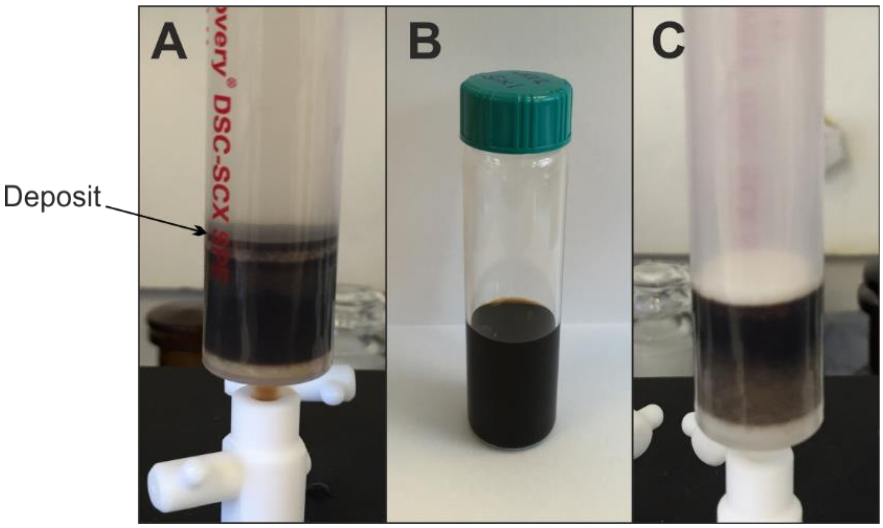

Figure 4-2. (A) Deposited ether insoluble material on cartridge frit, (B) toluene fraction recovered from the SCX SPE cartridge and (C) cartridge after the toluene elution from the separation of ANS crude.

Initial work on the SCX → SAX framework was focused on developing a solvent scheme that would enable maximum recovery of crude oil samples. Similar cartridge loadings to those applied to the modified 'Snyder' method were used (as discussed in Chapter 3). An aliquot (~0.5 g) of the ANS crude oil was introduced on to the SCX cartridge. The solvents employed to dilute and introduce the crude oils were also the same as those used

in the modified 'Snyder' method. Ammonia (NH_3) and formic acid (FA) modified DEE were used for the SCX and SAX cartridges respectively.

On introduction of samples to the SCX cartridge in DEE/H_2O/FA (7 mL/0.1%/0.1%, *v/v/v*), flocculation and subsequent deposition of a black ether-insoluble material on the cartridge frit was observed (

Figure 4-2A). The 20 μm Teflon frit appeared to act as a filter, trapping the precipitated material before it could reach to the phase. A further elution of DEE/H_2O/FA (20 mL/0.1%/0.1%, *v/v/v*) was performed to elute the non-adsorbed/exchanged material. This elution did not appear to resolubilise any of the deposited material, leaving a thin deposited layer on top of the cartridge frit.

The subsequent utilisation of a toluene elution readily solubilised and eluted this deposited material. The jet-black colour (

Figure 4-2B) of the fraction and the observed flocculation in DEE would suggest this material is "asphaltenic" in nature, comprising large conjugated aromatic structures (Adams, 2014). Removal of the toluene from the fraction revealed a black solid, further supporting this supposition.

The tendency of the most polar and heaviest compounds in crude oils to self-associate has been extensively studied (reviewed Mullins, 2010; Svalova *et al.*, 2017). This group of compounds, more commonly referred to as the asphaltenes, are operationally defined by their insolubility in *n*-alkane solvents (*n*-pentane and *n*-heptane) and their solubility in aromatic solvents (benzene and toluene). Solubility theory is commonly employed to predict and model asphaltene precipitation; assuming that if solubility falls below a certain threshhold, precipitation will occur. In this instance, dilution of the whole crude oil sample in DEE/H_2O/FA (7 mL/0.1%/0.1%, *v/v/v*) resulted in the precipitation of a solubility class based on an insolubility in DEE. Therefore, this toluene soluble fraction

is comprised of a mixture of both these DEE insoluble and any material adsorbed to the SCX phase on account of π-π interactions.

Examination of the cartridge after elution with toluene (

Figure 4-2C) indicated that significant material still remained bound to the phase. If we conclude the toluene elution removed all crude oil components bound to the cartridge by π-π interations, the remaining material is likely ionically bound. Therefore, the following elutions were designed to remove the ionically bound material.

The evaluation of the 'Snyder' method (Chapter 3) had identified ammoniated methanol to be a poor choice of solvent for the elution of basic materials, only capable of solubilising a small percentage of the basic material. A suitable replacement solvent was required with the following criterea: a low boiling point (<100 °C) to allow for easy solvent removal, miscible with water to allow a sufficient volume of ammonia to be solubilised, a solvent strength similar to that of toluene (able to solubilise high molecular weight aromatics), non-toxic and universally available.

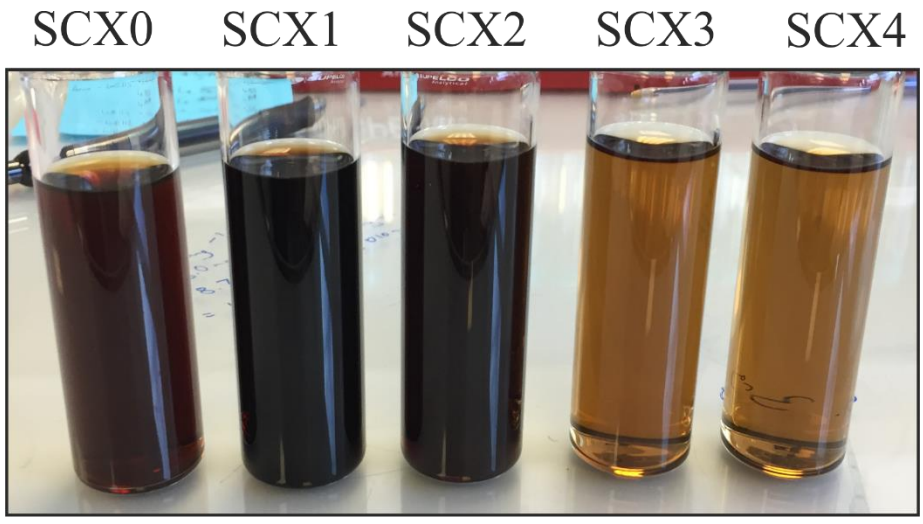

Figure 4-3. Illustration of the five fractions obtained from the separation of the ANS crude oil using SCX chromatography.

Initially, a binary mixture of THF/DCM, such as that employed by Simon *et al.*(2010) was tested. However, the mixture was incapable of solubilising sufficient volumes of ammonia to be effective. Ultimately, THF proved to be the most suitable solvent, having a boiling point of 66 °C, being miscible with water and having the ability to solubilise asphaltenic material (Zhang *et al.*, 2014; Gutierrez Sama *et al.*, 2016).

Prior to elution of basic material in modified THF, an elution of neat THF (20 mL) was performed to ensure that the basic fractions were not contaminated with non-ionic material. Interestingly, the THF removed significant material from the cartridge, leaving a dark brown solid after solvent removal. Basic materials were eluted first using 20 mL of 2% ammoniated THF. However, material still appeared to be retained on the cartridge so an additional elution of 5% ammoniated THF was performed. This final elution appeared to remove all remaining material from the cartridge completing the separation by SCX (final fractions shown in Figure 4-3).

Following separation by SCX, the solvent (DEE/0.1% H_2O/0.1% FA) was removed from the neutral fraction. The dried fraction was then solubilised in DEE/H_2O/NH_3 (7 mL/0.1%/0.1%) and introduced on to an SAX cartridge. Sample introduction was followed by a further elution (20 mL) of the ammoniated DEE to collect the neutral/non-adsorbed fraction. As performed in the SCX separation, collection of neutral material was followed by elutions of toluene (20 mL) and THF (20 mL). These elutions were designed to remove any deposited and adsorbed material from the cartridge. Isolation of acidic material was performed using an acidified THF (2% FA; v/v). The four SAX fractions are shown below in Figure 4-4.

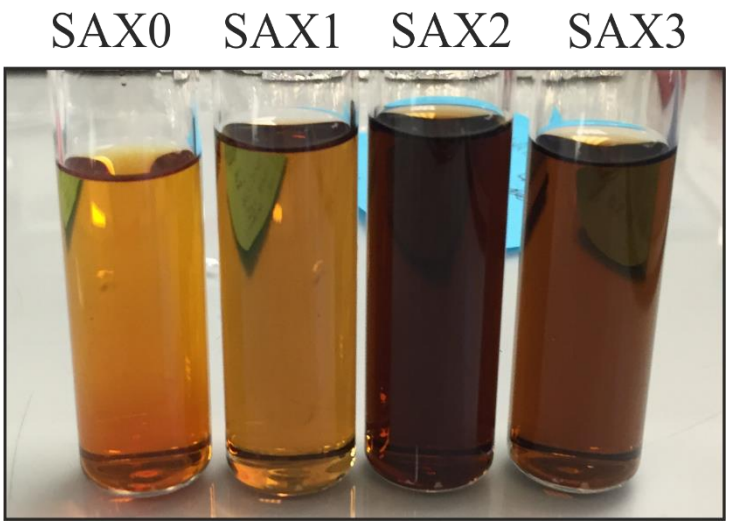

Figure 4-4. Illustration of the four fractions obtained from the separation of the ANS crude oil using SAX chromatography.

The effectiveness of the SCX separation at removing the high molecular weight material is illustrated by the colour of the resultant SAX fractions (Figure 4-4). Fraction SAX1 appears light in colour and no deposition onto the cartridge frit was observed during SAX separations. This suggests that fractions SAX1 and SAX2 are adsorbed to the phase, as opposed to being deposited. Thus, the fractions are likely composed of weakly acidic compounds, as the SAX phase possesses no mixed mode capabilities. The design of the 'Snyder' methodology was such that any fractions interacting with the SAX phase other than strongly bound acids were not utilised. However, it is evident from the colour of fractions SAX1 and SAX2 (Figure 4-4) that significant material could be isolated by employing these weaker interactions.

Initial separation by SCX suffered from higher losses than separation by SAX (Figure 4-5). Losses from the SCX separation can be attributed to the loss of volatile crude oil components, likely occurring during solvent removal under nitrogen (Appendix 2). This was confirmed by quantifying the gravimetric losses, by subjecting a neat sample of ANS crude oil to nitrogen blow down. Overall, recovery from the IEX separations was 84.6% with the majority of losses being attributable to losses of volatiles.

Separation by SCX chromatography resulted in the retention and elution of 10.8% of the mass of the crude oil sample. This was substantially greater than the 1.3% that was isolated from the previously performed 'Snyder' separation procedure (Chapter 3). Interestingly, when the gravimetry of the SCX1 fraction was compared with the equivalent fraction from the 'Snyder' separation (SAX1; Chapter 3) over double the mass was collected. This implies that the SCX1 fraction is indeed comprised of both materials adsorbed to the SCX phase and precipitating and depositing in DEE, as the SAX phase is afforded no mixed mode capability. The percentage mass obtained for the deposited SCX1 fraction (2.7%) is similar to the percentage asphaltene content of the ANS crude oil, determined by IP143 (2.1%).

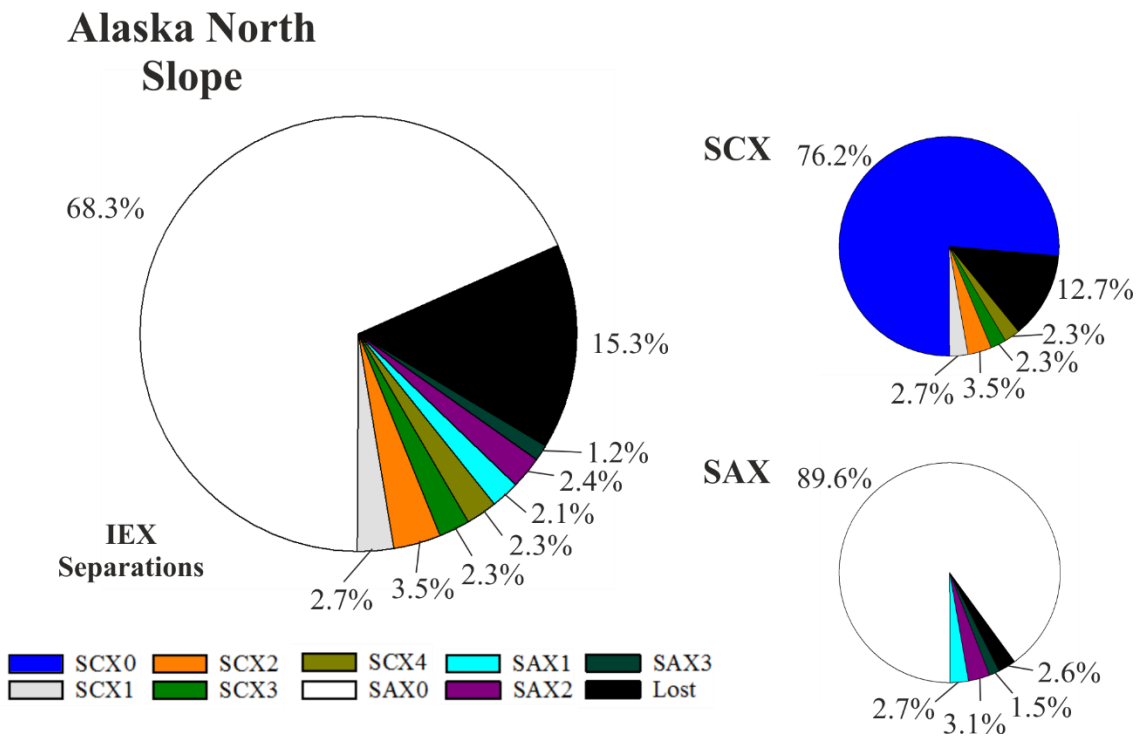

Figure 4-5. Mass distribution between fractions (where fraction SCX0 is re-introduced to the SAX column) from the separation of ANS crude oil. Distributions from each individual columns separation are presented alongside the total distribution.

In performing the SCX separation first, isolation of (ionic exchangeable) cationic material was substantially improved. The procedure performed herein resulted in the isolation of

4.6% of the crude oil sample within the cationic fractions compared to just 0.5% isolated by the 'Snyder' methodology. The large difference in the cationic material isolated by each method is the result of two factors. The first is the irreversible adsorption of cationic material to the phases used in separations prior to the SCX separation using the 'Snyder' method. The second is the insufficient elution strength of the ammoniated methanol employed previously to elute the cationic fraction.

SAX chromatography also appeared to perform more efficiently than in the 'Snyder' framework, allowing the isolation of 7.4% of the crude oil sample. The non-acidic fractions, that is those fractions not eluted in acidified ether, constituted 5.5% of the ANS sample. This highlights the benefit of utilising the SAX cartridge to isolate weakly acidic compounds. The efficiency of the acid isolation was also greater than that observed in the Snyder methodology, isolating 0.5% more material within the acidic fraction. This was likely a consequence of substituting the acidified DEE with the stronger acidified THF to elute the acidic material.

4.3.2 Development of normal phase separations

Fraction SAX0 comprises the neutral/non-ionic crude oil material that was not retained by either SCX or SAX cartridges. Examination of the SAX0 fraction by GC×GC-MS showed the fraction to be dominated by saturated and aromatic hydrocarbons (Figure 4-6). However, it is likely that the SAX0 fraction also contains a certain percentage of non-ionic NSO compounds. As such, further fractionation of this neutral fraction was required to separate the "neutral polar" compounds from bulk hydrocarbon material.

Four phases commonly used in crude oil separations: unbonded silica (SiOH), both cyano ($(CH_2)_3CN$), and aminopropyl ($(CH_2)_3NH_2$) functionalised silica and neutral alumina (Al_2O_3) were evaluated for their ability to separate such neutral fractions. Normal phase separations are typically employed to separate polar compounds from non-polar matrices.

In this instance, the separation was designed to isolate aromatic and NSO containing compounds from the bulk, saturated hydrocarbons. However, as observed with alumina separation performed in the 'Snyder' methodology, higher polarity phases tend to suffer from significant irreversible adsorption when employed to separate whole crude oils. The benefit of performing the normal phase separation after the IEX separations is that the highly polar, ionic material has already been isolated and removed from the crude oil matrix. Therefore, separation should proceed with minimal loss.

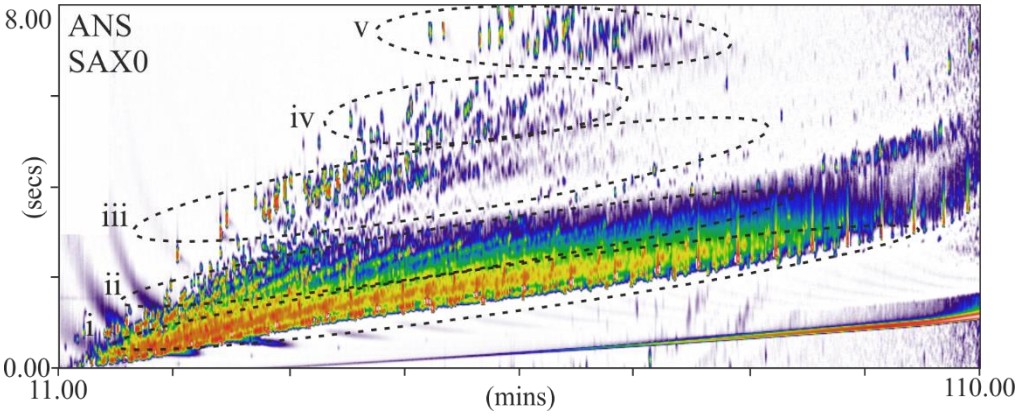

Figure 4-6. GC×GC-MS total ion chromatogram (TIC) of the SAX0 fraction obtained from the SPE separation of the ANS crude oil. Highlighted on the chromatogram are areas in which various compound classes elute: i; saturated hydrocarbons, ii; alkyl benzenes, iii; alkyl naphthalenes, iv; alkyl fluorenes and alky dibenzofurans, and v; alkyl phenanthrenes and alkyl dibenzothiophenes.

Unbonded silica (Figure 4-7A) is perhaps the most frequently used solid phase in crude oil separations (for example: Sutton and Rowland, 2014; Bissada *et al.*, 2016a; Bissada *et al.*, 2016b; Vargas *et al.*, 2017; Zhang *et al.*, 2017). Most commonly applied to obtain saturated and aromatic fractions, the high polarity of the silica phase makes it an attractive choice for crude oil separations. Polar analytes are strongly retained to unbonded silica due to hydrogen bonding interactions from hydroxyl groups. In this instance, separation on silica was tested on a silica SPE cartridge (Isolute® SI, 1 g, 6 mL, Biotage®, Hengoed,

U.K.), with an average particle size of 50 μm, pore diameter of 60 Å and a moisture content of 7% (±1%).

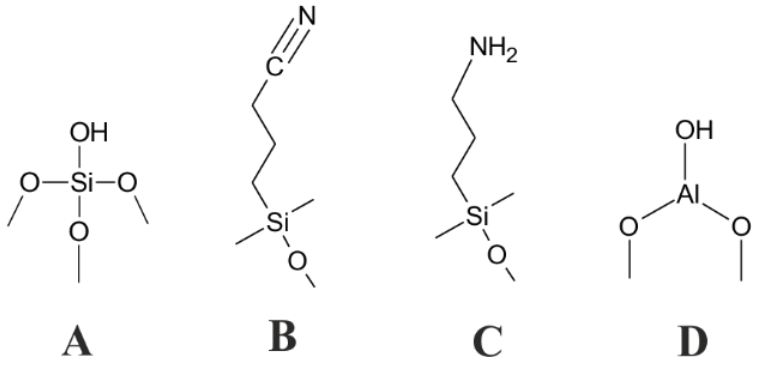

Figure 4-7. Structures for the normal phases evaluated from the separation of SAX0; silica (**A**), cyano (**B**), amino-propyl (**C**) and alumina (**D**).

Cyano bonded silica (Figure 4-7B) retains polar compounds due to strong dipole interactions generated by the C≡N functionality. Cyano functionalised silica separations are not as common as those employing unbonded silica, but have been employed to generate aromatic hydrocarbon fractions and other, more polar, fractions (Borgund *et al.*, 2007; Bissada *et al.*, 2016a; Bissada *et al.*, 2016b). The cyano functional group affords a lower polarity separation than unbonded silica, reducing losses to irreversible adsorption. Separation was conducted on a CN SPE cartridge (Isolute® CN, 1 g, 6 mL, Biotage®, Hengoed, U.K.) with an average particle size of 50 μm and a pore diameter of 60 Å.

The aminopropyl bonded silica (Figure 4-7C) is primarily used for the extraction of strongly acidic compounds using weak anion exchange retention mechanisms. However, aminopropyl separations can also be used for the extraction of polar compounds from non-polar matrices utilising the hydrogen bonding mechanism generated by the primary amine functional group. The aminopropyl bonded silica phase has been employed in crude oil separations for both acid extraction and for the retention of polar compounds (Kaminski *et al.*, 2004; Sutton and Rowland, 2014; Clingenpeel *et al.*, 2017). In this instance, separation was conducted on an aminopropyl SPE cartridge (Isolute® NH2, 1

g, 6 mL, Biotage®, Hengoed, U.K.) with an average particle size of 50 μm, pore diameter of 60 Å and an exchange capacity of 0.6 meq g^{-1}.

Alumina is commonly used in crude oil separations for similar applications to those utilising unbonded silica. The neutral surface allows the interaction of heteroatom containing compounds (e.g. N, O, S and P) and compounds with highly aromatic structures with the aluminium metal centre. Alumina has been used extensively in crude oil separations to isolate fractions of aromatic and polar compounds (Snyder and Buell, 1968; Strausz *et al.*, 2011; Machado *et al.*, 2013; Giraldo-Davila *et al.*, 2016). In this instance separation was conducted on an AL-N SPE cartridge (Isolute Al-N; 1 g, 6 mL; Biotage®, Hengoed, U.K.) with an average particle size of 50-200 μm, pore diameter of 120 Å and a nominal moisture content of <0.1%.

The same solvent scheme was applied in each of the four trials. A stepped gradient of a non-polar to polar solvent was used to elute compounds from the normal phases. As discussed previously (Chapter 3), the normal phase separation can be described as the separation of a polarity continuum. By applying solvent mixtures of increasing polarity, the SAX0 fraction can be separated into further fractions of increasing polarity. Examples of this approach can be seen regularly within the literature, applying elution gradients of *n*-hexane to dichloromethane (DCM) (Grizzle and Sablotny, 1986; Wang *et al.*, 2007; Arboleda *et al.*, 2015) and *n*-hexane to toluene (Li *et al.*, 1992b; Islas-Flores *et al.*, 2005; Sutton and Rowland, 2014). An *n*-hexane-DCM gradient was used to elute fractions in order to reduce the temperatures required for solvent removal from the resultant fractions.

Following conditioning in hexane (10 mL) and DCM (10 ml), four ~100 mg sub-samples of fraction SAX0 were diluted in 100 μL of *n*-hexane and introduced to the normal phase cartridges. An initial elution of *n*-hexane (10 mL) was conducted to elute the non-adsorbing components (fraction 0). Subsequent elutions with 20/80% DCM/*n*-hexane

(fraction 1), 50/50% DCM/*n*-hexane (fraction 2) and 100% DCM (fraction 3) were performed to elute fractions of increasing polarity. The primary elution in *n*-hexane was designed to remove the non-adsorbing saturated hydrocarbons and was followed by an elution of 20/80% DCM/*n*-hexane to remove aromatic hydrocarbons (PAHs). Subsequent elutions were designed to remove the higher polarity, NSO-containing hydrocarbons. During the first trial separations on unbonded silica, the DCM elution appeared to be of insufficient strength to remove all adsorbed material. A THF elution was added to remove this retained material (fraction 4); increasing recovery.

Results from the trial normal phase separations are presented in Table 4-2. Recoveries from all four separations were greater than 90%. Losses to irreversible adsorption were low. The two lower polarity phases, the cyano and aminopropyl bonded silica, presented the highest percentages of non-retained material (fractions CN0 and NH0; 88.3% and 85% respectively). These higher percentage masses suggest the inefficient retention of the lower polarity components, likely resulting in contamination of the saturated hydrocarbon fraction with aromatic compounds.

Table 4-2. Percentage distribution of fraction SAX0 subfractions when separated by silica, cyano, amino-propyl and alumina normal phases. S = silica, CN= cyano, NH= aminopropyl, A=alumina; suffix 0 refers to non-retained fractions and positive integers to the order of elution from SPE cartridges.

Silica		Cyano		Aminopropyl		Alumina	
Fraction	%	Fraction	%	Fraction	%	Fraction	%
S0	80.5	CN0	88.3	NH0	85.0	A0	79.6
S1	12.2	CN1	5.4	NH1	6.1	A1	8.4
S2	0.7	CN2	0.2	NH2	0.2	A2	4.0
S3	0.1	CN3	0.0	NH3	0.5	A3	0.7
S4	1.6	CN4	0.7	NH4	0.1	A4	0.3
Recovery	96.4	Recovery	94.6	Recovery	91.9	Recovery	93.0

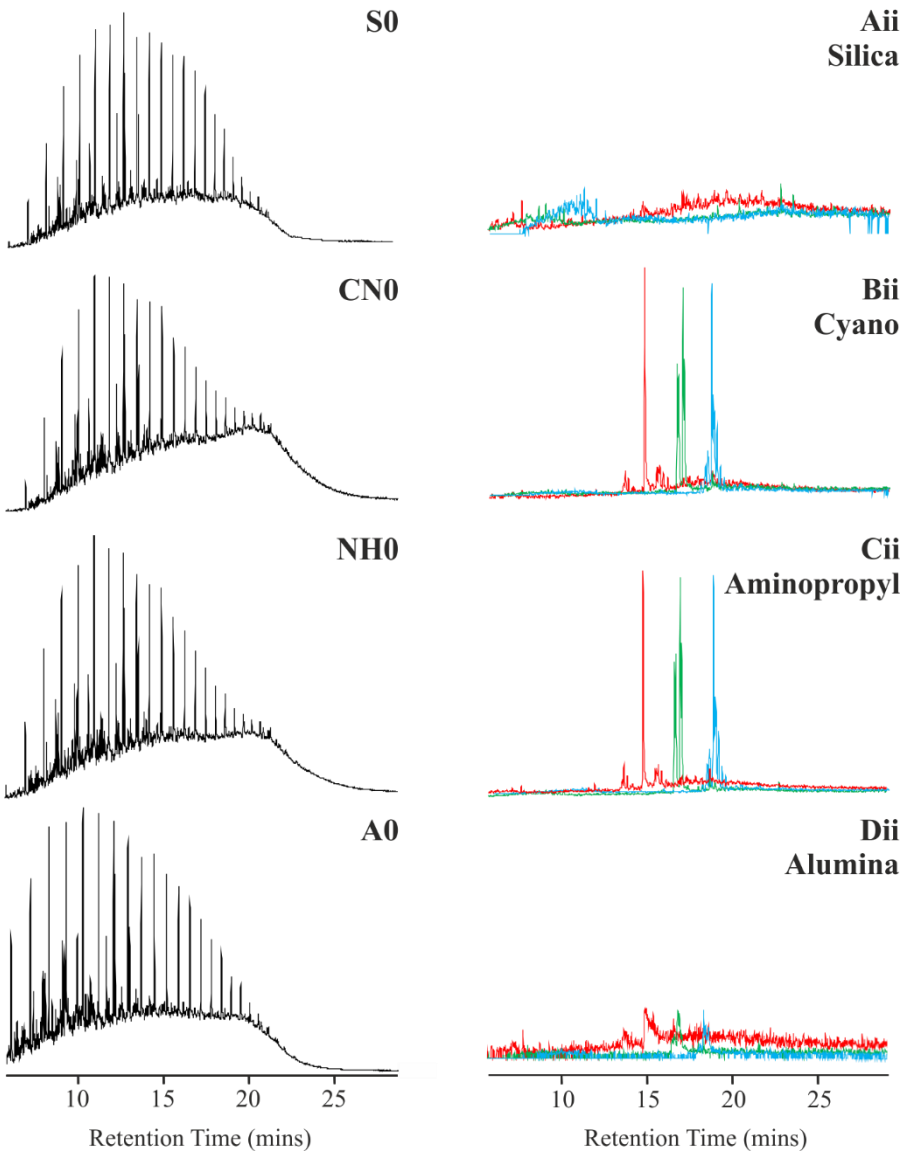

Figure 4-8. GC-MS TICs of the *n*-hexane SPE fractions analysed at equal concentrations (1 mgmL^{-1}) from the normal phase trial separations (left): unbonded silica (fraction S0), cyano bonded silica (fraction CN0), aminopropyl bonded silica (fraction NH0) and alumina (fraction A0) and extracted ion chromatograms (EICs; right) for phenanthrene (*m/z* 178; red) and C_1 (*m/z* 192; green) and C_2 (*m/z* 206; blue) alkyl phenanthrenes.

The compositions of the *n*-hexane fractions were examined by GC-MS to assess the degree of polycyclic aromatic hydrocarbon (PAH) contamination in the saturated hydrocarbons fractions. Phenanthrene and the $C_{1\text{-}2}$ alkyl phenanthrenes were used as a

marker for the presence of PAHs within the non-retained fractions, their presence suggesting poor retention of crude oil aromatics. High concentrations of phenanthrenes were observed in the CN0 and NH0 fractions (Figure 4-8Bii and Cii) confirming the poor separation between saturates and aromatics. Analysis of the fractions of the more polar unbonded silica and alumina trials was more encouraging. Phenanthrene and its alkyl homologues were absent in the GC-MS chromatograms of the silica *n*-hexane fractions (Figure 4-8Aii) and only very low concentrations were seen within the equivalent alumina fraction (Figure 4-8Dii). The lowest recovery (Table 4-2) was obtained using the alumina phase. After sequential elution of the unbonded silica and alumina cartridges with the *n*-hexane/DCM gradient, a black band of material was still adsorbed to both cartridges. A THF elution successfully removed this material from the silica cartridge however, did not remove all visible material from the alumina phase.

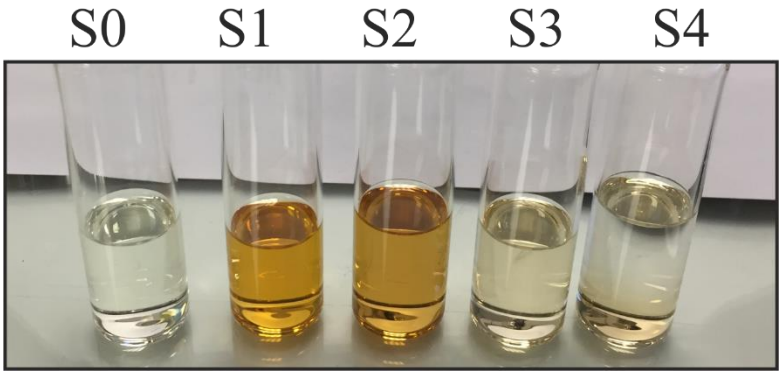

Figure 4-9. Illustration of the five fractions obtained from the separation of the fractions SAX0 by Silica chromatography following SCX/SAX separation.

Overall, the unbonded silica appeared to be the most suitable normal phase for the separation of the SAX0 fraction. The silica provided the highest recovery of the four tested phases, and allowed the elution of material, which could not be recovered during the equivalent alumina separation. Analysis of fractions S0 and S1 by GC-MS showed good separation of saturated from aromatic hydrocarbons (Figure 4-8). The five silica fractions (Figure 4-9) appeared varied in composition. The bulk of the mass (80.5%) was

concentrated within the colourless, saturated hydrocarbon fraction (S0). The colour of fractions S1 and S2 suggest aromatic character with S2 likely consisting of the larger aromatics and/or heteroatom containing structures.

4.3.3 The final SPE procedure

Combination of the ion exchange and normal phase procedures yielded a three-step method for the separation of crude oils (Figure 4-10). The procedure resulted in the collection of 12 fractions. The first four fractions consisted of those materials that adsorbed/exchanged to the SCX cartridge and included both ionic fractions and fractions resulting from hydrophobic interactions. The non-retained fraction from the SCX separation was subsequently introduced to a SAX cartridge. The second series of fractions, obtained from the SAX cartridge, consisted of weak to strong acids based on elution in a solvent series of increasing polarity. Finally, the non-ionic fraction, i.e. the neutral fraction from the SAX cartridge, were separated on an unbonded silica cartridge. The final five fractions were obtained from a solvent gradient of increasing polarity, separating the more polar components from the bulk saturated hydrocarbons.

Table 4-3. Total and individual cartridge recoveries (weight%) of the ANS crude oil when separated by the developed procedure and by the 'Snyder' method and average losses of the ANS crude oil when subject to N_2 blowdown.

Mode of Separation		Percentage Recovery	
		Developed Procedure	Snyder Methodology
IEX	SCX	87.0	87.9
	SAX	97.4	88.5
Normal Phase		96.4	82.9
Total		82.7	72.3
Blowdown loss		19.8	

Total recovery from the ANS separation was 82.7%, some 10% higher than the recovery obtained from the 'Snyder' separation procedure (Table 4-3; Chapter 3). Interestingly, the method devised herein exhibited the expected initial loss of volatile crude oil components when undergoing separation by SCX. This was not observed in the 'Snyder' method, where separation steps suffered consistently low recoveries. Indeed, the volatile losses occurring on the blowdown of the neat ANS crude oils were almost equivalent to those sample losses occurring during the devised separation procedure (Table 4-3). The almost negligible losses from the subsequent SAX and normal phase separations highlight the significant improvements afforded to the framework using the new method.

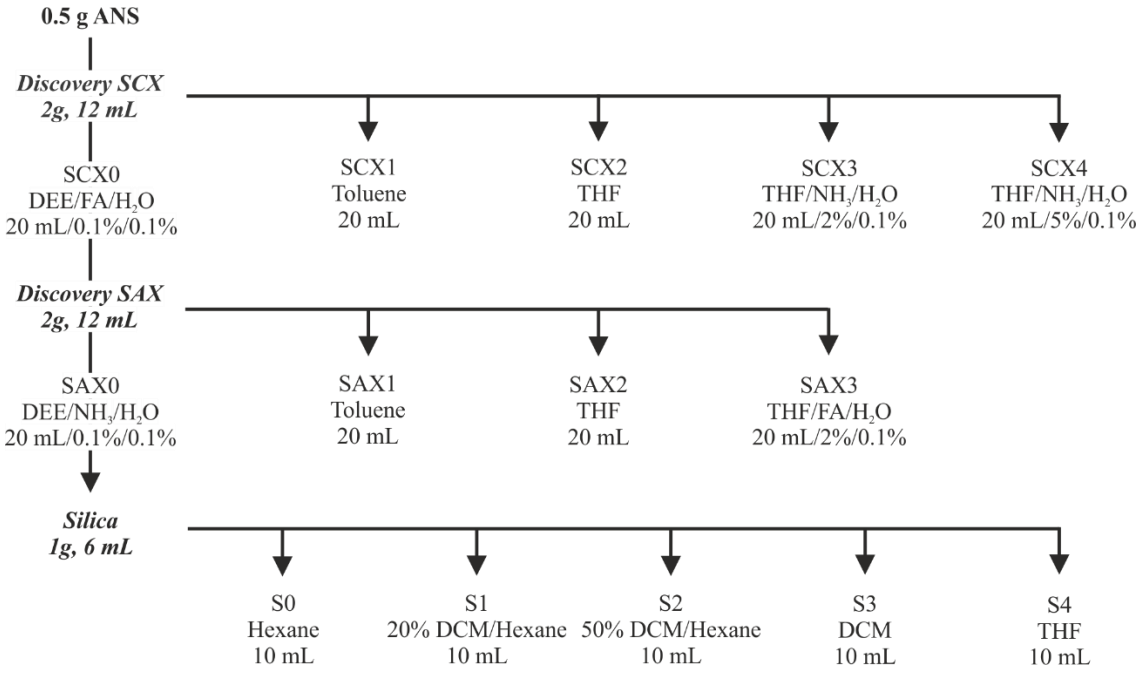

Figure 4-10. Flow diagram for the developed elution sequence for the SPE procedure. Fraction numbers are related to the solid phase extraction phase (e.g., SCX = strong cation exchange, SAX = strong anion exchange, S = silica; suffix 0 refers to non-retained fractions and positive integers to the order of elution from SPE cartridges).

Method repeatability was investigated by the separation of triplicate samples of the ANS crude. Average fraction masses with standard deviations are presented in Figure 4-11 and show low variability of individual fraction masses. Further quantification studies

conducted on individual fractions (utilizing more appropriate, synthesised alkylated standards) would allow a final sample composition to be obtained but currently these are not available.

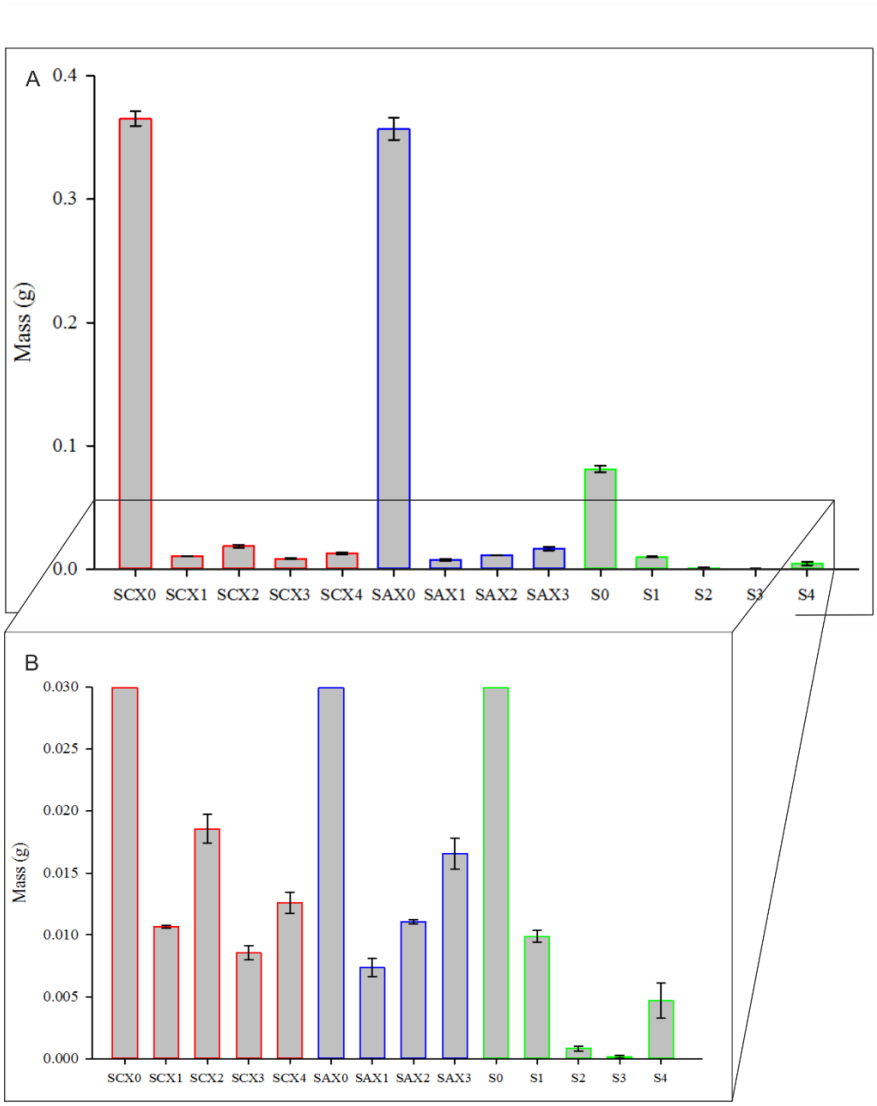

Figure 4-11. Average fraction mass recoveries from triplicate separations of ANS crude oil with standard deviations (A) and zoomed insert (B) showing lower mass fractions. Red= SCX fraction series, blue= SAX fraction series and green= silica fraction series.

4.4 Procedural blanks

The regular use of highly organic solvents in combination with plastics presents a likely source of contamination. To investigate the potential procedural contamination of the

fractions, a number of blank runs were performed to generate suitable procedural blanks. In the case of all 'blank' fractions, a negligible mass was collected. Thus, 50 µL of DCM was added to each of the fourteen fractions (SCX0 and SAX0 included) and these were subsequently analysed using GC-MS. Additionally, procedural blanks for the analysis of SCX4 fractions by liquid chromatography-high resolution-mass spectrometry (LC-HRAM-MS) were analysed. The procedural blanks were first solubilised in THF followed by dilution (10×) in methanol before instrumental analysis.

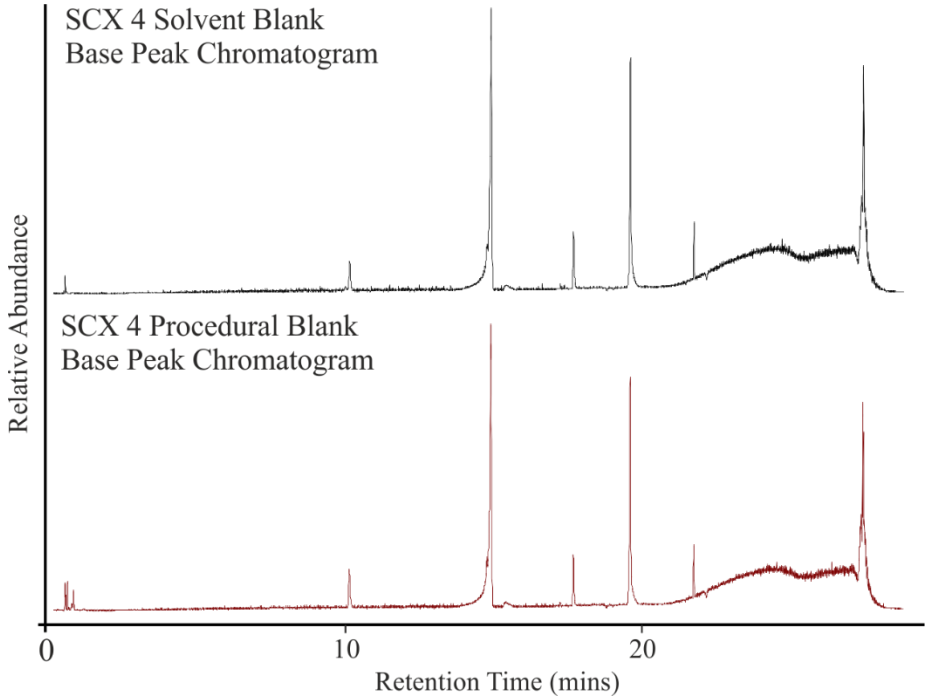

Figure 4-12. Base peak chromatograms from the LC-HRAM-MS analysis of procedural blanks for the SCX4 fractions.

Results from the LC-HRAM-MS analysis of the SCX4 procedural blank are presented in Figure 4-12. Comparison of the procedural blank analyses with that of the instrumental solvent blank run showed all significant peaks to be sourced from the eluents employed in the analysis. Comparison of accurate masses obtained from the peaks with a database of common contaminants suggested them to be primarily series of common phthalates and detergents.

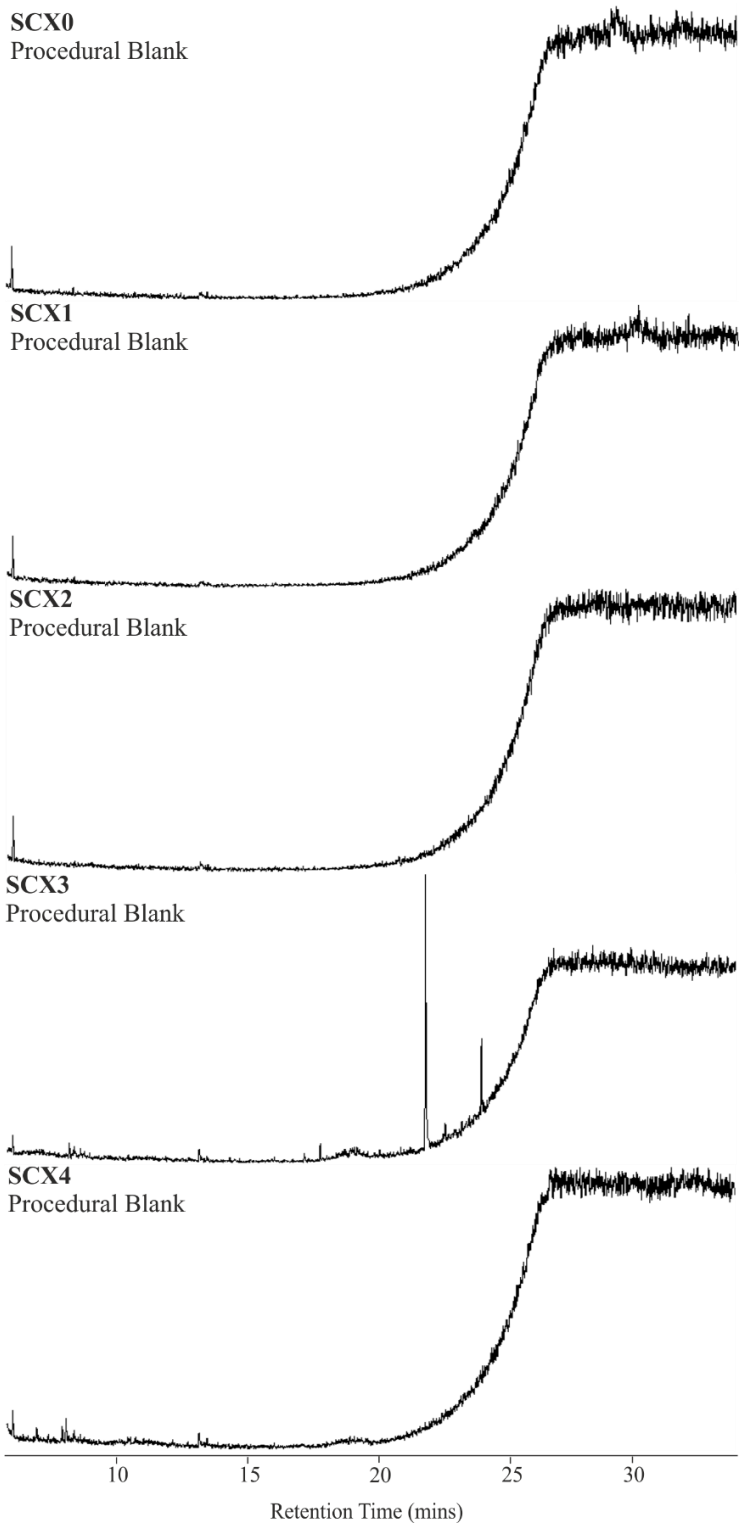

Figure 4-13. GC-MS TICs of the procedural blanks of the five SCX fractions (SCX0-4) from the SPE separation procedure.

GC-MS chromatograms of procedural blanks obtained from the cation exchange separation are presented in Figure 4-13. Overall, the procedural contamination of each fraction was minimal and no contamination was apparent in fraction SCX0-2. Minor

phthalate contamination was observed in fraction SCX3 and a small number of low abundance peaks were seen to elute before 10 minutes. The presence of similar low abundance peaks in fraction SCX4 suggests they are likely sourced from the ammonium hydroxide additive or result from its interaction with the stationary phase (i.e. phase stripping). Nevertheless, the abundance of these peaks suggests they would be negligible interferences in later analyses.

No contamination was present in the SAX1 and SAX2 fraction from the anion exchange separation (Figure 4-14). Minor contamination of the SAX0 fraction consisted of a number of low abundance peaks producing ions consistent with the presence of phthalates. A number of peaks were present in the SAX3 blank fractions. It is likely that given the absence of these peaks in the other fractions, that they are sourced from the FA modifier or its interaction with the stationary phase. The early eluting peaks could not be identified. Later eluting peaks produced mass spectra consistent with *n*-hexadecanoic acid, *n*-octadecanoic acid and diisooctyl phthalate. The presence of the C_{16} and C_{18} acids in the SAX3 fractions has been observed in previous experiments. However, the concentrations of these particular acids in the procedure blank is significantly lower, and unlikely to interfere with qualitative measurements.

The TICs from the analysis of the procedural blanks collected from the silica separation are shown in Figure 4-15 and no significant contamination was seen to be present in fraction S0-2. However, two substantial peaks were present in the chromatograms of the S3 and S4 fractions. The later eluting, and more abundant of the two peaks was identified as diisooctyl phthalate and the earlier eluting produced a mass spectrum consistent with the 2-(2-methoxyethyl)hexyl propyl ester of phthalic acid. Whilst significant in abundance, phthalates are common laboratory contaminants and were not compounds of interest within crude oil samples. Indeed, it is uncommon to see crude oil samples that are not contaminated by various phthalate derivatives because of regular contact with

plastics during sampling, storage, etc. These results however, do highlight the importance of preparing procedural blanks to minimise the misidentification of crude oil constituents.

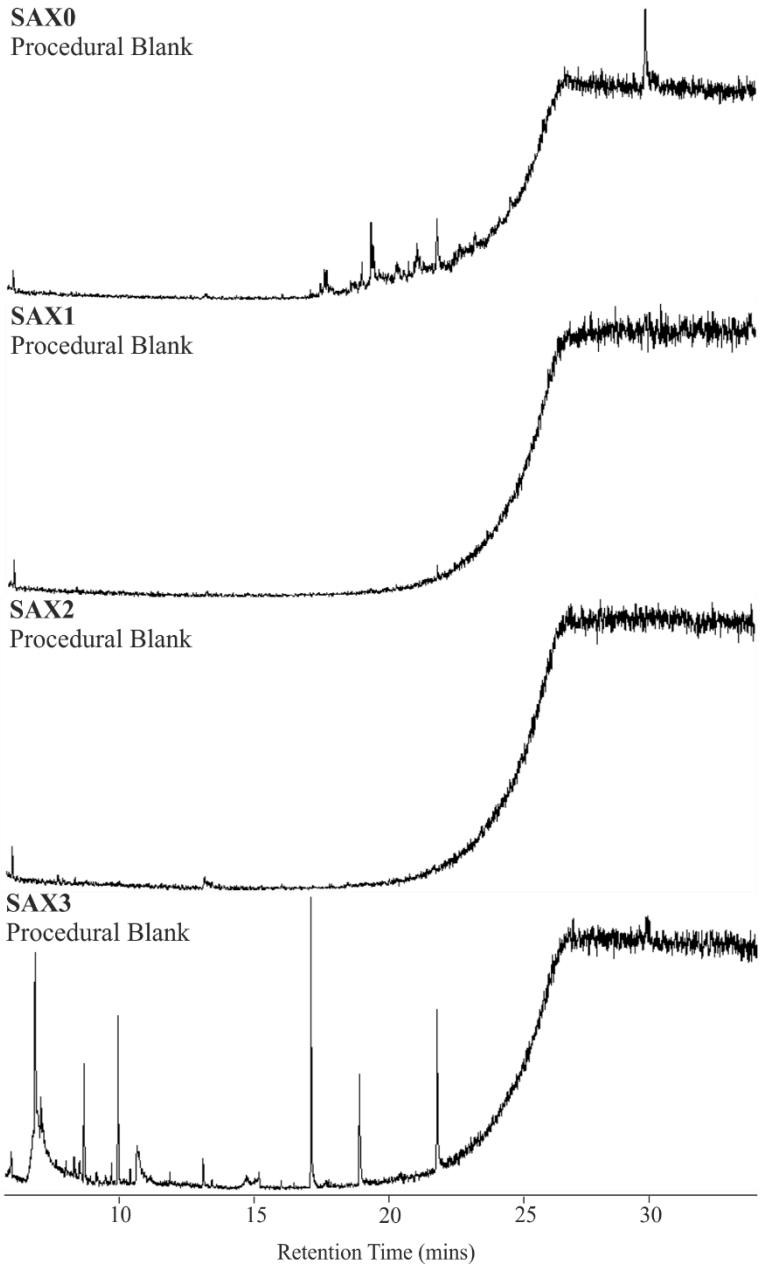

Figure 4-14. GC-MS TICs of the procedural blanks of the five SAX fractions (SAX0-3) from the SPE separation procedure.

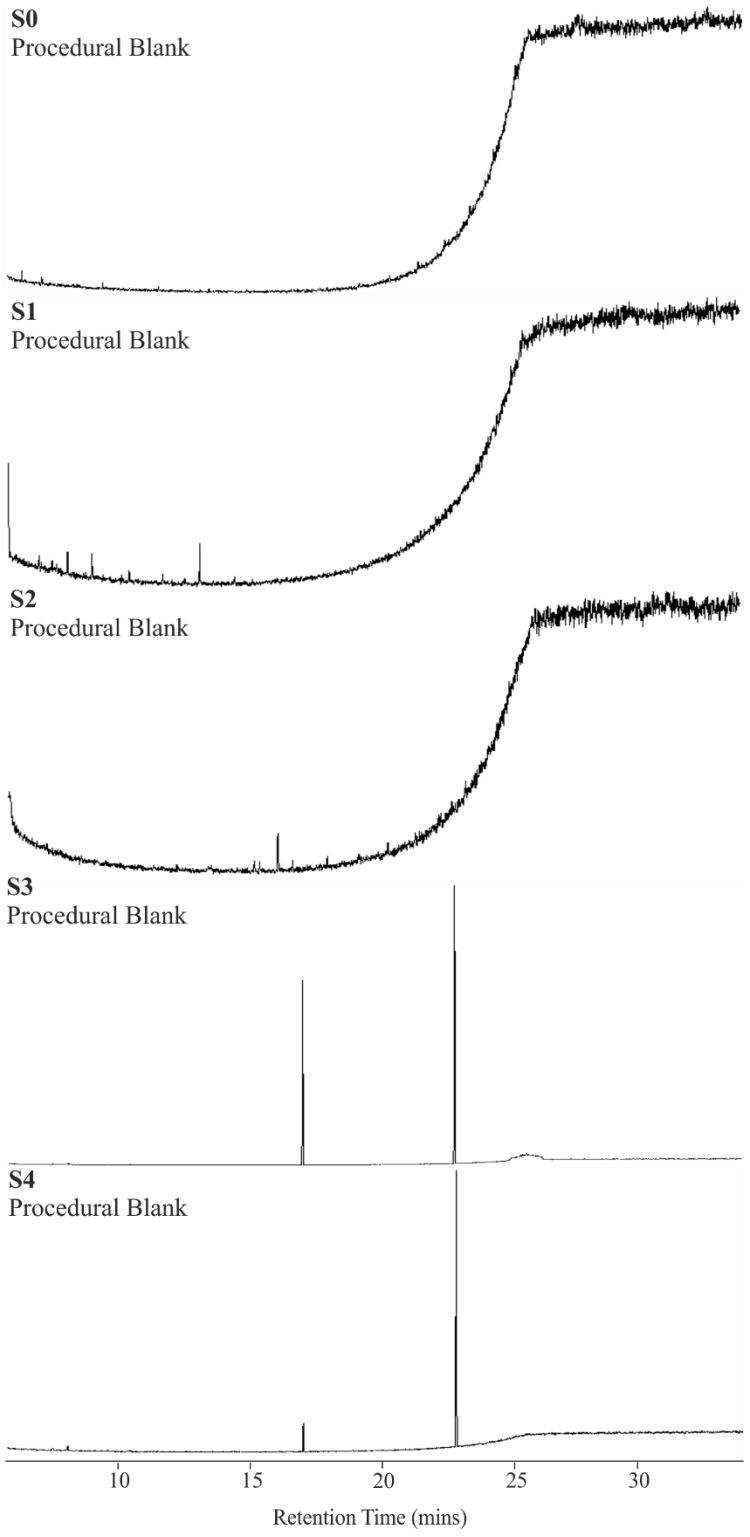

Figure 4-15. GC-MS TICs of the procedural blanks of the five silica fractions (S0-4) from the SPE separation procedure.

4.5 Separation of 'model' compounds by SPE

Separation and quantitation of the same model compound mixture (Table 2-1) as that employed to evaluate the 'Snyder' method (Chapter 3), enabled the location of various compound classes to be identified within the developed separation scheme (Figure 4-10). Separations were performed in triplicate to assess method repeatability. Overall, the method performed well, with all but three compounds (representing three classes) being isolated entirely within individual fractions (Figure 4-16). High recoveries of model compounds (Appendix 3) suggested that low losses of similar compounds would be observed on separation of crude oil samples.

4.5.1 SCX fractions

Initial separation using SCX SPE resulted in the successful isolation of two of the model compounds, benzene sulfoxide and benzoquinoline. The use of such phases for the isolation of benzoquinoline and other pyridine derivatives has been reported previously with similar success (Schmitter *et al.*, 1983; Conceição Oliveira *et al.*, 2004; Simon *et al.*, 2010). As observed in these previous studies, benzoquinoline was isolated completely in the basic fractions (Figure 4-16C; SCX4, quinoline fraction). Analysis of fractions by GC-MS showed no division of the quinoline model compound between the two basic fractions (SCX3 and SCX4), indicating strong ionic interactions between the basic nitrogen compound and the chromatographic phase.

No model compounds were observed to elute within the SCX1 fraction. Inclusion of proposed asphaltene 'model' compounds (López-Linares *et al.*, 2006; Nordgård and Sjöblom, 2008) in the test mix may have given an indication as to whether this fraction is asphaltenic or whether the asphaltene model compounds behave in the same manner as crude oil components when separated in this way. However, the validity of such compounds as reliable asphaltene 'models' is not unchallenged. The sulfoxide model

compound, dibenzyl sulfoxide, was recovered using THF from both of the IEX cartridges (SCX2 and SAX2; Figure 4-16B), although was predominantly found within the SCX 2 fraction.

4.5.2 SAX fractions

Chromatography utilising the SAX SPE cartridge resulted in the successful isolation of all the carboxylic acids (dibenzofuran carboxylic acid, adamantane carboxylic acid, 4-pentylbicylco[2,2,2]octane-1-carboxylic acid, dibenzothiophene carboxylic acid, cholanic acid) in a single fraction (SAX3; Figure 4-16D). Ionic interactions between carboxylic acids and the quaternary amine phase appear to be unaffected by the presence of other functional groups or structural features. Interestingly, as observed in the work of Sutton and Rowland (2014) acid isolation appears improved when SCX is performed prior to SAX separations. Unlike in the Snyder methodology, no early elution of any of the acid model compounds was observed.

Retention of carbazoles and phenols to anion exchangers has been reported previously by Snyder and Buell (1968) but was considered counterproductive. In the current study however, exploitation of these interactions allowed isolation of carbazole (SAX2; Figure 4-16C) and phenyl phenol (SAX2; Figure 4-16A) within one fraction with no carryover into later fractions observed in either instance. Nitroindole was also recovered in the SAX3 fraction, suggesting the addition of the nitro group increases the dissociation of the indole functionality, thus increasing the ionic interactions with the phase.

4.5.3 Silica fractions

Normal phase chromatography conducted on silica provided separation of those neutral compounds that were not retained by the SCX or SAX SPE cartridges. Quantitation of dibenzothiophene in the silica fractions revealed the compound to be divided between fractions S0 and S4 (Figure 4-16B). Despite subsequent elution with increasingly polar

mixtures of *n*-hexane and DCM, 10% of the dibenzothiophene was only collected upon elution with THF. Whilst this suggested the method did not provide fractions ideally suitable for quantitation of thiophenic compounds, subsequent separations of crude oils resulted in an S4 fraction composed of a number of thiophene and other sulphur containing compounds. Separation of oxygen compounds on silica was successful with furan, fluorenone and xanthone eluting in separate fractions (S0, S2 and S4 respectively; Figure 4-16A).

Dibenzofuran eluted in fraction S0, indicating minimal retention of the compound to the silica phase. Similarly, aromatic hydrocarbon model compounds (fluoranthene, phenanthrene and benzo[*a*]pyrene) eluted in fractions S0 and S1, indicating limited retention (Figure 2E). Increasing numbers of rings resulted in an increase in retention, with benzo(a)pyrene eluting within fraction S1. This observation is contradictory to the results observed during the development of the adsorption phase separation procedures. Separation of fraction SAX0 on unbonded silica had seen the successful separation of tri-aromatics and saturated hydrocarbons. The poor retention of the tri-aromatic model compound here suggests the crude oil matrix has a positive effect on the separation of saturated and aromatic hydrocarbons.

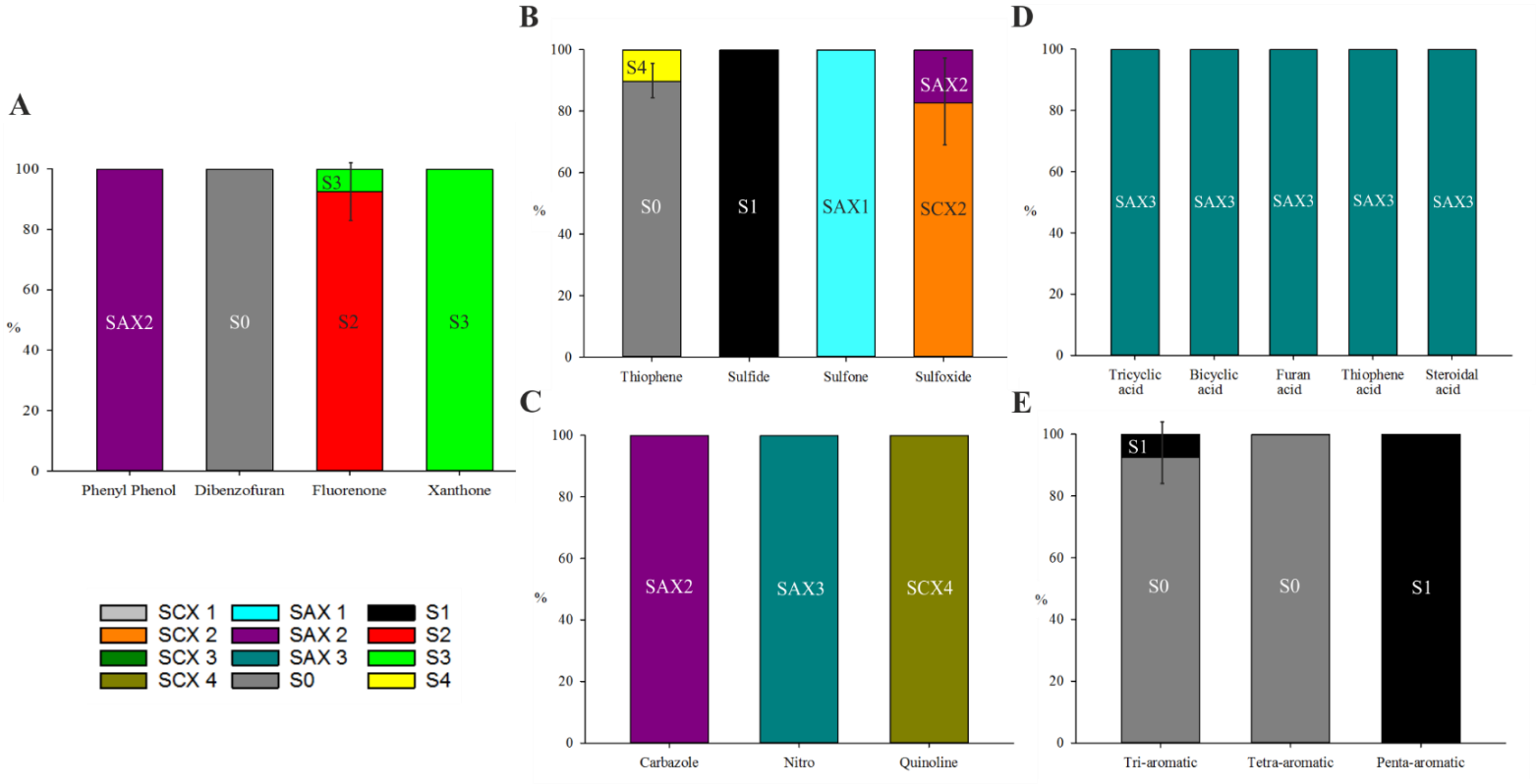

Figure 4-16. Averaged gravimetric data (n = 3; error bars represent separation of compounds between fractions) illustrating which chromatographic fraction contained each of the model compounds. Compounds are grouped into charts of similar functionality: oxygen-containing (non-acid) compounds (A), sulphur-containing compounds (B), nitrogen-containing compounds (C), acids (D), and aromatic compounds (E). Single coloured bars indicate a model compound was recovered in a single fraction.

4.5.4 Crude oil spiked fractions

Authentic model compounds were then spiked into the ANS crude oil in order to investigate the effect of the matrix on compound separation. Only minor differences were observed in the distribution of model compounds (Figure 4-17) when the chromatographic scheme was applied to the model compounds in a crude oil matrix compared to the model compounds mixture alone. In particular, no matrix effects were found for sulfide, sulfoxide, carbazole, phenol, and acidic and basic fractions.

Dibenzothiophene sulfone eluted later in the scheme, divided slightly between fractions SAX1 and SAX2 when dosed into the crude oil. Aromatic compounds eluted later, with penta- and tetra- aromatic compounds eluting completely in fractions S1. Separation of phenanthrene remained largely unchanged, but tetra- and penta- aromatic compounds eluted later (S1 rather than S0).

Separation of oxygen containing compounds also showed a slight increase in retention with dibenzofuran eluting in both fractions S0 (83%) and S1 (17%). Fluorenone and xanthone eluted later with the former separating between fractions S2 (88%) and S3 (12%) and the latter between fractions S3 (9%) and S4 (91%). Finally, thiophene splitting appeared reduced with >98% present within fractions S0 and only slight retention and elution in fraction S4.

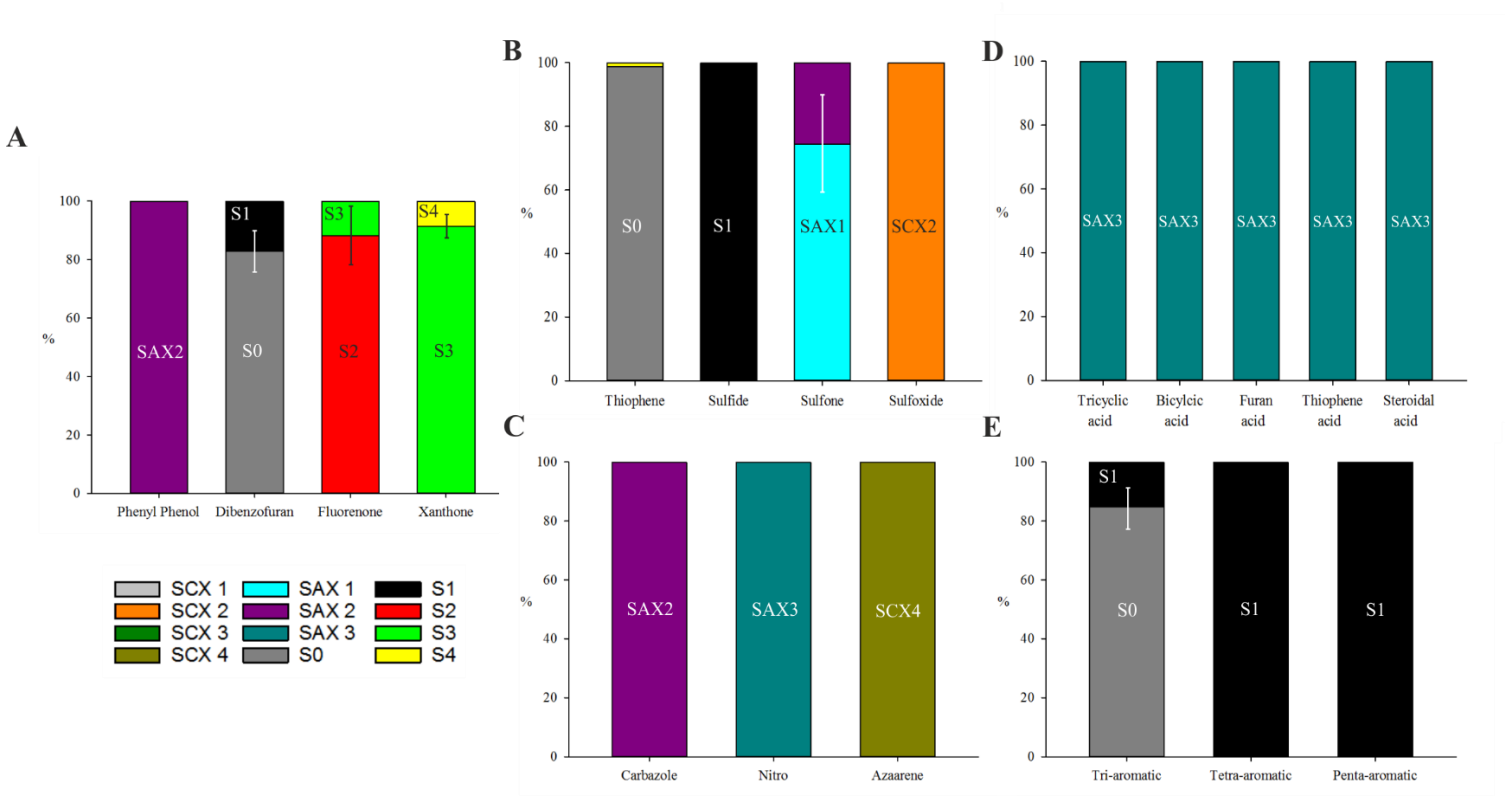

Figure 4-17. Averaged gravimetric data (n = 3; error bars represent separation of compounds between fractions) illustrating which chromatographic fraction contained each of the model compounds. Compounds are grouped into charts of similar functionality: oxygen-containing (non-acid) compounds (A), sulphur-containing compounds (B), nitrogen-containing compounds (C), acids (D), and aromatic compounds (E). Single coloured bars indicate a model compound was recovered in a single fraction

4.6 Conclusions

A method for the fractionation of crude oils was developed. The method utilises both ion exchange and normal phase chromatography to generate twelve fractions from each separated oil. By designing the method around the separation of a crude oil sample, losses to irreversible adsorption were minimised. Losses were observed to occur primarily during the first stage of the separation and could be almost entirely attributed to the loss of volatile components. Triplicate fractionation of the ANS crude oil demonstrated the reproducibility of the developed procedure with average standard deviations of 4.7% for fractions of significant mass (all except S2-4); higher deviations (26.4-41.7%) were seen for these fractions as recorded masses were <1 mg.

Separation of a suite of nineteen representative 'model' compounds demonstrated the selectivity of the method, with only three instances of the overlap of compound classes (nitro- and acid compounds; SAX3, furans, thiophenes and aromatics; S0, and the carbazoles and phenols; SAX2). Despite instances of lower chromatographic resolution between certain fractions, the developed method appears to provide significant advantages over some of those previously developed. By employing commonly available SPE cartridges and solvents, the method was found to be highly reproducible and was quick to conduct (6 hours for a complete separation).

The fractionation method developed herein could now be employed for the separation of a variety of crude oils that differ in physical properties (e.g. API gravity; Chapter 5) or for the investigation of geochemical, operational or engineering problems. Some of these approaches are illustrated in Chapter 6.

Chapter 5. Separation of crude oils with different API gravities using the newly developed SPE procedure and analysis of selected fractions

Chapter 5 describes the application of the method developed in Chapter 4 (for separation of crude oils) to a series of five crude oils of varying chemical (e.g., TBN, TAN, and % asphaltene) and physical properties (e.g., API, viscosity and % sulphur), followed by characterisation of the fractions using gas chromatography-mass spectrometry (GC-MS), multidimensional gas chromatography-mass spectrometry (GC×GC-MS), Fourier transform-ion cyclotron resonance-mass spectrometry (FT-ICR-MS) and liquid chromatography-high resolution accurate mass-mass spectrometry (LC-HRAM-MS).

Deployment of the solid phase extraction (SPE) procedure resulted in the collection of twelve discrete fractions from each of the five crude oils. Sample recoveries from the scheme were high (77−98%) with simple evaporative losses correlating closely with total deficit from mass balance. Subsequent analysis of fractions by appropriate chromatographic and mass spectrometric techniques showed predictions of fraction composition, informed by separation of the 'model' compound suite, to be accurate. Alkylated series of quinolines, carbazoles, fluorenones and xanthones were identified successfully within their predicted fractions.

In addition to known crude oil polar compounds, analysis of fractions by GC and LC techniques enabled the tentative identification of compounds hitherto not previously reported in crude oils. Analysis of cationic fractions by LC-HRAM-MS enabled the identification of individual $C_{1\text{-}3}$ benzoquinolines and phenyl quinolines. GC×GC-MS analysis of the S3 xanthone fraction enabled thioxanthone and its alkylated homologues to be identified in crude oils for the first time. Also tentatively identified were the

tocopherols (E vitamins), present in the SAX2 (phenol/carbazole) fraction of the Bonga crude oil (W. Africa).

5.1 Introduction

Chapter 4 discussed the development of a three stage, SPE separation of crude oil into twelve individual fractions differing in sorption behaviours and polarities. The separation procedure was designed to mitigate the shortcomings observed in literature separations reported previously (e.g., Snyder and Buell, 1968; Jewell *et al.*, 1972; Willsch *et al.*, 1997). Preliminary results from the separation of the ANS crude oil and a mixture of model compounds suggested that the development of a high recovery, compound class specific separation procedure had been successful. However, the immense variety in the physical and chemical properties of different crude oils is such that separation of additional samples is required to evaluate further the performance of the method. The present investigation therefore aimed to evaluate the performance of the method when applied to a series of crude oils encompassing a range of physical and chemical properties.

Five crude oils from different geographical locations were separated to assess the effect of changing physical and chemical properties on the 'quality' of the fractions obtained. Additionally, separation of such a series should allow for the effects of variable crude oil parameters (e.g., viscosity, percentage wax and percentage asphaltene content) on fraction reproducibility to be investigated. The crude oil series was selected to contain a sufficient variety of oils to enable the assessment of these potential issues.

The separation of a wider number of crude oils also allowed the reliability of the separations of the 'model' compound mixtures to be evaluated more fully. Whilst the selected model compounds should adequately represent the lower alkylated homologues of the parent compound (because only lower molecular weight compounds were available from commercial sources), whether their behaviour represents that of higher alkylated homologues and benzologues present in crude oils required investigation. The characterisation of all fractions obtained from the separation of the five crude oil samples

by chromatographic and mass spectral techniques facilitated molecular and structural identifications. This, in turn, allowed for thorough evaluation of previously observed ‘model’ compound behaviour.

5.2 Crude Oil Selection

In order to evaluate the wider performance of the separation procedure developed in Chapter 4, five crude oils of differing API gravity and from different geographical locations were studied. By separating such a series, the effects of changing chemical and physical properties on fraction composition and reproducibility could be examined. Additionally, by investigating the composition of polar fractions obtained from the selected crude oils, the ease with which new series of NSO biomarkers could be identified could be evaluated. The following five export crude oils were selected to be a part of the initial performance tests: Alaska North Slope (ANS), Brent Blend, Kuwait Blend, Tia Juana Heavy TJP and Bonga (Figure 5-1).

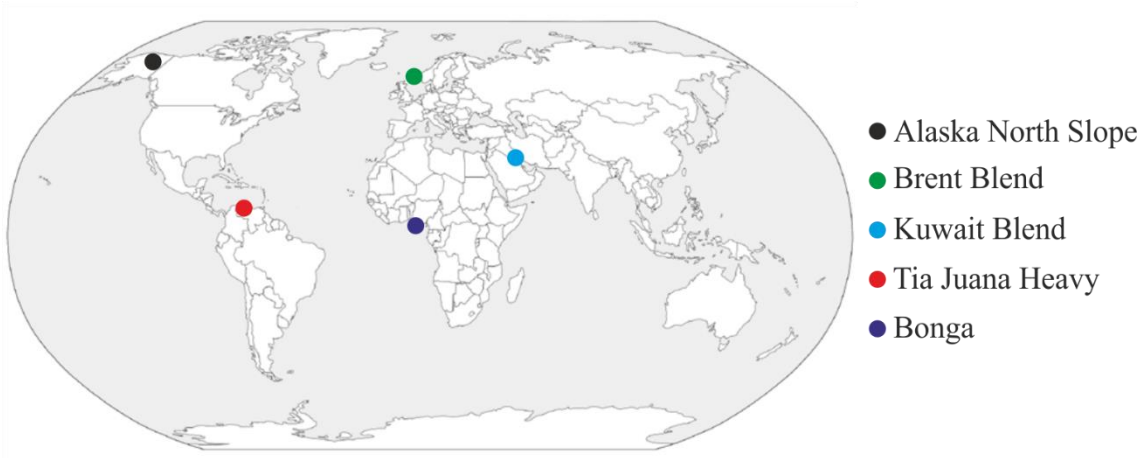

Figure 5-1. World map showing the geographical origins of the five crude oil samples used to assess method performance.

5.2.1 Alaska North Slope (ANS)

Alaska North Slope crude oils are blended oils from fields located across the Alaska North Slope region; major fields include Prudhoe Bay, Kaparuk, Lisburne and Endicott. The resulting blend is a medium grade crude with an API gravity of approximately 30.3 ° and a sulphur content of 0.96%. The ANS region was estimated by the United States Geographical Survey (USGS) to hold more than 50 billion barrels of crude oil.

Geochemical interest in the ANS export crude is also associated with its accidental release in the 1989 *Exxon Valdez* oil spill in Prince William Sound (AL, USA).

Crude oils accumulating on the North Slope of Alaska are geochemically challenging, as reservoirs are typically fed by multiple source formations. Crude oils in the ANS region have historically been classified into five oil types: Kuna and Lisburne (Carboniferous), Kingak and Blankenship (Jurassic), Shublik and Otuk (Triassic), Pebble-GRZ-Torok-Hue (Cretaceous) and Canning (Paleogene; Lillis *et al.*, 2006).

The Kuna and Lisburne oil types originate from the Lower Carboniferous to Lower Permian Lisburne Group that is widely distributed throughout the ANS. The group largely consists of shallow marine carbonate rocks which, due to its high TOC, has been proposed as a potential source rock (Lillis *et al.*, 2002). However, oils derived from the Lisburne Group are widely scattered and few in number. The Kingak and Blankenship type are largely generated from the Kingak Shale (Jurassic). This particular formation has been proposed as an oil source rock in a number of studies and is thought to contribute to the large Prudhoe Bay oilfield (Sedivy *et al.*, 1987). The Shublik and Otuk type are formed from the Shublik Formation (Triassic) which is widely regarded as the source rock for the largest volumes of crude oil in the ANS. Certainly, the substantial Prudhoe Bay and Kuparuk fields are largely derived from the Shublik Formation (Lillis *et al.*, 2006). The Pebble-GRZ-Torok-Hue types originate from a number of Lower Cretaceous formations and studies have shown these source rocks to be a significant contributor to the Prudhoe Bay oilfield (Lillis *et al.*, 2006). The Canning type oils are sourced from the Canning Formation (Paleogene). These crude oils tend to be located in the Eastern sector of the ANS region.

5.2.2 Brent Blend

Brent Blend is comprised of 15 crude oils extracted from fields in the Brent and Ninian systems, in the East Shetland Basin of the North Sea. The resulting blend is a high quality, low sulphur (0.40%), light crude oil with an API gravity of approximately 38.3 °. The high quality of the crude oil produced from the Brent oilfield led to it serving as a major economic benchmark, dictating the price of approximately two thirds of the world's internationally traded crude oil. However, after being produced for the last 41 years and with an output of over 4 billion barrels of oil, the Brent oilfield will soon no longer be economically viable to produce; decommissioning has already begun (Shell, 2017).

Most of the oil within the Brent oilfield is found in both the Brent (sandstone) and Statfjord (sandstone) formations. The Brent formation is unconformably overlain by transgressive Upper and Middle Jurassic shales less than 50 m thick. Above this lie transgressive Cretaceous mudstones and marls. The Statfjord formation is of poorer quality and occurs some 200 m deeper than the Brent formation (Kirk, 1980). Evaluation of source rock potential of the Cretaceous and Jurassic mudstones indicates the oil prone Kimmeridge Clay (Upper Jurassic) and gas prone Brent Formation coals and coaly mudstones to be the richest, most likely source rocks (Goff, 1983). In the case of the Brent oilfield, the size of the accumulation and the thinness of the source rock suggests the main source of the oil lies outside of the discussed formation. It is thought the source of the oil is in the Upper Jurassic formations in the flanking troughs and that migration through faults has led to the vast accumulations (Chapman, 1983).

5.2.3 Kuwait Blend

The Kuwait blend is a high sulphur (2.52%) crude with an API gravity of approximately 31.4 °. Kuwait has proven crude oil reserves of 104 billion barrels, which is estimated to constitute ~9% of the world's crude oil reserves. The Burgan oil field, located in South

Eastern Kuwait, is the world largest sandstone oil field and is predicted to produce between 66 and 75 billion barrels of crude oil.

The Burgan oil field is produced from three Cretaceous age formations found within the Wasia Group: Wara, the Mauddud limestone and the Burgang formation (Strohmenger *et al.*, 2006). The large Burgang formation is separated into the Third and Fourth Sands; the former is then separated into the Upper, Middle and Lower units. The Third Sand is thought to have contributed to approximately 75% of the Burgan oil field (Strohmenger *et al.*, 2006). The high sulphur content of the Kuwait crudes is attributed to the sulphur rich carbonate source rocks that were likely deposited under anoxic conditions. The oils produced from each of these formations have varying API gravities. Oil in the Wara formation varies from 29-36 °, while oil in the Third Sands formation varies from 28-34 ° (Kaufman *et al.*, 2002).

5.2.4 Tia Juana Heavy

The Tia Juana Heavy or Tia Juana Pesado (TJP) is a heavy (12.1 ° API), high sulphur (2.70%) Venezuelan crude oil. The Tia Juana oilfield is located in the Maracaibo Basin in Eastern Venezuela and produces both heavy and light crude oil. The lighter crude oil and gases are found at lower levels and the heavy variant is found at shallow depths. This highlights the effects of the loss of light fractions by evaporation, flushing and biodegradation that occurs in the shallower deposits, yielding the heavier crudes (James, 2000a). As of 2009, the Venezuelan government claimed proven oil reserves of 211 billion barrels of conventional crude oil. Geochemical interest in the TJP is also associated with its accidental release in the 1989 Mersey Oil Spill (Davies and Wolff, 1990).

The major petroleum system in the Maracaibo Basin involved the migration of hydrocarbons from the La Luna formation (Upper Cretaceous) to reservoirs in the Misoa,

(Eocene), Lagunillas (Miocene) and La Rosa (Miocene) formations. The most efficient of these systems is the La Luna to Misoa formation, which accounts for ~50% of migration. The source rocks for the Tia Juana oilfield are the calcareous limestone shale of the La Luna formation, which are widely considered to be the world's best known source rocks (James, 2000a; James, 2000b). The higher of the two Tia Juana deposits has been subject to extensive biodegradation, initiated by exposure to sub-surface waters resulting in microbial action. The effects of biodegradation of crude oil composition are well studied (Reviewed Peters *et al.*, 2005) with the selective removal of normal and branched paraffins being the most notable alteration. Given that the paraffins typically constitute ~40% of non-biodegraded crude oils, their removal has significant consequences on the physical properties of the crude oil; most notably, a substantial increase in viscosity and decrease in API gravity.

5.2.5 Bonga

The Bonga field is an offshore oilfield located 120 km southwest of the Niger Delta in Nigeria. The Bonga is a medium gravity (29.4 ° API), low sulphur (0.25%) naphthenic crude oil. The Bonga oilfield is estimated to have 1.4 billion barrels of crude oil in place and is currently produced at a rate of 202,000 barrels per day.

The stratigraphy of the Niger Delta basin is divided into three significant formations: Benin, Agbada and Akata. The Akata formation (Paleocene) consists of mainly over pressured shale with marine origins. The overlying Agbada formation (Eocene), some 4 km thick, is composed of interbedded sands and shales. The Benin formation is the youngest of the three (Eocene to Recent) and is mainly composed of gravels and sands (Sonibare *et al.*, 2008). The source rocks for the petroleum in the Niger Delta are thought to exist mainly within the lower regions of the Agbada Formation and the uppermost strata of the Akata Formation marine shales. The hydrocarbon reservoirs tend to reside

within the sandstone of the Agbada Formation, where oil and gas are typically trapped by rollover anticlines (Tuttle *et al.*, 1999).

5.3 Methods

5.3.1 Experimental Detail

Crude oil samples were separated using the sequential SPE procedure developed in Chapter 4 and described in detail in Chapter 2.

5.3.2 Crude Oils

The crude oils used in this study were: Alaska North Slope, Brent Blend, Kuwait Blend (all provided by British Petroleum), Bonga (provided by the National Nigerian Oil Company) and Tia Juana Pesado crude oil (provided by Royal Dutch Shell). The general characteristics of the five crude oil samples are presented in Table 5-1. Crude oils were sampled as described in Chapter 2.

Table 5-1. General characteristics of the five crude oil samples (API Gravity- an inverse measure of a petroleums liqid density relative to that of water; total acid number- TAN)

Crude Oil	Region	API Gravity (°)	Sulphur (%)	TAN (mg KOH)	Asphaltenes (%)
Alaska North Slope	North America	30.3[1]	0.96[1]	0.1[1]	2.1[1]
Kuwait Blend	Middle East	31.4[2]	2.52[2]	0.15[2]	3.0[3]
Brent Blend	North Sea	38.3[4]	0.40[4]	0.1[4]	0.2[4]
Bonga	West Africa	29.4[4]	0.25[4]	0.46[4]	0.0[4]
Tia Juana Heavy	South America	12.1[4]	2.70[4]	3.61[4]	11.0[4]

(1) Data obtained from an externally conducted crude oil assay (Intertek, Sunbury, UK)
(2) Stratiev, D., R. Dinkov, K. Petrov, and K. Stanulov. Petroleum and Coal. 2010, 52, 35-43
(3) AlHumaidan, F.S., A. Hauser, M.S. Rana, and H.M.S. Lababidi. Energy Fuels. 2016, 30, 2892-2903
(4) Data obtained from Exxon crude oil repository (http://corporate.exxonmobil.com/en/company/worldwide-operations/crude-oils; accessed 2017)

5.3.3 Analytical Procedures

The instrumentation used for the analysis of crude oil fractions is detailed in Chapter 2. The GC-MS analyses were performed using was a (5% phenyl)-methylpolysiloxane HP5-MS (30 m × 0.25 mm × 0.25 μm) with the following temperature program: 40 ºC (1 min hold), then heated to 300 ºC at 10 ºC min^{-1}. GC×GC-MS analysis were performed using conditions B in which the oven was programmed from 100 ºC (1 min hold), to 190 ºC at 3 ºC min^{-1}, then to 250 ºC at 0.7 ºC min^{-1} and finally to 330 ºC at 6 ºC min^{-1} (10 min hold). The hot jet was programmed to a temperature of 105 ºC (1 min hold), heated to 210 ºC at 3 ºC min^{-1}, then to 285 ºC at 0.9 ºC min^{-1} and finally to 340 ºC at 5 ºC min^{-1}. The secondary oven was heated from 150 ºC (1 min hold) to 230 ºC at 3 ºC min^{-1} and finally to 350 ºC at 1.2 ºC min^{-1}. The modulation times were 5 and 6 s. The MS transfer line temperature was maintained at 330 ºC. Mass spectral identifications were aided by comparison of the obtained mass spectra with those in the NIST mass spectral library (2011).

LC-HRAM-MS analyses were conducted using configurations A and B. Configuration A: used a Waters XBridge BEH C18 (50 × 2.1 mm, 3.5 μm) column (Waters, U.K.) with a solvent gradient of 0.1% formic acid (FA) (aq)/ 0.1% FA acetonitrile (100:0 to 0:100, 10-minute runtime). Configuration B: used an ACE Excel 3 SuperC18 (100 × 2.1 mm, 2.5 μm) column (Advanced Chromatography Technologies Ltd, UK) with a solvent gradient for the analysis of basic fractions of 0.1% FA (aq)/ 0.1% FA in acetonitrile/ 0.1% FA in IPA (90:10:0 to 15:85:0 to 0:10:90; 30-minute runtime).

FT-ICR-MS data was obtained by Dr. Steven M. Rowland at Maglab, Florida State University, USA. Data were collected using custom-built FT-ICR mass spectrometer equipped with a 9.4 T horizontal 220 mm bore diameter superconducting solenoid magnet operated at room temperature with a micro ESI emitter. Samples were analysed at a

concentration of 50 μg mL^{-1} in 50/50 toluene:methanol with 1% formic acid, the flow rate was 50 μL min^{-1}, and ESI voltage was 2.5 kV.

5.4 Results and Discussion

The major focus of the work presented herein was to assess the performance of the developed separation method when applied to crude oils of varying physical and chemical properties. The five selected crude oils were all subjected to the developed SPE separation as described in Chapter 2 and initial investigations were focused on identifying trends in the gravimetry of the fractions. Additionally, comparison of gravimetric data with a number of industrially relevant properties (e.g., API, TAN, % sulphur, *etc.*) was investigated as a further means of method evaluation.

The second stage in evaluating the procedure was to assess the reliability of predictions made by separation of the 'model' compound series. In order to investigate composition, fractions were subjected to analysis by chromatographic and mass-spectrometric methods. The ability of the separation method to isolate 'chemically discrete' fractions was important, and was the main driver for the development of the separation scheme. Therefore, successful isolation of the targeted compound classes from all crude oil samples was necessary in proving the methodology was fit for purpose.

The lack of available library spectra and of reference compounds hindered the rigorous identification of many of the fraction components, but many unknowns could be better identified from *ab initio* interpretation of mass spectra. Whilst reference mass spectra often exist for the parent compounds and occasionally their $C_{1\text{-}2}$ alkyl homologues, they were not available for the more abundant and more complex higher alkylated homologues. A comprehensive characterisation of each fraction was however, not within the aims of the current work, which was instead focussed on isolation of discrete fractions for future detailed studies.

In addition to identifying the more commonly studied compound groups (*i.e.* thiophenes, carbazoles and naphthenic acids), attempts were made, where possible, to identify novel

or more rarely studied compound groups. By showing the ease with which previously elusive compounds could be isolated and studied by deployment of the separation method, the potential for use of the method in crude oil characterisation studies could be demonstrated.

5.4.1 Gravimetric Data

Total recoveries from separation of the five crude oils were good (77.4 - 97.5%; Table 5-2), with simple evaporative losses correlating closely with loss of volatiles from the sample under N_2 blowdown (Appendix 2). By attributing the vast majority of sample losses to the evaporation of volatile crude oil components (likely occurring during solvent removal), a near 100% recovery of the non-volatiles was achieved. This again demonstrated the benefits of employing ion exchange phases prior to the normal phases, which resolved many issues of irreversible adsorption of the high molecular weight and highly polar material, allowing its separation and isolation.

Table 5-2. Total and individual cartridge recoveries (weight percent) of crude oil samples separated in this study and average losses of crude oil sample during N_2 blowdown.

Mode of Separation		Percentage Recovery				
		Alaska North Slope	Kuwait Blend	Brent Blend	Bonga	Tia Juana Heavy
IEX	SCX	87.0	91.5	94.1	86.3	98.6
	SAX	97.4	95.3	94.1	96.3	99.7
Silica		96.4	95.4	91.4	92.1	95.6
Total		82.7	84.9	83.1	77.4	97.6
Blowdown loss		19.8	16.6	14.7	15.2	1.8

This is particularly emphasised by the excellent recovery of the TJP crude oil (97.6%; API gravity 12.1°). As previously discussed, the TJP has been subject to extensive biodegradation and, as a result, is highly enriched in polar NSO compounds and has a comparatively low volatiles content. High recovery of the summed fractions of this oil

thus indicated that losses due to irreversible adsorption were exceptionally low when compared to other methods. For example, recoveries obtained by Willsch et al. (1997) varied from 56.6%-76.3%, with losses likely due to irreversible adsorption on the numerous employed silica separations, in addition to the loss of volatile components during solvent removal. Snyder et al. (1968) reported no recoveries, but attempts to reproduce their separation using ANS crude oil herein (Chapter 3), resulted in a recovery of only ~67%.

The gravimetry data for the individual fraction masses from each crude oil are presented in Figure 5-2. To investigate potential correlation with masses of the NSO fractions, the data are presented in order of increasing API gravity. The API gravity is a measure of crude oil density, typically increasing with thermal maturity and decreasing when oils are subject to biodegradation. As immature or heavily biodegraded crude oils also tend to be enriched in NSO compounds, one might expect lower API gravity oils to be composed of higher molecular weight material, to be enriched in NSO containing compounds and to, contain proportionally less saturated hydrocarbons than an oils of high API gravity.

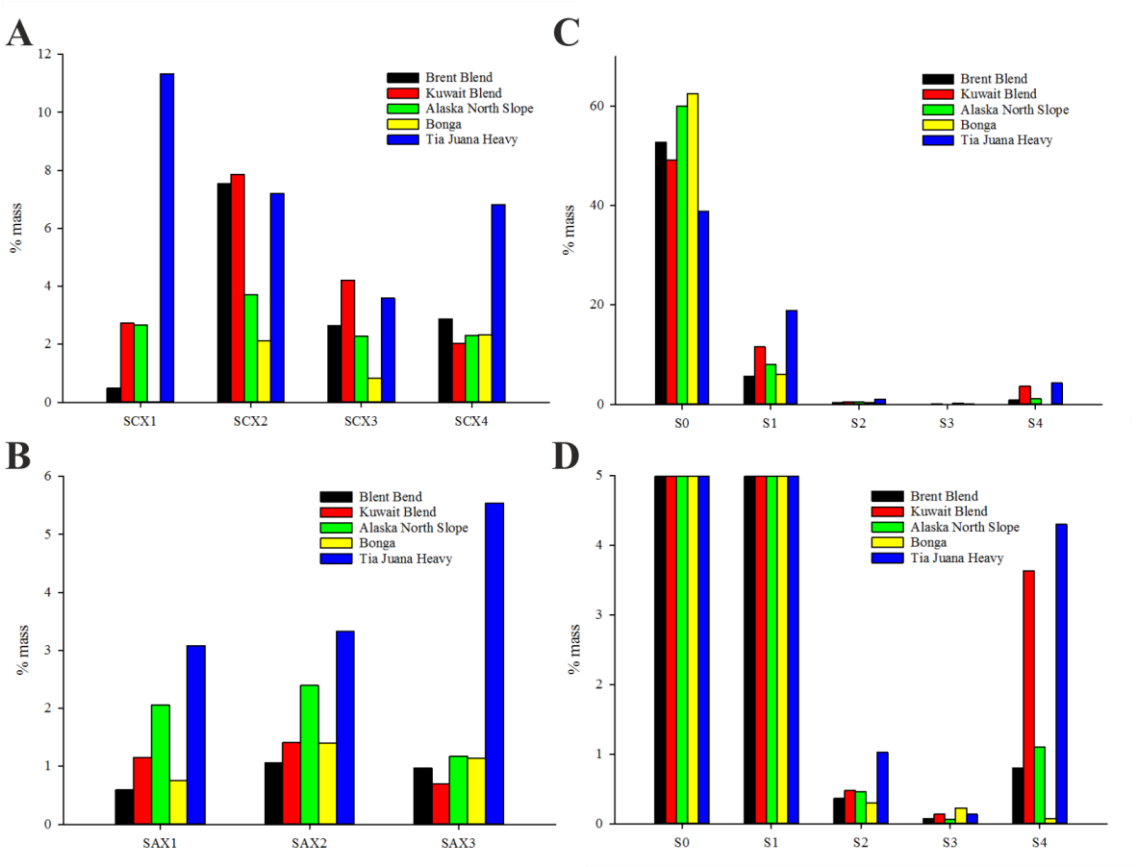

Figure 5-2 Gravimetric data (weight percent) of individual fractions from the SCX (**A**), SAX (**B**) and silica (**C**; with zoomed insert to show lower mass fractions, **D**) from the separation of the Brent Blend, Kuwait Blend, ANS, Bonga, and Tia Juana Heavy crude oils (in order of decreasing API gravity; 38.3 °, 31.4 °, 30.3 °, 29.4 ° and 12.1 °).

Previous studies have had some success in identifying relationships between the composition of crude oils and a number of physical properties. For example, trends in the masses of SARA (saturates, aromatics, resins and asphaltenes) fractions and certain physical properties, such as density and viscosity, have been well studied (Tissot and Welte, 1984). This compilation of work showed the existence of strong positive correlations (sample size 349, average regression coefficient = 0.8) between the four SARA fractions of crude oils; as the percentage of saturated hydrocarbons increased the percentage of asphaltenes decreased. Whilst a negative correlation between saturated hydrocarbon concentrations and crude oil density exists, it is weaker and it is now known

that the density and viscosity of crude oils are far more dependent on heavier crude oil components. Indeed, studies into the effects of biodegradation on the physical properties of crude oils have attributed changes in viscosity to the selective removal of the lower molecular weight *n*-alkanes (Peters *et al.*, 2005).

In the present study there appeared to be little correlation between fraction masses and API gravity (Figure 5-2), suggesting that detailed compositional variations are more subtle. Identifying gravimetric trends in individual fraction series was an important first step in evaluating method performance. Correlations identified by comparison of fraction masses with industrially relevant parameters (e.g. TAN and "acid fractions") helped to further evaluate the procedure.

As discussed in Chapter 4, **Fraction SCX1** is composed of the toluene soluble material that aggregated and deposited on the cartridge frit, and was considered 'asphaltenic' in nature. The masses of the SCX1 fraction (Figure 5-2A) show a general increase as crude oil API increases. However, the Bonga crude oil is an outlier, with no mass being eluted in the SCX1 fraction. Indeed, several studies have identified links between asphaltene concentration and crude oil density (e.g. Alboudwarej *et al.*, 2006; Malkin *et al.*, 2016; Padula *et al.*, 2016). However, these studies were only conducted on small sample groups and a more comprehensive investigation conducted by Evdokimov (2005), utilising over 350 crude oil samples, identified more subtle trends in asphaltene-density relationships. The result was the identification of two groups of crude oils, one in which density is greatly affected by low asphaltene content and another in which is determined by another parameter. This could help to explain the observation that the Bonga crude oil, with an API gravity of 29.4 °, did not deposit any material during separation and no material was collected in Fraction SCX1. Further support for this is the correlation between the mass of the SCX1 fractions and the percentage asphaltene content determined by a standard industry method (IP143; Figure 5-3A). The strong correlation between the IP143

(Institute, 2004) values and that of the SCX1 fraction, suggests the separation method developed herein could be employed to provide approximate values for crude oil asphaltene content. The SCX1 fraction can be rapidly obtained and data would be far cheaper to acquire than those obtained by the lengthy IP143 method.

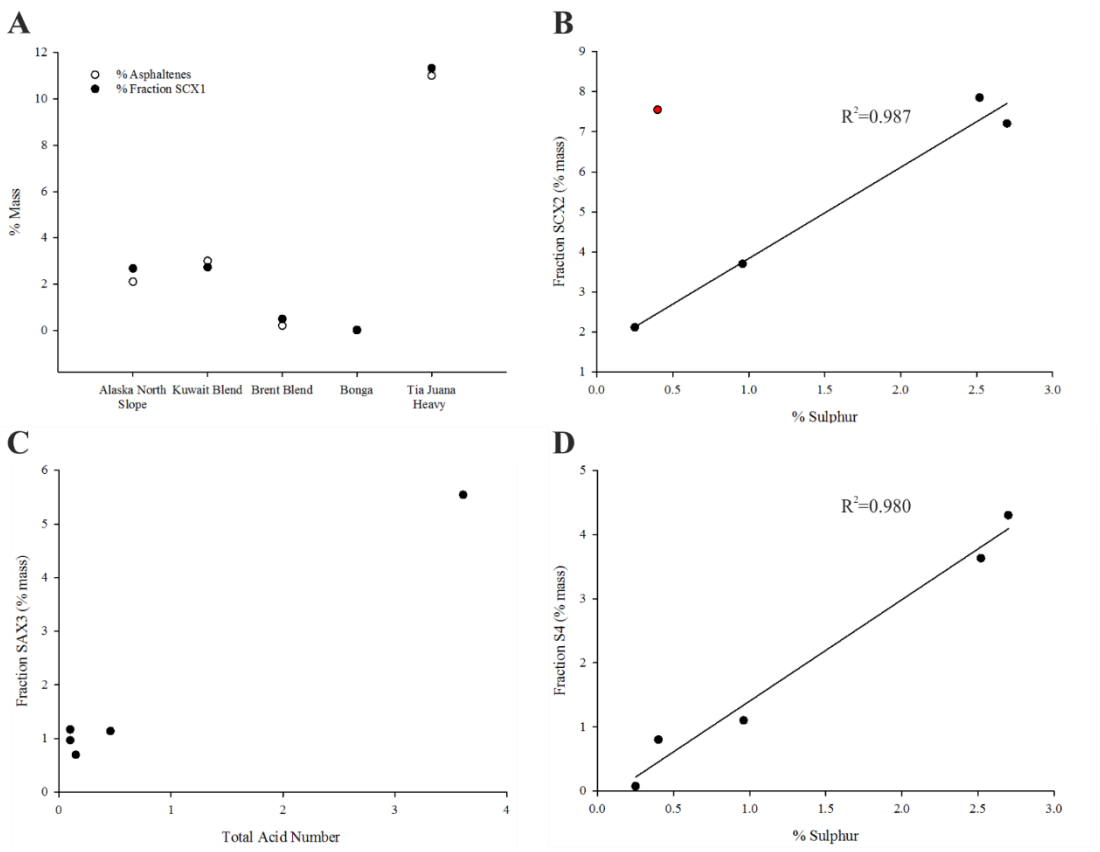

Figure 5-3. Plots showing the correlation between certain fraction masses and crude oil properties: **A**, a direct comparison between % mass of Fraction SCX1 and % asphaltene; **B**, % mass of Fraction SCX2 and % sulphur with outlier (Brent Blend) highlighted in red; **C**, % mass of Fraction SAX3 and Total Acid Number and **D**, % mass of Fraction S4 and % sulphur.

Fraction SCX2 was identified as containing the sulfoxide functionalised crude oil components by separation of the standard mixture of 'model' compounds. The data comparing the % sulphur and the % mass of Fraction SCX2 for the crude oils used in this study are presented in Figure 5-3B. The regression line plotted in Figure 5-3B excludes

the outlying Brent Crude oil data point (coloured red). This improves the regression coefficient to 0.987 from 0.382, showing excellent correlation between the SCX2 fraction mass and sulphur content of four of the crude oil samples. The elevated mass of the Brent Crude in relation to the percentage of sulphur can be attributed to a number of potential factors. Sulfoxides are not thought to occur naturally in crude oils but to be the product of the oxidation of sulfidic species when the oil is exposed to air (Payzant *et al.*, 1986). As a result, it is likely that the composition of crude oil sulfoxides is dependent on the conditions under which the samples are stored. It is also possible there is an additional input increasing the sulfoxide concentration within the sample or, more likely, the presence of another compound class with a similar chemistry.

The masses of the two ionic fractions, **SCX3 and SCX4** showed little correlation with known crude oil parameters and are not shown in Figure 5-3. Interestingly, the percentage mass of the **SCX4** fractions is significant for all five crude oil samples (2-7%). With crude oils containing on average only 0.03 ~% basic nitrogen (Tissot and Welte, 1984), the high masses observed in these 'basic' fractions was unexpected. Whilst the composition of **SCX4** can be predicted from the elution of the benzoquinoline 'model' compounds, the composition of the **SCX3** fraction remains unknown.

The masses of the **SAX 1 and SAX2** fractions showed similar trends when compared to the crude oil API gravities (Figure 5-2). With the exception of the Bonga crude oil, samples showed an increase in fraction mass with increasing API gravity (Figure 5-3). Interestingly, the mass of the **SAX2** (carbazole) fraction did appear to correlate with API gravity, unlike the trends seen for the basic **SCX3** and **SCX4** fractions.

The anionic fraction (**SAX3**) was identified as the acidic fraction by the elution behaviour of all five 'model' acids. Comparison of the gravimetric data with both API Gravity (Figure 5-2B) and TAN showed little correlation (Figure 5-3C). The Tia Juana Heavy

crude oil proportionally contained the highest percentage of acidic compounds (TAN; Table 5-1) which was reflected by the high fraction mass obtained from SPE separation. However, the four other crude oil samples had significantly lower acid concentrations and showed no relationship to the fraction masses obtained from the SPE separation (Figure 5-3C). In order to investigate further the efficiency of acid isolation, a suite of crude oils with a sequentially increasing TAN should be separated.

The gravimetric data for the saturated hydrocarbon fraction (**S0**; Figure 5-2C) do not appear to show a strong correlation with crude oil density. However, this correlation is greatly improved if it is assumed that the volatile losses occurring during solvent removal under N_2, solely affect the lower molecular weight hydrocarbons in the **S0** fraction. If the losses that occur during N_2 blowdown are summed to the masses of the **S0** fractions, the regression coefficient changes -0.66 to -0.82, thus suggesting a potential negative relationship between API gravity and saturated hydrocarbons.

'Aromatic' and ketone fraction masses (**S1-S3**) showed no relationship with the API gravity of the crude oils from which they were isolated (Figure 5-2A; B). There is however, a strong negative correlation (regression coefficient = -0.94) between the aromatic (**S1**) and saturated hydrocarbon (**S0**) fractions. This observation is in agreement with the aforementioned SARA correlations. The two ketone (i.e**. S2** and **S3**) fractions were only minor constituents (average 0.65% mass) of the five separated oils and masses showed little correlation to any of the available parameters. Interestingly, there appeared to be no correlation between either the masses of the ketone fractions (**S2** and **S3**) themselves, or the ketone fractions and acidic fractions (**SAX3**). This suggests the oxygen-functionalised compound classes in crude oils may be independent of each other, *i.e*. that ketone concentrations do not follow the same trends as those of the naphthenic acids.

Thiophenic compounds were identified previously in the **S4** fraction of the crude oil sample separations. However, both the quantification study and GC-MS analysis of the **S4** fraction of the ANS crude oil identified that this fraction only constituted a small percentage of the total thiophenic compounds in the sample (10% of dibenzothiophene standard in 'model' compound study). Therefore, the masses of the **S4** fractions could not be compared directly to the concentrations of sulphur within the samples. However, if there is good correlation between the percentage mass of the **S4** fraction and the total sulphur percentage, it could be assumed that the fractionation is unbiased in the relative amount of dibenzothiophenes that are retained per sample. This plot is shown in Figure 5-3 and shows a strong correlation (regression coefficient = 0.98).

5.4.2 Fraction SCX1 (unidentified compounds)

As described previously in Section 5.4.1 and in Chapter 4 the SCX1 fraction, was thought to be composed of asphaltenic material. With an average molecular weight of ~750 $gmol^{-1}$ and a tendency to aggregate (Subramanian *et al.*, 2016), the asphaltenes as a compound class are not amenable to traditional GC techniques. Attempts at employing high temperature GC (HTGC) to analyse both derivatised and non-derivatised fractions were unsuccessful (Appendix 4). Analysis by LC-HRAM-MS (reversed phase; ESI ionisation) also failed, likely due to issues with compound ionisation and solubility.

Analysis of fractions by Fourier Transform-Infrared Spectroscopy (FT-IR) provided limited information on the functionality of the SCX1 fractions (data not shown). The spectra of all five SCX1 fractions were dominated by peaks at ~2990 cm^{-1} and 2850 cm^{-1} corresponding to the symmetrical and antisymmetrical stretching of the C-H bond. A shoulder on the C-H peak at 3000-3050 cm^{-1} consistent with C=C-H stretching and a sharp peak at 1490 cm^{-1} caused by the C=C-C stretching of benzene rings, evidence the high aromaticity of these fractions.

Typically, investigations into the composition of asphaltenes and asphaltene like material employ the use of FT-ICR-MS instruments with atmospheric pressure photo/laser ionisation (APPI or APLI) to characterise samples. Studies such as those by Gaspar *et al.* (2012) and Pereira *et al.* (2014a) have demonstrated the successful analysis of asphaltenic material by such techniques. Whilst this instrumentation provides no structural information, it does allow for unequivocal molecular assignments, allowing the degree of unsaturation/aromaticity and the distribution of compound functionality to be obtained.

Whilst further characterisation of the SCX1 fraction was not conducted as a part of this study, attaining information on the distribution of the various compound classes within this fraction is of interest. However, at this time suitable analytical techniques are not

available. Further plans for investigating the composition of the SCX1 fraction are discussed in Chapter 2.

5.4.3 Fraction SCX2 (sulfoxides)

Separation of the 'model' compound mixture identified the SCX2 fraction as containing the benzyl sulfoxide model compound and can thus be crudely labelled as a "sulfoxide fraction" for simplicity. Such an assignment also agrees well with the results of previous uses of cation exchange resins to isolate sulfoxides from crude oils (Okuno *et al.*, 1967; Snyder and Buell, 1968).

The five different crude oil SCX2 fractions were each subjected to analysis using GC-MS in order to study their broad composition. No attempt was made at detailed characterisations of each oil fraction as this was beyond the scope of the present work. For present purposes, it was deemed sufficient simply to identify some sulfoxides in order to demonstrate the general nature of this fraction. Sulfoxides are in any event usually assumed to be the products of the secondary oxidation of sulphides in crude oils and thus their distributions likely reflect sample history and storage (Liu *et al.*, 2010b).

SCX2 fractions were analysed using GC-MS at equal concentrations (5 $mgmL^{-1}$) and results (Figure 5-4) showed the compositions of each oil fraction to be varied. Thus, chromatograms obtained from the Kuwait Blend and TJP samples (Figure 5-4 B and E) suggested that much of these particular SCX2 fractions was likely comprised of higher molecular weight (>550 $gmol^{-1}$) materials, since relatively low proportions of each fraction eluted within the 36 minutes GC analysis time. In contrast, the chromatograms obtained from the Brent, ANS and Bonga crude oils (Figure 5-4 A, C and D) were characterised by larger responses within the analytical window; however, much of the material was present as an unresolved complex mixture by GC (*viz* so-called UCM).

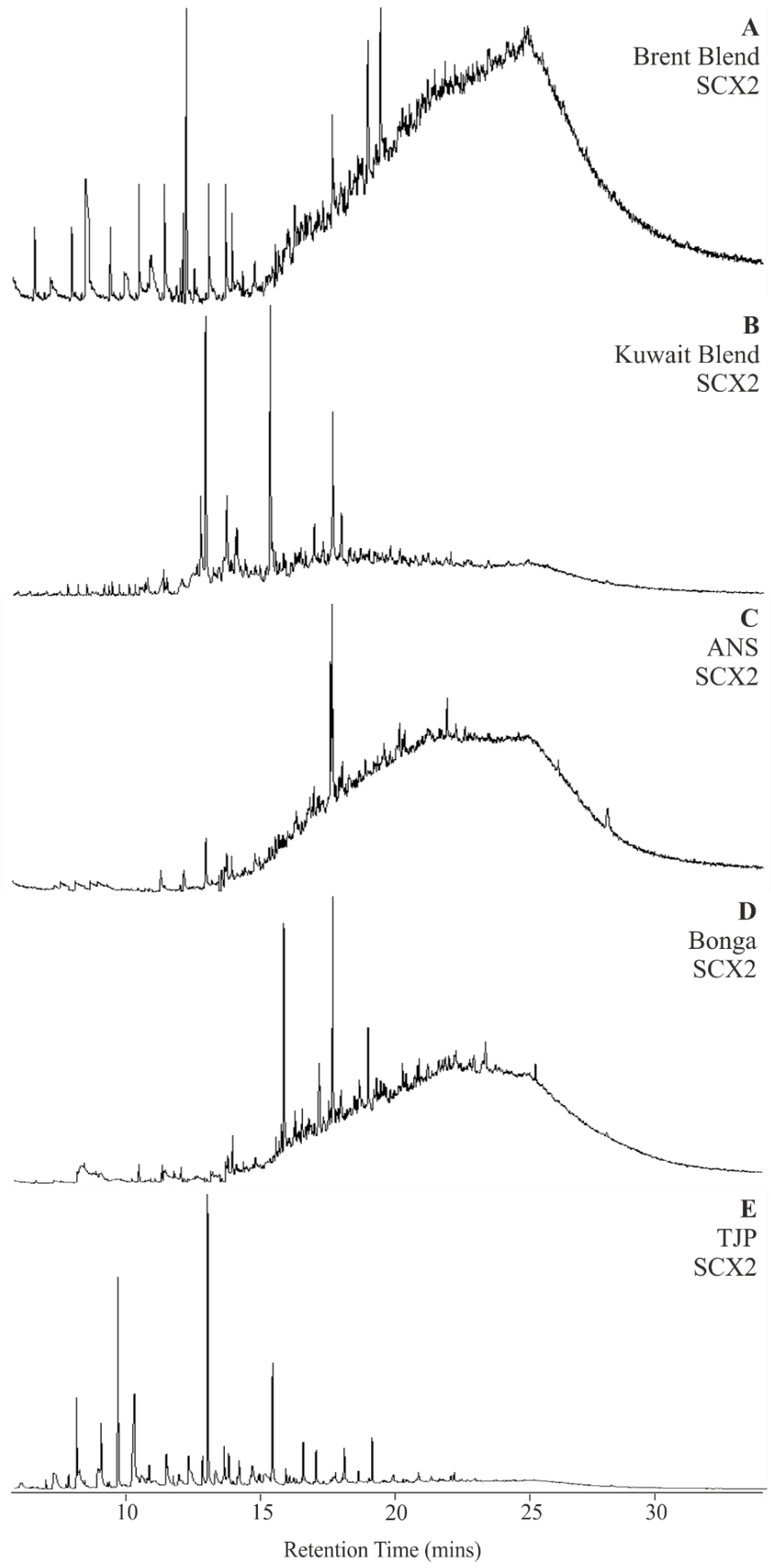

Figure 5-4. GC-MS TICs of the SCX2 fractions obtained from the SPE separation of the Brent Blend (**A**), Kuwait blend (**B**), ANS (**C**), Bonga (**D**) and TJP (**E**) crude oils.

Further investigation into the molecular composition of the SCX2 fractions were focused on the fraction isolated from the ANS crude oil. Analysis of this fraction using GC×GC-MS provided improved chromatographic resolution, allowing clear mass spectra of individual compounds to be obtained. Inspection of the GC×GC-MS TIC (Figure 5-5) showed the presence of a number of abundant component peaks. The mass spectrum (Figure 5-7D) of the most abundant of these peaks (Figure 5-5A) possessed a molecular ion of *m/z* 228 and an intense $M^{+\cdot}$-17 ion, indicative of the loss of an -OH moiety, suggesting possible sulfoxide functionality (Budzikiewicz *et al.*, 1967; Seizo and Shigeru, 1972).

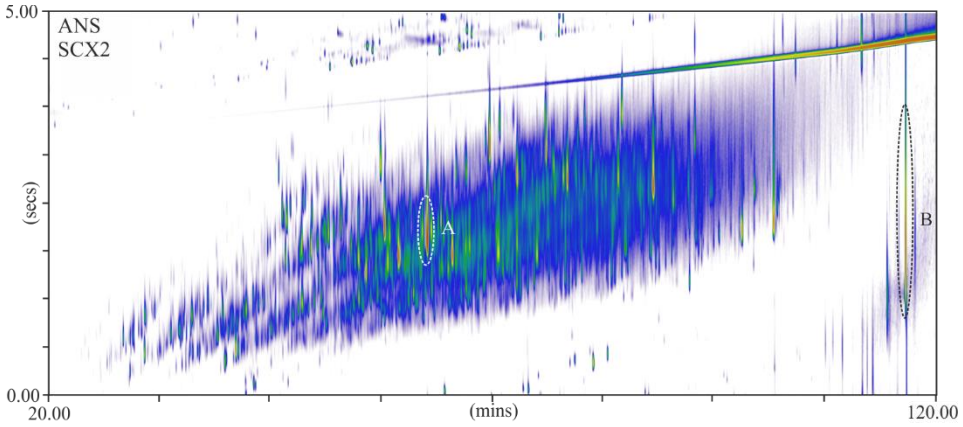

Figure 5-5. GC×GC-MS TIC from the analysis of Fraction SCX2; abundant peaks (**A** and **B**) are highlighted and labelled.

The presence of a compound producing a similar spectrum was observed in a study on the composition of sulfides and sulfoxides in an Athabasca Bitumen (Payzant *et al.*, 1983), where it was tentatively assigned as a terpenoidal bicyclic sulfoxide, consisting of condensed cyclohexane and cyclopentane rings. This assignment was corrected in their later work (Payzant *et al.*, 1988), when synthesis of reference compounds showed the compound in fact to be comprised of two condensed cyclohexane rings (structure shown in Figure 5-6A). Comparison of the mass spectrum of peak A (Figure 5-7D) in the ANS crude oil with the mass spectra obtained by Payzant *et al.* (1988) allowed for confident

assignment as the bicyclic terpenoid sulfoxide structure. Also identified by Payzant *et al.* (1983; 1988) was a larger, tetracyclic terpenoid sulfoxide structure (Figure 5-6B). Extraction of the molecular ion (*m/z* 364) in the SCX2 fraction isolated from the ANS crude oil revealed a late eluting peak. The mass spectrum of the peak (Figure 5-7E) was characterised by an intense ion at *m/z* 347, corresponding to a loss of -OH ($M^{+\cdot}$-17) moiety as well as a series of low *m/z* ions, comparable to those of the bicyclic sulfoxides. The mass spectrum compared well with that presented by Payzant *et al.* (1988) leading to a confident assignment of the peak as the tetracyclic terpenoid sulfoxide (Figure 5-6B).

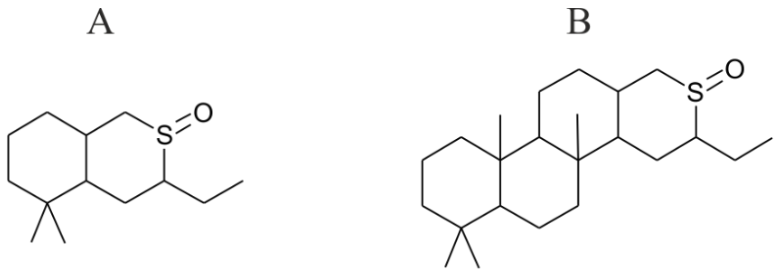

Figure 5-6. Structures of the tentatively identified bicyclic (**A**) and tetracyclic (**B**) terpenoid sulfoxides in the ANS crude oil

Extraction of the molecular ions of lower alkylated homologues of these compounds (*m/z* 186, 200 and 214; C_1, C_2 and C_3 substituted) of the C_2 substituted bicyclic terpenoidal sulfoxide (228 Da; Figure 5-6A) revealed the presence of the expected series. A reasonable library match was obtained for the C_1 homologue (*m/z* 186; Figure 5-7A and Ai; RMatch 889 for example). The tentative identification of the peak at *m/z* 186 further evidenced the presence of this series as a group of methyl substituted bicyclic sulfoxides. The C_2 and C_3 homologues (Figure 5-7 B and C) were tentatively assigned based on similarities in their mass spectra and their position within the chromatographic series.

The mass spectra of the bicyclic sulfoxides (Figure 5-7A-D) were dominated by an ion due to the loss of the -OH moiety ($M^{+\cdot}$-17), as well as a series of high intensity ions at *m/z* 55, 69, 81, 95, 109 and 123, characteristic of the dimethyl-substituted cyclohexyl ring

(Figure 5-6A). Common losses of $M^{+\cdot}$-31 (loss of -OH followed by loss of CH_2 or loss of OCH_3) and $M^{+\cdot}$-49 (loss of -OH followed by loss of S) can only be mechanistically rationalised by sequential loss of an –OH moiety followed by loss of an additional fragment. The mass spectrum of the ethyl-substituted structure (Figure 5-7D) exhibits a loss of $M^{+\cdot}$-45, corresponding to the loss of –OH followed by the loss of C_2H_4.

Attempts to identify the dibenzyl sulfoxide 'model' compound and its alkylated homologues in the SCX2 fractions by extraction of their molecular ions (*m/z* 230, 244, 258 and 272), did not reveal their presence in any of the five crude oils. Nonetheless, the positive identification of the above sulfoxide biomarkers (Figure 5-5 to 6) within the ANS SCX2 fraction suggests that isolation of a "sulfoxide" fraction had been successful. However, the high complexity and variability of the fractions combined with the absence of sufficient reference mass spectra, makes their characterisation challenging. Additionally, the natural presence of sulfoxides in crude oils is unlikely. It is largely agreed that sulfoxides in crude oils are generated by the in-air oxidation of sulfidic species. It is therefore likely that these identified sulfoxide structures were originally associated sulfides. Indeed, in the work of Payzant *et al.* (1983; 1986; 1988), sulfides were deliberately oxidised to the sulfoxides in order to facilitate their separation, implying the likely sulfidic origin of the species studied herein.

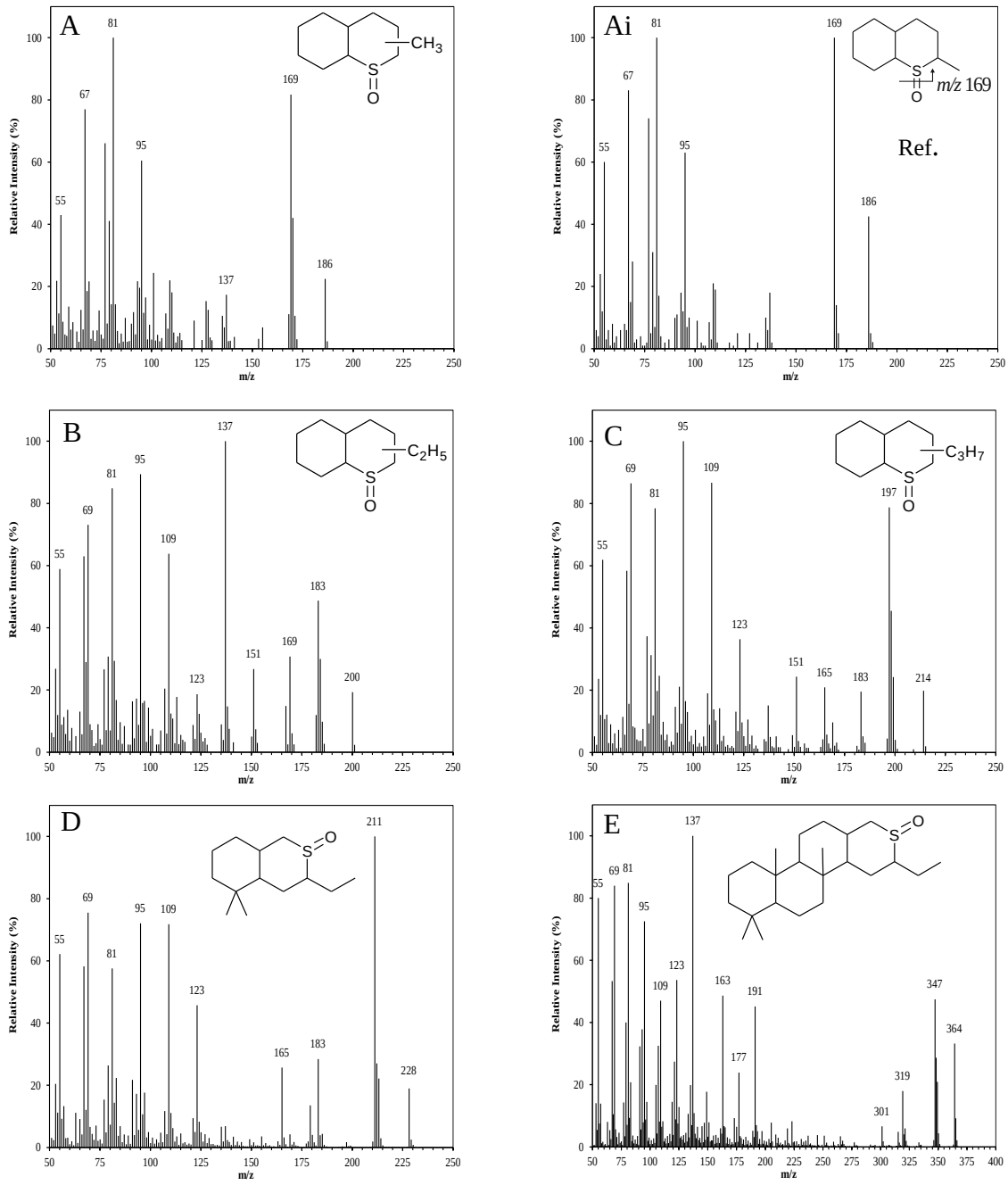

Figure 5-7. Examples of tentative mass spectral identification of alkylated bicyclic sulfoxides from the analysis of Fraction SCX2 (ANS crude oil separation; **A**-**C**) and of bicyclic and tetracyclic terpenoid sulfoxides (**D** and **E**). Individual compounds identified by comparison of spectra obtained from crude oil analyses with the NIST library (**A**-**A**i) and from position within the homologous series and mass spectral interpretation (**B**-**E**).

5.4.4 Fraction SCX3 (unidentified compounds)

Attempts to investigate the composition of the SCX3 fractions were met with significant challenges. Initial screening using GC-MS was unsuccessful in the cases of all five SCX3 fractions, in that no GC-MS amenable compounds were observed (data not shown). Attempts to derivatize the fraction with derivatising agents of increasing potency (BSTFA and SYLON BTZ) to render a more GC-amenable mixture were also unsuccessful (data not shown). Assuming that the issue was related to the high average molecular mass and/or high polarity of components of this fraction, attempts were made to analyse the fraction using LC-HRAM-MS but ionisation using electrospray was unsuccessful. Possible future strategies for the analysis of the SCX3 fraction are discussed in Chapter 7.

5.4.5 Fraction SCX4 (basic nitrogen compounds)

Separation of crude oils by cation exchange chromatography facilitated isolation of basic materials. Fraction SCX4 consisted of the most basic crude oil components, requiring the use of aggressive solvent conditions (THF/H_2O/ammonia; 20 mL; 0.1%/5%; v/v/v) to remove the strongly bound ionic material. Pyridinic compounds are thought to comprise the majority of crude oil bases (Yamamoto *et al.*, 1991), and elution of the benzoquinoline model compound within the SCX4 fraction suggested successful isolation of a basic nitrogen fraction. Attempts at analysis by GC were largely unsuccessful, with neither benzoquinoline (179 Da) nor its alkylated homologues (193, 207, 221 Da) being detected in any of the five SCX4 fractions. Failure of the GC analysis was thought to be due to the absence or low abundance of low boiling point constituents, suggesting the need for an approach in which a higher mass range could be accessed.

Analysis of the higher molecular weight species in crude oil presents a number of unique challenges. Higher molecular weight compounds will have a larger number of carbon

atoms per structure, resulting in a dramatic increase in the number of potential structural arrangements. Additionally, the higher molecular weight fractions of crude oils are typically enriched in heteroatoms, and complex isotopic distributions require high or ultra-high mass resolution instruments to assign molecular formula confidently. Fortunately, the development of high-resolution accurate mass/mass spectrometers (HRAM-MS) such as Fourier transform-ion cyclotron resonance (FT-ICR), Orbitrap and time-of-flight (ToF) mass spectrometers satisfy such requirements, achieving mass resolutions of >300,000, >70,000 and >10,000 respectively (at *m/z* 200).

Many atmospheric pressure ionisation techniques are employed to analyse petroleum mixtures in combination with HRAM-MS techniques. Techniques such as electrospray ionisation (ESI), atmospheric pressure chemical ionisation (APCI), atmospheric pressure photoionisation (APPI) and atmospheric pressure laser ionisation (APLI) are all regularly employed in petroleum analysis (Lababidi *et al.*, 2013). Recent work by Huba *et al.* (2016) utilised a series of model compounds to investigate the ionisation efficiency of various atmospheric pressure ionisation techniques. This publication highlighted substantial variations in the ionisation efficiency for commonly studied crude oil derived compound classes. Many authors (e.g., Bae *et al.*, 2010; Purcell *et al.*, 2010; McKenna *et al.*, 2013; Pereira *et al.*, 2014a; Silva *et al.*, 2016) have published work in which the relative abundances of various compound classes are compared, assuming that this abundance reflects the true ratio of compound classes in the samples. However, in no cases have they employed reference compounds, adjusting their analyses for potential differences in ionisation efficiency.

Isolation of the benzoquinoline model compound in the SCX4 fraction, suggested components were characterised by a pyridinic functionality. The work of Huba *et al.* (2016) showed electrospray ionisation (ESI) operating in positive mode to be the most efficient mode of ionisation for such compounds. Therefore, initial HRAM-MS analyses

employed +ESI FT-ICR-MS to characterise molecular compositions of the SCX4 fractions.

Broadband mass spectra obtained from the analysis of the SCX4 fractions showed only minor differences in molecular composition (example shown in Figure 5-8). Ions detected in this fraction ranged from *m/z* 270-1200, with maximum ion abundance occurring between *m/z* 500-600. The dominance of even ions in the mass spectra suggested the compounds are detected as protonated species $[H]^+$, consistent with previous reports of the ionisation of pyridinic nitrogen species (Vasconcelos *et al.*, 2017). Approximately 14000 peaks were detected in each mass spectrum (range 11000-19000) and peaks were assigned molecular formulae based on the following criteria: C 0-100, H 0-200, N 0-10, S 0-10 and O 0-20.

Examination of the lower mass regions (*m/z* 200-300; *e.g.*, Figure 5-8) showed a distinct absence of ions. Ions corresponding to the presence of the $C_{2\text{-}5}$ benzoquinolines ([H]; *m/z* 208, 222, 236, 250) were not present in any of the five mass spectra. Potential reasons for the absence of lower molecular weight ions are numerous. Most likely, is that these constituents are too low in abundance relative to the higher molecular weight species. Whilst ESI is typically a sensitive ionisation method (Ikonomou *et al.*, 1990), the linearity of ESI efficiency is often lost at high concentrations ($> 10^{-5}$ M). In experiments where highly complex samples are infused directly, competition for charge or space charge results in a significant loss in sensitivity for compounds of lower abundance. Therefore, in order to detect less abundant species, it would be beneficial to conduct additional pre-separations (i.e., SPE) or online separations.

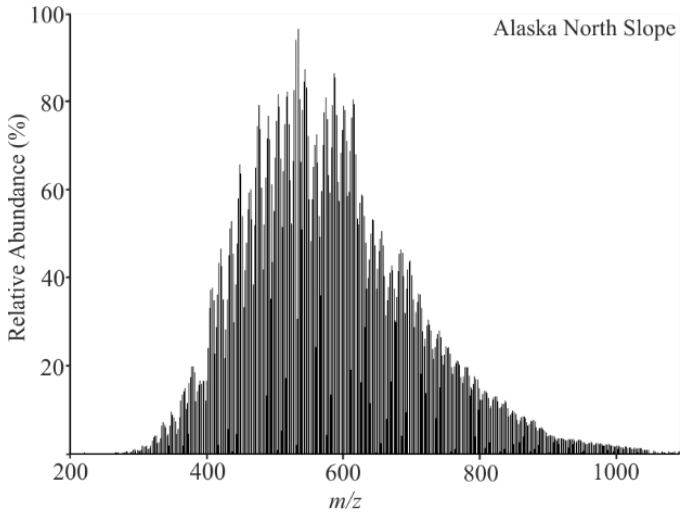

Figure 5-8. Example of the FT-ICR-MS mass spectrum obtained from the analysis of the SCX4 fractions of ANS crude oil.

The distribution of the assigned compound classes are presented in Figure 5-9. Most notable is the dominance of the N1 compound class, demonstrating the model compound prediction for the SCX4 fraction was successful. Indeed, all assigned formula contained at least one nitrogen atom, suggesting all fraction components possess a basic nitrogen functionality. Interestingly, the Kuwait Blend and TJP, both contain a higher relative concentration of the N1S1 species, reflecting their high sulphur content. The presence of the O2 species (N1O2 and N1O2S1) in the TJP crude oil is also of interest, and is likely linked to its high state of biodegradation.

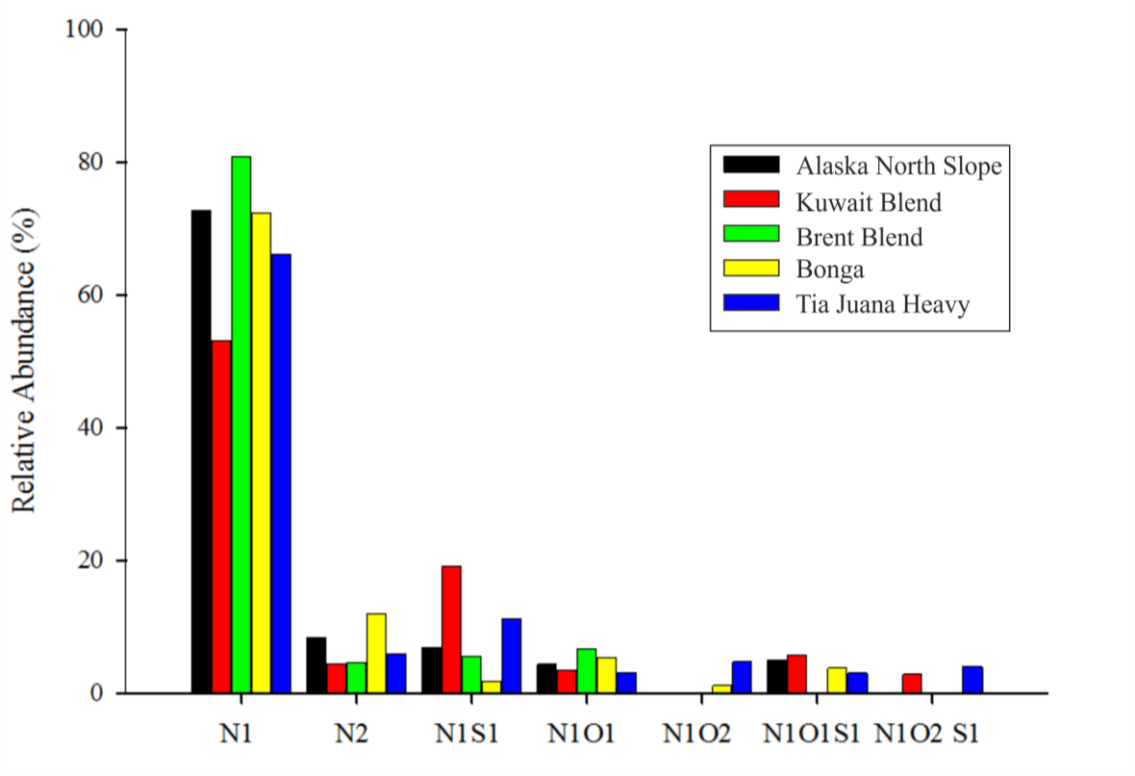

Figure 5-9. Compound class distribution obtained from the FT-ICR-MS analysis of the SCX4 fractions from the separation of the five crude oil samples.

In an attempt to identify compositional differences, three-dimensional Van Krevelen diagrams were plotted. The diagrams were plotted for the N1 compound series, showing changes in the degree of alkylation (plotted as the ratio of hydrogen/carbon; a higher value being indicative of higher degrees of alkylation) against increasing carbon number. Examination of the generated plots (Figure 5-10) show only minor differences in the composition of the SCX4 fractions. The plot obtained from the Bonga SCX4 fraction shows the most significant differences, showing a slight increase in the abundance of the lower molecular weight compounds and a smaller H/C range. The more abundant N1 species all show similar distributions, with hydrogen/carbon ratios ranging from ~1.30 to 1.80 and a carbon numbers ranging from ~25 to 55. These data sets compare well with those observed in previously conducted FT-ICR-MS studies on N1 compounds, suggesting highly conjugated aromatic, nitrogen containing cores with varying degrees of alkylation (Chen *et al.*, 2012; Xiaobo *et al.*, 2014).

Interestingly, two or three areas of high relative abundance can be easily identified within each of the plots (relative abundance of 80-100; orange/red; Figure 5-10). These areas of increased abundance occur within the same region in each of the five samples, and are concentrated at the C_{34} (Bonga), C_{38} and C_{42} carbon numbers. The reasons for the dominance of these particular carbon numbers in the N1 series are unknown. Indeed, such carbon numbers are common in biologically derived material, and a number of geochemical biomarkers possessing different functionalities are found in these ranges (*e.g.*, C_{39} alkanones, C_{40} isorenieratene and derivatives and others). However, without additional structural information, no further significance can be attributed to these more abundant series.

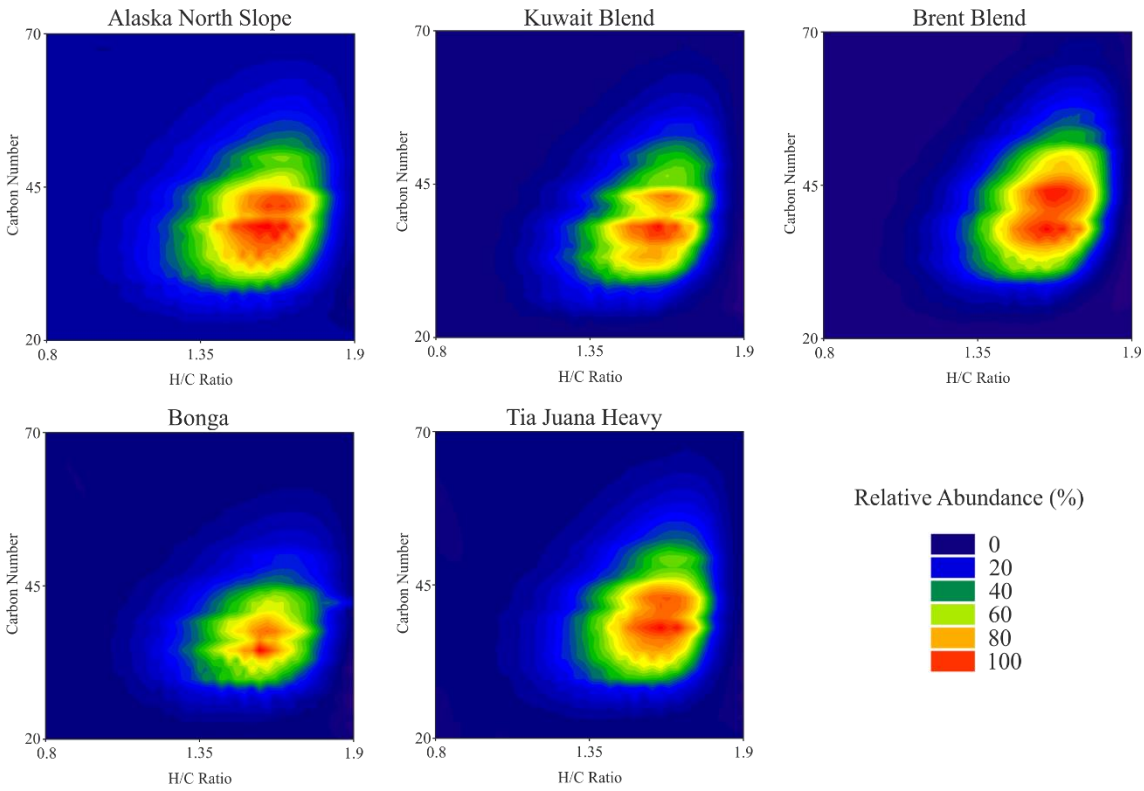

Figure 5-10. Van Krevelen diagrams of the N1 compounds in the five crude oil samples.

Whilst Van Krevelen diagrams are a valuable tool for presenting FT-ICR-MS data, they are only suitable for observing trends in compound distributions. In this instance, as crude oil samples are independent, and not part of a defined series, the plots provide only limited

information. Additionally, although the FT-ICR-MS instruments provide unparalleled mass resolution, information is only gathered on a molecular level, and no information on the structural iterations for each generated molecular formula is available. Despite this, it is common to see such assignments made within the literature (e.g., Xiaobo *et al.*, 2014; Kong *et al.*, 2015). Without any addition information, these assignments are speculative, and in order to make any structural identifications, a chromatographic separation must be performed prior to mass analysis. A number of authors have attempted to couple liquid chromatography (LC) with FT-ICR-MS instrumentation to improve the selectivity of their experiments (Lababidi *et al.*, 2013; Lababidi and Schrader, 2014). However, the high acquisition time (>1 scan sec^{-1}) of ICR instrumentation results in poor chromatographic resolution and only bulk, class type separations have been achieved.

The application of LC-MS to crude oil samples has historically encountered a number of difficulties. Issues with solvent compatibility, solubility, sufficient sensitivity and ionisation, have all made the analysis of crude oils problematic. Recently technological advances have resulted in substantial improvements in ionisation efficiency and separation techniques and, as a result, the application of LC-MS is becoming more commonplace in petroleum analysis (Molnárné Guricza and Schrader, 2015b; Ghislain *et al.*, 2017; Thiäner and Achten, 2017).

Applications utilising routine LC-MS analysis typically employ reversed phase LC, coupled with ESI ionisation. This set up is particularly useful for the analysis of polar species, but is largely incompatible with the majority of crude oil components, especially if the whole oil has not been pre-fractionated. Solubility issues, likely due to the high aromaticity of basic crude oil fractions and previously poor instrumental limits of detection have likely made previous attempts at such analysis challenging. As a result, this appears to be the first instance that LC-high resolution accurate mass (HRAM)-MS has been applied to characterise the structures of basic crude oil components.

LC-HRAM-MS analyses were first focused on the development of optimised chromatographic conditions for the separation of the ANS crude oil SCX4 fraction. Whilst initial attempts afforded no chromatographic separation, extraction of the molecular ions for the alkylated benzoquinolines revealed their (putative) presence in the fraction (Figure 5-11A). As predicted, the LC separation vastly improved the sensitivity towards the lower molecular weight fraction components. Indeed, the ions for $C_{2\text{-}7}$ alkyl benzoquinolines were sufficiently abundant to be seen within the base peak chromatogram and were employed as markers to optimise the chromatographic separation.

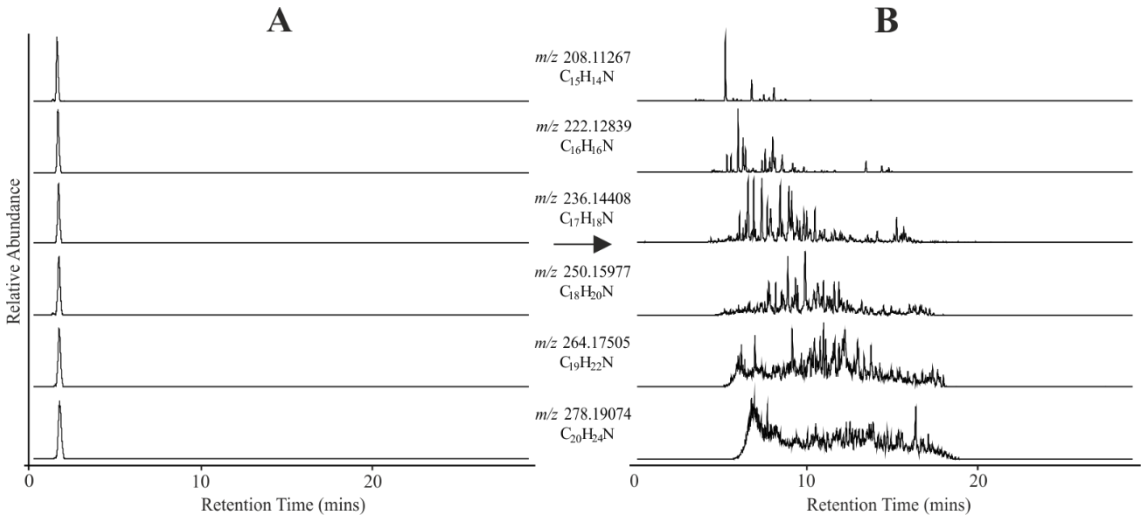

Figure 5-11. EICs of the protonated adducts of the $C_{2\text{-}7}$ alkyl benzoquinolines (accurate masses shown) from the LC-HRMS analysis of the ANS, SCX4 fraction, showing no separation (**A**) and the optimised separation conditions (**B**).

Figure 5-11 highlights the successful development of the chromatographic separation, with Figure 5-11B showing the separation of the tentatively assigned $C_{2\text{-}7}$ alkyl benzoquinoline ions under the optimised conditions. Also emphasised in Figure 5-11B, were the increasing number of structures present for each molecular formula, information that had not been accessible by FT-ICR-MS analysis.

In the absence of suitable mass spectral libraries, a series of reference compounds were employed to assign individual structures within the SCX4 fractions. Comparison of retention times and mass spectra, obtained from fragmentation experiments, allowed for the tentatively identified series of quinolines to be further confirmed in the fractions, some for the first time. A series of benzoquinolines (including C_{1-3} alkylated homologues) and phenylquinolines (including C_{1-2} alkylated homologues) were obtained to facilitate these investigations (Figure 5-12). Compounds were separated and subject to fragmentation experiments in order to generate mass spectra for comparison, and to identify any trends in quinoline fragmentation.

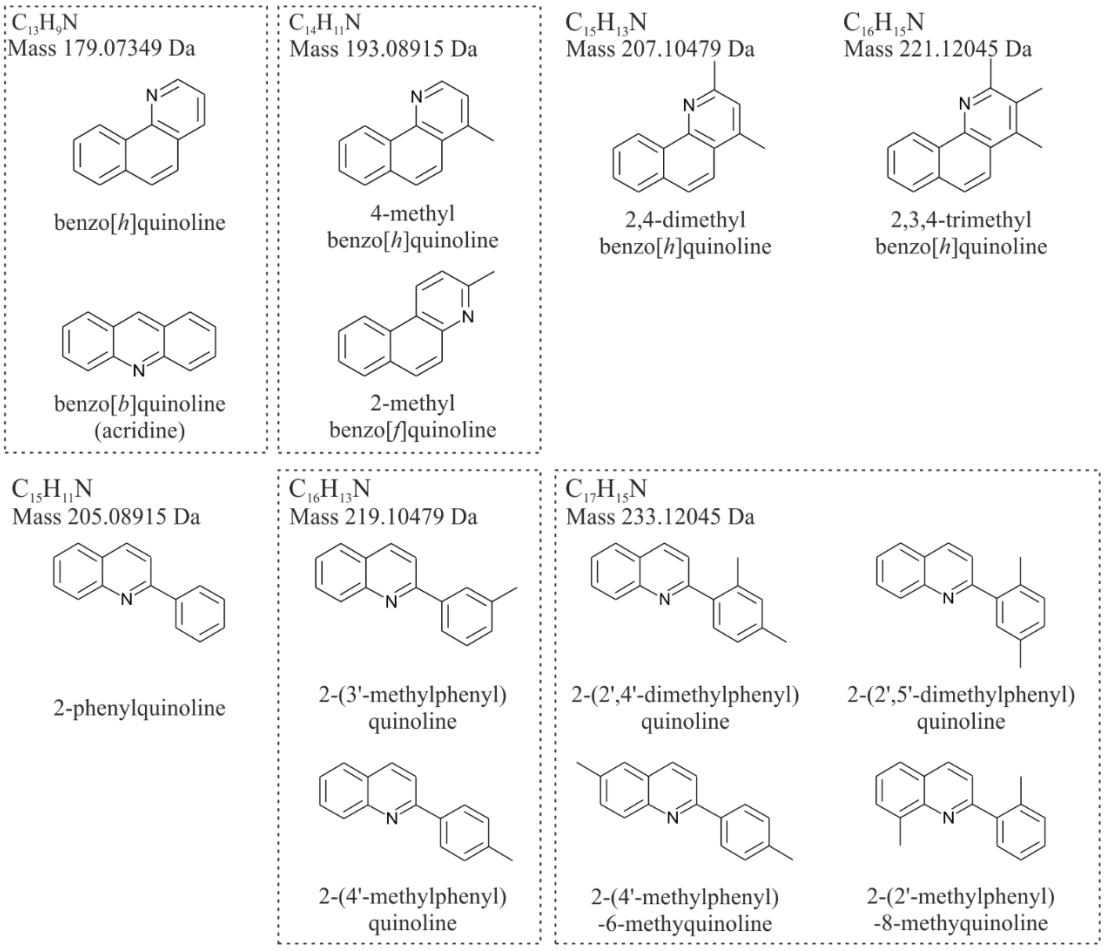

Figure 5-12. Labelled structures, molecular formulae and accurate mass of the six model benzoquinoline compounds and the seven model phenylquinoline compounds used to investigate the composition of the SCX4 fractions.

Unlike electron impact (EI) ionisation (used in GC-MS applications), ESI does not typically induce source fragmentation and is considered a 'soft' ionisation technique. Therefore, fragmentation must be conducted on the generated ions before detection. In the case of Orbitrap instruments (Thermo Fisher Scientific), fragmentation is conducted in a higher-energy collisional dissociation (HCD) cell. Developed by Olsen *et al.* (2007), HCD is a collision induced dissociation (CID) technique in which collision occurs in a dedicated multipole collision cell. In this cell, ions are accelerated and allowed to collide with nitrogen molecules, resulting in bond breakages and fragmentation (Wells and McLuckey, 2005). By altering the electrical potential, the kinetic energy of the collisions can be controlled, thus varying the degree to which ions fragment. In this work, model compounds were fragmented at multiple collision energies (CE) allowing the creation of a "fingerprint" mass spectrum for each model compound. This fingerprint could then be compared to equivalent mass spectra obtained from crude oil derived samples. The thirteen model compounds were fragmented at the following CE: 25, 35 and 50 eV.

Mass spectra obtained from the HCD fragmentation of 2,4-dimethylbenzo[*h*]quinoline are shown in Figure 5-13. Low energy collisions resulted in only minor fragmentation, with a base peak ion consistent with the protonated adduct of the dimethylbenzoquinolines ($[M+H]^+$; *m/z* 208.11218). The mass spectrum obtained at a collision energy of 35 eV gave significant product ions at *m/z* 193.08879, 165.07013 and 152.06213, identified as $C_{14}H_{11}N^+$, $C_{13}H_9^+$ and $C_{12}H_8^{\cdot+}$, respectively, by accurate mass measurements. Losses are rationalised in Figure 5-13, with the product ion at *m/z* 193.08879 being rationalised by the loss of either methyl group ($\cdot CH_3$; $[M+H]^+$-15). The product ion at *m/z* 165.07013 forms from the likely loss of a neutral ethanimine (C_2H_5N; $[M+H]^+$-43) molecule, rationalised by the structure shown in Figure 5-13, with a potential rearrangement to the positively charged fluorene structure, common to heterocyclic systems containing diphenyl substituents (Bowie *et al.*, 1968). Finally, the product ion at

m/z 152.06213, is rationalised by the formation of the biphenylene ion, also commonly observed in the fragmentation of condensed heterocyclic systems (Porter and Baldas, 1970). The highest energy collisions (50 eV) show a substantial reduction in the higher molecular weight ions, with a new base peak at *m/z* 165.07013. Additionally, two lower molecular weight product ions at *m/z* 128.06235 ($C_{10}H_8^{\cdot+}$) and *m/z* 115.05470 ($C_9H_7^+$) were assigned.

Table 5-3. Summary of the benzoquinoline HCD (25, 35 and 50 eV) collision experiments.

Model Compound	Monoisotopic Mass	$[M+H]^+$	Product Ion 1		Product Ion 2		Product Ion 3	
			m/z	Formula	*m/z*	Formula	*m/z*	Formula
Benzo[*h*]quinoline	179.07349	180.08077	152.06213	$C_{12}H_8^+$				
Benzo[*b*]quinoline			152.06213	$C_{12}H_8^+$	128.04979	$C_9H_6N^+$		
4-methyl benzo[*h*]quinoline	193.08915	194.09642	178.06529	$C_{13}H_8N^+$	165.07009	$C_{13}H_9^+$	152.06213	$C_{12}H_8^{\cdot+}$
2-methyl benzo[*f*]quinoline			179.07315	$C_{13}H_9N^{\cdot+}$	165.07013	$C_{13}H_9^+$	152.06213	$C_{12}H_8^{\cdot+}$
2,4-dimethyl benzo[*h*]quinoline	207.10479	208.11207	193.08879	$C_{14}H_{11}N^{\cdot+}$	165.07013	$C_{13}H_9^+$	152.06213	$C_{12}H_8^{\cdot+}$
2,3,4-trimethyl benzo[*h*]quinoline	221.12045	222.12773	207.10452	$C_{15}H_{13}N^{\cdot+}$	192.08083	$C_{14}H_{10}N^+$	165.07013	$C_{13}H_9^+$

Results from the fragmentation by HCD of the benzoquinoline series are summarised in Table 5-3. Both benzoquinoline isomers readily form a product ion at *m/z* 152.06213 ($C_{12}H_8^{\cdot+}$), however the linear, benzo[*b*]quinoline forms an additional product ion at *m/z* 128.06235 ($C_9H_6N^+$), likely taking the structure of quinoline. Fragmentation of the methyl benzoquinolines resulted in similar fragmentation patterns. Both isomers showed the initial loss of the methyl substituent (Table 5-3), with 2-methylbenzo[*f*]quinoline losing a neutral methane molecule (CH_4; 16 Da) forming a product ion at *m/z* 178.06529 ($C_{13}H_8N^+$) and 4-methylbenzo[*h*]quinoline losing a $\cdot CH_3$ radical forming a product ion at *m/z* 179.07315 ($C_{13}H_9N^{\cdot+}$). The methylated isomers also form *m/z* 165.07013 ($C_{13}H_9^+$) and *m/z* 152.06213 ($C_{12}H_8^{\cdot+}$) product ions, of which the *m/z* 152.06218 dominates. The

di- and tri-methylbenzoquinoline structures also show the initial loss of the methyl substituents (·CH_3; $[M+H]^+$-15) followed by the formation of smaller, condensed aromatic product ions (e.g., *m/z* 165.07013 and 152.06213), forming from the higher energy collisions. In this way, differences between molecular ion adducts and product ions can be useful in differentiating which benzoquinoline structures are present.

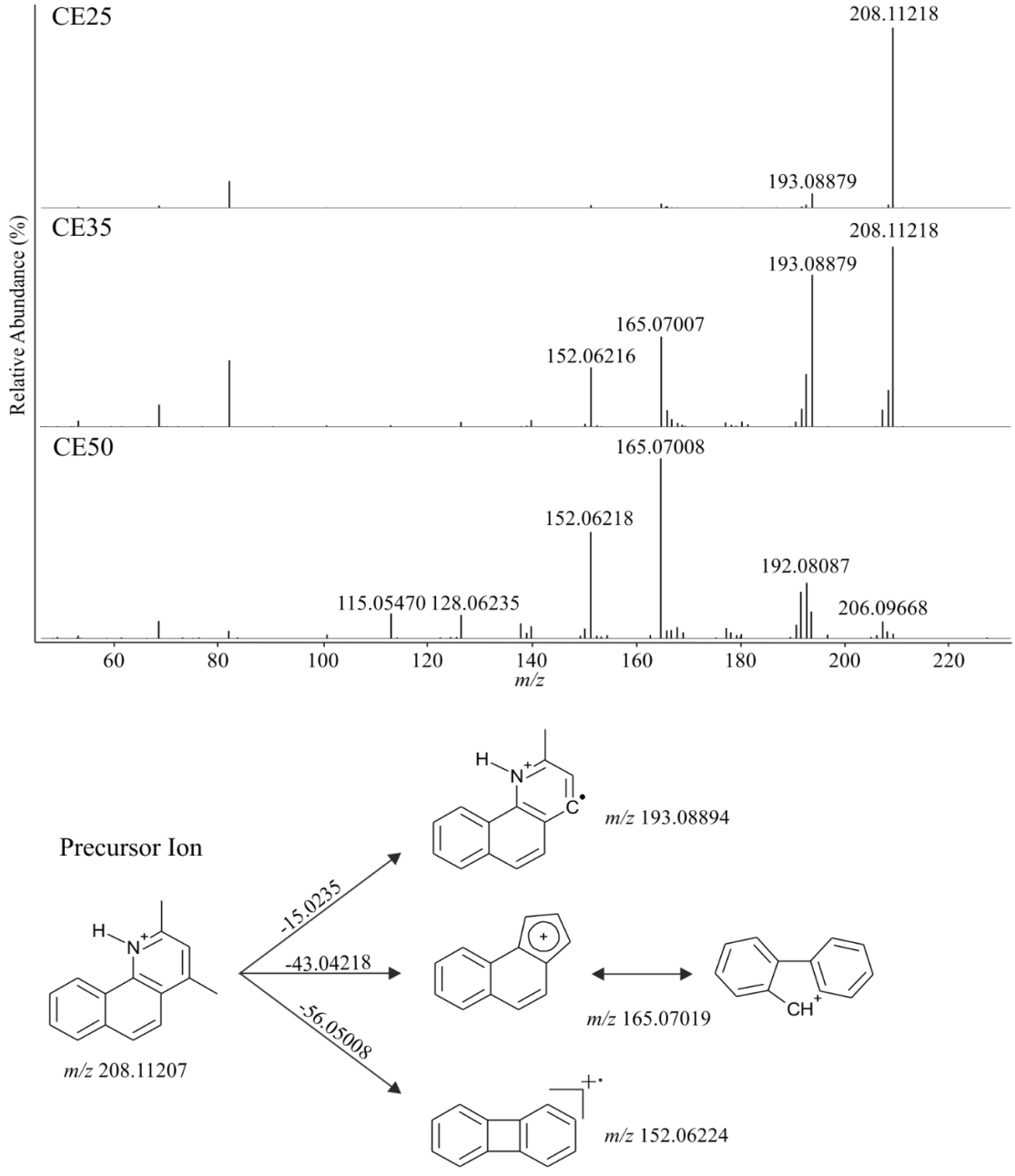

Figure 5-13. Positive ion ESI-HCD spectra of 2,4-dimethylbenzo[*h*]quinoline at (top) CE of 25, 35 and 50 eV and (bottom) postulated fragmentation pathways for the most abundant product ions.

The mass spectra generated by the fragmentation of 2-(4'-methylphenyl)-6-methylquinoline are shown in Figure 5-14. The low CE (25 eV) experiment showed little fragmentation producing a base peak at *m/z* 234.12794, corresponding the protonated adduct of a dimethyl-phenylquinoline. The low abundance ion at *m/z* 142.06513 is formed from the loss of the methylphenyl substituent, rationalised by the structure shown in Figure 5-14, and is potentially followed by a rearrangement to the expanded ring structure, commonly observed in the mass spectra of substituted quinolines (Porter and Baldas, 1970). Increased collision energy (35 eV) resulted in the *m/z* 142.06513 ion becoming the base peak and the formation of a product ion at *m/z* 115.05474 ($C_9H_7^+$), rationalised by the structure in Figure 5-14. Finally, under high-energy conditions (50 eV) the base peak changed to the lower molecular weight product ion at *m/z* 115.05474, an ion corresponding to the positively charged phenyl substituent is also present (*m/z* 91.05493; $C_7H_7^+$).

Table 5-4. Summary of the phenylquinoline HCD (25, 35 and 50 eV) collision experiments

Model Compound	Monoisotopic Mass	$[M+H]^+$	Product Ion 1		Product Ion 2		Product Ion 3	
			Mass	Formula	Mass	Formula	Mass	Formula
2-phenylquinoline	205.08915	206.09643	128.04979	$C_9H_6N^+$				
2-(3'-methylphenyl) quinoline	219.10479	220.11207	128.04982	$C_9H_6N^+$	91.05496	$C_7H_7^+$		
2-(4'-methylphenyl) quinoline			128.04968	$C_9H_6N^+$	91.05496	$C_7H_7^+$		
2-(2',4'-dimethylphenyl) quinoline	233.12045	234.12772	128.04977	$C_9H_6N^+$	105.07040	$C_8H_9^+$		
2-(2',5'-dimethylphenyl) quinoline			128.04973	$C_9H_6N^+$	105.07040	$C_8H_9^+$		
2-(4'-methylphenyl) -6-methyquinoline			142.06531	$C_{10}H_8N^+$	115.05474	$C_9H_7^+$	91.05423	$C_7H_7^+$
2-(2'-methylphenyl) -8-methyquinoline			142.06529	$C_{10}H_8N^+$	115.05470	$C_9H_7^+$	91.05493	$C_7H_7^+$

Fragmentation of the phenyl quinoline series produced largely similar mass spectra, often dominated by the loss of the phenyl substituent. 2-phenylquinoline showed very little

fragmentation, forming only a product ion at *m/z* 128.04977, indicative of formation of the quinoline ion ($C_9H_6N^+$). Both methyl-phenylquinoline structures showed the loss of toluene, forming the *m/z* 128.04977 product ion, as well as the positively charged phenyl substituent (*m/z* 91.05423; $C_7H_7^+$). Differences in the position of the substituent methyl group did not result in any observable difference in the mass spectra, and the isomers could not be distinguished. The mass spectra of the dimethyl quinolines also showed only minor differences. The two isomers with both methyl groups attached to the phenyl substituent are dominated by the loss of the neutral xylene molecule (C_8H_{10}; 106.07825 Da), resulting in the common *m/z* 128.04977 product ion. The two isomers in which both the quinoline core and the phenyl substituent are methylated also are dominated by the loss of the phenyl group (C_7H_8; 91.05423 Da). However, both also exhibit a fragment at *m/z* 115.05474, previously rationalised in Figure 5-14.

After thorough mass spectral and chromatographic characterisation of the model aromatic nitrogen compounds, their presence within the crude oil samples could be investigated. Comparison of the retention times of the benzoquinoline and phenylquinoline model compounds with that of peaks present in the appropriate EICs of the SCX4 fractions allowed the tentative identification of four benzoquinoline, and six phenyl quinoline structures. These assignments were confirmed by the comparison of model compound retention times and mass spectra with those of the suspected quinoline peaks.

Benzo[*h*]quinoline was identified in the ANS crude oil (Figure 5-15A; *m/z* 180.08077) along with two additional benzoquinoline isomers, neither with a comparable retention time to the benzo[*b*]quinoline. The benzoquinoline parent structures were present at a substantially lower concentration than that of its higher alkylated homologues. Of the two methyl-benzoquinoline model compounds, only the benzo[*h*]quinoline isomer (Figure 5-15A; *m/z* 194.09642) could be identified. The trimethyl-benzoquinoline was also identified within the SCX4 fraction (Figure 5-15; *m/z* 222.12773).

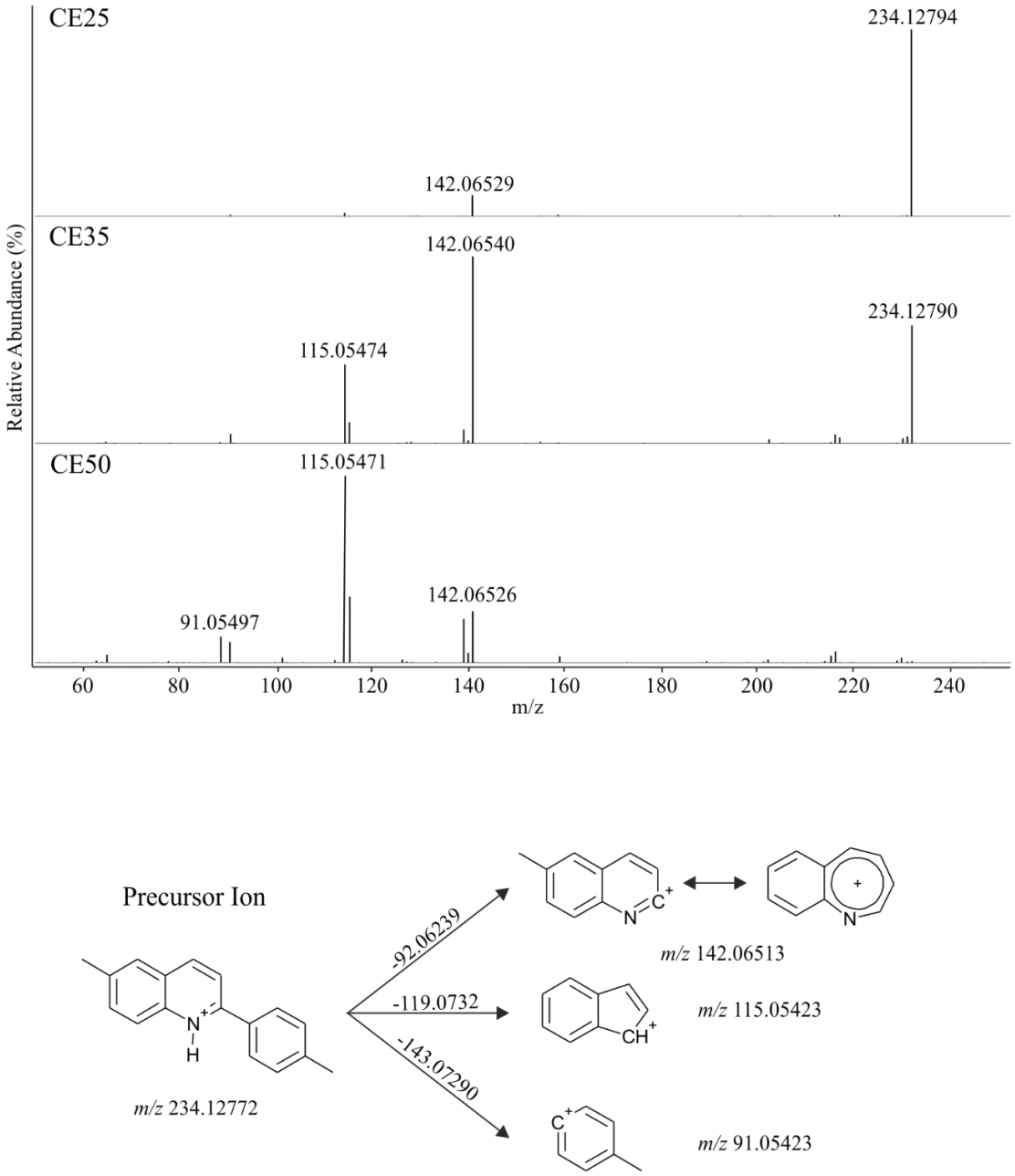

Figure 5-14. Positive ion ESI-HCD spectra of 2-(4'-methylphenyl)-6-methylquinoline at (top) CE of 25, 35 and 50 eV and (bottom) postulated fragmentation pathways for the more abundant fragments.

Only one phenyl quinoline isomer, 2-phenylquinoline, appeared to be present within the crude oil samples (Figure 5-15B; *m/z* 206.09643). Both methyl-phenylquinoline structures were positively identified in the samples (Figure 5-15B; *m/z* 220.11207) as well as three of the four dimethyl-phenylquinoline isomers (Figure 5-15B; *m/z* 234.12772).

The positive identification of the benzoquinoline and phenylquinoline alkylated series in the SCX4 fraction, indicated that prediction of fraction composition was correct.

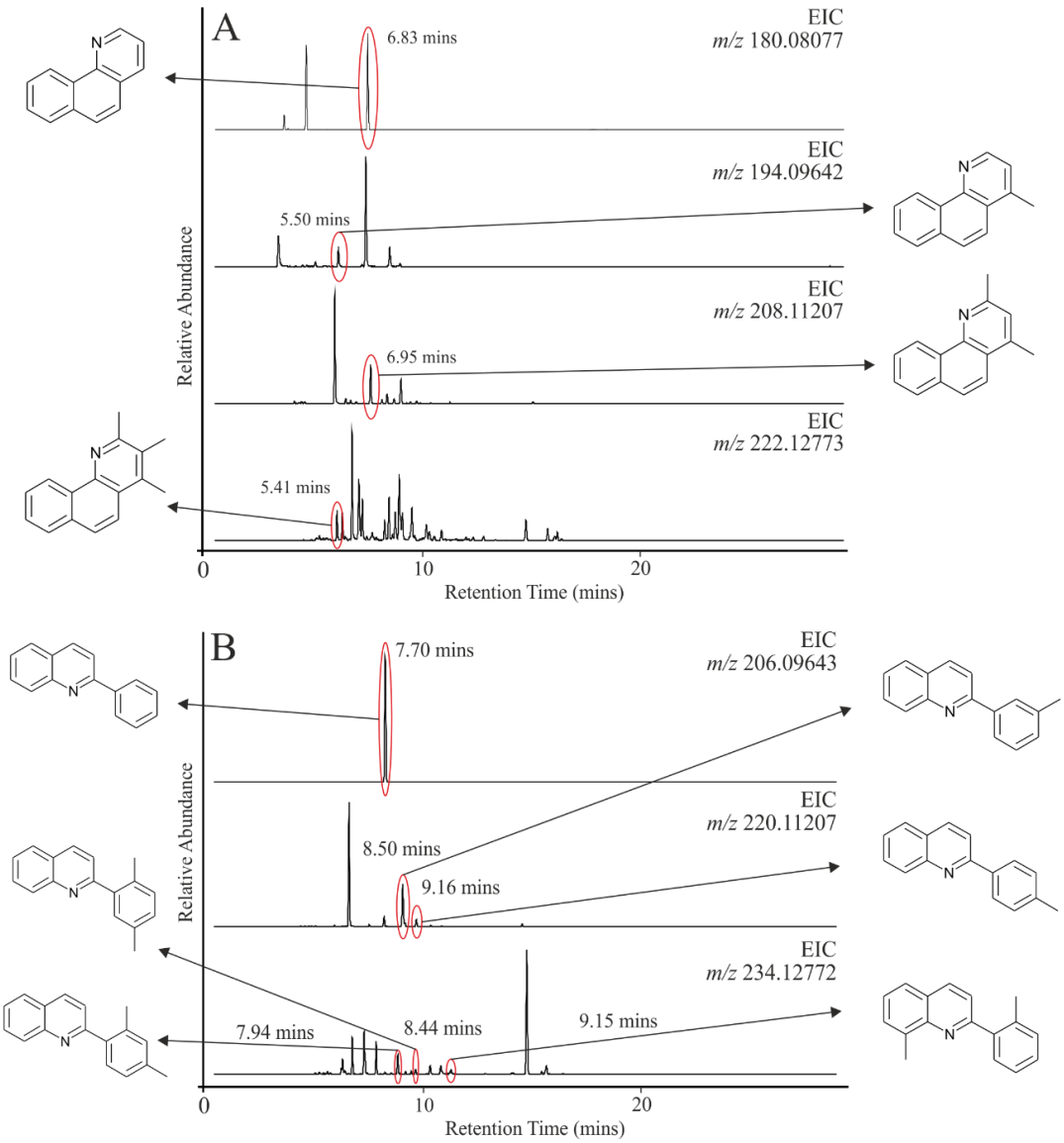

Figure 5-15. EICs of the protonated adducts ($[M+H]^+$) of benzoquinoline (**A**; *m/z* 180.08077) and its C_{1-3} alkylated homologues (*m/z* 194.09642, 208.11207 and 222.12773) and of phenylquinoline (**B**; *m/z* 206.09643) and its C_{1-2} alkylated homologues (*m/z* 220.11207 and 234.12772), showing individual structural identifications, from the analysis of the SCX4 fraction obtained from the ANS crude oil.

Further investigations into the composition of the SCX4 fraction attempted using mass spectral interpretation in order to identify other benzoquinoline structures. Unfortunately,

as with the EI mass spectra of condensed aromatic structures, the mass spectra obtained from HCD experiments on the $C_{2\text{-}4}$ alkyl benzoquinoline isomers were largely indistinguishable. For example, the EICs of the dimethyl-benzoquinolines are dominated by three peaks (Figure 5-15A; *m/z* 208.11207), and all peaks are characterised by product ions at *m/z* 193.08915, 165.07013 and 152.06213 (CE 40 eV), with only minor differences in abundance. As such, identification of methyl isomers within the SCX4 fractions without suitable reference compounds was not possible. Despite these difficulties in assigning individual structures, similarities between mass spectra of quinoline isomers and the relevant alkylated model compounds, allowed these series to be confidently identified as alkyl quinolines.

Comparison of alkyl-benzoquinoline isomer distribution in the five crude oil samples, showed them to be remarkably similar (Figure 5-16). The C_2 benzoquinolines were dominated by three abundant isomers, with the first peak being typically higher in abundance than the two later eluting isomers. However, in the case of TJP crude oil, all three peaks were of similar abundance suggesting a possible influence of biodegradation on distribution.

Interestingly, the EICs of the C_3 benzoquinolines showed the presence of a later eluting group of isomers (highlighted in Figure 5-16). Earlier eluting peaks also appeared to elute in two resolved clusters, suggesting the possible presence of different structural series within the C_3 benzoquinolines. As mentioned previously, the HCD fragmentation study afforded no information as to the differences in these structures, with all isomers producing largely identical mass spectra. The presence of these groups could be explained by the existence of alkylated series for the five-benzoquinoline isomers ([*b*], [*c*], [*f*], [*g*] and [*h*]). Indeed, fragmentation experiments conducted on the methylated benzo[*f*] - and benzo[*h*]quinoline isomers had shown them to have almost identical fragmentation pathways, and chromatographic separation of the benzo[*b*]- and benzo[*h*]quinoline

isomers showed substantial differences in retention, eluting some 5.5 minutes apart. However, without appropriate reference compounds to confirm the elution order of the alkylated benzoquinoline isomers could not be established. The relative abundance of the later eluting group appears to vary between samples and are most abundant in the Brent Blend and TJP crude oil samples. Interestingly, the relative abundance of the earlier eluting peaks are extremely similar in the five crude oil samples, suggesting the structures may have a common origin.

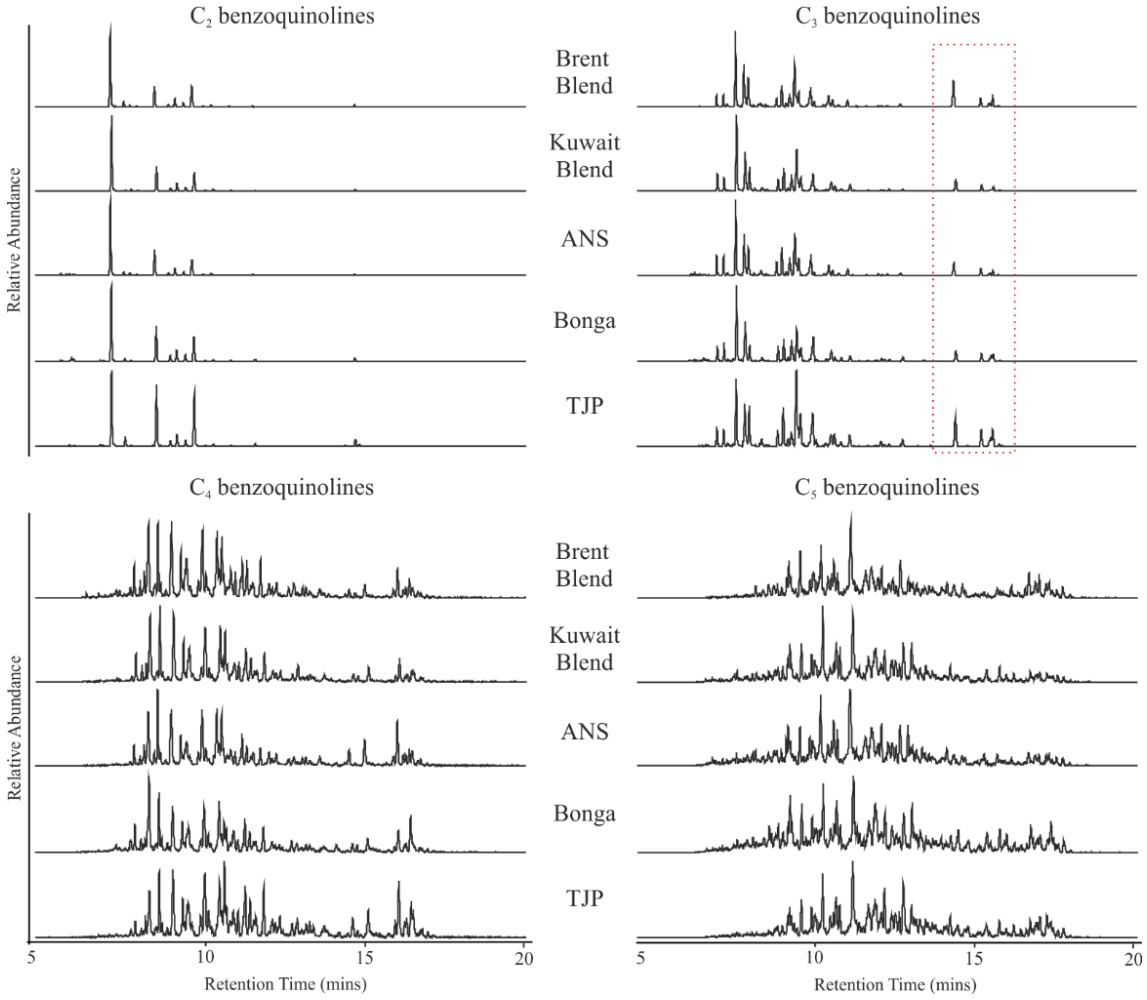

Figure 5-16. LC-HRAM-MS EICs of the protonated adducts of the $C_{2\text{-}5}$ benzoquinolines (*m/z* 208.11207, 222.12773, 236.14338 and 250.15903) obtained from analysis of the SCX4 fractions of the Brent, Kuwait, ANS, Bonga and TJP crude oils. Later eluting groups of C_3 benzoquinolines are highlighted (red box).

The distribution of the C_4 and C_5 benzoquinolines are also largely consistent across the sampled oils. Again, in both series a later eluting group of peaks is present, however, this is less pronounced in the C_5 benzoquinolines on account of the substantial increase in complexity. This complexity associated with the C_4 and C_5 benzoquinolines highlights the substantial number of individual structures associated with a single molecular formula.

5.4.6 Fraction SAX1 (sulfone compounds)

Analysis of the SAX1 fractions using GC-MS revealed a series of UCMs with several large, abundant peaks emerging from the chromatographic 'humps' (Data not shown). The model compound study had identified the sulfone compound to elute within in this fraction. Sulfones are the oxidation productions of sulfoxides and much like their sulfoxide precursors, are not thought to occur naturally in crude oils (Sharipov, 1988). Whilst sulfones have not been specifically studied in many crude oil samples, several studies applying FT-ICR-MS to resin and asphaltene fractions, report the presence of SO_2 species (Juyal *et al.*, 2010; Gaspar *et al.*, 2012). Extraction of the molecular ion for the dibenzothiophene sulfone compounds (*m/z* 216) and M+14n did not reveal the presence of the model compound or its alkyl homologues within any of the fractions. Plans for future analysis of the SAX1 fraction are discussed in Chapter 7.

5.4.7 Fraction SAX2 (pyrrolic and phenol compounds)

Isolation of the carbazole and phenyl phenol 'model compounds' in the SAX2 fraction suggested the likely presence of both pyrrolic and phenol functionalities within the fraction. The GC-MS analysis of the SAX2 fractions revealed a series of UCMs, all of which were characterised by a large number of components that were sufficiently abundant to be visible in the TICs (Figure 5-17). As was the case for many of the SPE fractions when examined by simple GC-MS (*e.g.* Figure 5-4), TICs of the SAX2 fractions

(Figure 5-17) were characterised by a series of UCMs. Interestingly, the UCMs observed in the Kuwait, ANS and TJP crude oils (Figure 5-17B, C and E) appear to be composed of two overlapping humps. The TIC of the SAX2 fraction obtained from the Bonga Crude (Figure 5-17D) also showed the presence of a series of late eluting compounds, not observed in any of the other crude oil samples.

To investigate the composition of the ANS crude oil SAX2 fraction in more detail, it was subjected to analysis using GC×GC-MS. Extraction of the molecular ions for carbazole (*m/z* 167) and its $C_{1\text{-}3}$ alkylated homologues (*m/z* 181, 195 and 209) revealed the presence of the homologous series (Figure 5-18A). The mass spectrum of the first peak in the chromatographic series compared well to that of authentic carbazole (also employed as a 'model' compound; Figure 5-19 A and Ai) and comparison of GC×GC retention times further confirmed its presence. The mass spectrum of carbazole (Figure 5-19Ai) is dominated by a molecular ion at *m/z* 167, reflecting the stability of the carbazole ring system under electron ionisation conditions. A minor fragment peak at *m/z* 139 ($M^{+\cdot}$-28) corresponds to a loss of the dihydrogen cyanide radical ($H_2CN\cdot$). The mass spectra of the C_1 carbazoles were dominated by strong molecular ions (*m/z* 181) as well as by a common fragment ion at *m/z* 152 ($C_{12}H_8^{+\cdot}$). Good matches between library mass spectra of the methyl carbazoles and the suspected peaks in the chromatogram of the ANS SAX2 fraction were also obtained (Figure 5-19 B and Bi; RMatch 948 for example, 1-methylcarbazole). Similarly, mass spectra of the C_2 carbazoles compared well to those of library spectra, allowing both dimethyl and ethylcarbazoles to be identified within the SAX2 fraction (Figure 5-19 C and Ci; RMatch 957 for example, 1,3-dimethylcarbazole). The two ions of significance in the mass spectra of the C_2 carbazoles are the molecular ion (*m/z* 195) and the $M^{+\cdot}$-15 ion (*m/z* 180) corresponding to the loss of a methyl group ($\cdot CH_3$). The mass spectra of the dimethylcarbazoles and the ethylcarbazoles differ in the abundance of the $M^{+\cdot}$-15 ion (*m/z* 180). In the latter case, the $M^{+\cdot}$-15 ion (*m/z* 180) is

significantly more abundant, becoming the base peak in the mass spectrum (data not shown).

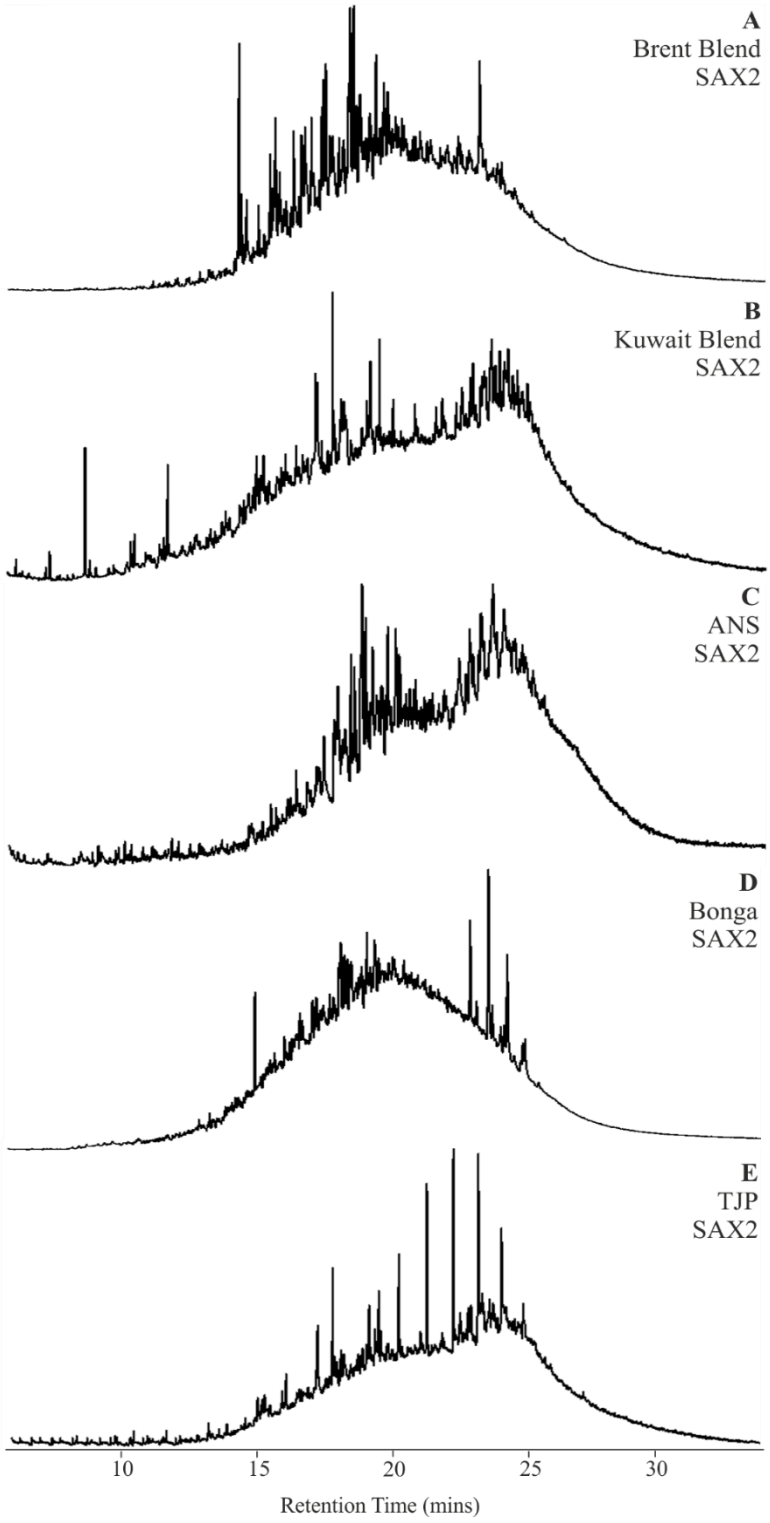

Figure 5-17. GC-MS TICs of the SAX2 fractions obtained from the SPE separation of the Brent Blend (**A**), Kuwait blend (**B**), ANS (**C**), Bonga (**D**) and TJP (**E**) crude oils.

The second, later eluting UCM seen in the GC-MS SAX2 TICs (Figure 5-17) were identified as benzocarbazole and its alkylated homologues. Extraction of the molecular ions of benzocarbazole (*m/z* 217) and the $C_{1\text{-}3}$ alkyl homologues (*m/z* 231, 245 and 259) in the GC×GC-MS chromatogram revealed the EIC presented in Figure 5-18B. Interestingly, two isomers of benzocarbazole are present in the EIC of SAX2 (Figure 5-18B). Investigation into the structures of the individual isomers revealed two identical mass spectra. Benzo[*a*]carbazole, benzo[*b*]carbazole and benzo[*c*]carbazoles have almost identical mass spectra (Figure 5-20 Ai-Aiii) making structural assignments without the appropriate reference compounds impossible by MS. Much like those of the carbazoles, mass spectra of benzocarbazole and its alkylated homologues are dominated by strong molecular ions; very little fragmentation occurs. Thus, the C_1 and C_2 benzocarbazoles were assigned based on their chromatography and strong molecular ions (Figure 5-20 B and C).

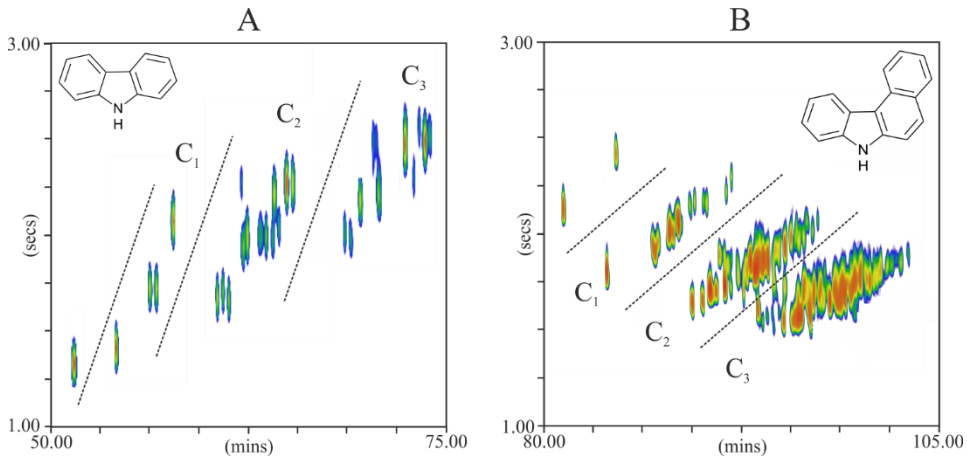

Figure 5-18. GC×GC-MS EICs of carbazoles and $C_{1\text{-}3}$ homologues (**A**; *m/z* 167, 181, 195 and 209) and benzocarbazole and $C_{1\text{-}3}$ homologues (**B**; *m/z* 217, 231, 245 and 259) obtained from Fraction SAX2 from the SPE separation of the ANS crude oil.

The occurrence and geochemical significance of pyrrolic nitrogen species, such as the carbazoles, has been the focus of a several studies over the last twenty years. Obtaining fractions of such compounds is of great interest to aid future work. For example, initial

work by Li *et al.* (1992b) and Larter *et al.* (1996) saw the development of chromatographic methods for the isolation of pyrrolic and pyridinic nitrogen and for the use of benzocarbazoles as molecular markers for crude oil migration distances. More recently, the ratio of benzo[*a*]carbazole/benzo[*a*]carbazole + benzo[*c*]carbazole (or BC ratio) was shown to decrease with crude oil migration distances and has been used to model migration paths for a series of Omani crude oils (Terken *et al.*, 2001). By applying, the method developed herein to isolate fractions of benzocarbazoles and carbazoles it is possible that future studies of the geochemical and environmental behaviour of these compounds will be facilitated.

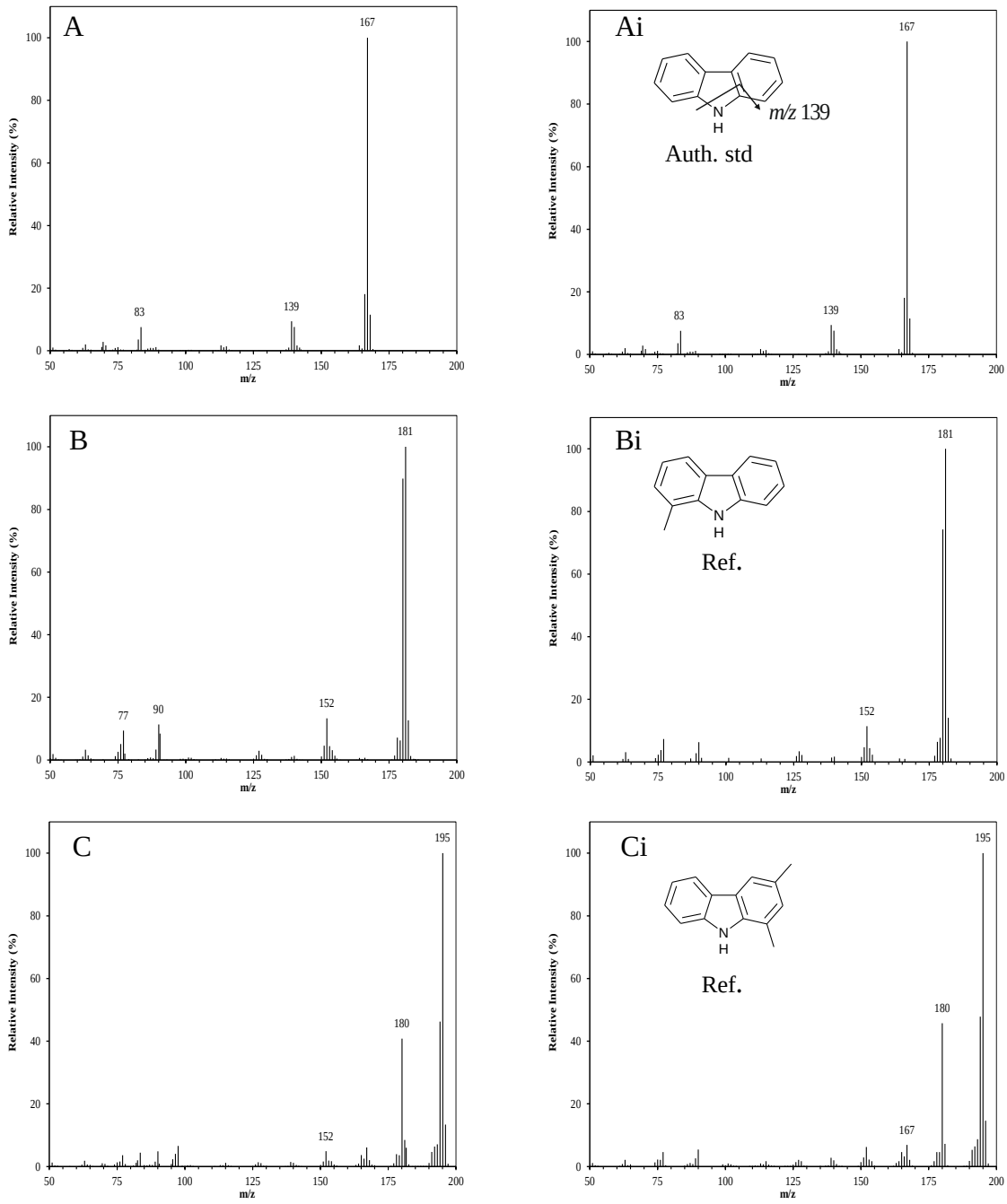

Figure 5-19. Examples of mass spectral identification of alkylated carbazoles from the analysis of fraction SAX2 (ANS crude oil separation; **A**-**C**). Individual compounds identified by comparison of spectra obtained from crude oil analyses with a carbazole authentic standard (**A**-**Ai**) and from position within the homologous series and comparison with NIST library spectra (**B**-**Bi** and **C**-**Ci**).

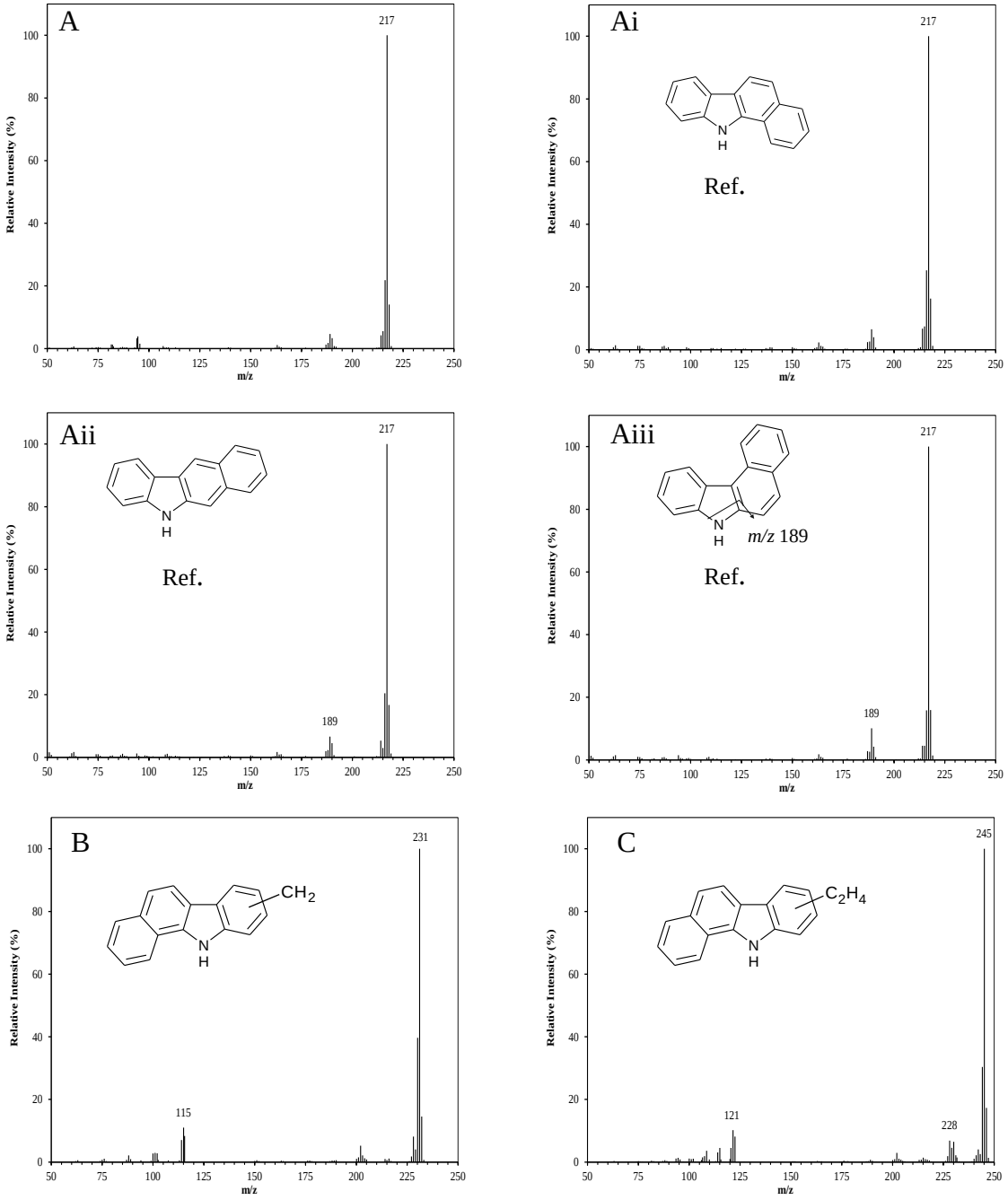

Figure 5-20. Examples of mass spectral identification of alkylated benzocarbazoles from the analysis of fraction SAX2 (ANS crude oil separation; **A-C**). Individual compounds identified by comparison of spectra obtained from crude oil analyses with NIST library spectra (**A-Ai**; benzo[*a*]carbazole, **Aii**; benzo[*b*]carbazole and **Aiii**; benzo[*c*]carbazoles) and from position within the homologous series (**B** and **C**).

Separation of the 'model' compound mixture had also identified the SAX2 fraction as containing phenyl phenol. Extraction of the molecular ions of the 'model' compound phenyl phenol (*m/z* 170) and its alkylated homologues (*m/z* 184, 198 and 212) did not reveal the presence of the series within the SAX2 fractions. Further investigations into the composition of the fractions led to the identification of a series of alkylated phenols (Figure 5-21).

The mass spectra of the alkylated phenols are dominated by the $M^{+\cdot}$-15 loss, corresponding to the losses of a methyl group. Identifications were based on reasonable comparison of mass spectra with those in a mass spectral library (NIST 2011). The C_3 phenol, 2,3,5-trimethyl phenol was identified with a RMatch of 897, the C_4 phenol, 3-methyl-4-isopropylphenol was identified with a RMatch of 903 and the C_5 phenol, 4-(1,1-dimethylethyl-2-methylphenol was identified with a RMatch of 888. The phenols were present at significantly lower abundances than that of the carbazoles in all five of the crude oil samples.

Isolation and quantification of phenols from crude oils is of importance given their relatively high associated toxicities and solubilities in water (Bennett *et al.*, 2007b). Laboratory experiments have suggested the likely source of the alkyl phenols is the acid-catalysed hydroxylation of the alkylbenzenes (Bastow *et al.*, 2005). The concentrations of alkylated phenols are routinely measured as part of environmental monitoring programmes connected with crude oil production and, as such, there is a need for reliable reproducible methods for their isolation.

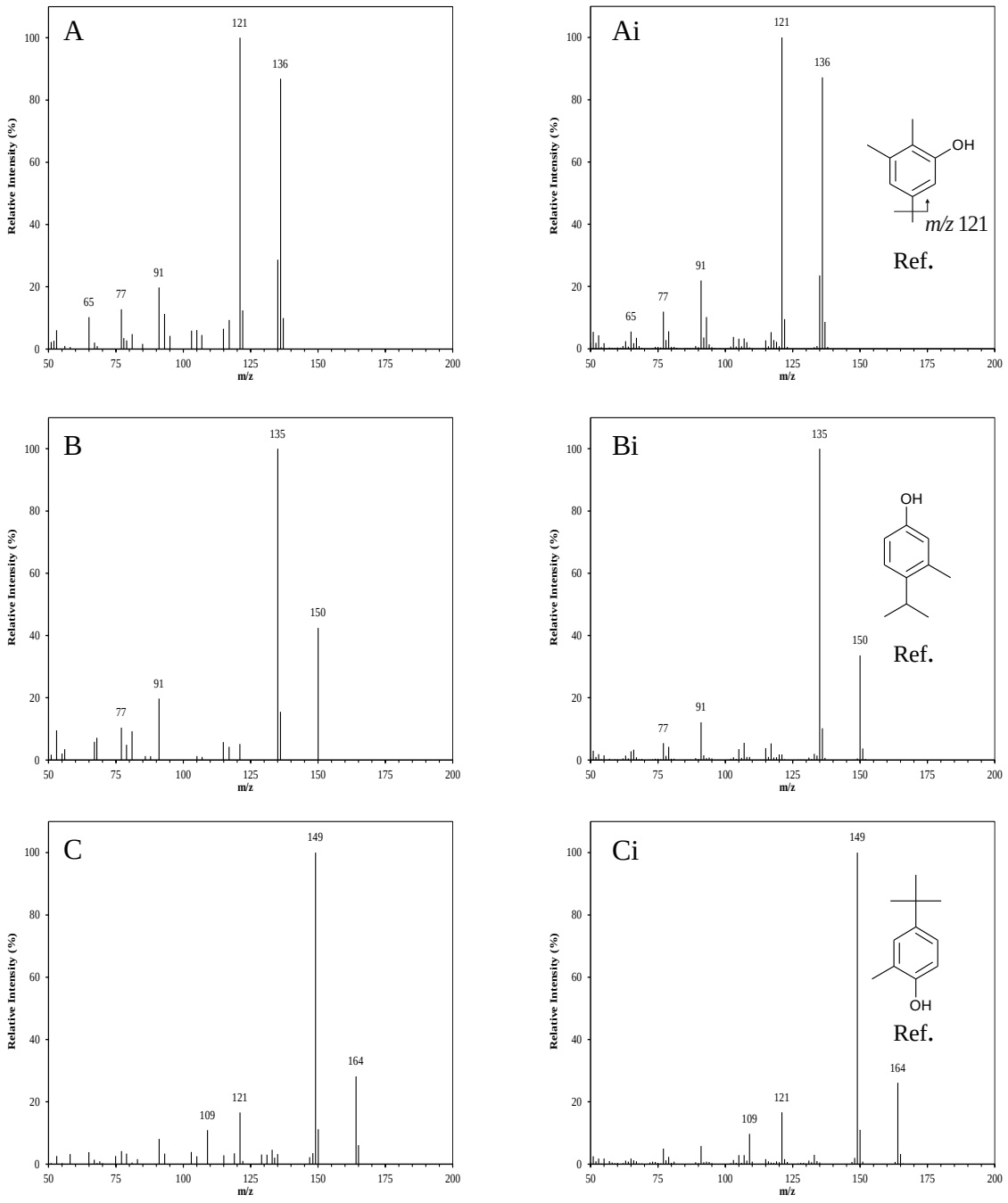

Figure 5-21. Examples of mass spectral identification of alkylated phenols from the analysis of fraction SAX2 (ANS crude oil separation; **A-C**). Individual compounds identified by comparison of spectra obtained from crude oil analyses with NIST library spectra (**A-Ai**, **B-Bi** and **C-Ci**).

The GC-MS TIC of the Bonga crude oil SAX2 fraction (Figure 5-17D) showed the presence of a later eluting series of compounds. Investigation into the composition of this series resulted in their tentative identifications as tocopherols (E vitamins; Figure 5-22).

Tocopherols are minor constituents of plants and algal lipid membranes, where they serve as antioxidants (Peters *et al.*, 2005) and have been identified as potential precursors for the formation of pristane in crude oils (Goossens *et al.*, 1984; Li *et al.*, 1995). Whilst tocopherols have been identified in a variety of sediment extracts (Brassell *et al.*, 1983), they do not appear to have been identified in a crude oil previously, to the author's knowledge current.

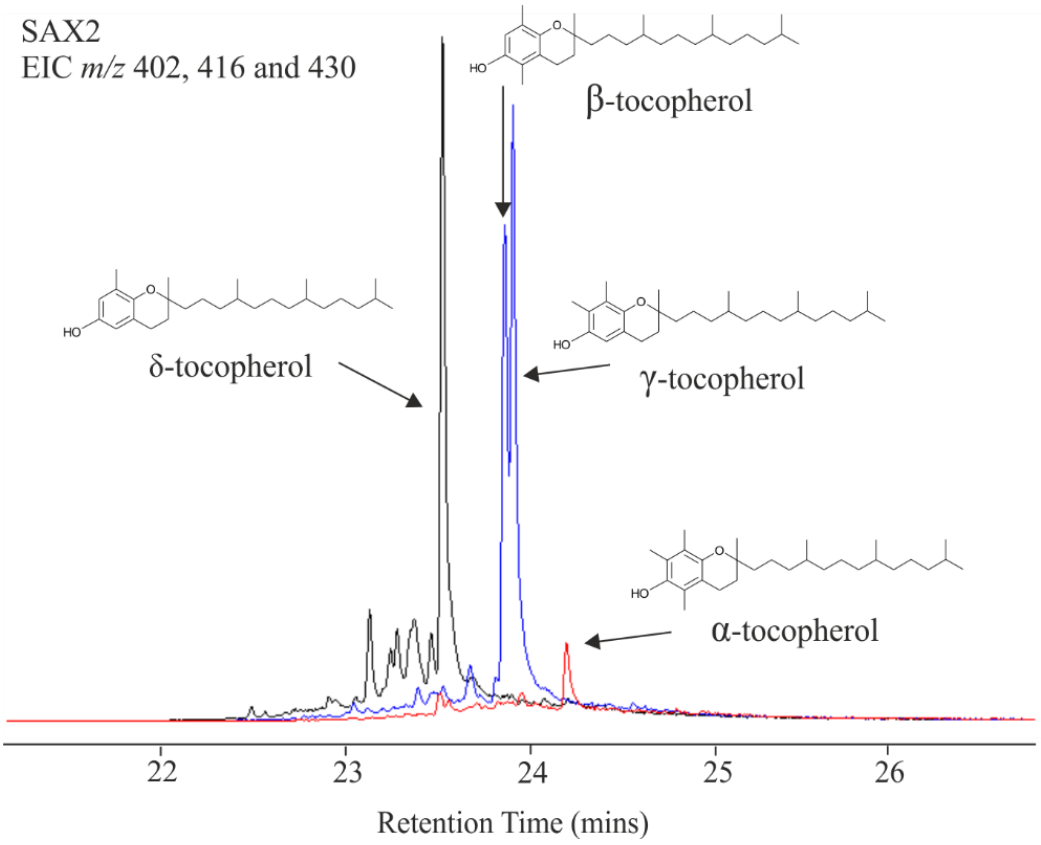

Figure 5-22. GC-MS EICs of the SAX2 fraction obtained from the SPE separation of the Bonga crude oil, showing the extracted molecular ions of the tocopherols: δ-tocopherol (*m/z* 402; black), β-tocopherol and γ-tocopherol (*m/z* 416; blue) and α-tocopherol (*m/z* 430; red).

The α-, β-, γ- and δ-tocopherol isomers, differ in the number of methyl substituents attached to the benzene ring and in the position of those methyl substituents (structures shown in Figure 5-22. All four tocopherols were identified in the SAX2 fraction of the

Bonga oil, by comparison of their mass spectra with those in the mass spectral library (Figure 5-23). The mass spectra of the tocopherols are characterised by strong molecular ions (α- *m/z* 430; β- and γ- *m/z* 416 and δ- *m/z* 402) and losses of $M^{+\cdot}$-225 and $M^{+\cdot}$-265 corresponding to the loss of the isoprenoid side chain ($C_{16}H_{33}$) and the breaking of the tetrahydropyran ring and loss of the isoprenoid side chain ($C_{19}H_{37}$).

The mass spectrum of the first major peak in the series (Figure 5-22; EIC *m/z* 402, black) compared well to that of δ-tocopherol (Figure 5-23 D and Di; RMatch of 945). The two co-eluting peaks (Figure 5-22; EIC *m/z* 416, blue) were identified as the two isomers of the $C_{28}H_{48}O_2$ tocopherol, β- and γ-tocopherols. The two isomers were distinguished based on the relative abundance on the molecular ion and the ion at *m/z* 151 ($M^{+\cdot}$-265). The first of the two peaks in the *m/z* 416 EIC was identified as β-tocopherol (Figure 5-23 B and Bi; RMatch 889) and the second as γ-tocopherol (Figure 5-23 C and Ci; RMatch 901). The last peak to elute (Figure 5-22; EIC *m/z* 430, red) was identified as α-tocopherol (Figure 5-23 A and Ai; RMatch 879).

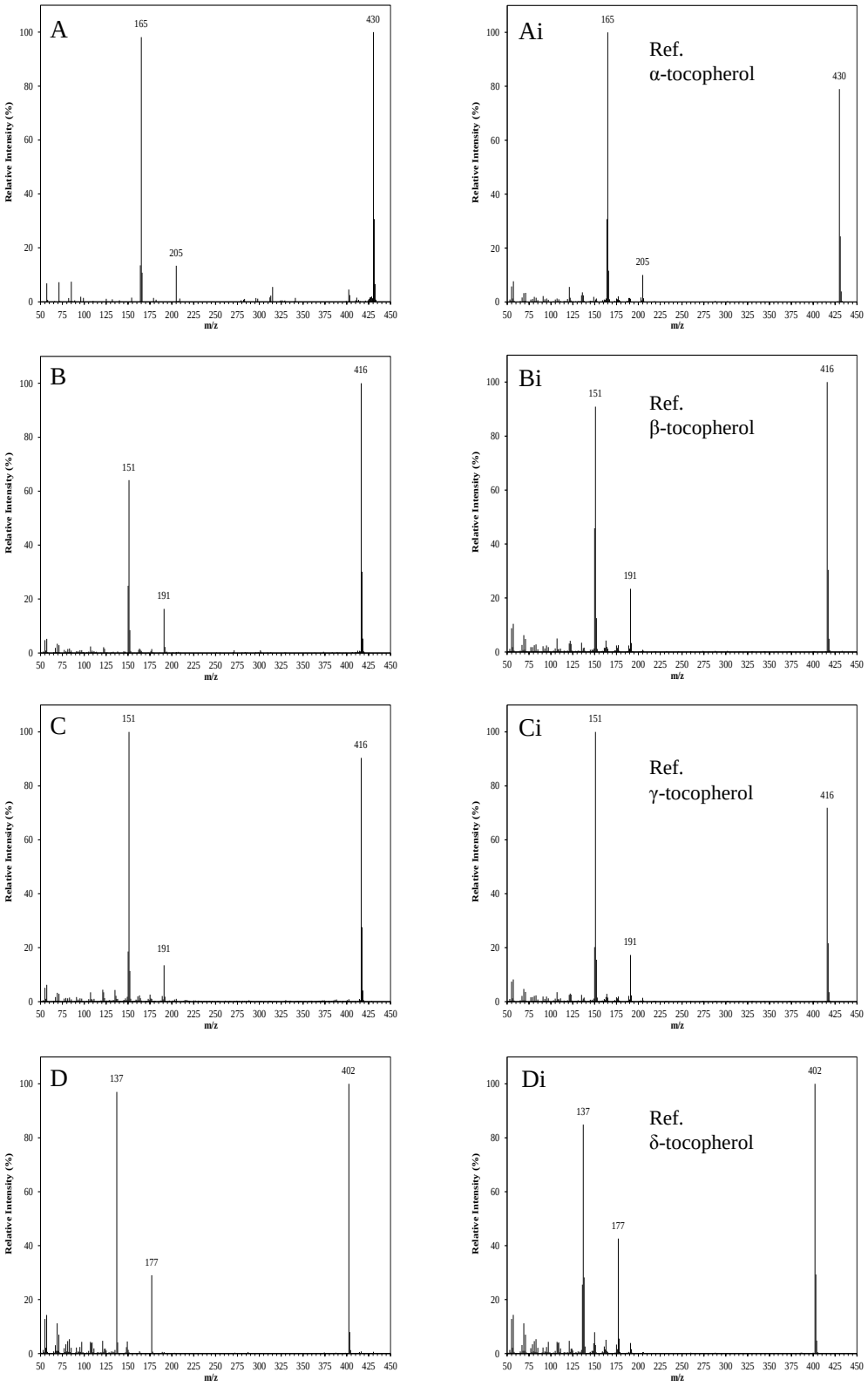

Figure 5-23. Mass spectral identification of tocopherols from the analysis of Fraction SAX2 (Bonga crude oil separation; **A-D**). Individual compounds identified by comparison of spectra obtained from crude oil analyses with NIST library spectra (**A** and **Ai**, **B** and **Bi**, **C** and **Ci** and **D** and **Di**).

5.4.8 Fraction SAX3 (acids)

The SAX3 fractions obtained from the separation of the five crude oils were subjected to analysis using GC-MS. Using 'model' compounds the SAX3 fraction was shown to contain carboxylic acids (i.e. to be broadly a 'naphthenic acid' fraction), with the successful elution of all 'model' acids wholly within the fraction. In order to ensure that acids in these fractions would be amenable to GC-MS analysis, they were analysed as their trimethylsilyl esters (Stalling *et al.*, 1968). The TICs obtained from the analyses are presented in Figure 5-24. With the exception of the fraction isolated from the TJP oil, all the fractions are dominated by *n*-hexadecanoic (C_{16}) and *n*-octadecanoic (C_{18}) *n*-acid TMS esters. The high abundance of the C_{16} and C_{18} acids in these samples was discussed previously (Chapter 3). Chromatograms obtained from the analysis of the ANS and the Kuwait Blend oil fractions (Figure 5-24 B and C) compare well to those obtained from use of the Snyder separation method (Chapter 3) with the notable absence of the previously observed phthalate peak, a likely contaminant that was present in the SAX3 procedural blank (Chapter 4). The SAX3 fraction obtained from the TJP crude oil was by far the most complex of the five fractions. Given the extent of biodegradation which TJP crudes have undergone resulting in a high TAN (3.61; Table 5-1), such a highly complex acid fraction was somewhat expected.

In recent years, significant progress has been made in the molecular and structural characterisation of petroleum derived naphthenic acids (Reviewed: Brown and Ulrich, 2015; Wilde, 2015). Methods such as that of Wilde and Rowland (2015), demonstrate the extensive lengths taken by researchers to facilitate the structural characterisations of individual naphthenic acids. In this instance, elution of all 'model' acids, and the tentative identification of a number of common petroleum derived acids was sufficient evidence that isolation of an acid fraction had been successful. For these reasons, investigation into the composition of the naphthenic acids of these crude oils was not a focus of this study

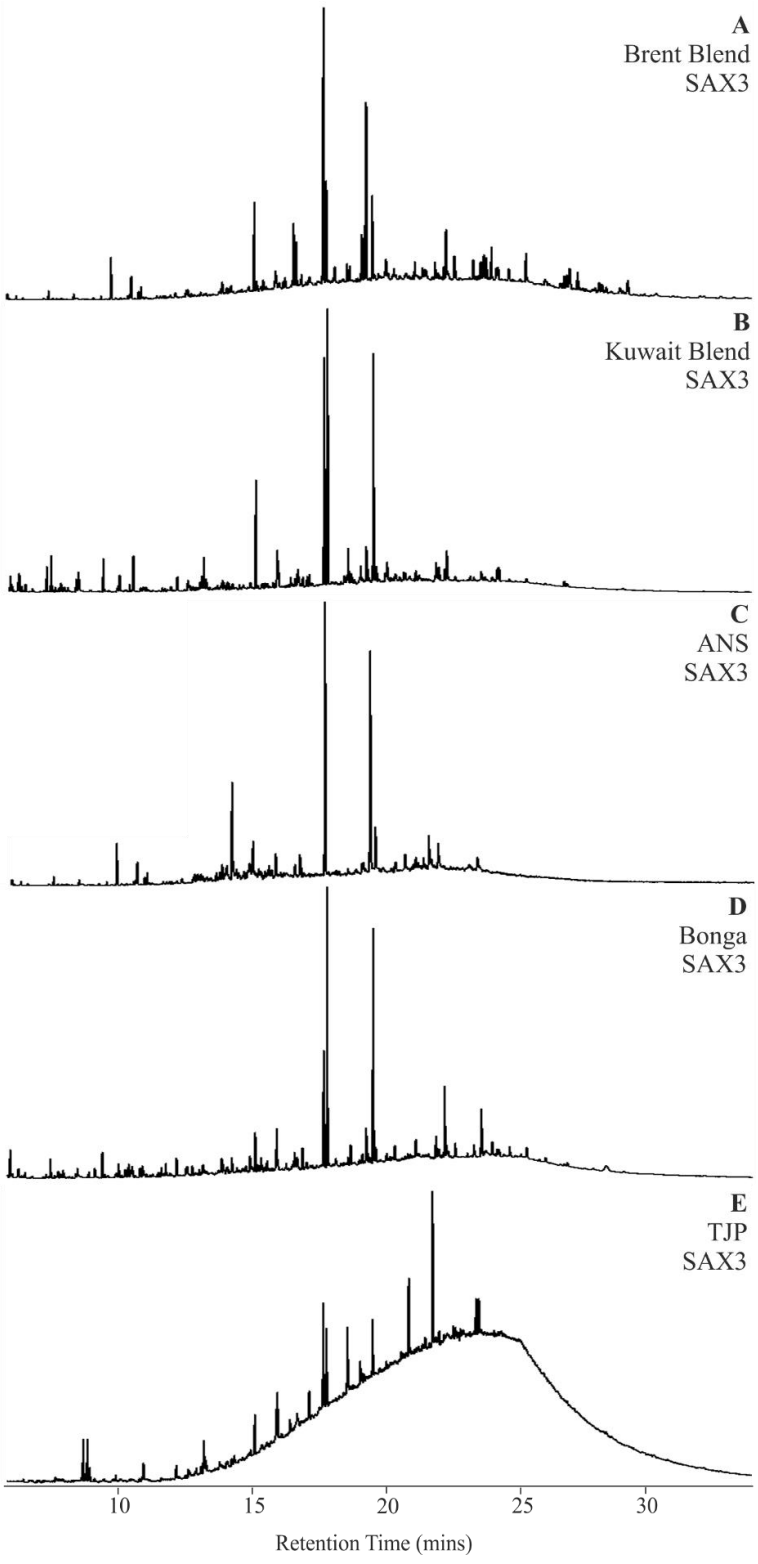

Figure 5-24. GC-MS TICs of the SAX3 fractions (analysed as the trimethylsilyl esters) obtained from the SPE separation of the Brent Blend (**A**), Kuwait blend (**B**), ANS (**C**), Bonga (**D**) and TJP (**E**) crude oils.

5.4.9 Fraction S0 (saturated hydrocarbons)

The composition of the S0 and S1 fractions has been briefly discussed in Chapter 4, Section 3.3.2, where fractions had been subject to GC-MS analysis to assess the efficacy of the separation between the saturated and aromatic hydrocarbons. The results discussed showed the complete absence of the tri-aromatics within fraction S0, implying good separation between the saturated and aromatic hydrocarbons. Investigations into the composition of the S0 (saturated hydrocarbon) fractions were not in the remit of this study because hydrocarbons have been studied extensively as major components of crude oils. However, isolation of fractions of saturated hydrocarbons free of aromatics are of great importance when conducting sample assessments based on traditional biomarkers. The high relative abundance and ease of analysis has resulted in a large number of source-, age- and maturity related biomarkers being identified within the saturated hydrocarbon fractions of crude oils (reviewed Peters *et al.*, 2005). For this reason, S0 fractions were subjected to analysis using GC-MS in order to profile the five crude oil samples and to ensure sufficient separation between saturated and aromatic compounds had been achieved. The TICs obtained from the GC-MS analysis are presented in Figure 5-25. With the exception of the TJP, all S0 fractions were dominated by peaks corresponding to a series of *n*-alkanes. The relative abundance of the alkanes appeared to correlate with the API gravities, with the abundance of the individual alkanes decreasing as the API decreased (Figure 5-25 A→E). Indeed, extraction of the characteristic ions for the alkanes (*m/z* 57, 71 and 85) showed the absence of the series in the TJP sample (data not shown), a direct consequence of the extensive biodegradation (discussed in Section 5.2.4).

The molecular ions of phenanthrene and the C_1 and C_2 alkyl phenanthrenes (*m/z* 178, 192 and 206) were extracted (data not shown) in order to investigate whether a good separation between the saturated and aromatic hydrocarbon fractions had been achieved (S0 and S1, respectively). In all cases, early elution of the phenanthrenes into fraction S0

was negligible, highlighting the successful collection of well-defined fractions of saturated and aromatic hydrocarbons.

Extraction of the molecular ions of dibenzothiophene and its alkyl homologues confirmed their presence in all five of the S0 fractions (data not shown). Elution of the dibenzothiophenes within the saturated hydrocarbon fraction is problematic. Previous studies quantifying thiophenes and alkyl thiophenes in crude oils have also made use of silica gel to separate crude oil samples into fraction of saturated and aromatic hydrocarbon fractions (Li *et al.*, 2012; Li *et al.*, 2014b; Fang *et al.*, 2016). However, these did not identify which of the two silica fractions were used for the dibenzothiophene analysis. These studies also employ a 'topping' step, in which the lower weight, volatile hydrocarbons were removed. It is possible that in using whole oils, the saturated hydrocarbon fraction produce a solvating effect, reducing the retention of the dibenzothiophenes. The use of sulphur chemiluminescence detectors (SCD) coupled to GCs is also regularly employed when working with sulphur compounds in crude oils (West *et al.*, 2013). Given the abundance of the thiophene series, use of such techniques conveniently avoids the need for involved preparative separations as pre-concentration is often not necessary (Ruiz-Guerrero *et al.*, 2006; West *et al.*, 2013; Dijkmans *et al.*, 2015).

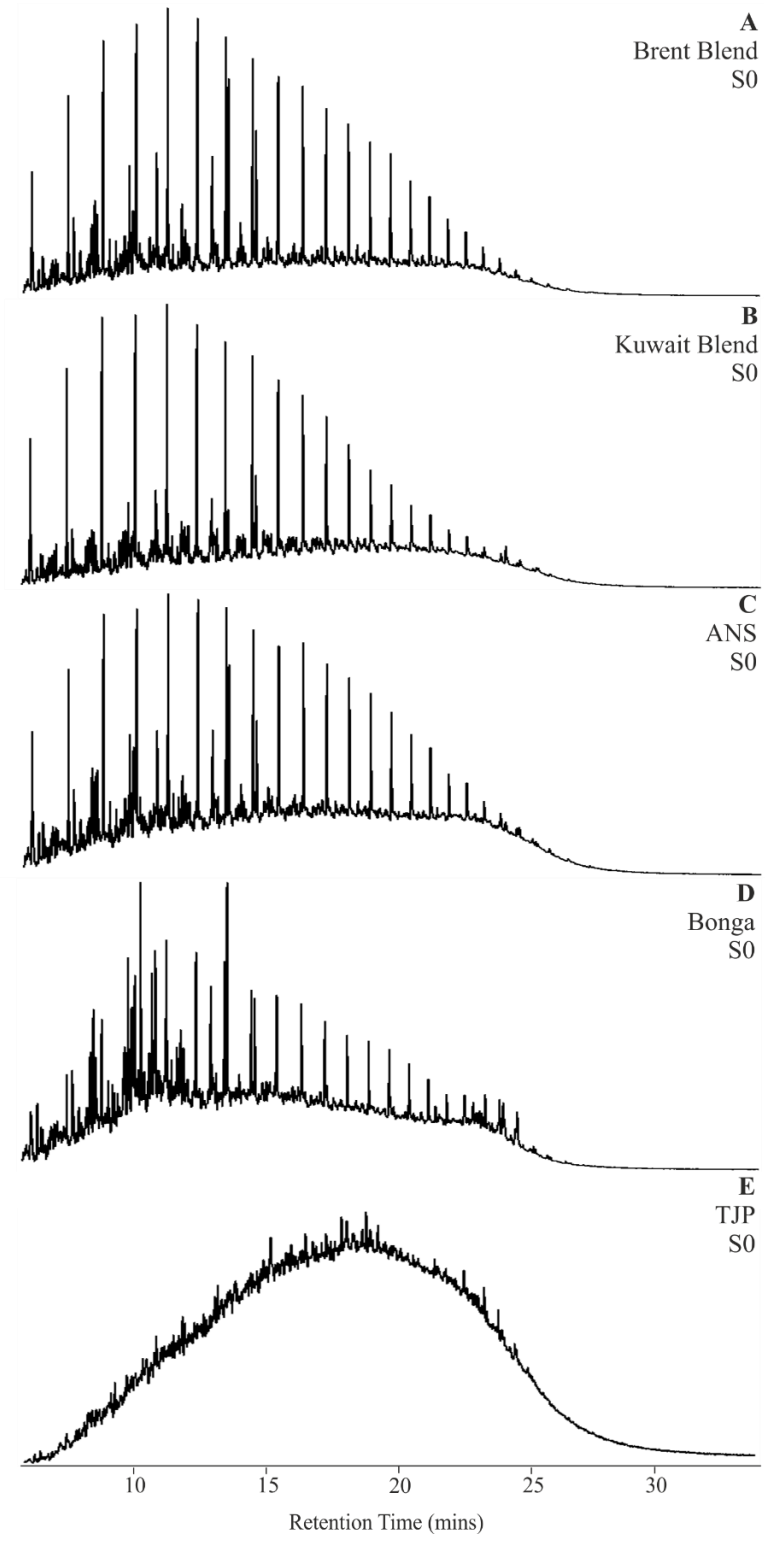

Figure 5-25. GC-MS TICs of the S0 fractions obtained from the SPE separation of the Brent Blend (**A**), Kuwait blend (**B**), ANS (**C**), Bonga (**D**) and TJP (**E**) crude oils.

5.4.10 Fraction S1 ('aromatic')

Separation of the 'model' compound mixture identified fraction S1 as an 'aromatic' hydrocarbon fraction by elution of the fluorene and benzo[*a*]pyrene 'model' compounds within the S1 fraction. The isolation of aromatic hydrocarbons fractions that are free of saturated hydrocarbons is of equal importance to that of discrete saturated hydrocarbons (S0). The aromatic hydrocarbons of crude oil are frequently used as tools to model a number of reservoir parameters. Most commonly employed are the methylphenanthrene and methyl-/ethylnapthalene indices for thermal maturity, which ratios various structural isomers to assess the degree of thermal maturation (Peters *et al.*, 2005). Similarly, the biphenyls and alkyl diphenylmethanes have been used as biodegradation indicators due to systematic changes in composition when oils are subject to biodegradation in reservoirs and surface sediments (Trolio *et al.*, 1999). Whilst detailed investigation into the composition of the aromatic hydrocarbons was not within the remit of this particular study, it is important that the developed method is demonstrated to be capable of generating PAH fractions, suitable for such assessment studies. As such, S1 fractions were subjected to preliminary analysis by GC-MS to confirm that appropriate aromatic fractions had indeed been generated by using the separation scheme.

The GC-MS TICs from the analysis of the S1 fractions are presented in Figure 5-26. The five chromatograms are characterised by UCMs overlain by some resolved components. The resolved peaks were identified as series' of alkylated fluorenes and alkylated phenanthrenes. Additionally identified within the S1 fraction were alkylated series of fluoranthenes, pyrenes and benzopyrenes and chrysenes. Identification of numerous PAHs within the S1 fractions further supports its designation as an aromatic hydrocarbon fraction such that it should be useful for crude oil assessments.

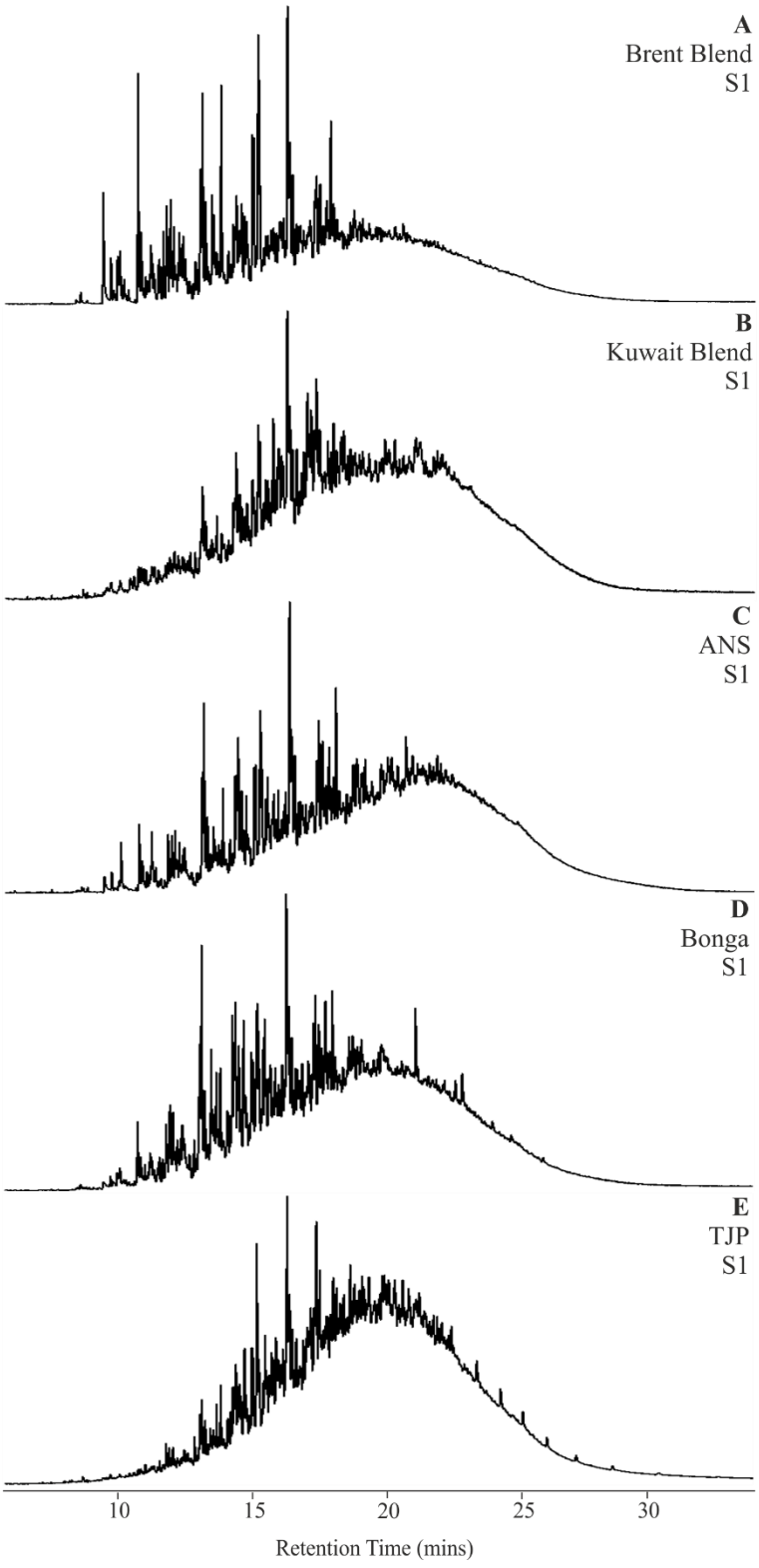

Figure 5-26. GC-MS TICs of the S1 fractions obtained from the SPE separation of the Brent Blend (**A**), Kuwait blend (**B**), ANS (**C**), Bonga (**D**) and TJP (**E**) crude oils.

5.4.11 Fraction S2 (ketones)

Separation of the 'model' compound mixture identified the S2 fraction as the fluorenone (or ketone) fraction. Preliminary GC-MS analysis of the S2 fraction (data not shown) obtained from the ANS crude oil showed the fraction to be highly complex with the fluorenone series was only revealed when the appropriate extracted ion chromatograms were generated. To address this, fractions by were analysed using GC×GC-MS, which allowed for improved separation (Figure 5-27). Under optimal conditions, clear distinguishable mass spectra could be obtained for individual compounds, many possibly for the first time. The resulting data sets allowed for the tentative identifications of many novel aldehydes and ketones by co-chromatography with authentic compounds and by comparison of mass spectra with library mass spectra.

Preliminary investigations were focused on the S2 fraction obtained from the ANS fractionation. The TIC obtained from GC×GC-MS analyses (Figure 5-27A) showed the presence of a low polarity UCM that extended across the whole chromatogram but which was still largely unresolved, even by GC×GC. However, two dominant series of higher polarity compounds could be clearly distinguished (Figure 5-27Ai and ii), having been successfully resolved in the second dimension. Closer inspection of the lower polarity, unresolved mixture revealed a series of compounds that were also sufficiently abundant to be visible in the TIC (Figure 5-27Aiii). Each of these series appeared to be made up of a repeating series of five peaks, eluting in a similar pattern in this S2 fraction to that of *n*-alkanes (in the S0 fraction).

Investigation into the composition of this repeating series of five peaks focused on identification of the latest eluting peak of each repeat unit. The mass spectra of first three of these peaks compared well to the spectra of nonanal, decanal and undecanal (Figure 5-28), indicating the likely presence of a series of aliphatic aldehydes. Much like the mass

spectra of the *n*-alkanes, the spectra of the *n*-aldehydes are dominated by a base peak ion at *m/z* 57, but are also characterised by the uncommon fragment ion *m/z* 82, which allowed good quality EICs for the aldehyde series to be generated (Figure 5-27Bii).

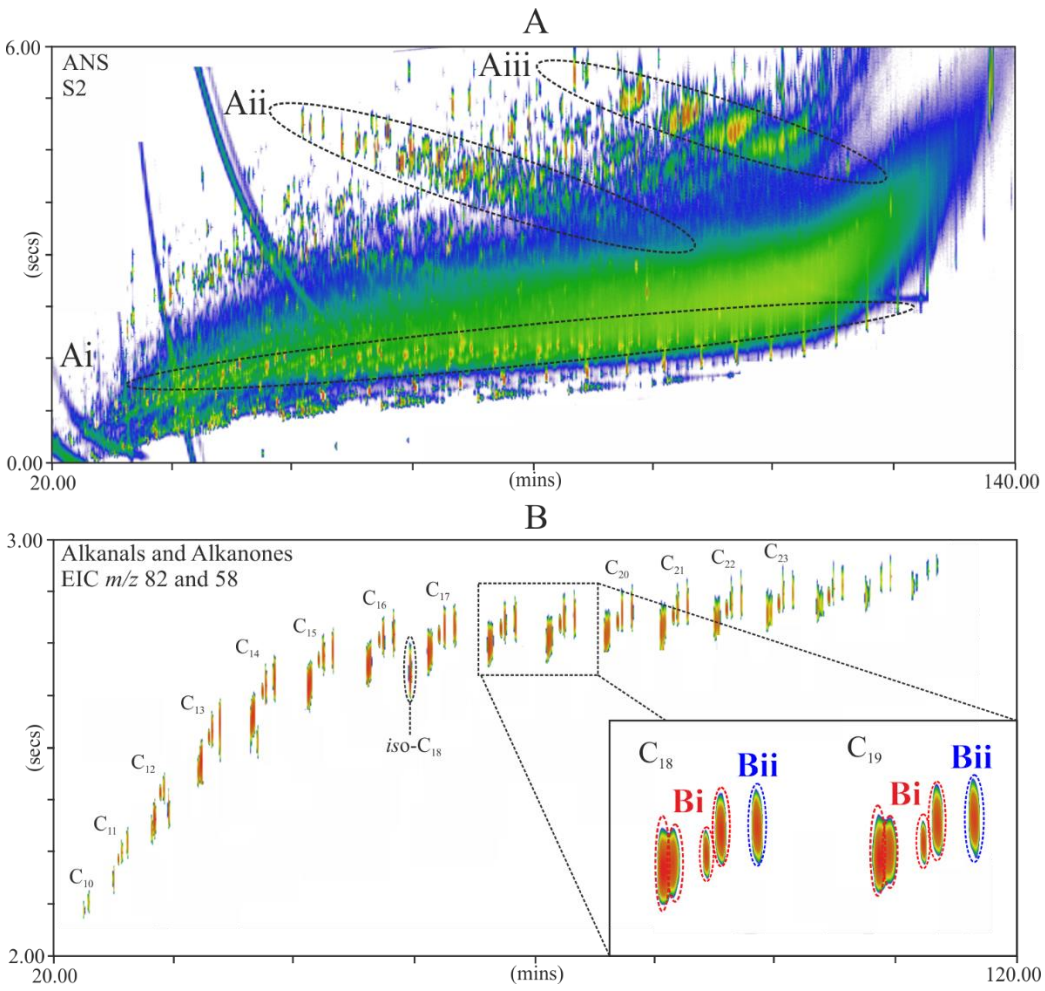

Figure 5-27. GC×GC-MS TIC from the analysis of Fraction S2 (**A**), showing the three observed compound series (Ai, Aii and Aiii) and GC×GC-MS EIC showing alkanal (*m/z* 82) and alkanone (*m/z* 58) homologous series (**B**) with a zoomed extract showing the ketone isomers (Bi) and aldehyde (Bii) elution order obtained from the SPE separation of the ANS crude oil. The peak labelled as *iso*-C_{18} is tentatively identified as 6,10,14-trimethyl pentadecan-2-one.

Examination of the slightly earlier eluting peaks (Figure 5-27Bi) within the repeat units revealed mass spectra dominated by the base peak ion at *m/z* 58 (Figure 5-29 A-C). The ion at *m/z* 58 is characteristic of aliphatic ketones (alkanones), forming in the MS ion

source as a result of a McLafferty rearrangement (McLafferty and Turecek, 1993). The first three peaks in this series were identified as nonan-2-one, decan-2-one and undecan-2-one based on comparison to library mass spectra (Figure 5-29). EICs generated from the extraction of the *m/z* 58 ion showed the presence of a repeating series of two resolved peaks and 2 partially resolved peaks (Figure 5-27 Bi).

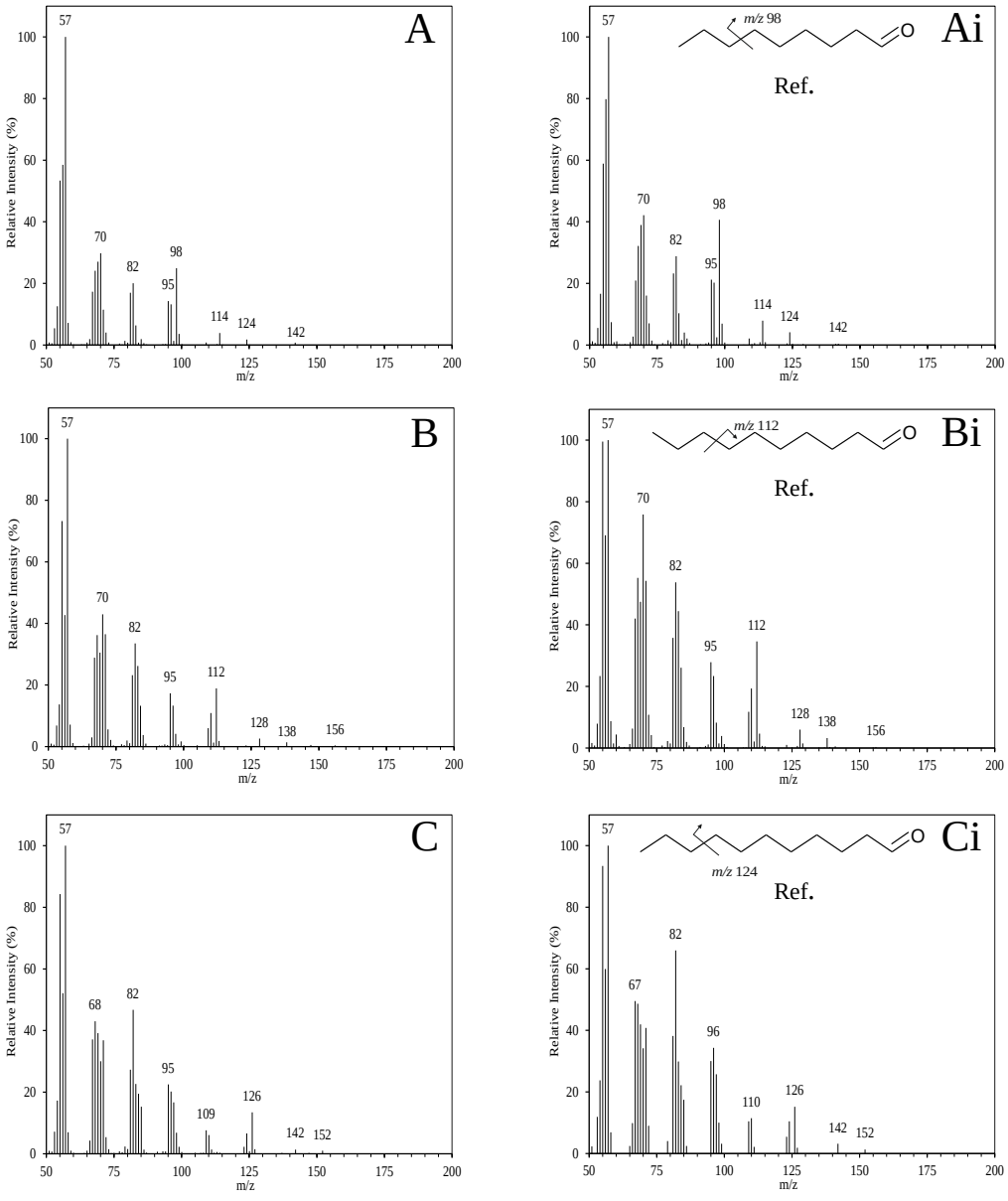

Figure 5-28. Examples of mass spectral identification of *n*-alkanals from the analysis of Fraction S2 (ANS crude oil separation; nonanal; **A**, decanal; **B**, undecanal; **C**). Individual compounds identified by comparison of spectra obtained from crude oil analyses with NIST library spectra (**A**; **Ai-C**; **Ci**).

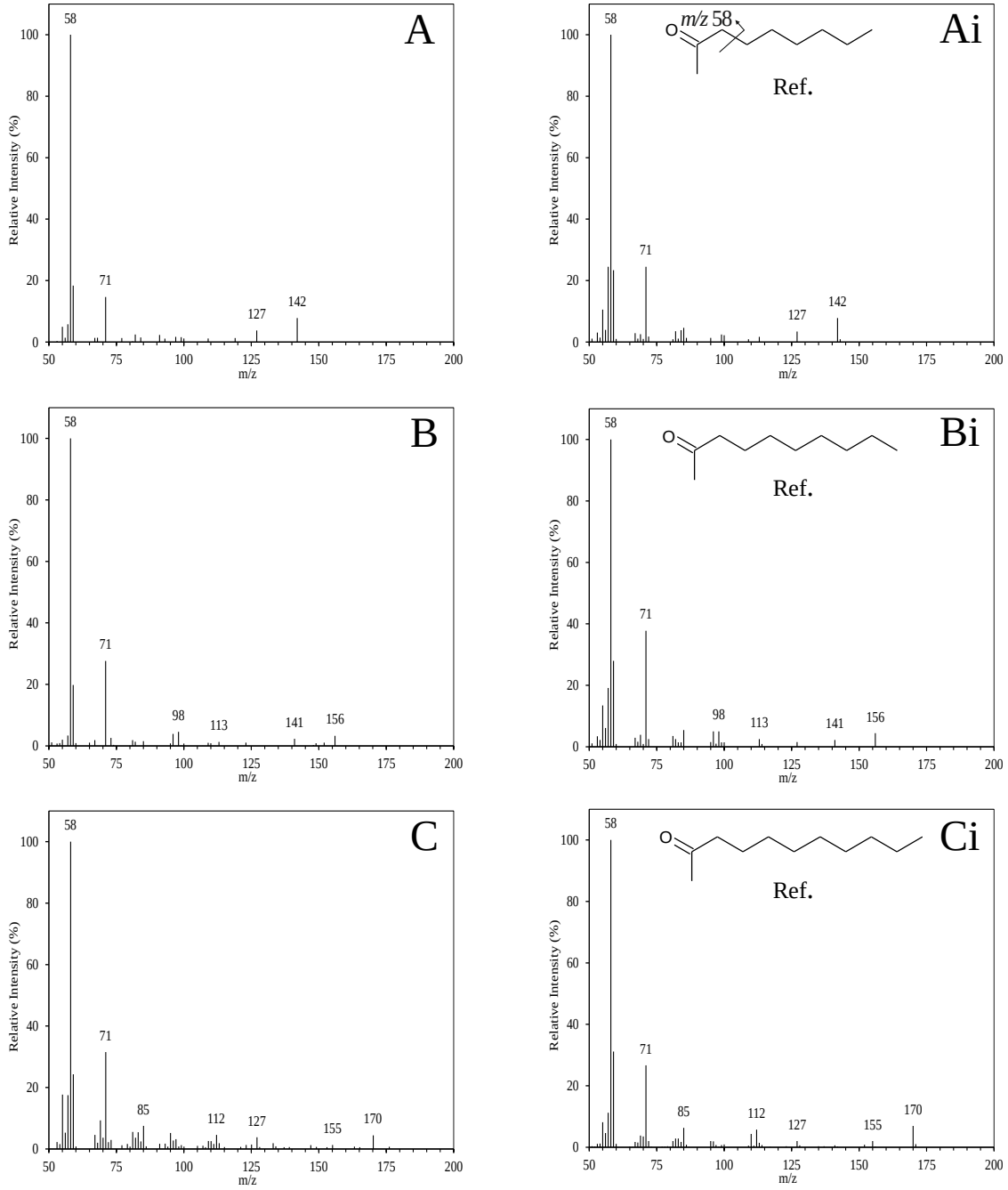

Figure 5-29 Examples of mass spectral identification of ketones from the analysis of Fraction S2 (ANS crude oil separation; **A-C**). Individual compounds identified by comparison of spectra obtained from crude oil analyses with NIST library spectra (**A**; **Ai-C**; **Ci**).

The elution order of these tentatively identified alkanone and alkanal series compared well with data in previously reported studies (George and Jardine, 1994; Leif and Simoneit, 1995; Riboulleau *et al.*, 2000). The GC×GC-MS EIC (*m/z* 82 and 58; Figure

5-27B) shows that the ANS crude oil *n*-alkanals and *n*-alkanones extended from C_9 to C_{26} (mostly C_{13} to C_{22}). The C_{12} series of peaks are shown as an example of the elution order (Figure 5-30) with v and vi corresponding to decan-2-one and decanal respectively (Figure 5-31 A and B).

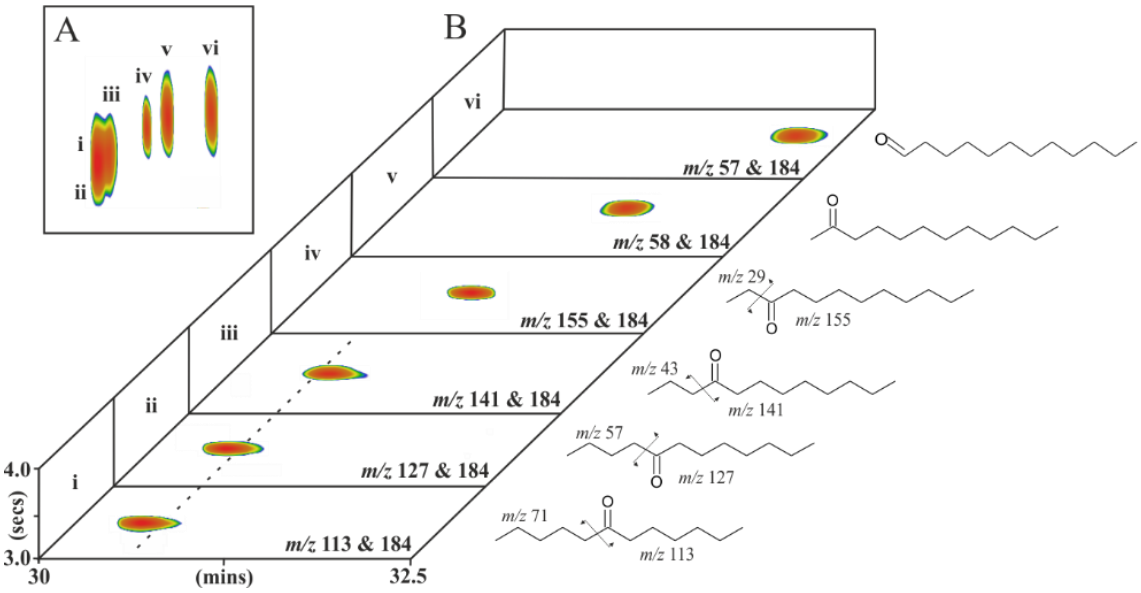

Figure 5-30. GC×GC-MS EIC (**A**) of the C_{12} alkanal (*m/z* 82) and alkanones (*m/z* 58) and a 3D graphic illustrating the elution order and structures of 6-dodecanone (i), 5-dodecanone (ii), 4-dodecanone (iii), 3-dodecanone (iv), 2-dodecanone and dodecanal showing the fragmentation resulting in the unique mass spectrum for each isomer (**B**).

The individual ketone isomers within the repeating alkanone units were tentatively identified based on their mass spectra. The spectrum of the first of the resolved peaks (*e.g.* Figure 5-30Biv) was characterised by a loss of M-29, indicative of the loss of·C_2H_5 and corresponding to an alkan-3-one. The mass spectrum obtained for the example of the C_{12} series shows the characteristic M-29 loss resulting in a peak at *m/z* 155. Identification of the remaining isomers is less straightforward owing to co-elution. As in the example of the C_{12} series (Figure 5-30A i/ii and iii), the two earlier eluting peaks were typically sufficiently well resolved that a good quality mass spectrum could be obtained for the later eluting peak (iii). These spectra are characterised by a loss of M-43, consistent with

a loss of $\cdot C_3H_7$ and suggesting an alkan-4-one. In the example of the C_{12} series (Figure 5-30Biii) the M-43 loss can be assigned in the mass spectrum, resulting in a fragment ion at *m/z* 141 (Figure 5-31D).

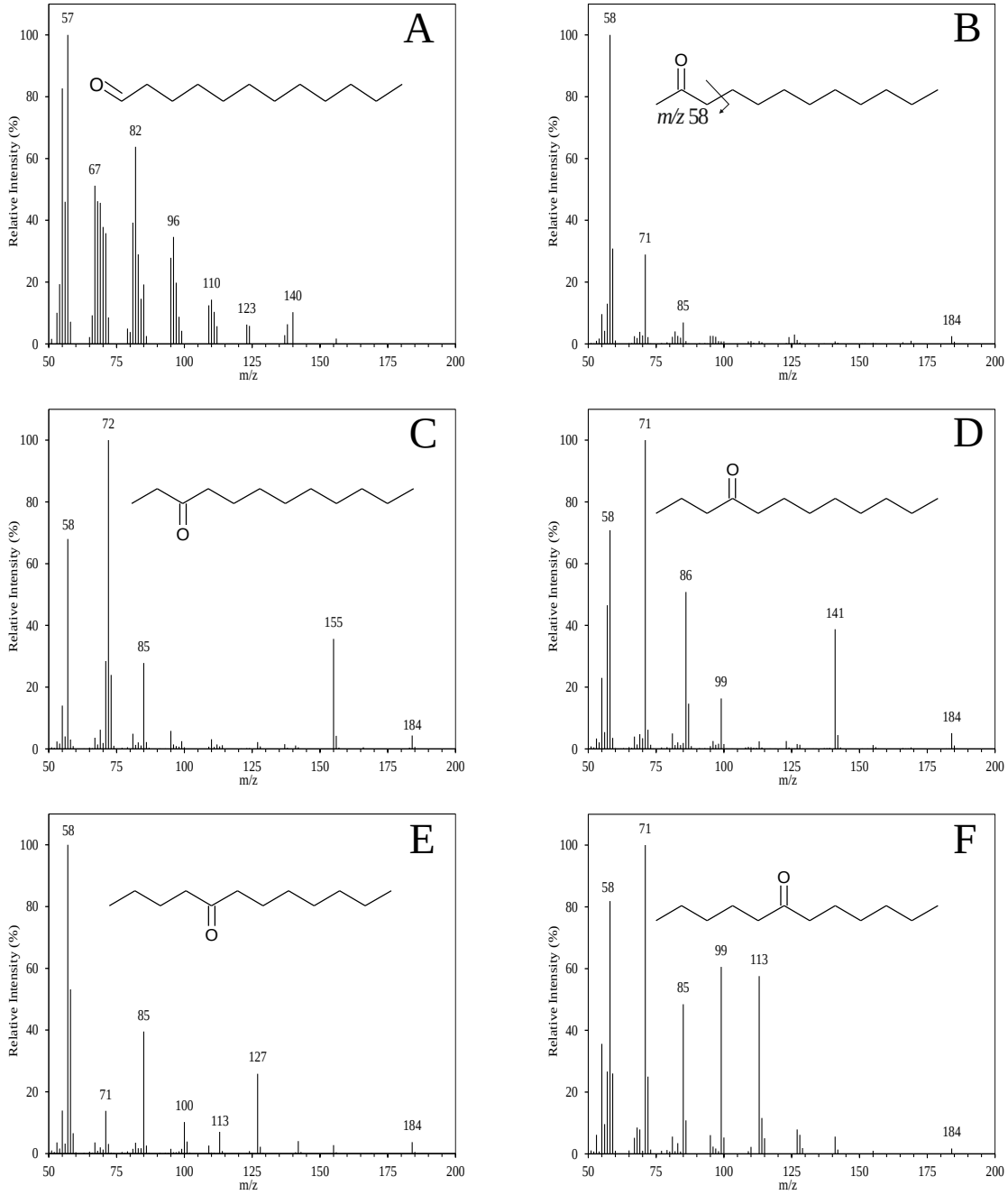

Figure 5-31. Mass spectra of the peaks tentatively identified as dodecanal (**A**), 2-dodecanone (**B**), 3-dodecanone (**C**), 4-dodecanone (**D**), 5-dodecanone (**E**) and 6-dodecanone (**F**) from the GC×GC-MS analysis of Fraction S2

The remaining isomers were typically too structurally similar to be resolved by GC techniques. In the case of the C_{12} ketones, only the 5- and 6-dodecanone isomers (Figure 5-30Ai and ii) could not be resolved chromatographically. By assuming a similar pattern of losses in the mass spectra of the 5- and 6- isomers, (i.e. M-57 and M-71 respectively), the EICs for the 5- and 6- isomers could be generated (Figure 5-30Bi and ii). By employing spectral subtraction, good quality mass spectra for 5-dodecaone and 6-dodecanone were obtained (Figure 5-31E and F). Both mass spectra indeed show the expected losses exhibiting the corresponding fragments ions, *m/z* 127 and 113 for the 5-dodecanone and 6-dodecanone isomers respectively.

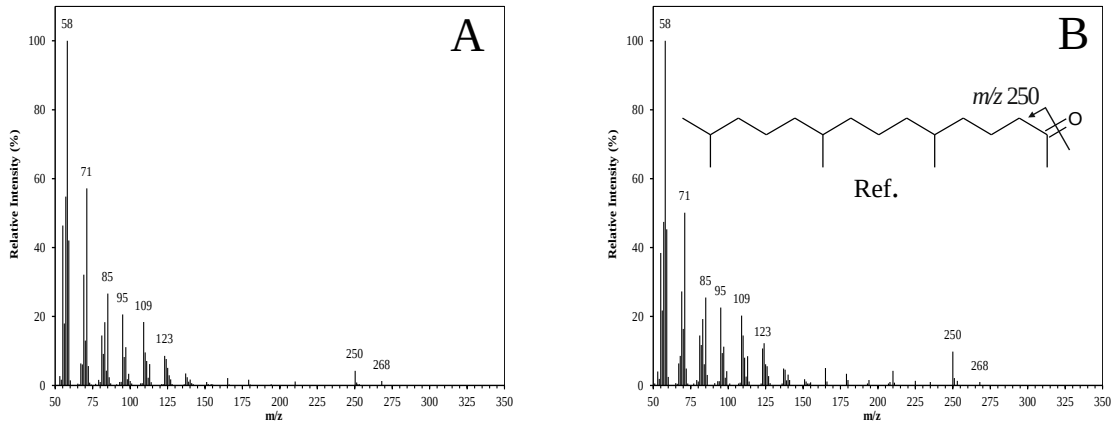

Figure 5-32. Mass spectrum of a C_{18} branched ketone (**A**) obtained from the GC×GC-MS analysis of fraction S2 of the ANS oil fractionation tentatively identified as 6,10,14-trimethyl-pentandecan-2-one by comparison with the NIST reference mass spectrum (**B**).

Closer inspection of the alkanal and alkanone EICs revealed a number of peaks that eluted outside of the previously discussed sequence. The most abundant of these peaks (Figure 5-27B; *iso*-C_{18}) had a molecular ion (*m/z* 268) consistent with a C_{18} alkanone. However, it eluted some 10 minutes earlier than the C_{18} *n*-alkanones. The mass spectrum of the compound (Figure 5-32) was characterised by the *m/z* 58 fragment ion and exhibited a loss of M-18, indicative of the loss of H_2O. The compound was tentatively identified as 6,10,14-trimethyl pentadecan-2-one by comparison with the NIST mass spectral library

(RMatch 927; Figure 5-32B). The occurrence of C_{18} isoprenoid ketones in crude oils is thought to be due to the oxidation of the phytyl chain of chlorophyll *a* 'incorporated' into kerogen. Indeed, previous studies have reported that the thermal degradation of phytol yields 6,10,14-trimethyl pentadecan-2-one as one of the main products (Leif and Simoneit, 1995; Riboulleau *et al.*, 2001).

Aliphatic ketones have rarely been reported in crude oils (Jenisch-Anton *et al.*, 1999; Strelnikova and Serebrennikova, 2011; Alhassan and Andersson, 2013) but have been identified as common constituents of shale oil (the product of oil shale pyrolysis; Iida *et al.*, 1966; Ingram *et al.*, 1983; Riboulleau *et al.*, 2000; Alhassan and Andersson, 2013) and other forms of dispersed and concentrated sedimentary organic matter (e.g. George and Jardine, 1994; Leif and Simoneit, 1995; Deniau *et al.*, 2001). The origin of the alkanones is thought to be linked directly to the ester bonds that polymerise the aliphatic chains of lipids in the original kerogen. During the catagenesis of the kerogen, these linkages are broken under thermal stress resulting in the formation of the alkanones (Leif and Simoneit, 1995; Strelnikova and Serebrennikova, 2011). This is supported herein by the identification of *n*-alkanones with the ketone (C=O) group located in different positions along the hydrocarbon chain. Such a feature may reflect the presence originally of ester linkages to kerogen at various locations in the alkyl chain (Jenisch-Anton *et al.*, 1999).

Extraction of the molecular ions of fluorenone (*m/z* 180) and the alkylfluorenone homologues (*m/z* 194, 208, 222 and 236) revealed them to be one of the more abundant series present in fraction S2 (Figure 5-33B). Co-injection of authentic fluorenone allowed confirmation of the parent molecule by its GC×GC retention time and by mass spectral comparison (Figure 5-34 A and Ai). Interestingly, library spectra were available for the dimethyl fluorenones (Figure 5-34C and Ci; RMatch 964) but were not available for the methyl fluorenones. Despite the lack of library spectra, the assignment of the C_1

fluorenones was made based on the relative retention position (Figure 5-33B) and by interpretation of the mass spectra (Figure 5-34B). The mass spectra of the methylfluorenones are dominated by the molecular ion at *m/z* 194 and an ion at *m/z* 165 (M-29). The latter loss corresponds to the loss of CHO, originating from the initial loss of CO, followed by a hydrogen rearrangement and incorporation of the methyl group into a 7-membered ring (Porter and Baldas, 1970). Mass spectra of the dimethyl-fluorenones exhibit both the M-15 (loss of CH_3) and M-29 (loss of CHO) suggesting the formation of a methyl substituted 7-membered ring (*m/z* 165).

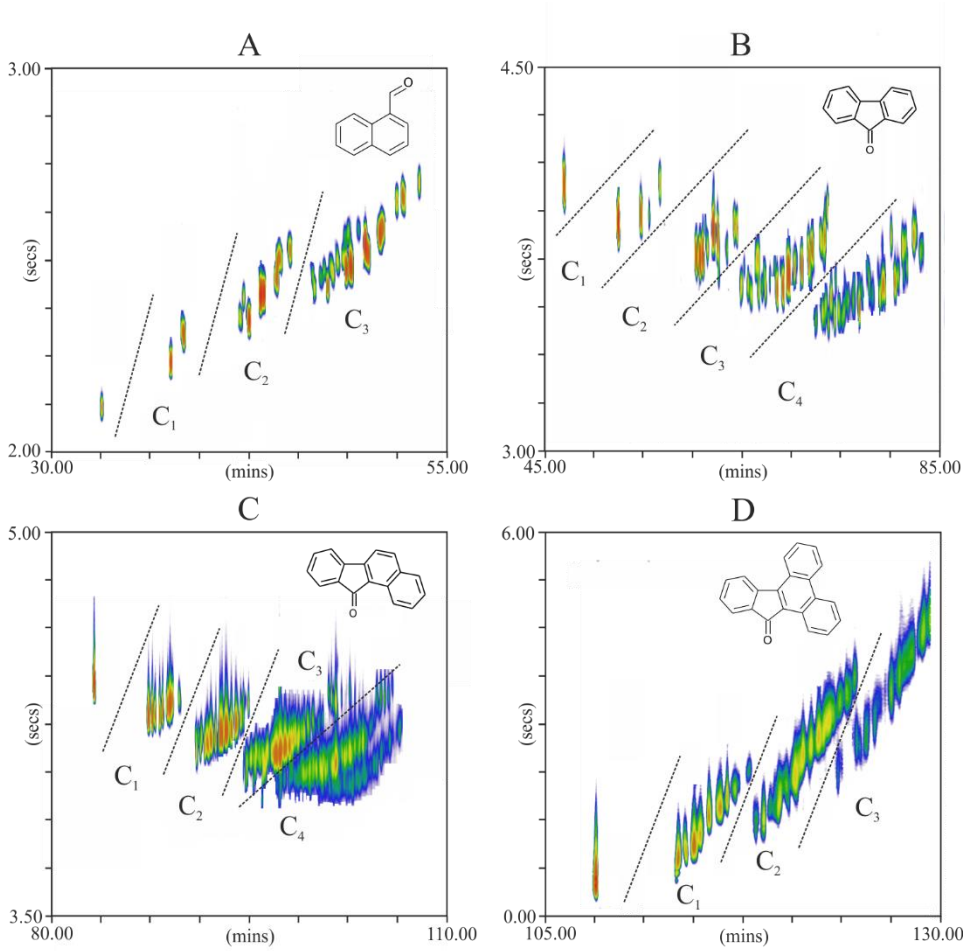

Figure 5-33. GC×GC-MS EICs of naphthalene carboxaldehyde and C_{1-3} homologues (**A**; *m/z* 156, 170, 184 and 198), fluorenone and C_{1-4} homologues (**B**; *m/z* 180, 194, 208, 222 and 236), benzofluorenone and C_{1-4} homologues (**C**; *m/z* 230, 244, 258, 272 and

286) and dibenzofluorenone and C_{1-3} homologues (**D**; *m/z* 280, 294, 308 and 322) obtained from Fraction S2 from the SPE separation of the ANS crude oil.

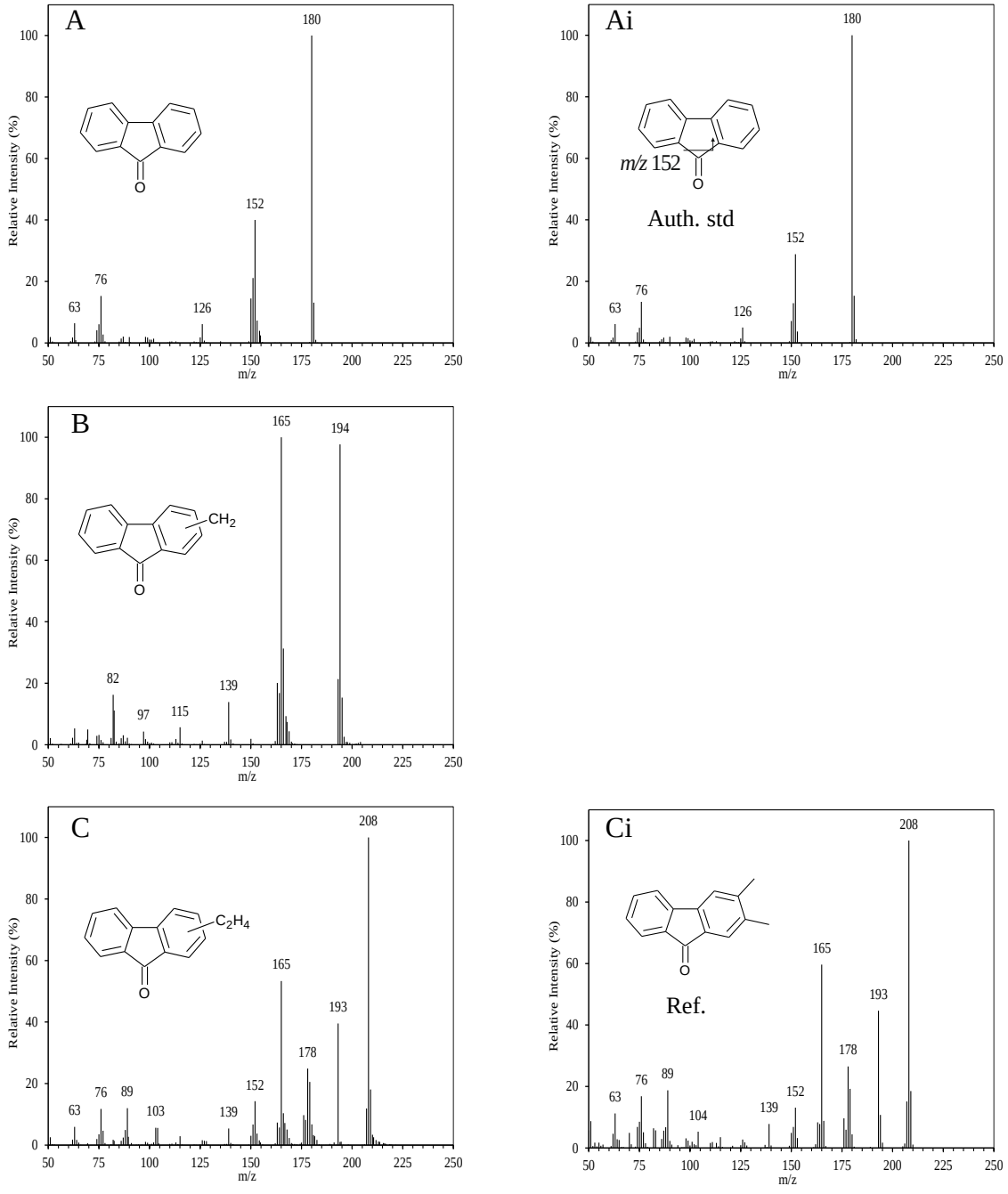

Figure 5-34. Examples of mass spectral identification of alkylated fluorenones from the analysis of Fraction S2 (ANS crude oil separation; **A-C**). Individual compounds identified by comparison of spectra obtained from crude oil analyses with a fluorenone authentic standard (**A-Ai**), from position within the homologous series and mass spectral interpretation (**B**) and comparison with NIST library spectrum (**C-Ci**).

The second of the larger, resolved compound series was identified as benzofluorenone and its alkylated homologues (Figure 5-33C). A previous study identified benzofluorenones as major constituents of crude oils, constituting ~50% of fluorenone material in each of four crude oil samples (Strelnikova and Serebrennikova, 2011). Comparison of the first peak within the series to the mass spectral library supported assignment as benzo(a)fluorenone (Figure 5-35A and Ai; RMatch 982). The mass spectrum of the second group of peaks in the series (*m/z* 294; Figure 5-35B) compared well with the mass spectrum of 10-methyl-benzo(a)fluorenone (Figure 5-35Bi; RMatch 901) again, with the typical M-29 losses. Interestingly, the M-29 loss was observed for all ten methyl-benzofluorenone isomers, implying the rearrangement and formation of the 7-membered ring is not exclusive to only those homologues with methyl groups attached to either of the substituted benzene rings.

Detection of benzofluorenone and its alkylated homologues prompted investigations into the presence of higher fluorenone benzologs. Extraction of the dibenzofluorenone molecular mass ion (*m/z* 280) and that of the alkylated homologues (*m/z* 294, 308 and 322) revealed a series of compounds with molecular ions matching those of the predicted compounds (Figure 5-33D). Comparison of the mass spectrum of the first chromatographic peak in the series to the mass spectral library allowed it to be identified tentatively as dibenzo(c)fluorenone (Figure 5-36A and Ai; RMatch 952). The mass spectrum of the parent compound was typical of those observed for fluorenone and benzofluorenone, the main loss being M-28, indicating the loss of the C≡O. The C_1 and C_2 alkyl dibenzofluorenones also exhibited similar fragmentation patterns to the lower fluorenone benzologs (Figure 5-36 B and C) and were also tentatively assigned based on their mass spectra and their retention position.

The origins of fluorenones in crude oils are not clear. Direct entry of the fluorenones from the initial kerogen is unlikely as currently there are no reports of suitable precursors

existing in living organisms. Oxidation of fluorenes has also been considered as a potential mechanism for fluorenone formation as the latter are easily oxidised at the methylene bridge. Certain authors seem to favour this theory (Bennett and Larter, 2000), based on observations of increasing fluorenone concentrations over time once samples are exposed to air. However, Strelnikova and Serebrennikova (2011) argue that fluorenes do not exist at sufficient concentrations in crude oils to explain the observed high fluorenone concentrations and instead propose fluorenone formation via a Friedel-Crafts acylation of 2-carboxyphenols during maturation as a more likely source.

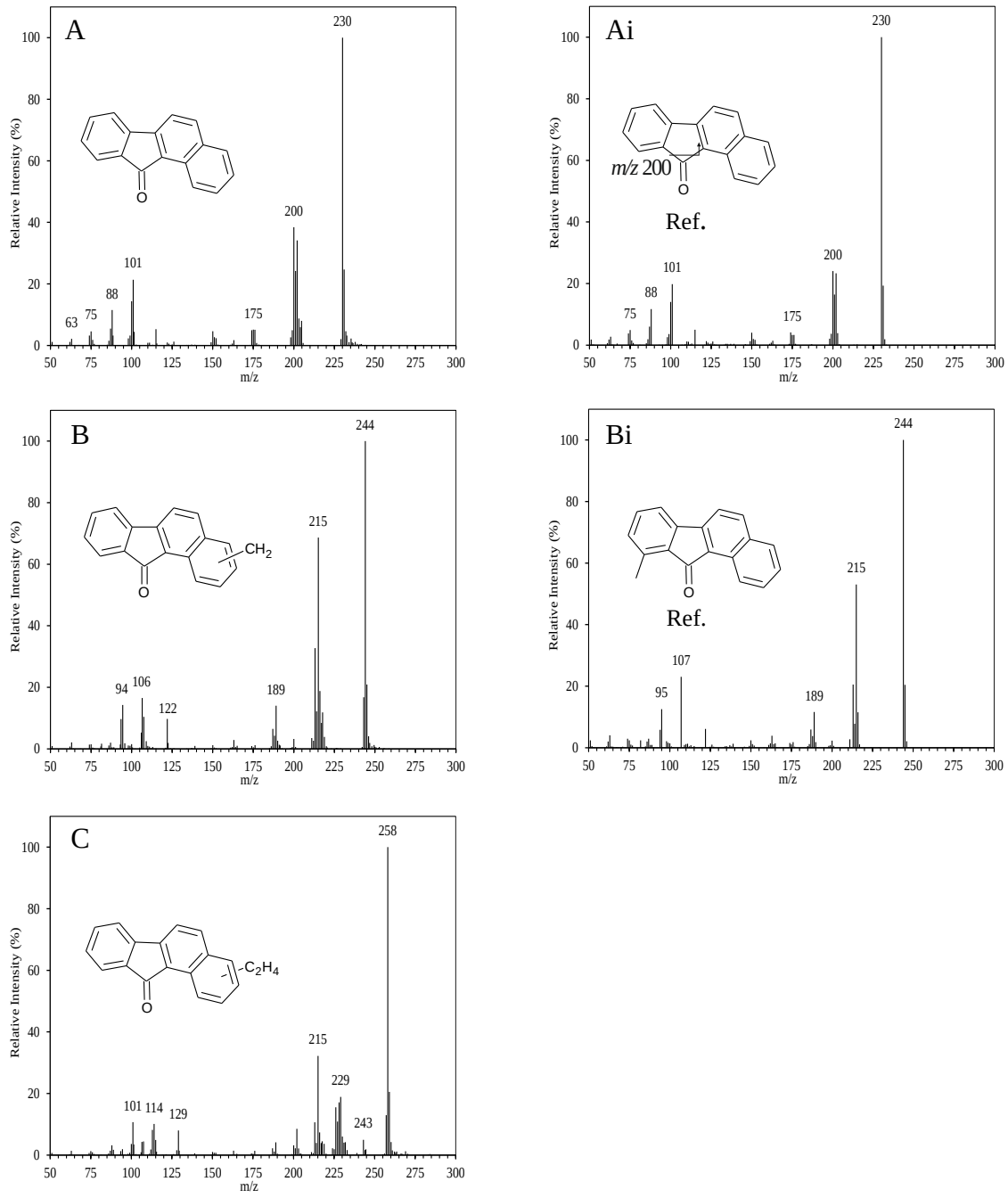

Figure 5-35. Examples of mass spectral identification of alkylated benzofluorenones from the analysis of Fraction S2 (ANS crude oil separation; **A-C**). Individual compounds identified by comparison of spectra obtained from crude oil analyses with NIST library spectra (**A**; **Ai** and **B**; **Bi**) and mass spectral interpretation and chromatographic position.

The observation that fluorenone concentrations are affected by exposure to air is of concern when attempting to link the presence or concentrations to geochemical parameters. Certainly, both academic and industrial practices regarding the proper transport and storage of such crude oil samples rarely considers the impact of oxidation by exposure to air. Indeed, a number of the oils used in this study have been exposed to air for a number of years and as such, no geochemical significance can be assigned to this particular data set. Nonetheless, the data presented herein do show the use of the separation scheme to obtain appropriate fractions of fluorenones, and should the appropriate samples be obtained, a comprehensive investigation into the fluorenones of crude oils could be conducted.

The lower benzologues of fluorenone (i.e. indanones), could not be identified within the S2 fraction. However, whilst investigating the earlier region of the chromatogram a series of naphthalene carboxaldehydes were tentatively identified (Figure 5-33A). The mass spectrum of the first peak in the series compared well to the library spectrum for naphthalenecarboxaldehyde (Figure 5-37A and Ai; RMatch 945) as did the spectra of the methylnaphthalene carboxaldehydes (Figure 5-37B and Bi; RMatch 894). The spectra of both the parent and methyl naphthalenecarboxaldehydes exhibited similar fragmentation pathways to those of the fluorenone series, with the most common losses being the M-28 and M-29 for the parent and alkylated compounds respectively.

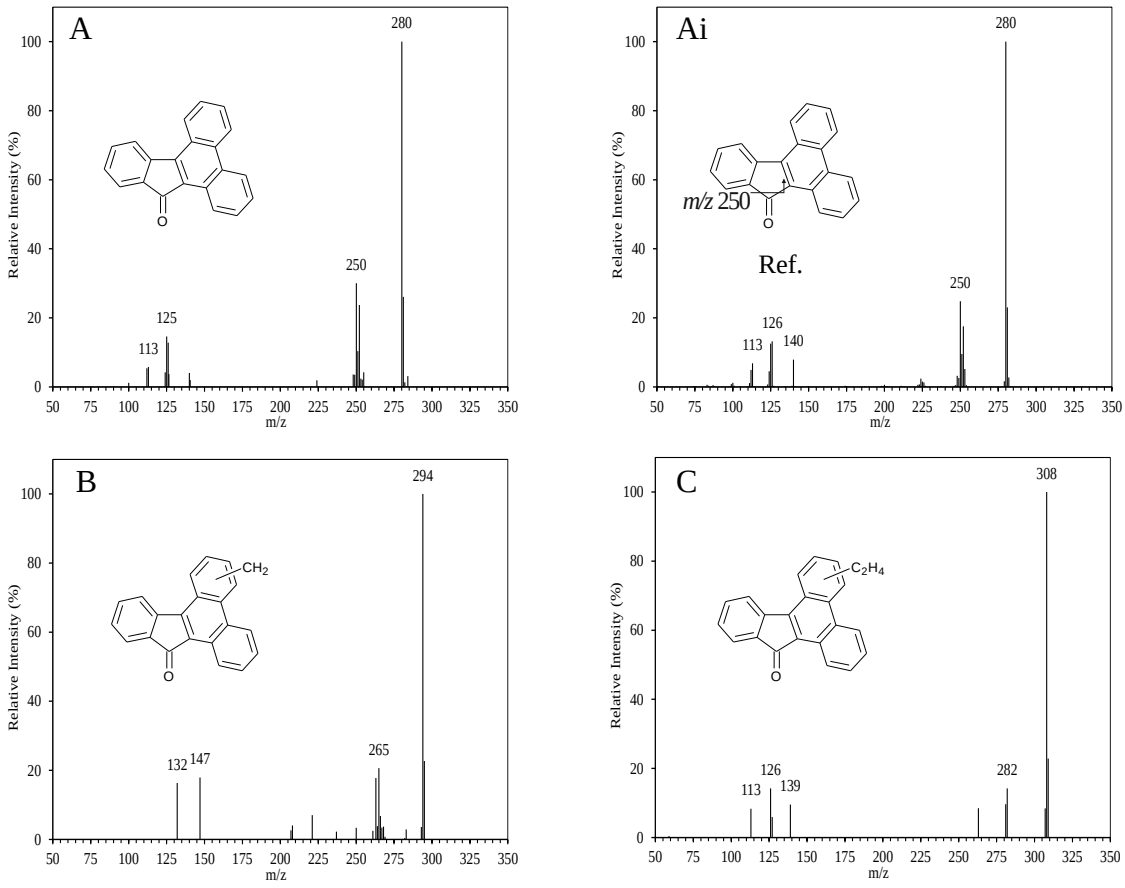

Figure 5-36. Examples of mass spectral identification of alkylated dibenzofluorenones from the analysis of Fraction S2 (ANS crude oil separation; **A-C**). Individual compounds identified by comparison of spectra obtained from crude oil analyses with NIST library spectra (**A**; **Ai**) and mass spectral interpretation and chromatographic position (**B** and **C**).

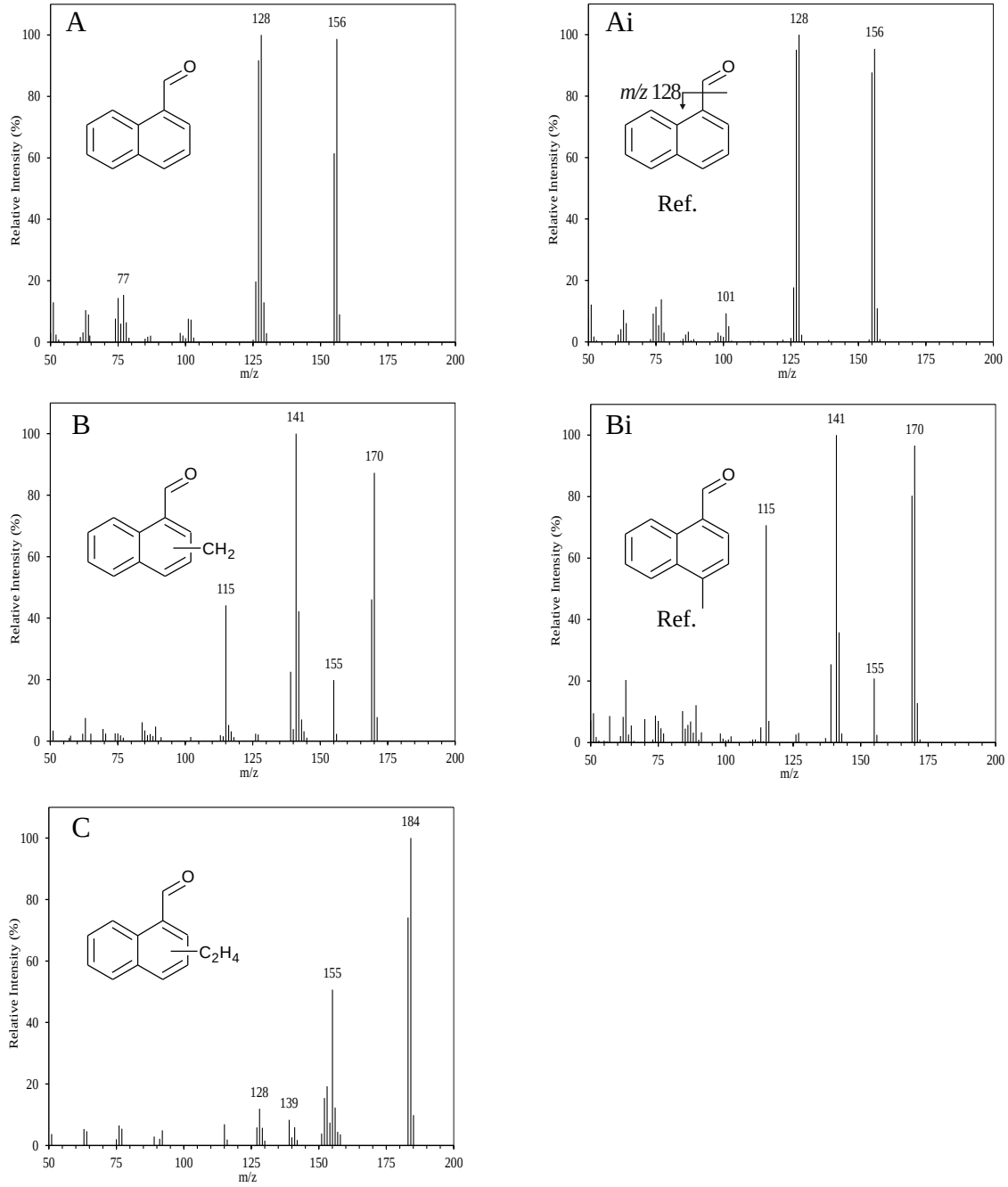

Figure 5-37. Examples of mass spectral identification of alkylated carboxaldehydes from the analysis of Fraction S2 (ANS crude oil separation; **A-C**). Individual compounds identified by comparison of spectra obtained from crude oil analyses with NIST library spectra (**A**; **Ai** and **B**; **Bi**) and mass spectral interpretation and chromatographic position (**C**).

Following the GC×GC-MS analysis of the ANS crude oil, the remaining four crude oil samples were examined under the same instrumental conditions. The resulting data are

presented in Figure 5-38. Examination of five chromatograms shows the Brent, Kuwait and ANS crude oils (Figure 5-38 A, B and C) to be very similar in composition. The fluorenone and benzofluorenones (Figure 5-38 ii and iii) appear to be the major constituents in all of the fractions and are easily visible in the TIC. Whilst broadly also similar, the S2 ketonic fractions of Kuwait and Brent samples do appear to be less complex than the ANS crude and the relative concentration of the fluorenone and benzofluorenone series are far higher in the Brent crude than in any of the other four samples.

The fractions from the TJP and Bonga oils (Figure 5-38 D and E) appeared significantly more complex than those of the other three samples. The chromatograms of the Bonga samples were characterised by a large UCM that could not be resolved by GC×GC-MS. Extraction of the *m/z* 58 ion revealed the presence of the alkanone series. Interestingly, in the case of the Bonga crude, the alkan-2-one appeared to be favoured, being far more abundant than the other ketone isomers. A series of higher molecular weight compounds were also present in the Bonga S2 fraction.

The S2 fraction for the TJP was also significantly complex and was characterised by a large UCM. Extraction of the alkanone ion (*m/z* 58) did not yield the previously observed sequence of alkanones. However, the data did yield a UCM of what were likely significantly branched alkanone structures. It is worth nothing that the relative concentration of the fluorenones and benzofluorenone was significantly lower in the TJP S2 fraction than in the other four samples.

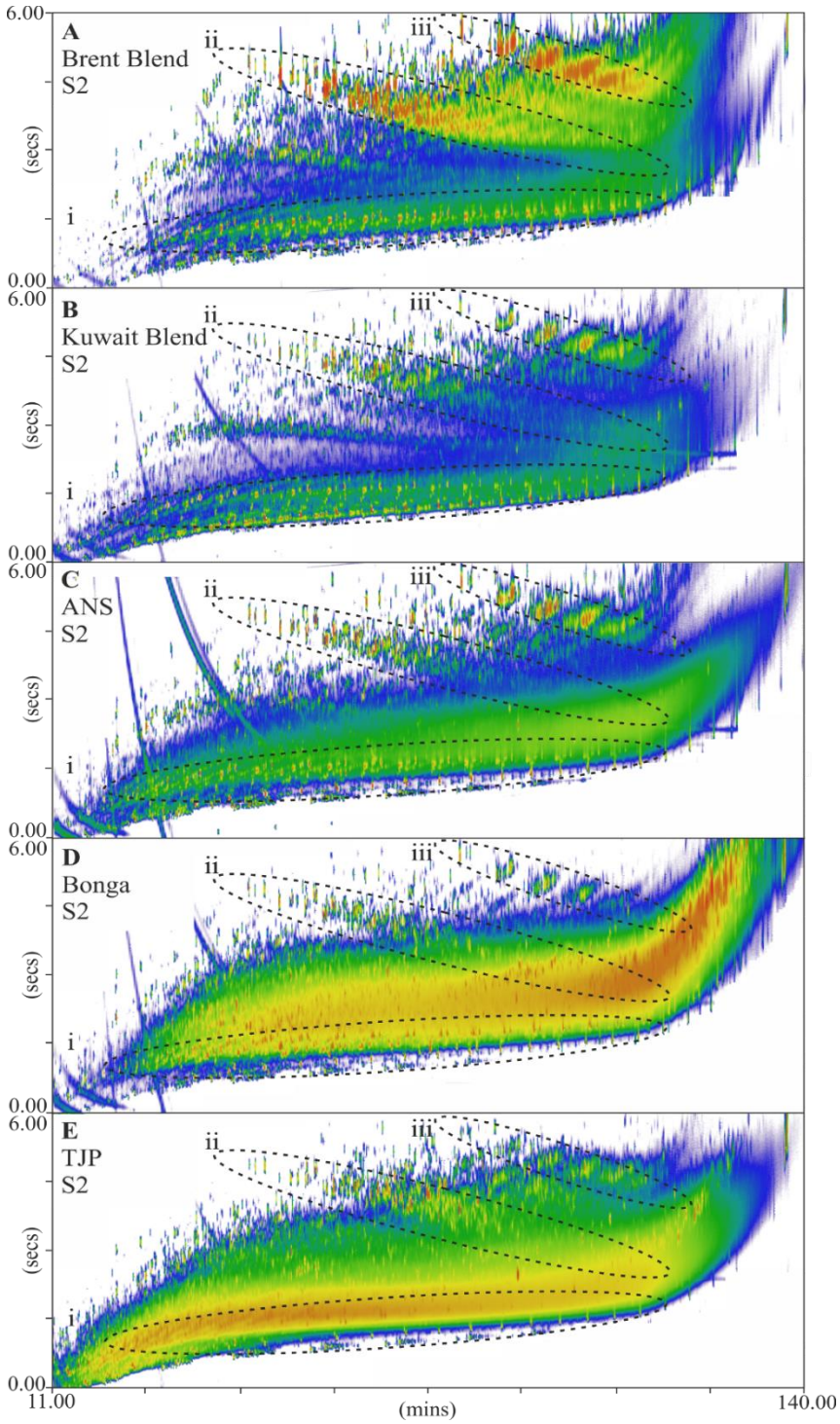

Figure 5-38. GC×GC-MS TICs of the S2 fractions obtained from the SPE separation of the Brent Blend (**A**), Kuwait blend (**B**), ANS (**C**), Bonga (**D**) and TJP (**E**) crude oils. Highlighted on each chromatogram are areas in which various compound classes elute: i; alkanals and alkanones, ii; alkyl fluorenones, iii; alkyl benzofluorenones.

Preliminary investigations into the composition of the fractions allowed the tentative identification of a number of other compounds and their corresponding alkyl homologues. For example, a series of OS containing compounds (*e.g.* phenoxathin and alkyl homologues) could be identified in the Kuwait oil, correlating with the high sulphur content of the oil. A series of cyclic ketones were identified within the Brent blend. It is likely that these compounds are present within the other samples but the increased degree of complexity makes their identification difficult. It is likely that as some of the overlying complexity of the crude oil matrix is removed by SPE separation, lower concentration components become easier to detect.

5.4.12 Fraction S3 (xanthone)

The 'Model' compound separation identified fraction S3 as containing the xanthone 'model' compound and was thus broadly labelled the "xanthone" fraction. GC-MS chromatograms of the S3 fraction were characterised by UCMs (data not shown), resulting in the need for application of GC×GC-MS to improve chromatographic resolution of the fraction components. Data from the GC×GC-MS analysis of the S3 fractions were treated similarly to those of Fraction S2. Much like the S2 datasets (Figure 5-38) a number of compound series were sufficiently abundant to be clearly distinguished in the GC×GC-MS TICs of the S3 fractions (Figure 5-39 i, ii and iii). Extraction of the molecular ion of xanthone (*m/z* 196) and $C_{1\text{-}3}$ alkylated homologues (*m/z* 210, 224, 238) revealed the likely presence of the xanthone series in the ANS crude oil (Figure 5-39B). Authentic xanthone co-injection eluted with comparable retention coordinated and produced an identical mass spectrum (Figure 5-40 A and Ai). No reference mass spectra for the alkylated xanthones were available for comparison and identifications were therefore made by interpretation of the mass spectra only.

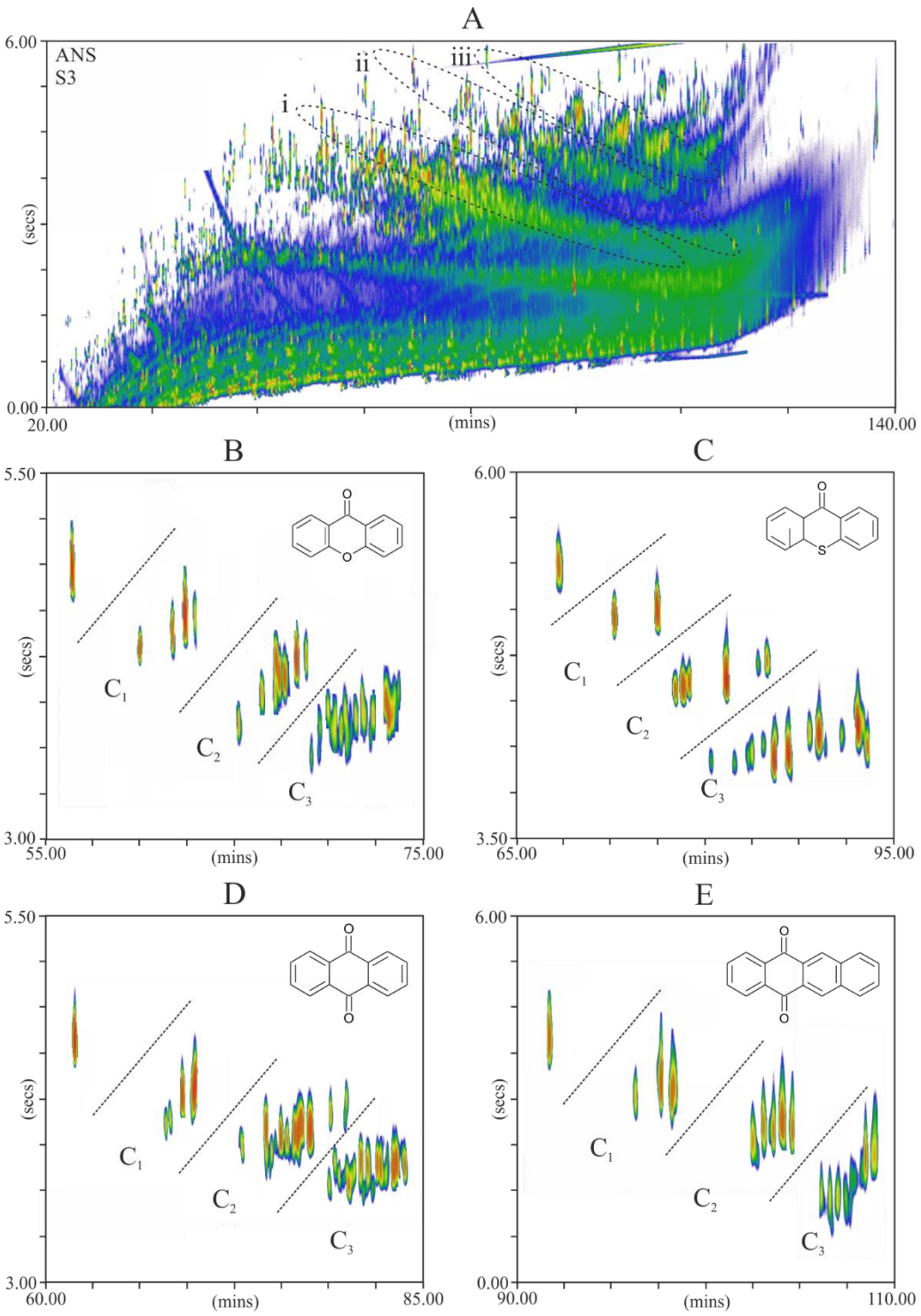

Figure 5-39. GC×GC-MS TIC from the analysis of the ANS crude oil Fraction S3 (**A**) and EICs of xanthone and C_{1-3} homologues (**B**; *m/z* 196, 210, 224 and 238), thioxanthone and C_{1-3} homologues (**C**; *m/z* 212, 226, 240and 254), anthraquinone and C_{1-3} homologues (**D**; *m/z* 208, 222, 236 and 250) and benzanthraquinone and C_{1-3} homologues (**E**; *m/z* 258, 272, 286 and 300).

In order to understand the mass spectral fragmentation of the alkylated homologues of xanthone a study was first made of the parent xanthone. The fragmentation pathways exhibited by xanthone were typical of polycyclic aromatic hydrocarbons (PAHs) containing a substituted methylene bridge (Porter and Baldas, 1970). Early studies by Beynon *et al.* (1959) on the fragmentation of anthraquinones, identified the successive loss of the C≡O from the molecule during electron ionisation. From these observations, the origin of the major fragment peaks within the mass spectrum could be predicted. Arends *et al.* (1973) were the first to study the fragmentation of xanthones specifically and allowed for a complete scheme for the fragmentation of xanthone to be drawn (Figure 5-41A). Ionisation occurs at the ketone functional group resulting in the loss of C≡O and the formation of the dibenzofuran ion (*m/z* 168; $C_{12}H_8O^{+\cdot}$). Successive loss of another C≡O moiety and a hydrogen atom yields the benzdehydrotropylium structure at *m/z* 139 ($C_{11}H_7^{+\cdot}$).

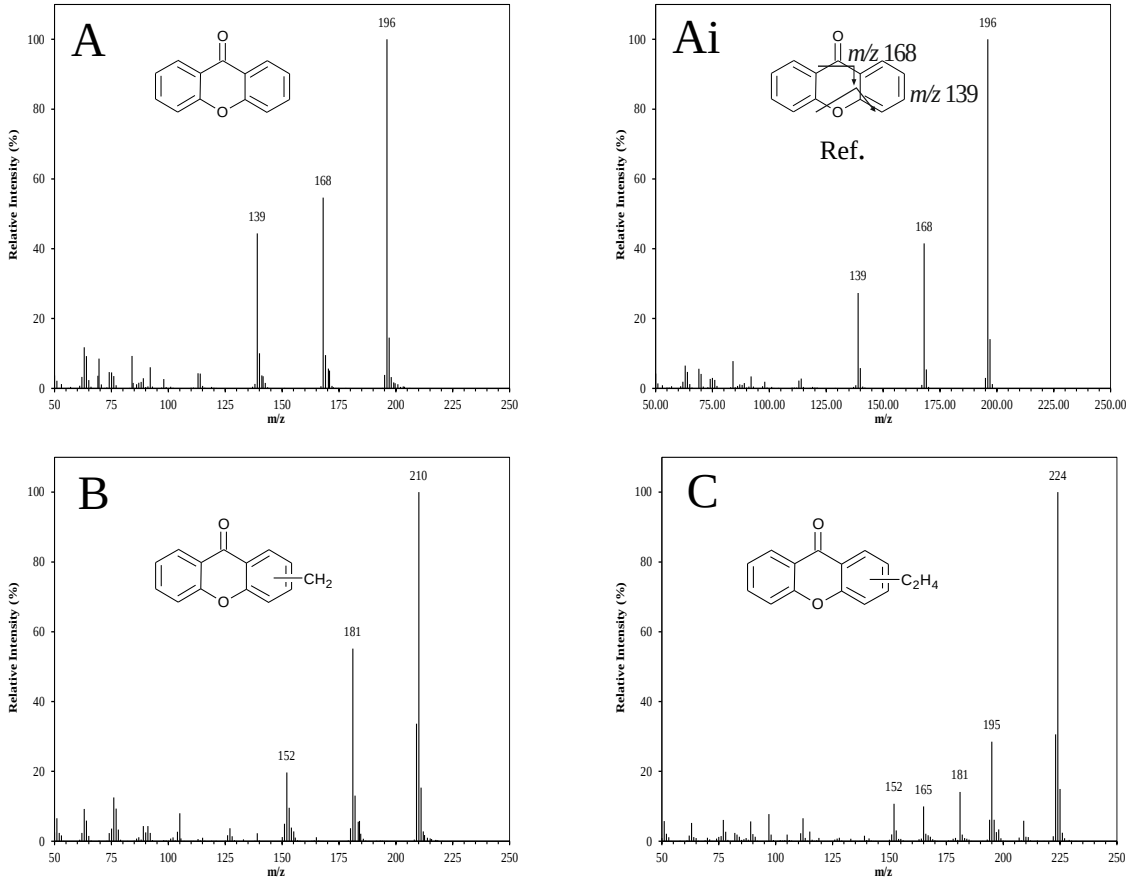

Figure 5-40. Examples of mass spectral identification of xanthone and its alkylated homologues from the analysis of Fraction S3 (ANS crude oil separation; **A**-**C**). Individual compounds identified by comparison of spectra obtained from crude oil analysis with co-injected model compounds (**A** and **Ai**) and mass spectral interpretation and chromatographic position (**B** and **C**).

Interestingly, mass spectra of the methyl-substituted compounds did not exhibit the common M-15 losses (Figure 5-40B), indicative of the loss of a methyl substituent (CH_3). Instead, there appeared a loss of a neutral -CHO (M-29) fragment. Whilst the fragmentation pathways of the alkyl xanthones have not been studied previously, commonalities can be observed between the losses and rearrangements that have been reported for other heteroatom-containing alkyl PAHs. For example, the fragmentation of 3-methyldibenzothiophene is thought to proceed with an initial loss of M-1, which is rationalised by the formation of a structure in which the methyl group is incorporated into

a 7-membered ring (Porter and Baldas, 1970). If a similar fragmentation pathway is assumed for alkylxanthones, the mass spectra of the methyl xanthones (Figure 5-40B) can be rationalised by loss of a neutral -CHO (M-29) fragment and subsequent rearrangement, with the alkyl substituent being incorporated into the benzene ring (Figure 5-41B). Indeed, the spectra of the three methylxanthone isomers (Figure 5-40B) all exhibited the same ions, and were confidently assigned. However, the similarity of the spectra are such that the position of the methyl groups on the parent xanthone structures could not be determined through mass spectrometry alone. Complete structural characterisation of the methyl xanthones would require synthesis of appropriate compounds in order to obtain unique retention characteristics.

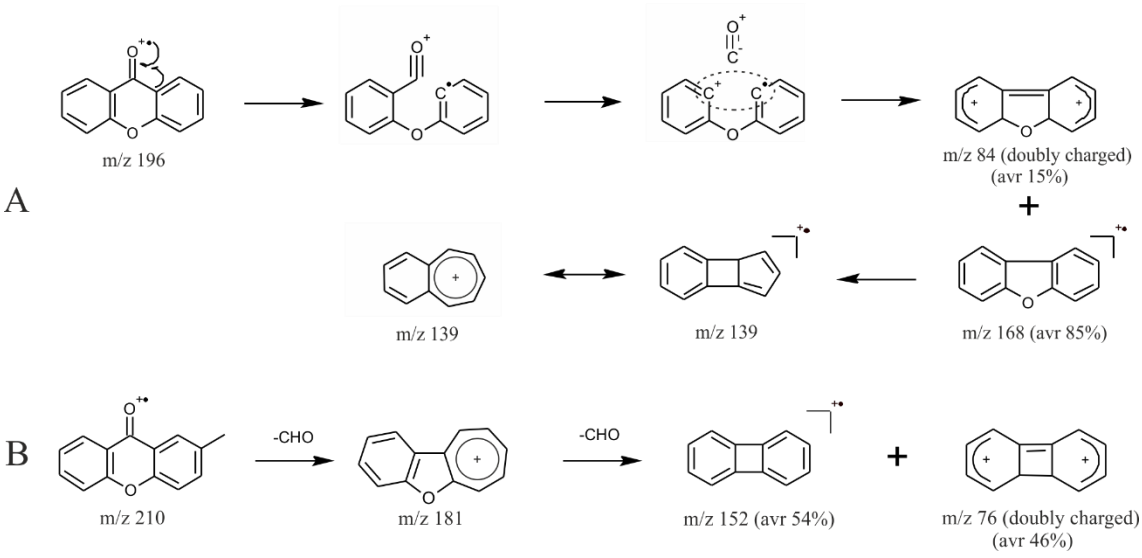

Figure 5-41. Fragmentation series for xanthone under electron ionisation (70 eV) showing the sequential losses of the two CO moieties (**A**) and the postulated fragmentation pattern for methyl xanthones loss of CHO (M-29) and incorporation of the methyl group into a 7-membered ring (**B**).

The mass spectra of the C_2 xanthones were not as simple (example shown in Figure 5-40C), with ions for both the loss of the -CHO (M-29) and -CH_3 (M-15) present in all spectra. Interestingly, the spectra of the earlier eluting peaks exhibited the preferential M-

15 loss, whereas the spectra of the later eluting peaks exhibited a higher loss of M-29, suggesting that positioning of the methyl groups affected the route of fragmentation.

Studies concerning the presence of xanthones in crude oils are uncommon, with perhaps only two reports in the literature (Oldenburg *et al.*, 2002; Bakr, 2009). Xanthones in crude oils are thought to originate from diagenetic transformation of functionalised biogenic xanthones, which lose their functional groups (Oldenburg *et al.*, 2002). This is evidenced by the common presence of highly functionalised biogenic xanthones in many terrestrial plants (*e.g.* Tomasek and Crawford, 1986) and from their absence in non-terrestrially sourced crude oils.

The xanthones are of both environmental and geochemical relevance. Xanthone has been identified as of the predominant oxygenated PAH in mutagenic fractions of diesel exhaust extracts (Strandell *et al.*, 1994), with subsequent investigations identifying xanthones in both urban aerosols (Fernandez and Bayona, 1992) and in North Sea water samples (Bester and Theobald, 2000). Geochemically, the xanthones have the potential to serve as markers for secondary crude oil migration based on the partitioning of xanthone and the alkyl xanthones between the oil and water phase, as well as being indicative of inorganic/organic interactions (Oldenburg *et al.*, 2002).

Further investigation into the composition of fraction S3 identified two series of compounds exhibiting a similar profile to that of the xanthones, but eluting sequentially later in both dimensions (Figure 5-39 ii and iii). The first of these series was identified as anthraquinone and its alkylated homologues (Figure 5-39C) by comparison of the mass spectrum of the parent compound with a reference spectrum from the mass spectral library (Figure 5-42 A and Ai; RMatch 924). Fragmentation of anthraquinone in the MS is similar to that of xanthone. However, the presence of the cyclohexane ring in place of a methylene bridge resulted in the successive loss of two CO moieties, resulting in a

fragment ion of *m/z* 152 ($C_{12}H_8^{+\cdot}$). In this instance, reference mass spectra were also available for the methyl (Figure 5-42Bi) and the dimethyl (Figure 5-42Ci) anthraquinones allowing their positive identification in the S3 fraction (RMatch 901 and 915 respectively).

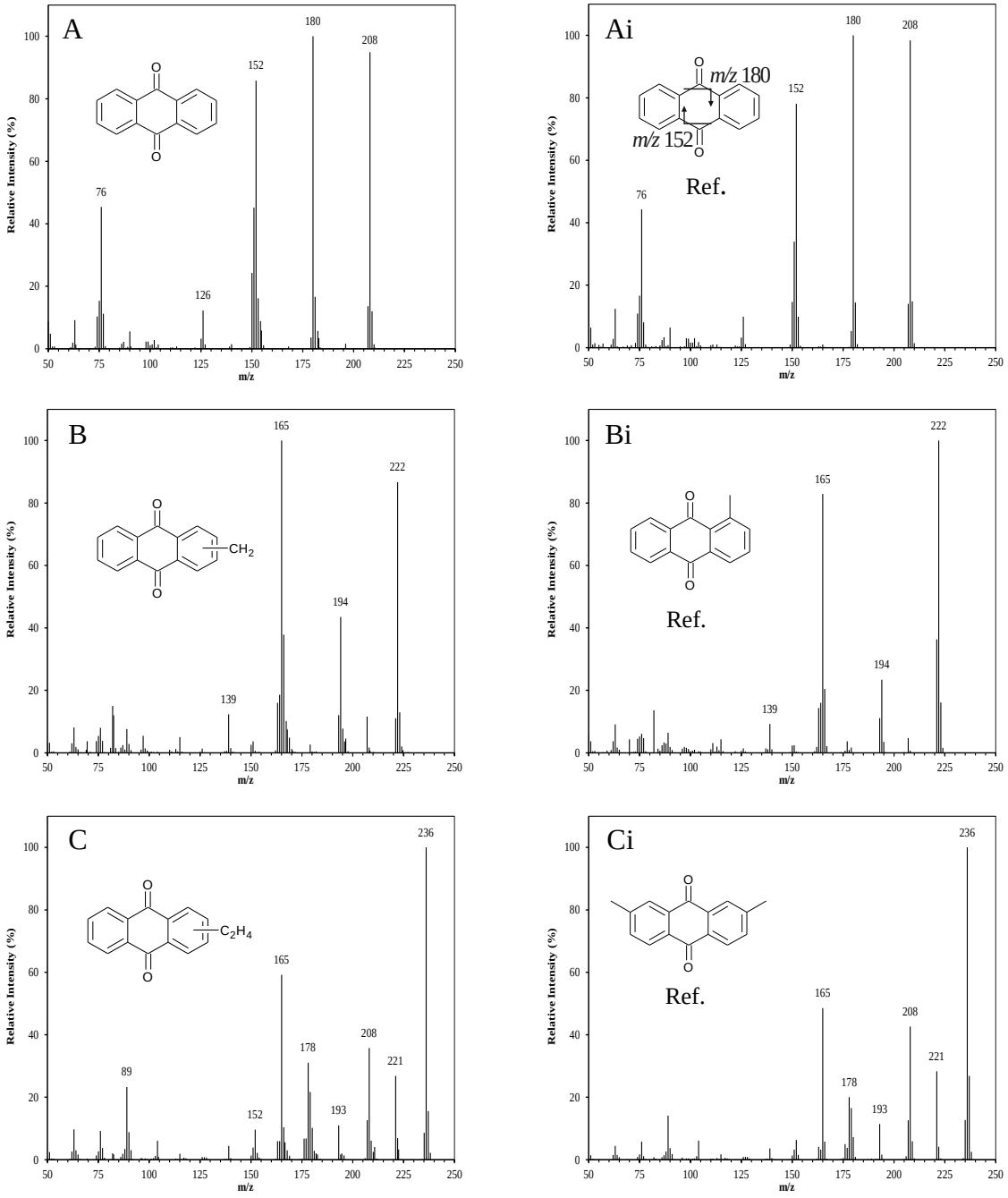

Figure 5-42. Examples of mass spectral identification of anthraquinone and its alkylated homologues from the analysis of Fraction S3 (ANS crude oil separation; **A-C**).

Individual compounds identified by comparison of spectra obtained from crude oil analysis with NIST library reference mass spectra (**A** and **Ai**; **B** and **Bi**; **C** and **Ci**).

The higher benzene homologues of anthraquinone and its alkylated homologues were also identified (Figure 5-39D). Benzanthraquinone was positively identified within the S3 fraction by comparison of the mass spectrum with a reference spectrum (Figure 5-43A and Ai; RMatch 882). The mass spectra of the C_1 and C_2 alkylated homologues were similar to that of the alkylated xanthones in that the dominant losses were of both the CO moieties and not of the methyl substituents.

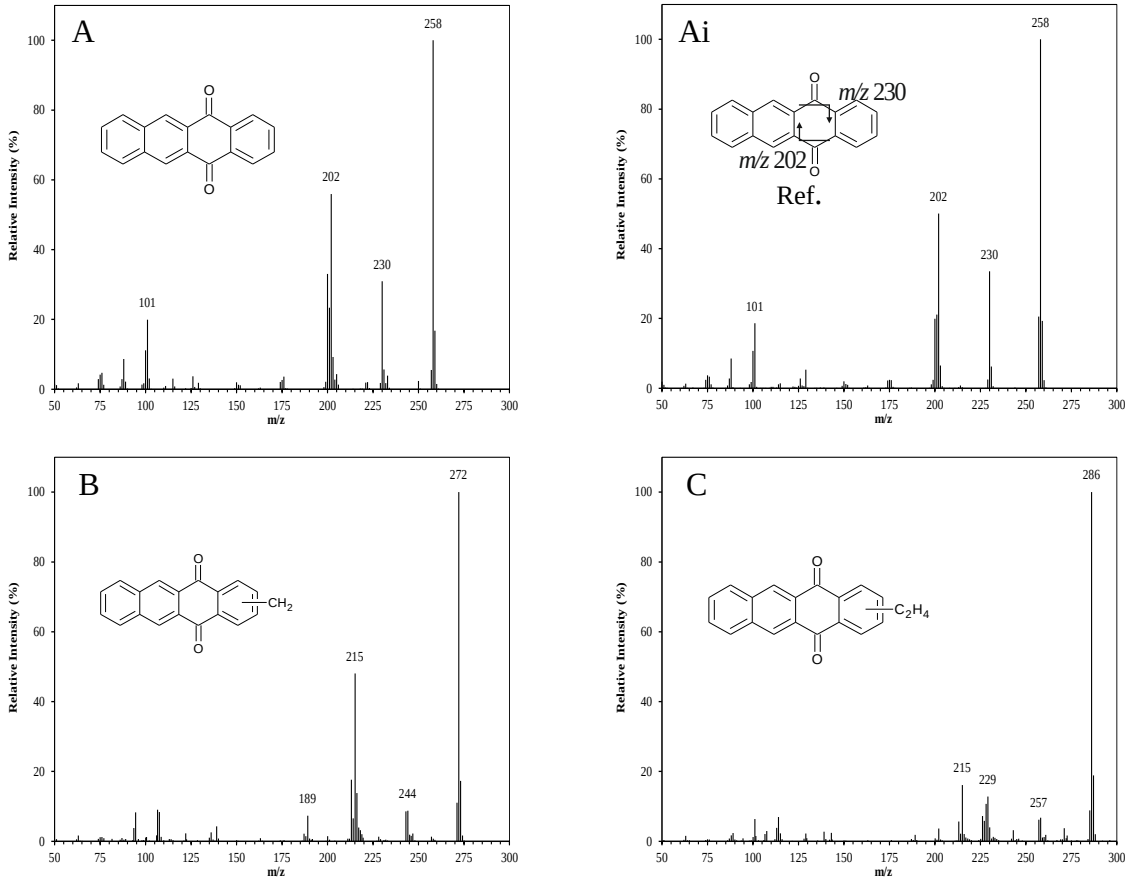

Figure 5-43. Examples of mass spectral identification of benzanthraquinone and its alkylated homologues from the analysis of Fraction S3 (ANS crude oil separation; **A-C**). Individual compounds identified by comparison of spectra obtained from crude oil analysis with NIST library reference mass spectra (**A** and **Ai**) and by mass spectral interpretation and chromatographic position (**B** and **C**).

The third series of compounds identified within the S3 fractions (Figure 5-39iii) was identified as a series of thioxanthones (Figure 5-39B) which, to the author's knowledge, is the first instance of their identification within crude oils. Identification of thioxanthone was facilitated by comparison of the mass spectrum with a library spectrum (Figure 5-44; RMatch 903). Fragmentation of the thioxanthone molecule proceeds very similarly to that of xanthone (Figure 5-41A). A loss of M-28 corresponding to the loss of CO is observed, leaving the dibenzothiophene fragment (*m/*z 184; $C_{12}H_8S^{+\cdot}$) instead of the dibenzofuran fragment (*m/*z 168; $C_{12}H_8O^{+\cdot}$) observed in the xanthone fragmentation. This is followed by the successive loss of the -CSH moiety (*m/z* 47) resulting in the *m/z* 139 fragment ($C_{11}H_7^{+\cdot}$). The alkylated thioxanthones were identified based on their retention position and interpretation of their mass spectra. Much like the parent thioxanthone, the fragmentation of the alkylated thioxanthones was extremely similar to that of the alkylated xanthones, allowing them to be identified within the crude oil samples.

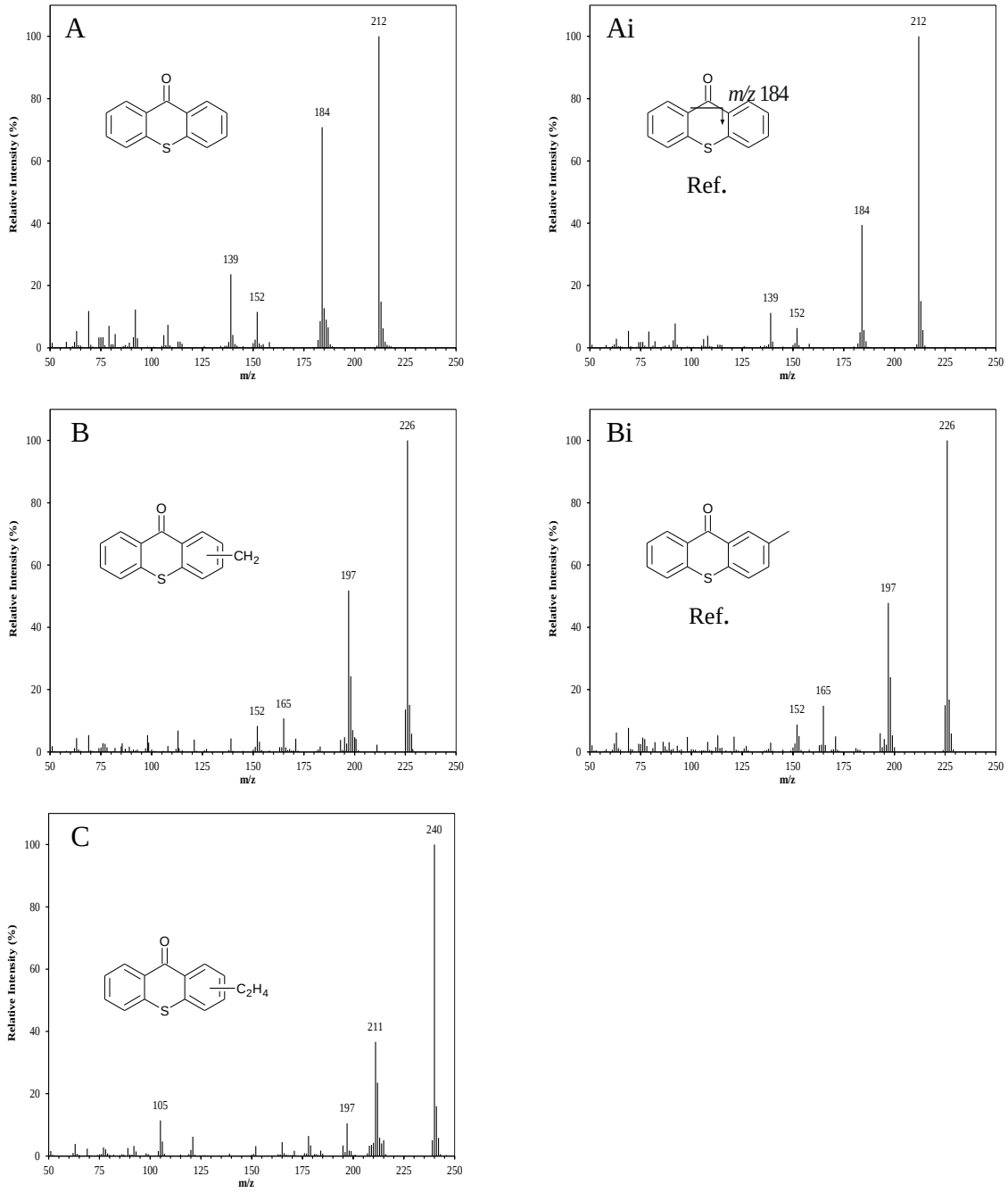

Figure 5-44. Examples of mass spectral identification of thioxanthone and its alkylated homologues from the analysis of Fraction S3 (ANS crude oil separation; **A**-**C**). Individual compounds identified by comparison of spectra obtained from crude oil analysis with NIST library reference mass spectra (**A** and **Ai**) and by mass spectral interpretation and chromatographic position (**B** and **C**).

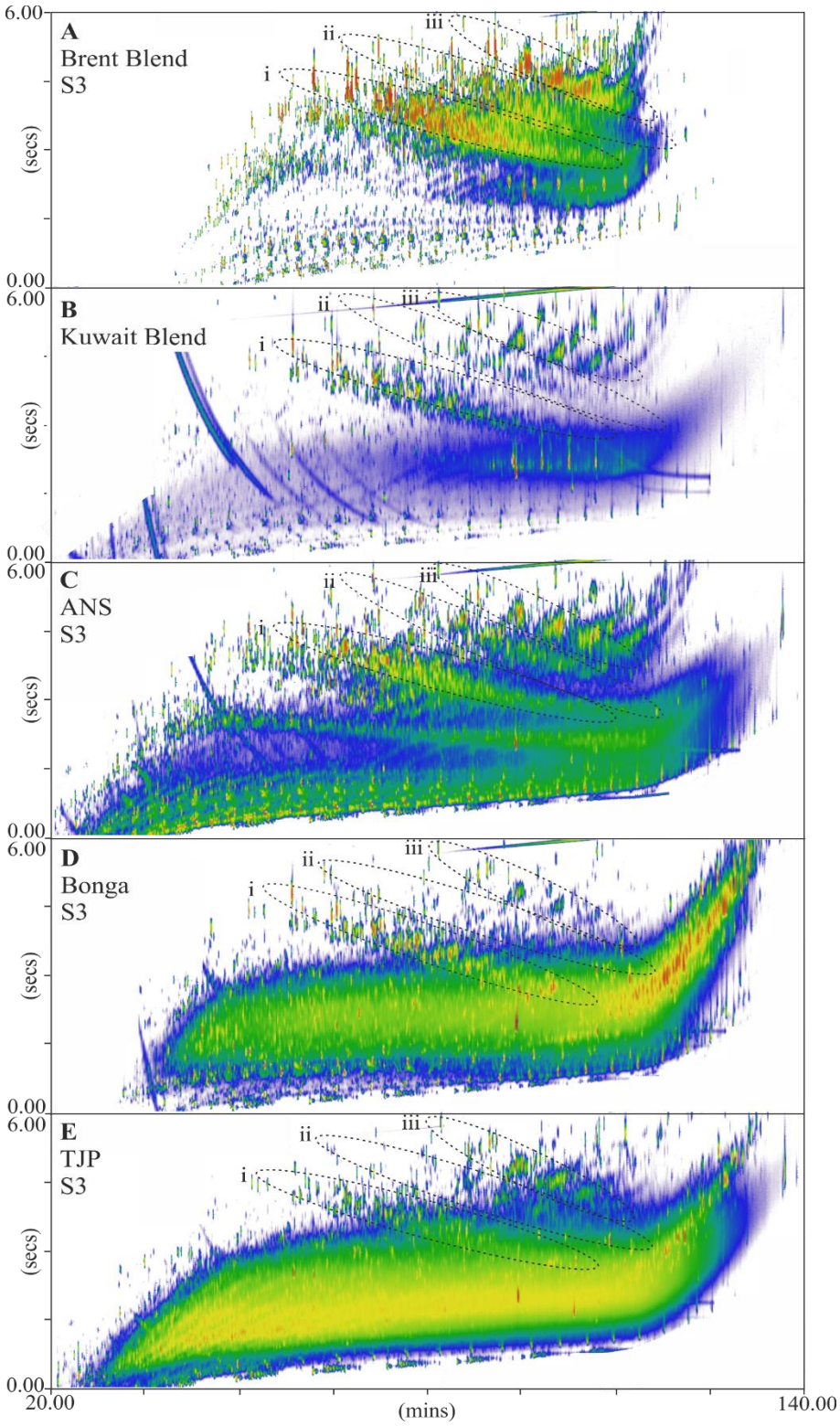

Figure 5-45. GC×GC-MS TICs of the S3 fractions obtained from the SPE separation of the Brent Blend (**A**), Kuwait blend (**B**), ANS (**C**), Bonga (**D**) and TJP (**E**) crude oils. Highlighted on each chromatogram are areas in which various compound classes elute: i; alkyl xanthones, ii; alkyl anthraquinones, iii; alkyl thioxanthones.

The S3 fractions obtained from the separation from the other four crude oil samples were also subject to analysis by GC×GC-MS. Examination of the five TICs showed each crude oil contained the xanthone, thioxanthone and anthraquinone series (Figure 5-45 A-E; i-iii). Fraction complexity appeared to increase throughout the API series, with the Bonga and TJP presenting the most complex chromatograms, dominated by UCMs. The relative concentrations of the three identified groups appeared to decrease with the associated increase in concentrations of the UCM. Despite few or no reports of some of these chemicals, they were present in all the oils tested.

A series of late eluting peaks were observed in the chromatogram of the S3 fraction obtained from the Bonga crude oil showed the presence of a late eluting series of peaks (Figure 5-46A). Comparison of the mass spectra of a number of these late eluting compounds with those in the mass spectral library suggested the series was likely a complex mixture of triterpenoids. However, whilst the lower *m/z*, 'fingerprint' region of the mass spectra compared well to the mass spectra of a number of reference pentacyclic triterpenoid structures, the molecular ions and some fragmentations were not consistent with such structures. Given the predominance of ketone-functionalised compounds in the S3 fractions, it can be expected that the structures present within the Bonga S3 fraction are ketone-functionalised triterpenoids.

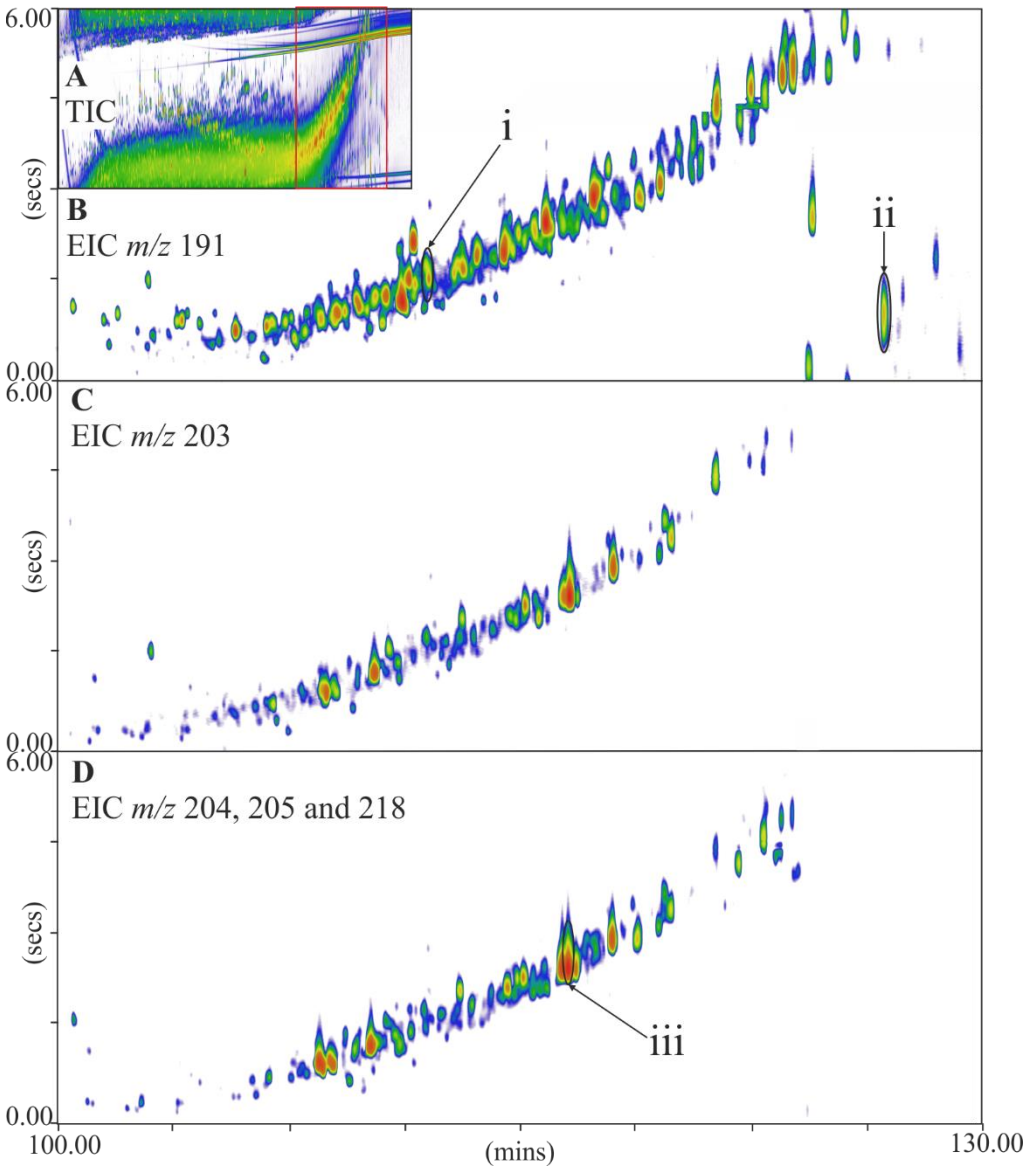

Figure 5-46. GC×GC-MS TIC of the S3 fraction (**A**) and EICs of the hopanes (**B**; *m/z* 191), pentacyclic triterpenoids (**C**; *m/z* 203) and oleananes/ursanes (**D**; *m/z* 204, 205 and 218) from the SPE separation of the Bonga crude oil. Identified on the EICs are the compounds 22, 29, 30-trinorhopan-21-one (**i**), homohopan-30-one (**ii**) and olean-12-en-3-one (**iii**).

Pentacyclic terpenoids are common constituents of geological samples and are found in abundance in many crude oils (Brooks, 1986). They include the more commonly observed hopanes and oleananes and, far less frequently, the lupane series (Tuttle *et al.*, 1999; Nytoft *et al.*, 2002; Peters *et al.*, 2005). Indeed, the oleananes were first identified in crude

oils from the Niger Delta (Whitehead, 1973) and have since, along with the lupanes, been employed as markers for a Tertiary/Late Cretaceous source for crude oils (Oriuma, 2015). However, whilst significant work has been conducted on these compounds, only a limited number of studies have investigated the occurrence of pentacyclic triterpenoid ketones (Budzikiewicz *et al.*, 1963; Barakat and Yen, 1990; Duan, 2001) and none could be found in which such compounds were identified in crude oils. The origins of the terrigenous triterpenoid ketones are thought to be either directly from bacterial action, or from diagenetic oxidation (Duan, 2001).

Extraction of characteristic ions for the hopanes (*m/z* 191), pentacyclic terpenoids (*m/z* 203) oleananes/ursanes (*m/z* 204, 205, 218) and lupanes (*m/z* 177) revealed the extent to which these were present in the S3 fraction (Figure 5-46). Comparison of mass spectra to those in the literature and the mass spectral library allowed a number of tentative structural assignments to be made. Thus, olean-12-en-3-one was identified by comparison of the spectrum to the mass spectral library (Figure 5-47 A and Ai; RMatch 901) and 22, 29, 30-trinorhopan-21-one (Figure 5-46Bi) and homohopan-30-one (Figure 5-46Biii) were identified by comparison to mass spectra (Figure 5-47 B and C) available in the literature and by mass spectral interpretation (Budzikiewicz *et al.*, 1963; Duan, 2001). Even these tentative assignments may represent the first report of such compounds in crude oils.

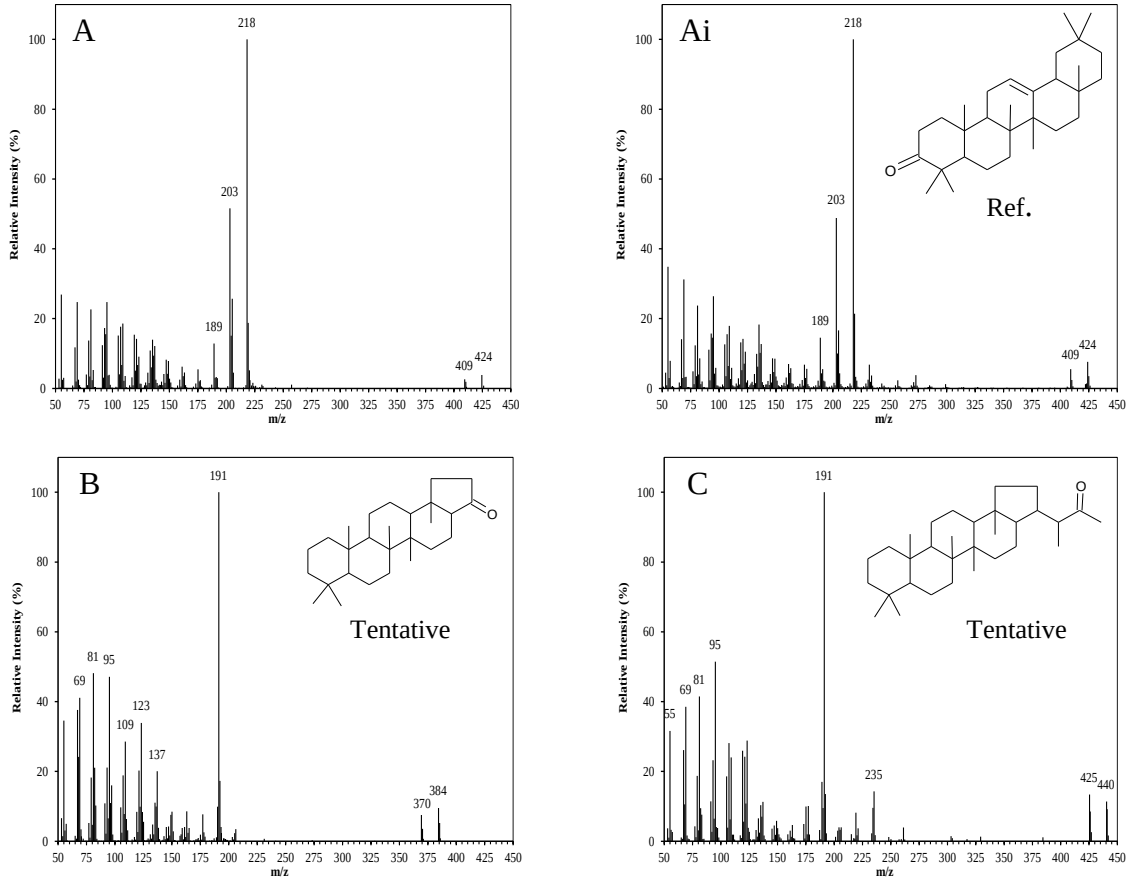

Figure 5-47. Tentative mass spectral identification of triterpene ketones in fraction S3 from the GC×GC-MS analysis of the Bonga crude oil. The mass spectrum of **A** was identified as olean-12-en-3-one by comparison to a NIST library spectrum (**Ai**), compounds **B** and **C** were tentatively identified as 22, 29, 30-trinorhopan-21-one and homohopan-30-one by comparison to mass spectra available in the literature (Barakat and Yen, 1990; Duan, 2001).

5.4.13 Fraction S4 (thiophenes)

Elution of the silica SPE cartridge with THF was necessary to remove strongly absorbed material not eluted from the silica cartridge using the previous solvents (S0-S3 inc). However, separation of the 'model' compound mixture provided only limited information as to the composition of the S4 fraction, suggesting the possible presence of the dibenzothiophene series (Chapter 4; Section 4.3.3). Analysis by GC-MS revealed the S4 fractions to be characterised by UCMs (Figure 5-48). Interestingly, both the Brent and

ANS crude oils showed the presence of homologous series of compounds that were sufficiently abundant to be visible in the TICs (Figure 5-48 A and C).

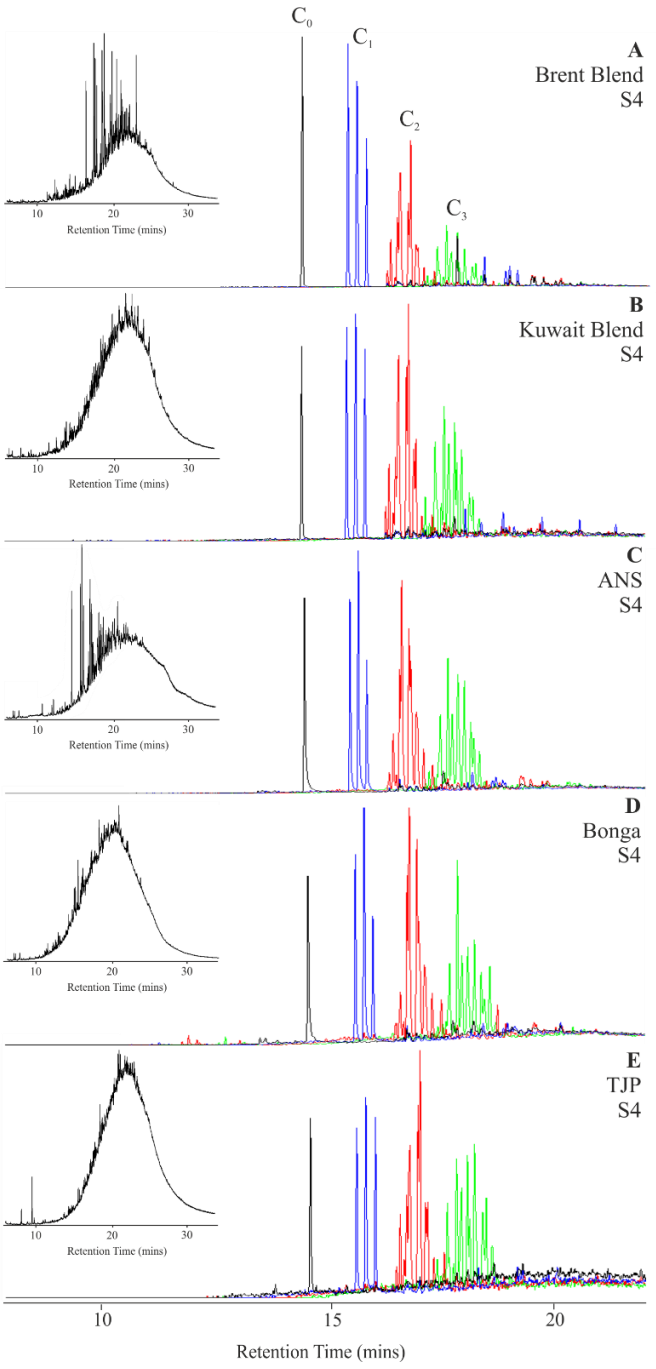

Figure 5-48. GC-MS EICs showing the extracted dibenzothiophene series: dibenzothiophene (*m/z* 184; black), C_1 dibenzothiophene (*m/z* 198; blue), C_2 dibenzothiophene (*m/z* 212; red) and C_3 dibenzothiophene (*m/z* 226; green) with TIC inserts (left) of the S4 fractions obtained from the SPE separation of the Brent Blend (**A**), Kuwait blend (**B**), ANS (**C**), Bonga (**D**) and TJP (**E**) crude oils.

Extraction of the molecular ions for dibenzothiophene (*m/z* 184) and C_{1-3} alkylated homologues (*m/z* 198, 212 and 226) showed the likely presence of these in the S4 fraction of all five crude oils (Figure 5-48). The mass spectrum of the peak thought to be dibenzothiophene compared well to that of authentic dibenzothiophene (Figure 5-49A-Ai). Thus, the mass spectrum of dibenzothiophene (Figure 5-48 Ai) was characterised by a base peak molecular ion at *m/z* 184 and abundant peaks at *m/z* 152 and 139. The peak at *m/*z 152 corresponds to the loss of sulphur ($M^{+\cdot}$-32), forming the biphenylene structure previously observed in the fragmentation of the methyl xanthones (Figure 5-41B). The peak at *m/z* 139 corresponds to a loss of the CHS· radical ($M^{+\cdot}$-45) and results in the formation of the benzdehydrotropylium ion observed previously in the fragmentation of xanthone (Figure 5-41A). The mass spectra of the methyl dibenzothiophenes compared well to spectra in the mass spectral library (Figure 5-49 B and Bi; RMatch 965 for example 1-methyldibenzothiophene) and were characterised by base peaks at the molecular ion (*m/z* 198). Low abundance peaks at *m/z* 165, rationalised by the loss of H ($M^{+\cdot}$-1) and subsequent loss of S (M-$1^{+\cdot}$-32) with incorporation of the methyl substituent into a 7-membered ring and at *m/z* 152 corresponding to a loss of the CH_2S·radical, forming the aforementioned biphenylene structure, were also observed. Mass spectra of the C_2 dibenzothiophenes also compared well to those in the mass spectral library (Figure 5-49 C and Ci; RMatch 954 for example 2,8-dimethyldibenzothiophene). The mass spectra of the C_2 dibenzothiophenes were also dominated by a base peak molecular ion (*m/z* 212) and showed a minor peak at *m/z* 196, likely corresponding to a loss of H ($M^{+\cdot}$-1) followed by a loss of CH_3 ($M^{+\cdot}$-15).

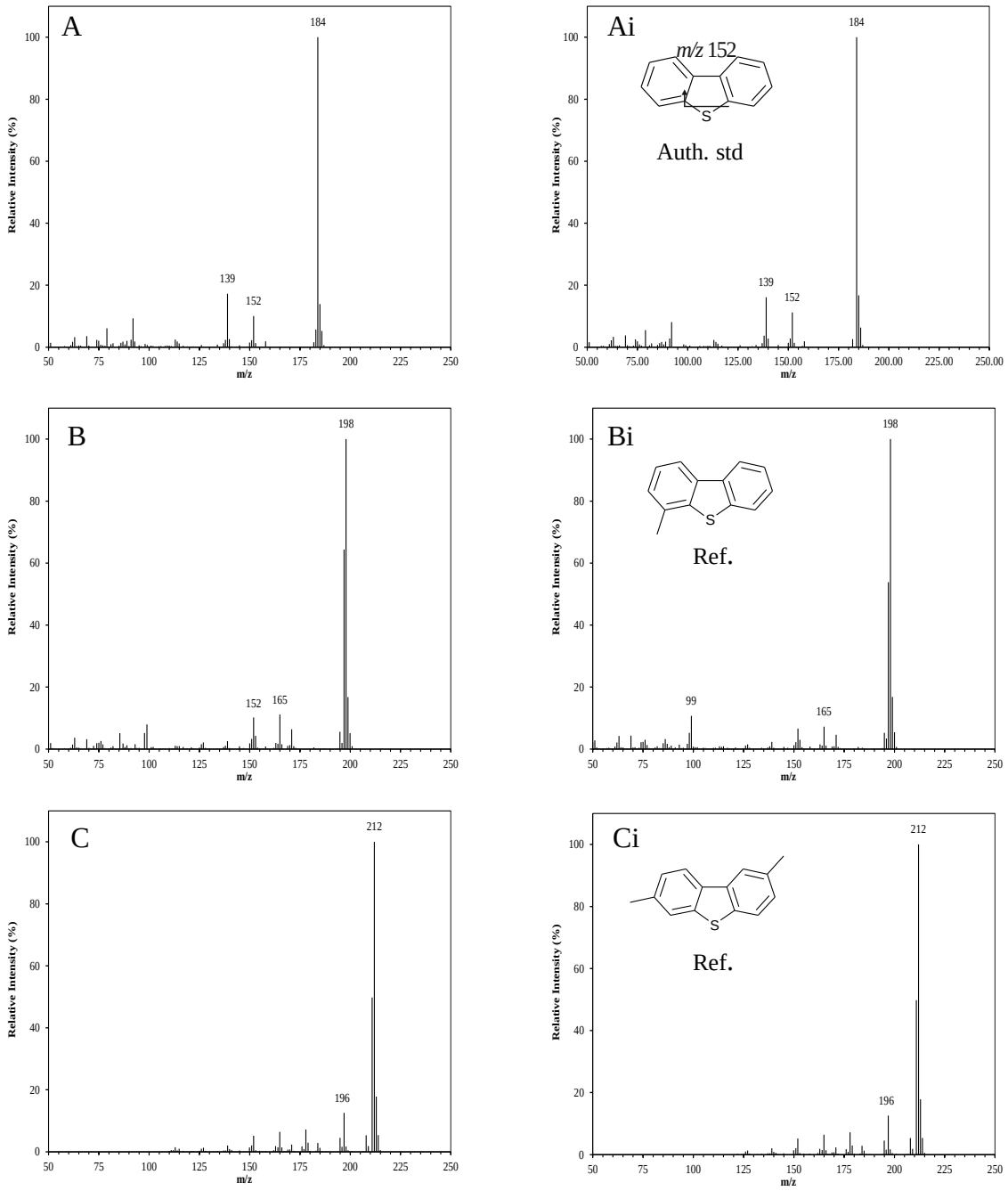

Figure 5-49. Examples of mass spectral identification of dibenzothiophene and its alkylated homologues from the analysis of Fraction S4 (ANS crude oil separation; **A-C**). Individual compounds identified by comparison of spectra obtained from crude oil analysis with previously analysed reference compounds (**A** and **Ai**) and by comparison to the NIST mass spectral library (**B** and **Bi**; **C** and **Ci**).

5.5 Conclusions

Results from the separation of Brent Blend, Kuwait Blend, ANS, Bonga and TJP crude oils (API gravity range 12.1-38.3°) presented herein have demonstrated a potential for wide ranging use of the SPE procedure developed in Chapter 4. Effects of crude oil chemical and physical properties on fraction 'quality' were found to be insignificant for the oils investigated herein. Indeed, recovery of the heavier, lower quality crude (TJP) was the highest (98%) in the series, highlighting the near complete recovery of non-volatile crude oil components.

Identification of commonly studied NSO-containing compounds herein, demonstrates the potential for the future use of the method in geochemical studies. Analysis of the fractions by appropriate chromatographic and mass spectral techniques established that the method is capable of providing quite well defined fractions of various compound classes, allowing rapid identification of common and rarely reported heteroatom-containing crude oil compounds (e.g. carbazoles, dibenzothiophenes, xanthones, thioxanthones, naphthenic acids, hydrocarbons). Mass spectral characterisations of the fractions also resulted in the identification of compound series that, to the authors' knowledge, have not previously been reported in crude oils. For example, identification of the tocopherols (E vitamins) and thioxanthones reported herein, demonstrates the use of the method for use in future characterisation studies.

Analysis of cationic fractions by LC-HRAM-MS shows promise as a technique for the separation and characterisation of such fractions. The coupling of LC to high-resolution mass spectrometers allows additional confidence in MS assignments based on elution retention times. Additionally, accurate mass measurements allow the assignment of elemental formula and provide an insight into the structural complexity of individual molecular formulas. Furthermore, the ability to assign individual structures, demonstrated

by the use of authentic compounds and MS/MS experiments, shows the power of LC-HRAM-MS techniques, allowing simultaneous molecular formula and structural characterisations.

Chapter 6. Separation of geochemically altered crude oil series using the newly developed SPE procedure and analysis of selected fractions

Chapter 6 describes the application of the method developed in Chapter 4 to crude oil 'series' exhibiting sequential geochemical alteration. Two 'series' of crude oils extracted from the North Sea and representing oils at (a) different stages of maturity and (b) different biodegradation levels, were separated by the procedure. This was followed by characterisation of a number of relevant fractions by gas chromatography-mass spectrometry (GC-MS) and liquid chromatography-high resolution accurate mass-mass spectrometry (LC-HRAM-MS).

The results presented herein demonstrate the potential for use of the separation as a tool to assist geochemical investigations. Isolation of class specific fractions enabled the effects of changing biodegradation and maturity on NSO functionalised hydrocarbons to be investigated. The success of this approach was demonstrated by the identification of numerous gravimetric correlations between NSO fractions and changes in sample geochemistry. Furthermore, investigations into the composition of benzoquinoline, carbazole, fluorenone and xanthone fractions yielded a number of potential heteroatom-containing molecular markers.

6.1 Introduction

Throughout their lifetimes, petroleum systems are subjected to numerous geochemical processes, which ultimately control the volumes and quality of crude oil available for extraction. The past 50 years have seen a great investment of time and resources into studying some of the geochemical effects of these processes and the application of this knowledge has led to significant improvements in petroleum exploration and production. Much of this work has relied on the use of molecular markers present within the crude oils to quantify or evaluate the processes. Due to their high abundance and previous instrumental limitations for the analysis of many other molecules, the majority of compounds employed as markers have been saturated hydrocarbons (Peters *et al.*, 2005). Comparatively little work has been conducted investigating the effects of geochemical processes on the NSO-containing classes of crude oils.

Thus, the focus of the present work was to employ the developed fractionation procedure, designed to facilitate isolation of more polar compounds from oils (Chapter 4), as a tool for investigating the effects of changes in some common reservoir parameters on the compositions of the NSO compounds. To achieve this, two oil sample 'series', one representing a crude oil at different stages of thermal maturity and one which has been subject to different extents of bacterial alteration, were fractionated using the developed SPE procedure. Selected NSO components of these fractions were then examined in order to determine that changes to these compounds coincided with well-known changes in the saturated (and aromatic) hydrocarbons (e.g. Peters *et al.*, 2005). These initial findings suggest that, in future, studies of the NSO fractions of petroleum (including perhaps, non-conventional hydraulic fracturing fluids and oil sands bitumen) may become as routine as studies of the hydrocarbons.

6.1.1 Thermal Maturity

Thermal maturity describes the degree to which source rocks have been subject to heat-driven reactions, transforming sedimentary organic matter into petroleum. The burial of sediments to depths reaching several kilometres results in a substantial increase in both temperature and pressure, driving the thermal degradation of kerogen into petroleum and gas (Tissot and Welte, 1984). Organic matter is often described as being 'immature', 'mature' or 'postmature', depending on the extent of this thermal alteration. 'Immature' organic matter has been subject to diagenesis, resulting in the formation of heavy heteroatomic compounds with only minor hydrocarbon generation. 'Mature' organic matter has been subjected to catagenisis, with resultant significant hydrocarbon production corresponding to the main zone of oil generation or "oil window". Finally, 'postmature' organic matter has been subjected to such high temperatures that only a hydrogen poor residue remains (Tissot and Welte, 1984).

As the thermal maturity of organic sediments increases, the structure of the kerogen adjusts in order to achieve an equilibrium with its surroundings. Compositional changes correspond to progressive structural rearrangements that result in a higher and more stable degree of ordering. These more stable arrangements require the elimination of steric hindrances and consequently, the removal of features such as nonplanar cycles, alkyl chains and heteroatomic linkages is observed. This continuous modification of kerogen by increasing temperature and pressure leads to the sequential removal of functional groups and linkages, forming medium to low molecular weight hydrocarbons, carbon dioxide and water (Tissot and Welte, 1984).

The development of parameters allowing the thermal maturity of organic matter to be described accurately is of great importance in petroleum exploration, as it allows petroleum generation to be better predicted. Peters *et al.* (2005) categorised existing

maturity parameters into two types: generation or conversion parameters used to indicate the stage of petroleum generation and thermal stress parameters describing the relative effects of temperature and time.

The most frequently employed thermal stress maturity parameter is vitrinite reflectance ($\%R_o$), which is a measure of the percentage of incident light reflected from vitrinite particles in sedimentary rocks (Tissot and Welte, 1984). Vitrinite reflectance is particularly suitable for assessing source rock potential due to a high sensitivity to temperature ranges largely corresponding with those of hydrocarbon generation (~60 – 120 °C). However, whilst being highly abundant in type III-kerogen, the maceral vitrinite is only moderately abundant in type II-kerogen and absent in type I-kerogen. Additionally, like many other thermal stress parameters, vitrinite reflectance can only be measured in sediments and source rocks, not in crude oils. Vitrinite reflectance measurements can be used to categorise samples into different degrees of maturity (Table 6-1).

Table 6-1. Ranges of vitrinite reflectance corresponding to increasing levels of maturity.

Level of Maturity		Vitrinite Reflectance ($\%R_o$)
Immature		0.20 - 0.60
Mature	Early	0.60 - 0.65
	Peak	0.65 - 0.90
	Late	0.90 - 1.35
Post Mature		>1.35

The need for accurate markers of crude oil maturity has seen the development of a number of molecular parameters, often based on ratios and distributions of both biomarkers and aromatic hydrocarbons. An ideal molecular maturity parameter involves measurement of the relative concentrations of compounds A and B; where compound B is formed only by the heat-driven conversion of compound A. In this scenario, compound B would be

thermally stable and its initial concentration would be zero, the concentration of A would not be affected by other factors and the conversion would only occur in the range of maturities in which petroleum is generated (Peters *et al.*, 2005).

Biomarker marker based maturity parameters are numerous and include those of terpanes (e.g., Ensminger *et al.*, 1977; Seifert and Michael Moldowan, 1978), polycadinenes (Alexander *et al.*, 1994; Sosrowidjojo *et al.*, 1996), steranes (reviewed Seifert and Moldowan, 1986), aromatic steroids (Mackenzie *et al.*, 1984), aromatic hopanoids (Wei and Songnian, 1990) and porphyrins (Baker and Louda, 1986; Sundararaman *et al.*, 1988). However, the majority of these parameters do not satisfy all of the above criteria, and as a result have only a limited range of specificity. For example, the Ts/(Ts + Tm) trisnorhopane ratio was shown by Moldowan *et al.* (1986) to be sensitive to source input in addition to maturity, thus compromising its use as a marker for maturity. Furthermore, the overall dynamic range of the biomarker ratios is typically limited to the lower levels of maturation, with cyclic hydrocarbons becoming depleted as crude oils reach higher levels of maturity (Rullkötter *et al.*, 1984).

To address the shortcomings of biomarker based maturity indicators, a number of maturity parameters utilising aromatic hydrocarbons have been developed. Radke and co-workers (1982a) identified a correlation between maturity and the distribution of methyl- and dimethyl-phenanthrenes and naphthalenes in crude oil samples. Further work by Radke *et al.* (1982b) was focused on the phenanthrenes and showed that the correlation with maturity existed throughout the oil window (0.6-1.6%R_o). Later studies concerning the alky naphthalenes produced similar results (Alexander *et al.*, 1985; Strachan *et al.*, 1988; van Aarssen *et al.*, 1999), demonstrating the potential use of aromatic hydrocarbons as indicators of maturity.

The culmination of these works saw the development of the methylphenanthrene index (MPI-1) and the methyl- and ethylnaphthalene ratios (MNR and ENR respectively). The MPI-1 was initially developed by Radke (1988) and is calculated using peak areas of phenanthrene and methylphenanthrene from gas chromatograms. The original MPI-1 equation was later modified by Cassani *et al.* (1988) to compensate for differences in response between phenanthrene and methylphenanthrenes when analysed by GC-MS and is as follows:

$$\text{MPI-1} = \frac{1.89(2\text{-MP} + 3\text{-MP})}{\text{P} + 1.26(1\text{-MP} + 9\text{-MP})} \quad (6\text{-}1)$$

The close correlation of the MPI-1 values and vitrinite reflectance allowed for the calculation of a vitrinite reflectance equivalence (VRE) value from MPI-1 datasets. The formula, developed by Radke and Welte (1983) is as follows:

$$\text{VRE} = 0.6 \cdot \text{MPI-1} + 0.4 \quad (6\text{-}2)$$

Whilst more robust than many of the biomarker based maturity parameters, a number of factors can nonetheless affect the use of the MPI-1 index. Variations in the organic matter in the source rock can influence methyl phenanthrene ratios. Additionally, crude oil migration is thought to effect the distribution of aromatic hydrocarbons, potentially effecting both naphthalene and phenanthrene indexes (Peters *et al.*, 2005).

The dominance of biomarker and aromatic indices for assessing maturity is likely associated with the ease with which fractions containing such compounds have been obtained until present. Recent years have seen a small number of studies investigating the potential use of the less abundant heteroatomic compounds as markers for crude oil maturity (e.g., Li *et al.*, 2013; Faboya *et al.*, 2014; Oldenburg *et al.*, 2014; Yang *et al.*, 2017). Previous difficulties in obtaining ‘clean’ fractions of such compounds has likely

discouraged investigations into their relationship with maturity. Such studies may be of of great interest with regard to petroleum exploration and the effects of maturity.

6.1.2 Biodegradation

The world's petroleum resources are dominated by petroleum that is biologically altered in the reservoir (Head *et al.*, 2003). The biodegradation (biotransformation at a molecular level) of petroleum by microbial action was long thought to primarily be an aerobic process (Tissot and Welte, 1984; Peters *et al.*, 2005). However, the last decade has seen this paradigm replaced with the view that this process is predominantly anaerobic (Aitken *et al.*, 2004), driven by methanogenic processes that are dominated by carbon dioxide reduction (Jones *et al.*, 2008). The dominance of anaerobic degradation is supported by the lack of sufficiently oxidised sub-surface waters (Horstad *et al.*, 1992), the recorded presence of anaerobic microorganisms in formation waters (reviewed Head *et al.*, 2014), the demonstration of anaerobic degradation in laboratories (Rueter *et al.*, 1994; Zengler *et al.*, 1999) and the elucidation of anaerobic petroleum degradation pathways (Jones *et al.*, 2008; Aitken *et al.*, 2017).

Observations from field studies typically observe the most severely degraded oil to be present at oil-water transition zones (OWTZ), implying the majority of degradation occurs at this interface (Head *et al.*, 2014). A number of authors (Bennett *et al.*, 2013 and references therein) have shown the presence of systematic gradients in the physical and chemical properties of oil throughout oil columns. These results suggest the majority of degradation occurs at the OWTZ at the base of filling reservoirs.

The extent of petroleum degradation is determined by a number of chemical and physical controls, the most important of which are temperature, salinity and the availability of inorganic nutrients. The upper temperature limit for effective bacterial biodegradation is generally accepted to be around 80 °C (Peters *et al.*, 2005) and it has been hypothesised

that once reservoirs reach temperatures greater that this they undergo paleopasteurization (i.e. that once they have been heated to temperatures within this range they are not recolonised by hydrocarbon degrading microorganisms) (Wilhelms *et al.*, 2001). Subsequent works have shown a close relationship to exist between biodegradation, reservoir depth and burial temperature (Adams *et al.*, 2006), further demonstrating the importance of temperature as a control on the bacterial alteration of petroleum. Head and co-workers (2014) recently reported on the importance of formation water salinity in determining the occurrence of biodegradation and presented "paleopickling" as mechanism whereby biodegradation is prevented. Experiments conducted therein, demonstrated a clear relationship between temperature and salinity, with the tolerance to increased salinity being greater at lower temperatures. Thus, in high saline conditions the temperature for paleopasteurization to occur will be purportedly less. The lithology of the reservoir has also been shown to control biodegradation, as rocks must be sufficiently porous and permeable to allow for bacterial movement and for the adequate dispersal of nutrients (Krumholz, 2000).

The effects of biodegradation on the composition of crude oil have been well-studied (Connan, 1984; Kennicutt, 1988; e.g., Peters *et al.*, 1996; Aitken *et al.*, 2004; Bennett *et al.*, 2013). The preferential removal of hydrocarbons produces crude oils with increased viscosity and density (or lower API gravity) that are enriched in the NSO containing components (resins and asphaltenes). This selective removal of hydrocarbons typically begins with the removal of the *n*-alkanes ($<C_{25}$) followed by the removal of isoprenoid alkanes and low-ring cycloalkanes and aromatics (Bennett *et al.*, 2013). There is also evidence for the degradation of biomarkers in heavily biodegraded crude oils. Indeed, of the latter, it appears steranes are the first to be biodegraded, followed by the hopanes, aromatic steroidal hydrocarbons, diasteranes and tricyclic terpanes (Peters *et al.*, 2005). Recent work has also shown biodegradation to effect the pyrrolic nitrogen species in

moderately to severely degraded crude oils, with preferential degradation of the alkyl carbazoles compared to alkyl benzocarbazoles (Huang *et al.*, 2003). Bacterial action also results in an increase in oxygenated compounds and the total acid number (TAN) of crude oils typically increase with the degree of biodegradation due partly to the conversion of alkylated hydrocarbons to carboxylic acids (Aitken *et al.*, 2017).

The degree to which crude oils have been biodegraded can be described by qualitative scales such as those proposed by Wenger *et al.* (2002). The latter scale is based on the extent to which the *n*-alkanes have been degraded, describing oils by terms such as "very slight", "slight" and "slight to moderate". More heavily degraded crudes in which biomarkers have been altered are described as "heavily" and "severely" biodegraded. Quantitative assessments of biodegradation often employ measurements of *n*- and branched alkanes relative to more resistant molecules, to evaluate slightly-moderately degraded crudes and then utilise analyses of biomarker ratios in more severely altered crudes, where the alkanes are no longer present.

Biodegradation parameters utilising ratios of *n*- to branched alkanes are based on the resistance of compounds containing multiple methyl groups, to resist degradation. This results in preferential degradation of the straight-chained compounds and, by comparing the relative abundance of the *n*- and branched alkanes, a relative degree of biodegradation can be measured. The most commonly employed ratios in this class of parameter are those of pristane/*n*C17 and phytane/*n*C18 (Peters *et al.*, 2005). These ratios are suitable for evaluating slightly to moderately degraded crude oils. However, higher levels of biodegradation will see the depletion of both the *n*-alkane and multi-methyl branched acyclic isoprenoid constituents, at which point the ratios above can no longer be used.

Measurements of polycyclic aromatic hydrocarbons (PAHs) have also been employed in order to evaluate degrees of petroleum biodegradation. In comparison to the *n*- and

branched alkanes, the PAHs exhibit an increased resistance to biodegradation, which is further enhanced by an increase when the number of aromatic rings increases. Several studies have examined the effects of biodegradation on aromatic hydrocarbons (Volkman *et al.*, 1984; Rowland *et al.*, 1986; Fisher *et al.*, 1998), observing significant changes in the ratios of mono-, di-, tri and tetra-methylnaphthalenes. These changes were likely the result of the preferential degradation of specific alkyl naphthalene isomers. Whilst further studies on this scale have not been conducted, similar observations were made in oils from the Liaohe Basin (Bao and Zhu, 2009), showing the potential use of aromatic hydrocarbons as markers for biodegradation.

Higher levels of biodegradation require the use of more resistant compounds to help quantify the extent of petroleum alteration. Much work has been conducted on the use of steranes, hopanes and terpane biomarkers to assess heavy to severe petroleum biodegradation (reviewed Peters *et al.*, 2005). The available parameters based on these biomarkers are numerous but many must be applied with caution. The relative susceptibility of individual hopane and sterane isomers to biodegradation has been shown to vary in both laboratory and naturally degraded petroleum. Examples of severely degraded crude oils in which the hopanes have been depleted prior to sterane alteration and in which the steranes have been depleted prior to hopane alterations have been observed in several instances (e.g., Seifert *et al.*, 1984; Peters and Moldowan, 1991).

The NSO compounds in petroleum are considered highly resistant to biodegradation, and as such little work has been done to investigate the potential alteration or generation of heteroatom-containing compounds during biodegradation. The small number of studies investigating such changes have been focused on those compounds containing an oxygen atom. Taylor *et al.* (2001) observed the removal of $C_{0\text{-}3}$ alkylphenols by bacterial action in series of biodegraded oils from the North Sea, Nigeria and California. However, concentrations of the alkyl phenols did not appear to correlate with the degree of

biodegradation. Oldenburg *et al.* (2002) investigated the effects of biodegradation on xanthone and its alkylated homologues in a series of offshore Norwegian crude oils. Bacterial alteration of the alkyl xanthones indeed appeared to alter distributions, and ratios of 4-methyl-/3-methylxanthone correlated well with the phytane/nC_{18} ratios for the studied sample suite.

The generation of carboxylic acids by bacterial action has been known for some time (reviewed Wilde, 2015). Most petroleum acids ('naphthenic' or naphthenoaromatics) are thought to be generated by the bacterial degradation of C_{18} or greater cyclic, aromatic and hetero-aromatic compounds (Thorn and Aiken, 1998). Despite the close association of TAN and biodegradation level, few studies have attempted to identify specific acidic biomarkers within acidic fractions of degraded crudes. Historically, studies into the composition of the so-called 'naphthenic acids' were greatly hindered by the available analytical techniques. However, the last decade has seen significant advances in instrumentation and sample preparation, allowing numerous, individual naphthenic acid structures to be identified (reviewed Wilde, 2015). The ability to identify individual acids should now enable the potential correlations between individual carboxylic acids and the extent of biodegradation to be investigated.

The ability to assess the level to which crude oils have been degraded is of great importance to the petroleum industry. Indeed, the amount of biodegraded oil is thought to exceed that of conventional oil and the cost of extraction can increase dramatically for biodegraded oil plays (Head *et al.*, 2014). Thus, the ability to easily and rapidly separate crude oils into fractions of discrete compound classes would facilitate investigations into compositional changes occurring at different levels of biodegradation.

6.2 Methods

6.2.1 Experimental Detail

Crude oil samples were separated using the sequential SPE procedure developed herein, described in detail in Chapter 2.

6.2.2 Crude Oils

Crude oils used in this study were provided by Shell Technology Centre, Rijswijk, NL. Two 'series' of oil extracted from the North Sea and representing oils at (a) different stages of maturity and (b) different biodegradation levels, were provided for investigations. Due to confidentiality agreements, only limited information regarding the oil origins and characteristics can be released here. Information relevant to the present study is shown below in Table 6-2 and Table 6-3. The biodegradation 'series' actually comprised two crude oils, each at different stages of biodegradation. These two crude oils are identified throughout the following work by colour coding. The first set, samples bA and bC and bD are coloured black and the second set, samples bB and bE are coloured green.

Table 6-2. Series of crude oils with increasing levels of thermal maturity as defined by Shell Technology *via* the estimated Vitrinite reflectance equivalence (VRE).

Sample Code		Estimated Maturity (VRE)	Maturation Level
FPC_62573	mA	0.58	Immature
FPC_60803	mB	0.71	Peak Maturity
FPC_60050	mC	0.79	
FPC_59986	mD	0.85	
FPC_60820	mE	0.93	Late Mature

Table 6-3. Series of crude oils as defined by Shell Technology *via* the estimated levels of biodegradation. Samples are presented in increasing order of biodegradation by Pr/nC_{17} ratios.

Sample Code		API Gravity (°)	Pr/nC_{17}
FPC_454108	bA	37.1	0.9
FPC_31648	bB	33.0	1.1
FPC_29722	bC	32.3	1.2
FPC_30603	bD	23.0	8.2
FPC_30041	bE	19.8	not present

6.2.3 Analytical Procedures

The instrumentation used for the quantification of 'model' compounds and the analysis of crude oil fractions is detailed in Chapter 2. The GC-MS analyses were performed using was a (5% phenyl)-methylpolysiloxane HP5-MS (30 m × 0.25 mm × 0.25 μm) with the following temperature program: 40 ºC (1 min hold), then heated to 300 ºC at 10 ºC min^{-1}.

LC-HRAM-MS analyses were conducted using set up B: the column was an ACE Excel 3 SuperC18 (100 × 2.1 mm, 2.5 μm) column (Advanced Chromatography Technologies Ltd, UK). The solvent gradient for the analysis of basic fractions was as follows: 0.1% FA (aq)/ 0.1% FA in acetonitrile/ 0.1% FA in IPA (90:10:0 to 15:85:0 to 0:10:90; 30-minute runtime).

6.3 Results and Discussion

The major focus of the work discussed herein, was to investigate only selected changes in NSO composition with increasing thermal maturity or with biodegradation. No attempt was made at this stage to conduct an exhaustive analysis of all twelve fractions from each oil (which would have entailed analysis of 120 fractions). Rather, the aim was to use analyses of selected NSO fractions, obtained in unusual purity by the methods developed herein (Chapter 4) to illustrate the likely utility of such measurements in future for crude oil studies.

To conduct this study, two North Sea crude oil 'series' were made available by scientists at the Shell Projects and Technology Centre, Rijswijk, NL. Included in these series were five crude oils of increasing estimated thermal maturity, ranging from immature to post mature (Table 6-2) and five crude oils of increasing biodegradation severity, ranging from very slight to heavy biodegradation (Table 6-3). Unfortunately, specific details pertaining to the origin of the crude oil samples cannot be published herein for legal reasons and only limited ancillary data was provided. Whilst this limited the scope of the study, an analysis of such samples provides a unique opportunity to investigate the effects of geochemical processes on the composition of NSO-containing compound groups. Additionally, data collected from the following separations demonstrates the potential for use of the method to aid geochemical investigations. The ten crude oil samples were each fractionated according to the developed SPE procedure (described in Chapter 2). Work focused on identifying trends in the gravimetric data obtained from the separation and on the changes in individual isomeric distributions of selected NSO-functionalised compounds.

6.3.1 Maturity

6.3.1.1 Gravimetry

Total recoveries from separation of the maturity series were good (70.9 – 92%; Table 6-4), with the most significant losses occurring due to initial volatile losses during separation by SCX. Interestingly, the recovery of crude oil decreased quite substantially as sample maturity increased (~20%). This corresponded to an equally substantial increase in the loss of sample observed during blowdown of whole crude oils (~28%). These changes likely reflect the increasing relative abundance of volatile saturated hydrocarbons with the increased level of maturity. As observed in separations of crude oil previously (Chapter 5), evaporative losses of whole crude oils samples correlated very closely to procedural losses; suggesting near 100% recoveries of non-volatile material.

Table 6-4. Total and individual cartridge recoveries (weight percent) of the maturity sample series and average losses of crude oil sample during N_2 blowdown.

Mode of Separation		Percentage Recovery				
		mA 0.58 VRE	mB 0.71 VRE	mC 0.79 VRE	mD 0.85 VRE	mE 0.93 VRE
IEX	SCX	97.4	82.3	84.3	85.5	78.3
	SAX	97.0	98.1	99.8	93.9	97.4
Silica		95.3	97.0	97.5	96.5	93.0
Total		**92.0**	**78.8**	**82.6**	**78.0**	**70.9**
Blowdown loss		4.7	15.3	21.7	24.2	33.0

The gravimetric data obtained from the separation of the five crude oil samples are presented in Figure 6-1 in order of increasing thermal maturity (i.e. mA→mE). Overall, fraction masses correlated exceptionally well with changes in thermal maturity. It is well understood that increasing thermal maturity results in the progressive removal of functional groups, resulting in the concentration of medium to low molecular weight saturated hydrocarbons (e.g., *n*-alkanes). These compositional changes are reflected in

the data, which show a sequential depletion of non-hydrocarbons and a corresponding rise in the abundance of the saturated hydrocarbons.

Overall, the gravimetry of the fractions obtained from the SCX cartridge were characterised by an incremental decrease in abundance as maturity increased (Figure 6-1A). The SCX1 fractions appeared to follow this trend; however, correlation was interrupted by an elevated mass in sample mC. Changes in the SCX 2 (sulfoxide) fractions also appeared to correlate closely with sample maturity. A plot of fraction abundance vs. maturity showed the extent of this relationship, generating a regression coefficient of 0.990 (Figure 6-2A). A similar decrease in the abundance of SO functionalised compounds was observed in a study conducted by Oldenburg *et al*. (2014), who investigated the effects of maturity on numerous NSO classes by FT-ICR-MS. The relative abundances of both cationic fractions (SCX3 and SCX4) were also observed to decrease with increasing maturity. Similar changes in composition were also observed by Oldenburg *et al.* (2014), who reported a decrease in the abundance of the aromatic N1 species as crude oils increased in maturity. Correlation between the cationic fractions and maturity was not as strong as for the sulfoxide fraction, generating a regression coefficient of 0.915 (Figure 6-2B).

Fractions obtained from the SAX separation also showed a strong correlation with maturity, with the relative abundance of all fractions decreasing incrementally (Figure 6-1B). The weights of the SAX2 (carbazole/phenol) fraction correlated particularly well with the changing maturity and produced a regression coefficient of 0.998 (Figure 6-2C). The depletion of carbazoles with increasing maturity has been observed previously in maturity suites from the North Sea and Gulf of Mexico (Clegg *et al.*, 1998; Bennett *et al.*, 2002; Oldenburg *et al.*, 2014), suggesting a close relationship between pyrrolic nitrogen species and maturity. The abundance of the acidic fraction also decreased as the degree

of thermal maturation increased, agreeing well with observations of the decarboxylation of naphthenic acids at high temperatures (Yang *et al.*, 2013a).

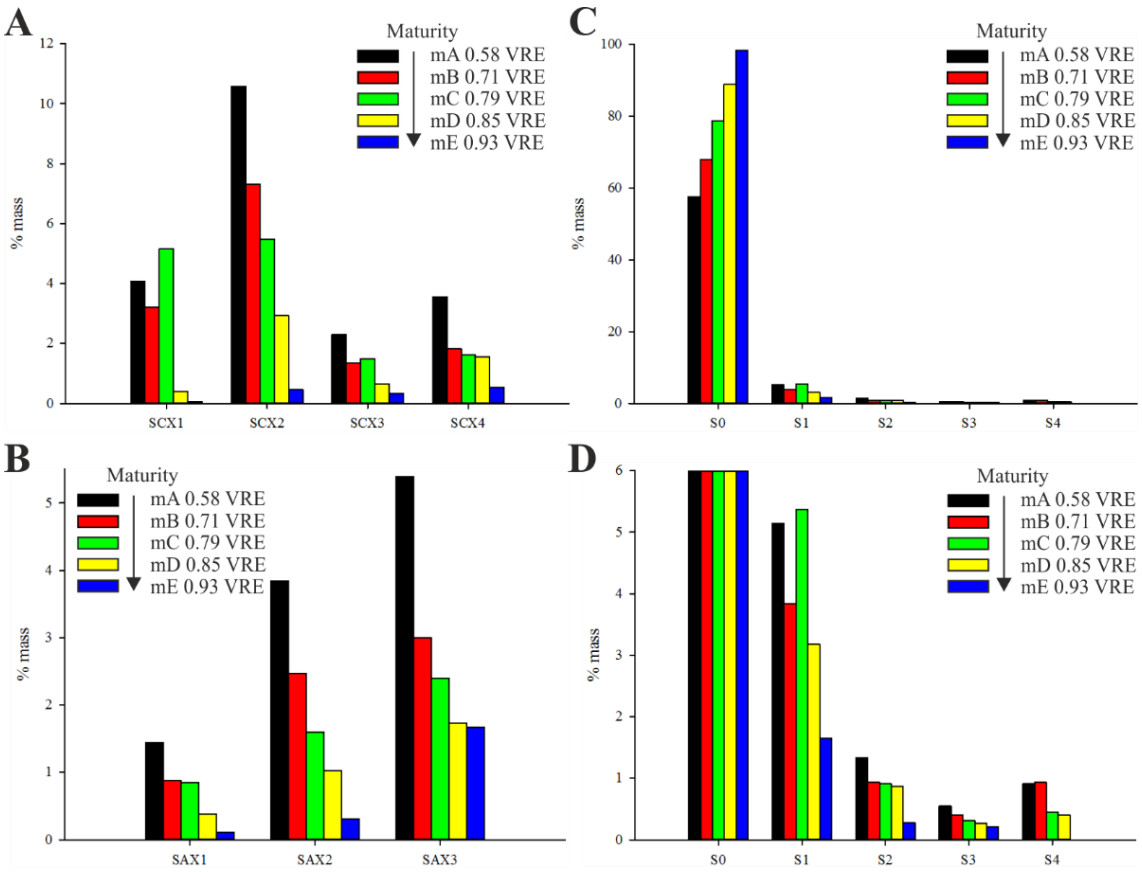

Figure 6-1. Gravimetric data (weight percent) of individual fractions from the SCX (**A**), SAX (**B**) and Silica (**C**; with zoomed insert to show lower mass fractions, **D**) from the separation of the crude oil maturity series.

The saturated hydrocarbon (S0) fractions showed an expected strong positive correlation with the maturity of the samples. By summing average evaporative losses to the S0 fractions, this correlation is further improved (Figure 6-1C), showing an incremental increase in the abundance of saturated hydrocarbons. A plot of percentage mass of S0 vs. maturity (Figure 6-2D) highlights this relationship, generating a regression coefficient of 0.970. The data for the aromatic hydrocarbon fractions (S1; Figure 6-1D) show a similar trend to that of the SCX1 fractions (Figure 6-1A). The fractions showed a general

decrease in abundance as maturity increases. However, the abundance of sample mC is again elevated, suggesting a higher level of aromaticity in the sample.

The masses of the two 'ketone' fractions (S2 and S3) also correlated with increasing maturity, incrementally decreasing in relative abundance throughout the series. Indeed, this correlation is highlighted by a plot of percentage mass of the S3 fraction vs maturity producing a regression coefficient of 0.992. The effect of changing maturity on the ketones of crude oils has been studied only rarely. Oldenburg *et al.* (2002) identified a potential relationship between the xanthones of crude oil and maturity, observing an overall decrease in abundance as the degree of maturation increased. In a more recent study, Oldenburg and co-workers (2014) reported on the decreasing relative abundance of O1 (non-hydroxyl) functionalised compounds with increasing maturity in North Sea sample series. Wilkes *et al.* (1998a) observed the abundance of fluorenone dominated, "low-polarity" fractions obtained from a Posidonia Shale (North Western Germany). The results showed an initial increase in abundance of the fluorenone fractions in immature to peak mature samples. This was followed by a sharp decrease in fraction abundance as the maturity of samples progressed further (late-mature to post-mature). This observed increase is of interest, as such a change is not observed within the present sample series. The lack of specificity afforded to the fractionation used by Wilkes *et al.*(1997) could explain the observation, with the increase being attributed to other classes within the low-polarity fraction (e.g. carbazoles).

Data obtained for the S4 fraction showed a slight increase in abundance of the thiophene fraction between samples mA and mB. This is followed by a decrease and the absence of the fraction in sample mE. Similar trends in the abundance of the thiophenes were observed by Oldenburg *et al.* (2014), who reported a sharp decrease in abundance as sample maturity surpassed 0.78 VRE and Radke (1988) also observed the depletion of thiophenic compounds with increasing maturity.

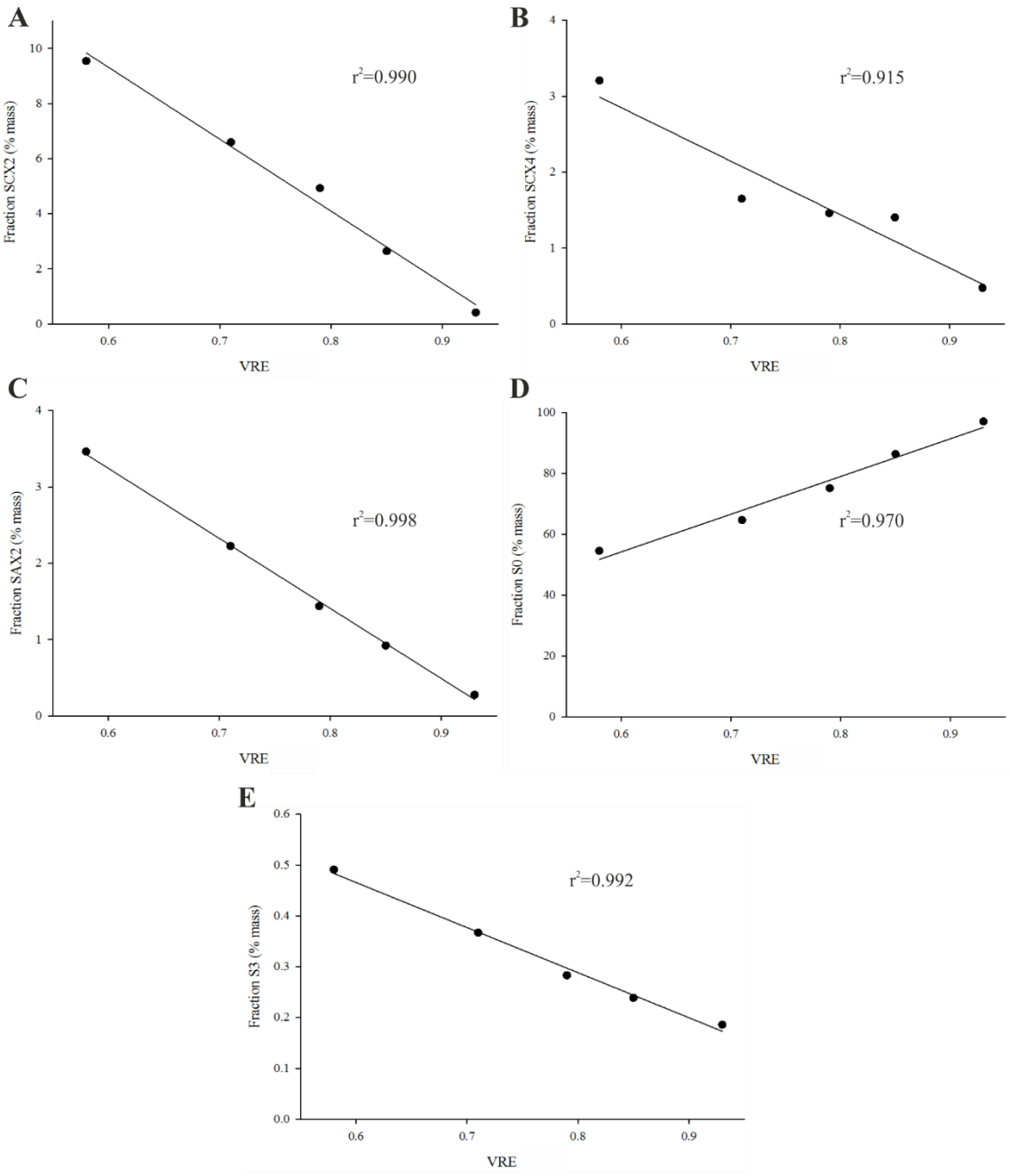

Figure 6-2. Plots showing the correlation between fraction masses and crude oil maturity: A, a direct comparison between % mass of Fraction SCX2 and maturity (VRE); B, % mass of Fraction SCX4 and maturity (VRE); C, % mass of Fraction SAX2 and maturity (VRE); D, % mass of Fraction S0 and maturity (VRE) and E, % mass of Fraction S3 and maturity (VRE).

6.3.1.2 Compositional Investigations

Analysis of the five whole crude oils (mA-E) by GC-MS revealed only minor differences in composition (Appendix 7), highlighting only the increasing abundance of the lower molecular weight *n*-alkanes and a slight decrease in the complexity of the lower abundance UCM components. By studying the composition of the NSO fractions, the effects of maturity on the structural distribution of the NSO functionalised hydrocarbons could not be determined. Existing maturity parameters such as the MPI-1, MNR and MER are based on the thermal rearrangement of alkylated species, with compounds rearranging to more thermodynamically stable structures on application of sufficient energy. These transformations are not specific to just alkyl phenanthrenes and naphthalenes. Similar changes in the distribution of alkylated isomers of carbazoles (Bennett *et al.*, 2002), fluorenones (Wilkes *et al.*, 1998a) and thiophenes (Radke, 1988) have been reported in crude oils of increasing thermal maturity. Therefore, the following work investigated the ability of the developed SPE procedure to isolate suitable NSO fractions for maturity assessment by comparison of observed trends with those reported previously in the literature. Additionally, isolation of discrete fractions allowed the changes in the abundance and isomeric distributions of novel compound series, enabling new maturity markers to be identified.

6.3.1.2.1. Fraction SCX4

The effects of thermal maturity on the structural distribution of the alkyl quinolines is yet to be investigated. Oldenburg *et al.* (2014) were able to identify a potential increase in the larger, more condensed quinoline type structures with increasing maturity and also reported on their de-alkylation. However, FT-ICR-MS measurements were not able to identify changes in individual isomer distributions because no chromatographic separation in involved. Application of the LC-HRAM-MS methods developed herein in

Chapter 5, allowed changes in the distribution of the alkyl quinoline structures to be investigated.

Previous work led to the identification of 2,4-dimethylbenzo[*h*]quinoline within crude oil samples (Figure 5-16) and whilst MS/MS experiments could not enable further structural assignments, similarities in the mass spectra of isomers led to the confident identification of a C_2 benzoquinoline series (Chapter 5). Changes in the distribution of the C_2 benzoquinolines of the maturation series are shown in Figure 6-3, with increasing thermal maturity appearing to influence significantly the distribution of isomers. Changes in maturity appear to drive the incremental depletion of isomers c and d, whilst also resulting in the gradual increase of peak b. Interestingly, an early eluting series of co-eluting peaks can be observed only in the chromatogram of most mature sample (mE). The origin of these peaks is unknown.

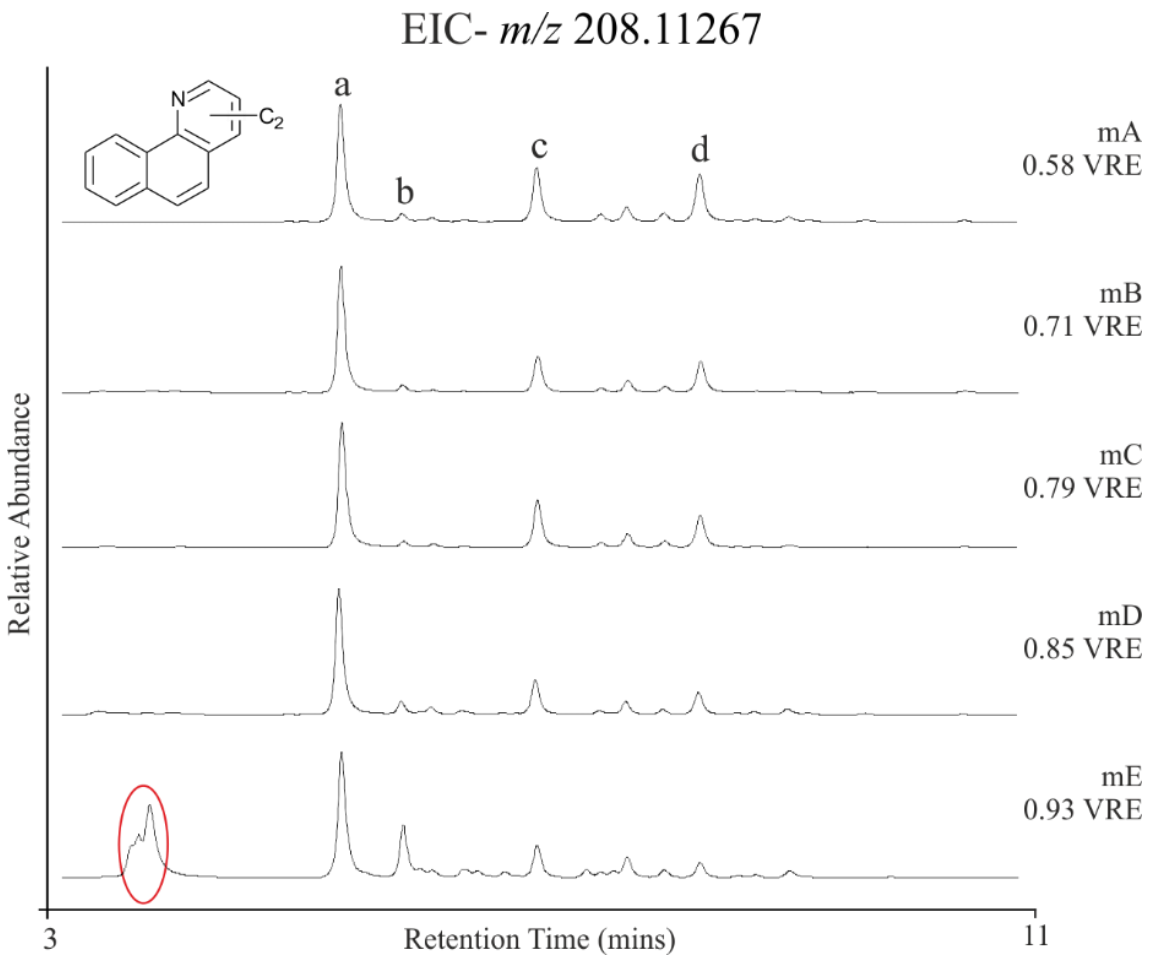

Figure 6-3. EICs of the protonated C_2 alkyl benzoquinolines from the LC-HRAM-MS analysis of the maturity crude oil suite. Important isomers are labelled (a, b, c and d) and the appearance of a peak series in sample mE is highlighted.

Changes in the relative abundance of the most significant C_2 benzoquinolines (peaks a-d) are shown in Figure 6-4. Peaks a, c and d all show similar trends, initially showing a gradual decrease in abundance between 0.58 and 0.79 VRE before increasing to a maximum at a maturity of 0.85 VRE and final decreasing in abundance. As observed in the chromatograms (Figure 6-3), peak b remains largely unchanged in the immature and early/early peak mature samples (0.58-0.79 VRE; mA-C) but then gradually increases in abundance, reaching a maximum in the most mature sample (0.93 VRE; mE).

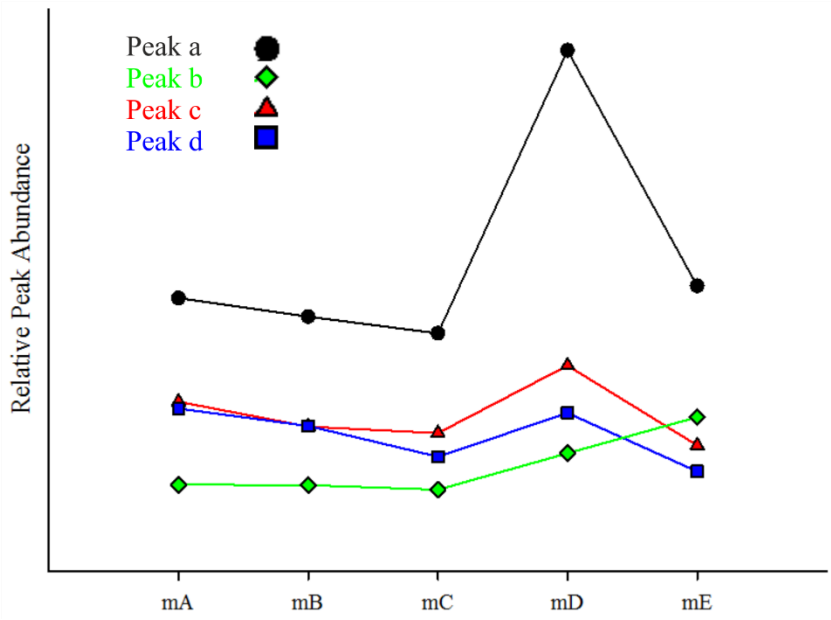

Figure 6-4. Changes in the relative abundance of the four most significant C_2 benzoquinoline isomers determined by LC-HRAM-MS analyses.

In order to show the effects of changing maturity on the C_2 benzoquinolines, isomer ratios were plotted for peaks showing significant changes. Peak ratios were calculated using Equation 3 and were plotted against sample maturity (VRE) to investigate the correlation with sample maturity.

$$\text{Peak Ratio} = \frac{(\text{area of peak x})}{(\text{area of peak y} + \text{area of peak x})} \qquad (3)$$

Interestingly, the plot comparing the ratio of peaks b:a to maturity appeared only to correlate with the more mature samples (> 0.79 VRE; Figure 6-5A), showing the potential for its application as a marker for high thermal maturity. The ratio of peaks d:a showed the closest relationship with maturity, demonstrated by a regression coefficient of 0.997 when plotted again maturity (Figure 6-5B).

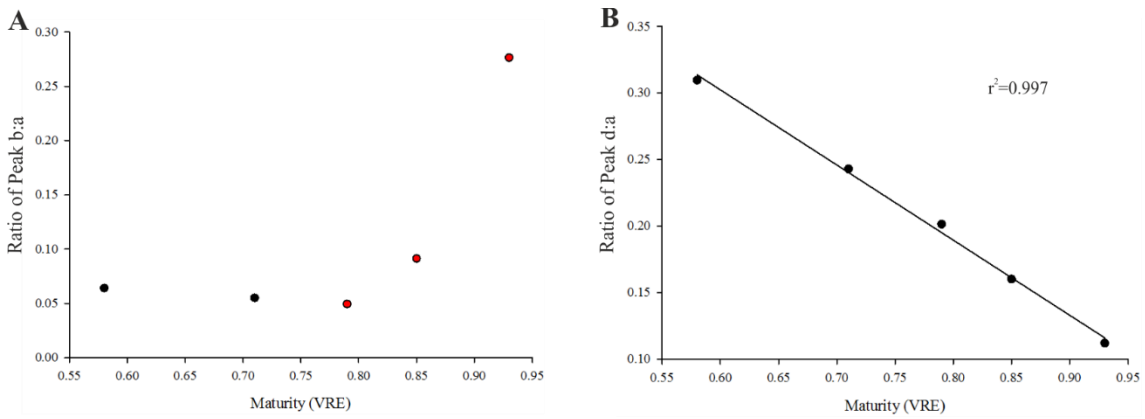

Figure 6-5. Scatter plots showing the correlation between the ratio of peaks a:b and maturity (VRE; A) and the ratio of peaks a:d and maturity (VRE;B) for the C_2 benzoquinolines.

In addition to the C_2 benzoquinolines, the C_3 benzoquinolines also appeared to be significantly affected by changes in maturity (Figure 6-6). The most significant of these changes was the progressive depletion of the late eluting series of peaks. The reduction of the most abundant of these peaks (peak c), appeared to correlate closely with increasing maturity, becoming completely absent in the most mature sample (mE). It was postulated previously (Chapter 5) that this late eluting series of peaks within the C_3 benzoquinolines were alkylated series not of benzo[*h*]quinoline but one of the other four potential benzoquinoline isomers ([*b*], [*c*], [*f*] or [*g*]). If this is the case, the preferential depletion of such isomers would be an interesting discovery, suggesting either the occurrence of the thermal rearrangement of the aromatic quinoline core, or the preferential thermal degradation of less stable benzoquinoline isomers. Changes in the earlier eluting, more condensed series of peaks are also noteworthy. The abundance of peak a relative to its surrounding peaks appears to increase, whilst the lesser abundant peaks (e.g., peak b) are progressively depleted as the degree of thermal maturation increases. In addition to these observations, the EIC of sample mE again shows the presence of a unique early eluting series of compounds which, as with the C_2 benzoquinolines, cannot be explained.

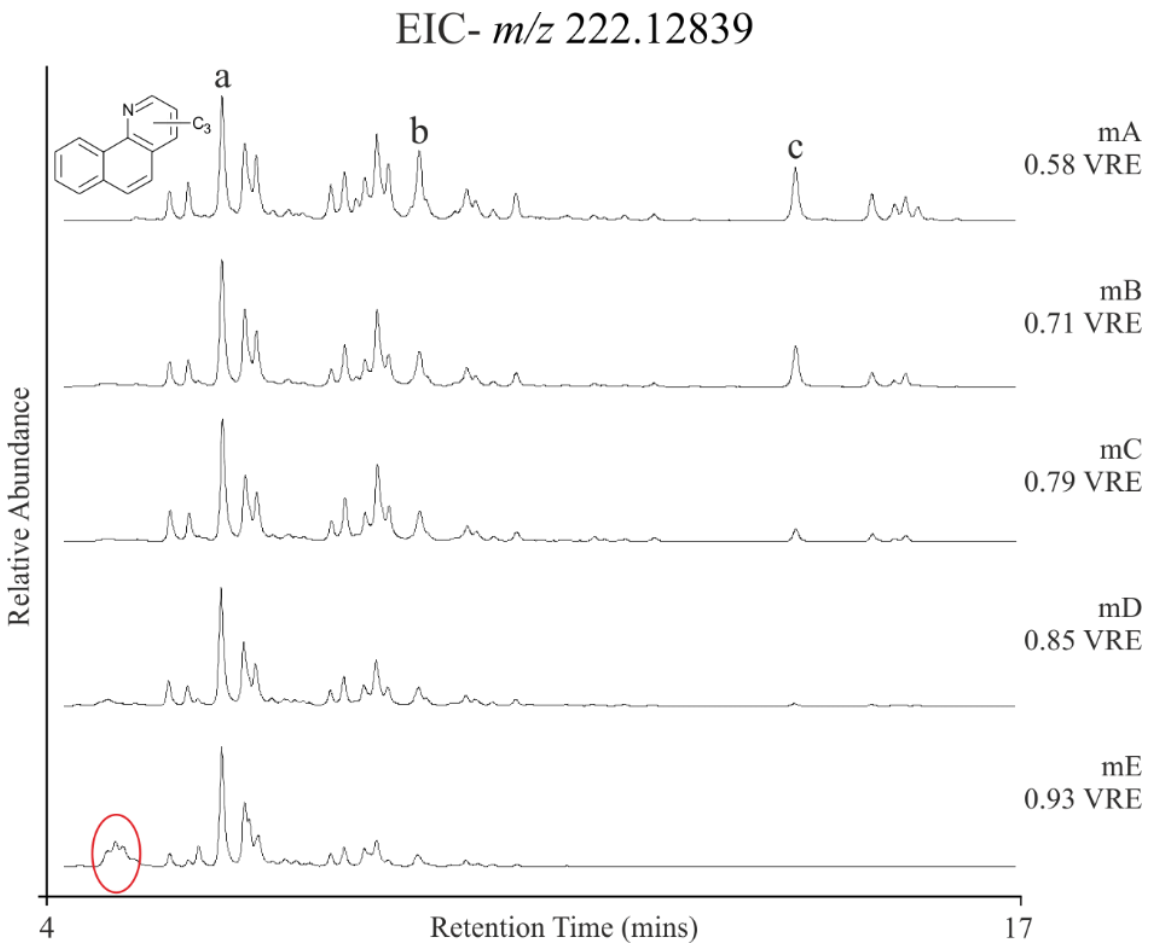

Figure 6-6. EICs of the protonated C_3 alkyl benzoquinolines from the LC-HRAM-MS analysis of the maturity crude oil suite. Important isomers are labelled (a, b and c) and the appearance of a peak series in sample mE has been highlighted.

The plots of the ratio of peaks b:a and peaks c:a vs maturity highlight (Figure 6-7A & B) the strong correlation between C_3 benzoquinolines and maturity. The regression coefficient of 0.991 obtained for the peak b:a ratio demonstrates its potential for a marker of thermal maturity across the range studied herein. However, in the case of the ratio of peaks c:a the complete absence of peak c in the late-mature sample (mE) weakens correlation with maturity (r^2= 0.972). Removal of this data point improves the correlation (r^2= 0.997), suggesting the ratio is only suitable for early-peak mature samples (<0.85 VRE).

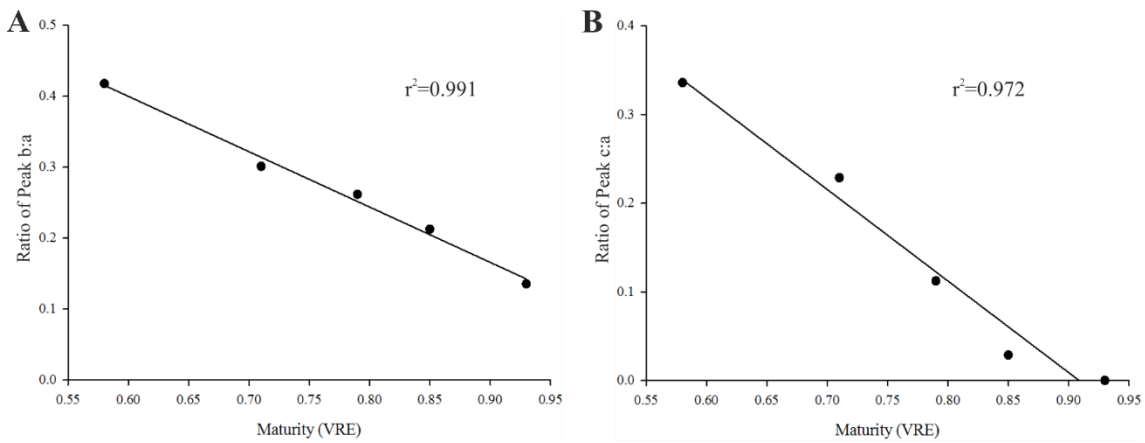

Figure 6-7. Scatter plots showing the correlation between the ratio of peaks b:a and maturity (VRE; A) and the ratio of peaks c:a and maturity (VRE; B) for the C_3 benzoquinolines.

The close correlation between the isomeric ratios of the C_2 and C_3 benzoquinolines and thermal maturity suggest great potential for use of the benzoquinolines as indicators of the level of thermal maturity of crude oils. However, in order to complete this study, ideally reference compounds should be obtained to allow for the confident identification of all C_2 and C_3 benzoquinoline isomers. Furthermore, the relationship of the benzoquinoline distributions with crude oil maturity should be tested on further maturity suites, preferably those that extend in to the extremes of early and post mature crude oils. This is discussed in greater depth in Chapter 7.

6.3.1.2.2. Fraction SAX2

The relationship between carbazoles and maturity is perhaps the most studied of the heteroatom containing classes. Initial interest in the carbazoles of crude oil was for use as markers of secondary migration (Larter *et al.*, 1996) and in addition to ratios of methyl-carbazoles, the ratio of benzo[*a*]- to benzo[c]carbazole was suggested as a potential marker for the degree of migration. However, in order to be suitable as migration markers the effects of source rock maturity on isomeric distribution must be negligible, as otherwise changes in distribution could not confidently be assigned to either maturity,

migration or both. Work by Li *et al.* (1997) identified a close relationship between the distribution of the benzocarbazoles and maturity, rendering them less suitable for use as migration markers. However, this discovery led to a number of further investigations in which the effects of maturity on carbazole distributions were studied in greater depth (Clegg *et al.*, 1998; Horsfield *et al.*, 1998; Bennett *et al.*, 2002; Zhang *et al.*, 2011).

To investigate the effects of thermal maturity on the distribution of pyrrolic nitrogen species in the North Sea series, carbazole and the benzocarbazole isomers were quantified in the SAX2 fractions. Results from the quantification (Figure 6-8A) show an initial decrease in carbazole and benzocarbazole concentrations (0.58-0.79 VRE), followed by a sharp increase as maturity progresses further (0.79-0.93 VRE). A similar correlation between carbazoles and thermal maturity was reported in a study by Clegg *et al.* (1998), who observed a slight decrease in initial carbazole concentrations (0.3-0.8%R_o) followed by a sharp increase in concentration to a peak abundance at 1.1%R_o. Bennett *et al.* (2002) also reported on the distribution of carbazoles and benzocarbazoles in a North Sea maturity suite. The authors observed the same initial decrease in the concentrations of benzo[*a*]- and benzo[*c*]carbazole in the early stages of maturity (0.68-0.75%R_o), followed by a 4× increase concentration as maturity progressed further (0.85%R_o). This initial decrease in benzocarbazole concentrations was attributed to a stage of dilution by more rapidly produced petroleum species prior to release from the source rocks. A more recent study by Zhang *et al.* (2011) also reported similar trend in carbazole concentrations in source rocks from the Western Qaidam Basin, NW China.

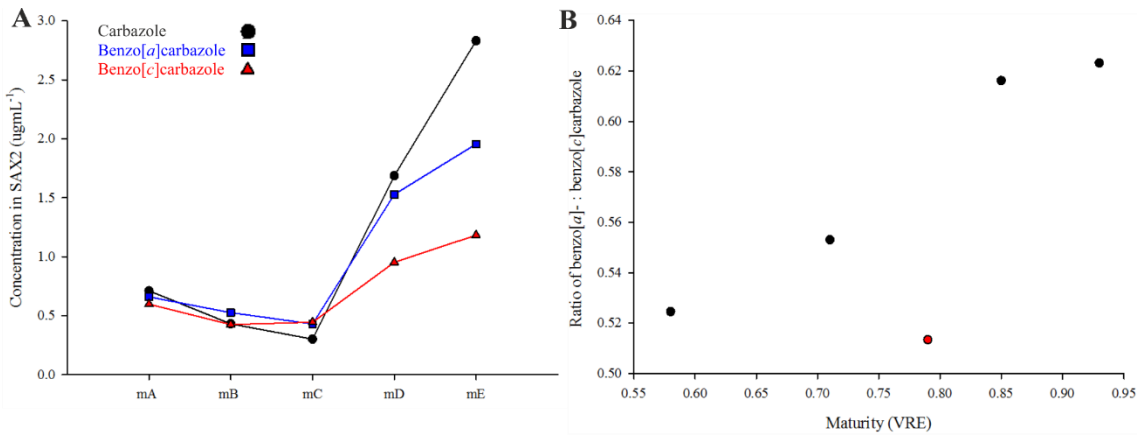

Figure 6-8. Plot showing changes in the relative abundance of carbazole, benzo[*a*]carbazole and benzo[*b*]carbazole (A) and a scatter plot showing the correlation between the ratio of benzo[a]:benzo[b]carbazole and maturity (VRE; B).

Correlation between the ratio of benzo[*a*]- and benzo[*c*]carbazole and maturity are shown in a plot in Figure 6-8B. Previous studies correlating benzocarbazole ratios to thermal maturity have observed that the relationship can be significantly affected if the samples in the series have been the subject of secondary migration processes. Horsfield *et al.* (1998) studied series of crude oils generated from the Sonda de Campeche formation, Mexico and identified that carbazole ratios were significantly effected in oils that had experienced migration over distances of 1-3 km. Later work by Bennett *et al.* (2002) reported similar trends in a series of North Sea crude oils. The sample set tested herein shows a generally positive correlation. However, this is interrupted by an outlier at 0.79 VRE (sample mC). It is possible that sample mC has been subject to secondary migration thus, affecting the ratios of the benzocarbazole isomers.

6.3.1.2.3. Fractions S2 and S3

Wilkes *et al.* (1998a; 1998b) were the first to investigate possible relationships between thermal maturity and aldehyde/ketones. Their work was focused on the characterisation of the fluorenone series, identifying a systematic increase in overall fluorenone concentrations as maturity increased (Wilkes *et al.*, 1998a). However, unlike the alkylated

carbazoles, the authors observed little correlation between the distribution of the alkyl fluorenones and maturity. One notable exception was that of 1-ethylfluorenone:1,8-dimethylfluorenone, which was reported to decrease linearly across the maturity range of the sample suite (0.48-1.45%R_o). Later work expanded on this, studying the effects of increasing maturity on the distribution of alkyl- naphthaldehydes, benzaldehydes, acetophenones, indanones and tetralones (Wilkes *et al.*, 1998b). The authors identified significant correlations between the distributions of these compound series and maturity. Indeed, ratios of α- and β- isomers were seen to behave similarly to those of their hydrocarbon counterparts (i.e. alkyl naphthalenes).

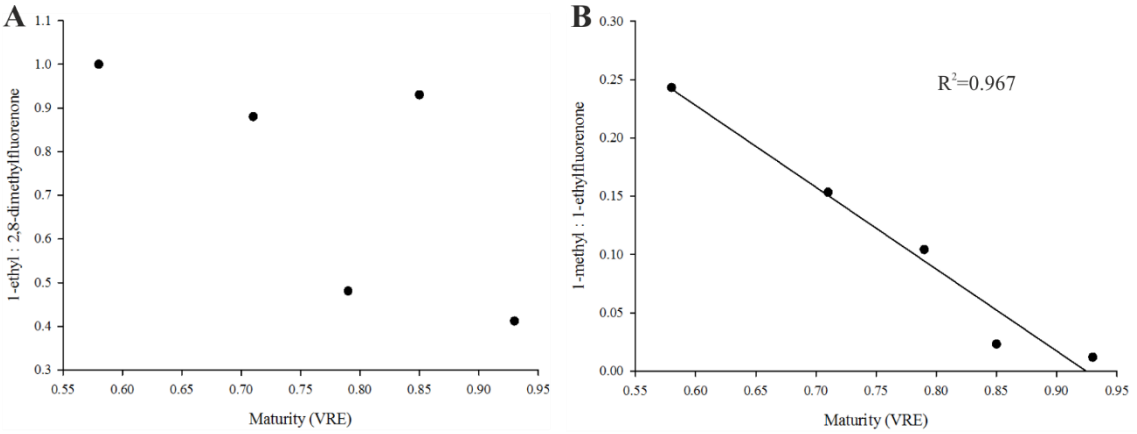

Figure 6-9. Plot showing relationship between 1-ethyl:2,8-dimethylfluorenone and maturity (VRE; A) and a plot showing the correlation between 1-methylfluorenone: 1-ethylfluorenone and maturity (VRE; B).

Investigations into the distributions of the alkylated fluorenones in the S2 fractions of the series studied herein, identified correlations between alkyl fluorenone isomers not observed by Wilkes *et al.* (1998a). Whilst a negative correlation did exist for the 1-ethyl:2,8-dimethylfluorenone isomers (Figure 6-9A), it was not as strong as that observed by Wilkes and co-workers (1998a). Additionally, unlike in the work of Wilkes *et al.*, linear trends in the abundance of individual fluorenone isomers were identified within the studied maturity series. For example, Figure 6-9B shows the close correlation between

the ratio of 1-methyl- and 1-ethylfluorenone and maturity, generating a regression coefficient of 0.967. The difference in observations between the two sample suites suggests that the distributions of the alkylated fluorenones may be affected by additional factors (e.g., migration, source).

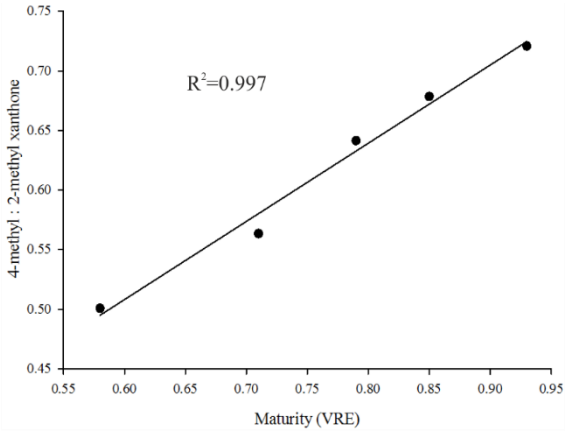

Figure 6-10. Plot showing relationship between 4-methyl:2-methylxanthone and maturity (VRE).

Oldenburg *et al.* (2002) investigated the correlation between the alkylated xanthones and thermal maturity. The authors reported strong correlations between the relative abundance of the C_1 and C_2 xanthones and maturity. Similar correlations between the relative masses of the various alkylated xanthones were seen in this maturation series. Furthermore, a strong correlation was observed between 4-methyl-:2-methylxanthone and thermal maturity, generating a regression coefficient of 0.997 (Figure 6-10) and demonstrating the potential for the use of the alkylated xanthones as a marker of thermal maturity.

6.3.2 Biodegradation

The biodegradation 'series' studied herein consisted of crude oils sampled from two reservoirs. The first sample set (bA, bC and bD) consists of samples classed as: very slightly biodegraded (bA), slightly biodegraded (bC) and heavily biodegraded (bD) and the second set (bB and bE) classed as: very slightly biodegraded (bB) and heavily biodegraded (bE). Indeed, it is likely that the impacts of bacterial alteration on the slightly biodegraded samples bA, bB and bC will be minor, and that changes to the highly degraded bD and bE samples will be substantial. Therefore, the 'series' is not capable of providing information on incremental changes in crude oil composition that occur as biodegradation progresses but should be suitable for indicating broad changes in NSO compounds occurring during biotransformation.

6.3.2.1 Gravimetric Study

Total recoveries from the separation of biodegradation 'series' were somewhat lower than those found in previous separations (Table 6-5). In this instance, evaporative losses could only explain sample losses for oils bA and bC and the remaining three samples (bB, bD and bE) suffered an additional loss of ~10% on separation. The majority of losses reported for samples bD and bE occurred during separation on silica (Table 6-5). A possible cause for this low recovery could be a result of insufficient drying of the SAX0 fraction, resulting in the recording of an incorrect mass. If this were the case, removal of this excess solvent during separation on silica or in later solvent removal steps would lead to the calculation of a lower recovery.

Nonetheless, the degree to which the individual samples had been subject to biodegradation appears to be reflected in the overall gravimetry. The less degraded samples (bA, bB and bC) show an elevated loss during the initial SCX separation (15.2-17.0%), suggesting a higher volatiles content. This is further supported by the observed

loss of volatiles when whole crude oils were subject to nitrogen blowdown (Table 6-5). Recoveries of >95% in both SCX and SAX separations of the heavily biodegraded samples (bD and bE) suggests a low volatiles content, highlighting the preferential removal of low molecular weight hydrocarbon species during biodegradation. This is also supported further by the blowdown losses from the whole crude oils, with only a 7.0% and 4.8% loss recorded for the bD and bE samples respectively (Table 6-5).

Table 6-5. Total and individual cartridge recoveries (weight percent) of the biodegradation sample series and average losses of crude oil sample during N_2 blowdown.

Mode of Separation		Percentage Recovery				
		bA 0.9 Pr/nC_{17}	bB 1.1 Pr/nC_{17}	bC 1.2 Pr/nC_{17}	bD 8.2 Pr/nC_{17}	bE n.d. Pr/nC_{17}
IEX	SCX	84.8	83.0	83.4	95.3	99.4
	SAX	97.5	94.8	95.0	99.6	98.8
Silica		90.3	93.1	94.8	83.2	82.6
Total		**69.0**	**70.4**	**75.8**	**82.1**	**84.0**
Blowdown loss		30.6	22.5	21.0	7.0	4.8

Gravimetric data for individual fractions are presented in order of increasing level of biodegradation in Figure 6-11. Overall, the dataset is less informative than that for the maturity series, with fewer fractions appearing to correlate with the level of biodegradation. Interestingly, the abundance of the deposited, asphaltene-type, SCX1 fractions appeared to decrease with increasing levels of biodegradation (Figure 6-11A). Whilst often considered recalcitrant to bacterial alteration, studies such as those by Liao *et al.* (2009), have shown that ‘asphaltenes’ and ‘resins’ are indeed affected during biodegradation. Nevertheless, this observed decrease is unexpected. The increasing relative abundance of asphaltenes in biodegraded crudes is well known and this result suggests the SCX1 fraction may not always provide equivalent asphaltenes concentrations.

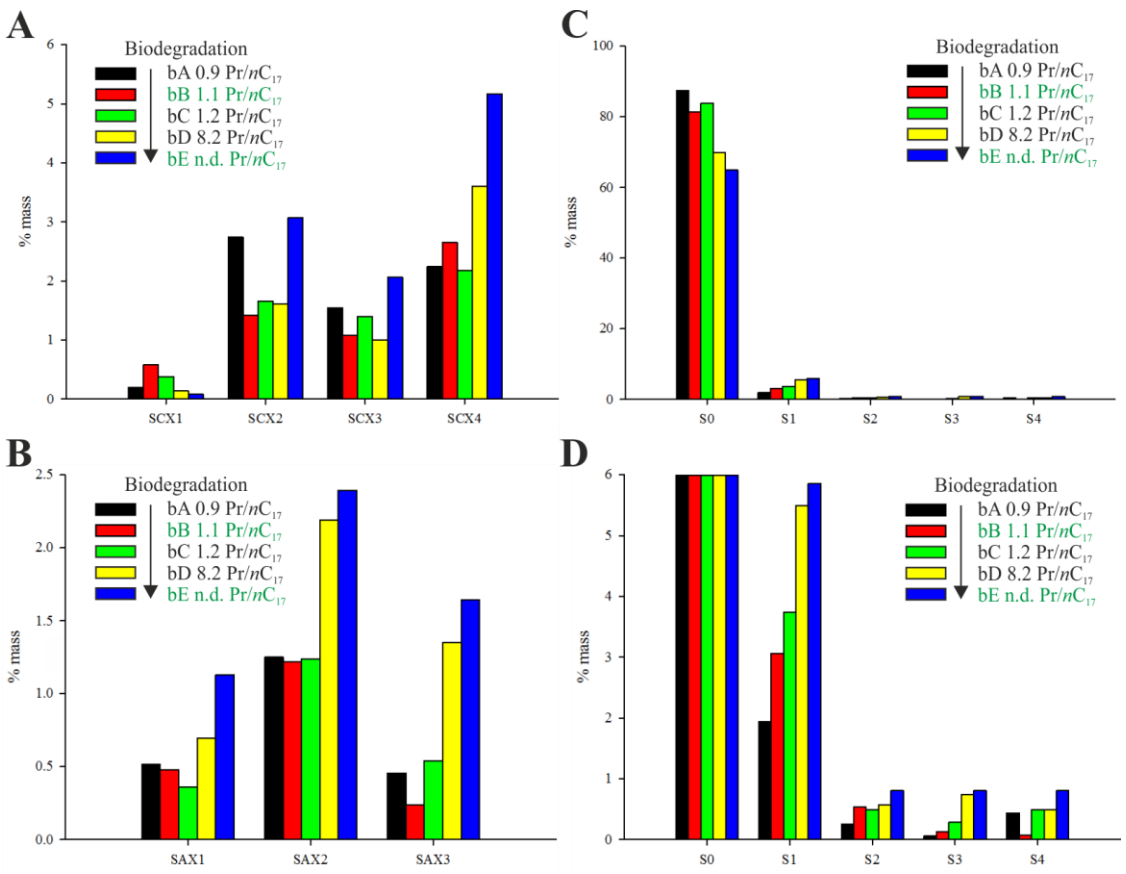

Figure 6-11. Gravimetric data (weight percent) of individual fractions from the SCX (**A**), SAX (**B**) and Silica (**C**; with zoomed insert to show lower mass fractions, **D**) from the separation of the crude oil biodegradation series.

Little correlation with biodegradation level was observed in the masses of the SCX2 and SCX3 fractions, suggesting the isolated classes are not affected by the level of biodegradation. However, the abundance of the SCX4 fractions (pyridinic nitrogen fraction) does appear to correlate with biodegradation, becoming enriched in samples bD and bE. The correlation is highlighted in a plot showing change in the ratio of SCX4:S0 as biodegradation progresses (Figure 6-12D). The plot shows little change in the ratio during the early stages of biodegradation but is clearly elevated in the biodegraded samples (bD and bE). The observed relative increase in nitrogen species agrees well with work conducted by Liao and co-workers (2009), who reported on the elevated nitrogen content of asphaltenes in increasingly biodegraded crude oils. Observed increases in the

abundance of nitrogen in biodegraded crudes likely reflects their resistance to microbial degradation.

Figure 6-11B shows the effect of biodegradation of the SAX fraction series. Little correlation can be seen in the SAX1 fractions. However, the abundance of the SAX2 fractions (pyrrolic nitrogen) appeared to be closely related to biodegradation. This correlation is highlighted in Figure 6-12A in a plot showing the change in the ratio of fractions SAX2:S0 with increasing levels of biodegradation. The three slightly biodegraded samples (bA, bB and bC) produce negligible changes in the ratio. However, the heavily biodegraded samples produced higher values, with their distributions reflecting the increased level of biodegradation in the bE sample. Much like pyridinic nitrogen cores, pyrrolic nitrogen compounds are relatively resistant to biodegradation and have been observed to increase in relative abundance with increasing biodegradation (Kim *et al.*, 2005). Huang *et al.* (2003) reported that biodegradation plays a significant role in the distribution of carbazoles, recording the preferential depletion of alkyl carbazoles compared to alkylated benzocarbazoles and naphthocarbazoles. The SAX3 fraction (petroleum acids) also appeared to correlate closely with the level of biodegradation (Figure 6-12B), producing a similar correlation to that of the SAX2 fractions (pyrrolic nitrogen). The generation of carboxylic acids during the microbial alteration of crude oil is well documented (Reviewed: Peters *et al.*, 2005).

Changes in relative abundance of fractions obtained by separation on silica are shown in Figure 6-11 C and D. Depletion of the saturated hydrocarbons by bacterial consumption is reflected well by the decrease in abundance of the S0 fraction. The samples subjected to only slight biodegradation (bA, bB and bC) show only minor changes in relative abundance (81.5 – 87.5%). The heavily biodegraded samples however, decrease some 20% in relative abundance, highlighting depletion of the saturated hydrocarbons. Interestingly, the mass of the S1 (aromatic hydrocarbon) fraction appeared to increase

across the samples series. The observed increase in the slightly biodegraded samples (bA, bB and bC) is likely unrelated to biodegradation and can be attributed to natural variations in the aromaticity of crude oils. Somewhat raised relative levels of aromatic hydrocarbons in the heavily biodegraded samples (bD and bE) would be expected, due to enrichment as the concentration of saturated hydrocarbons decreases.

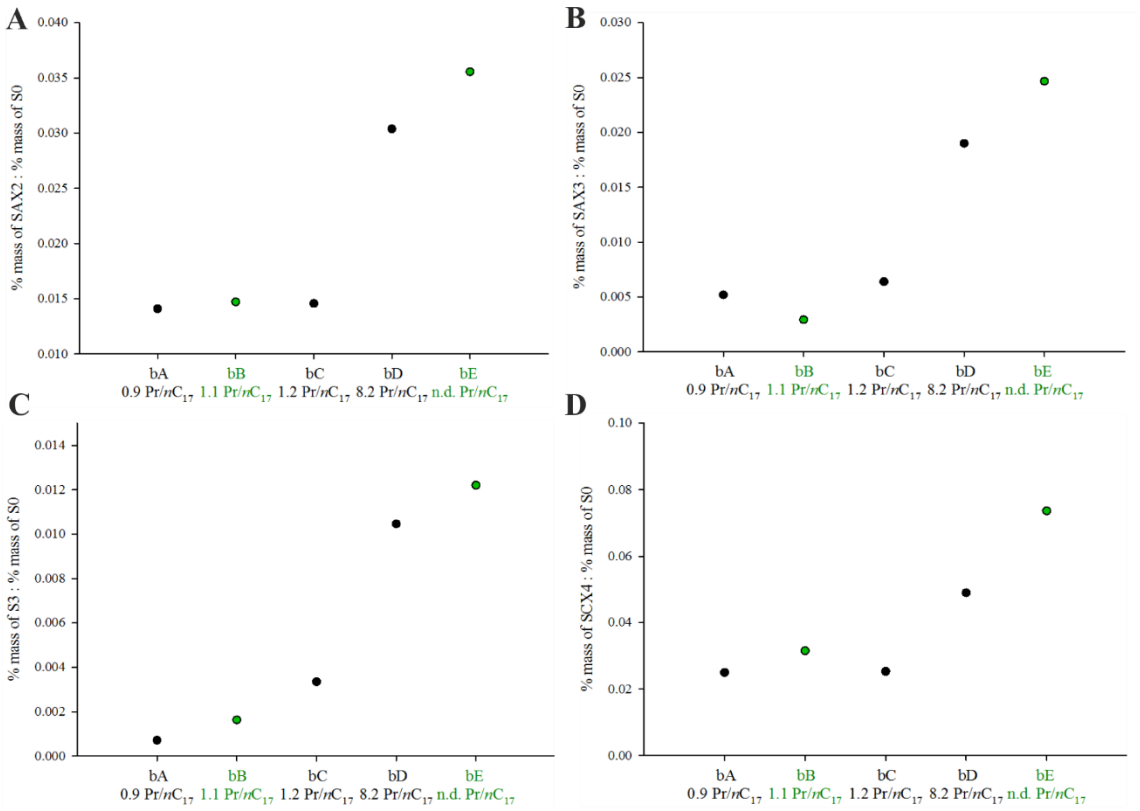

Figure 6-12. Plots showing the correlation between certain fraction masses and crude oils at different stages of biodegradation: A, ratio of the mass of Fractions SAX2:S0 vs samples of increasing biodegradation; B, ratio of the mass of Fractions SAX3:S0 vs samples of increasing biodegradation; C, ratio of the mass of Fractions S3:S0 vs samples of increasing biodegradation and D, ratio of the mass of Fractions SCX4:S0 vs samples of increasing biodegradation.

The proportional masses of the first of the ketone fractions (S2) showed little correlation with biodegradation, showing a general increase in abundance across the series but not correlating with the level of biodegradation. The masses of fraction S3 (xanthone)

however, appeared to correlate well with the extent of biodegradation. A plot comparing the ratio of S3:S0 to the degree of sample biodegradation is shown in Figure 6-12D and displays a similar correlation to that of the other plots. Masses of fraction S4 (thiophenes) did not show any relationship to the level of biodegradation, suggesting the bacterial alteration of thiophenes does not occur on a large scale, at least in these samples.

6.3.2.2 Compositional Study

Changes in the composition of biodegraded crude oils are most apparent in the saturated hydrocarbons fractions, which are well known. The preferential removal of the *n*-alkanes by bacterial action resulted in a relative increase in the abundance of the more bio-resistant compounds. These compounds consist of a highly complex mixture of highly branched acyclic, cyclic, aromatic and naphthenoaromatic structures. These changes are well illustrated in the GC-MS TICs of the whole crude oils of the biodegradation series studies herein (Figure 6-13). The samples exposed to only slight levels of biodegradation (bA, bB and bC) showed only minor differences in overall composition, with perhaps the slight depletion of earlier eluting *n*-alkanes ($C_9 - C_{14}$) visible in sample bC. However, changes in the profile when samples have been exposed to heavy biodegradation (bD and bE) were substantial. Depletion of the *n*-alkanes resulted in an unresolved 'hump' comprised of a highly complex mixture of these bio-resistant compounds. Peaks corresponding to pristane and phytane were still visible in sample bD but were undetectable in sample bE, leaving only a small number of resolved peaks.

Unfortunately, the lack of a sample suite in which biodegradation has progressed incrementally, made studying the effects of biodegradation on the composition of NSO functionalised hydrocarbons more difficult. As such, a comprehensive investigation in the composition of the fractions was not conducted in this particular study. However, the ability to obtain discrete fractions of the various NSO functionalised compounds in crude

oils provided a good unique opportunity to investigate compositional changes occurring during microbial degradation.

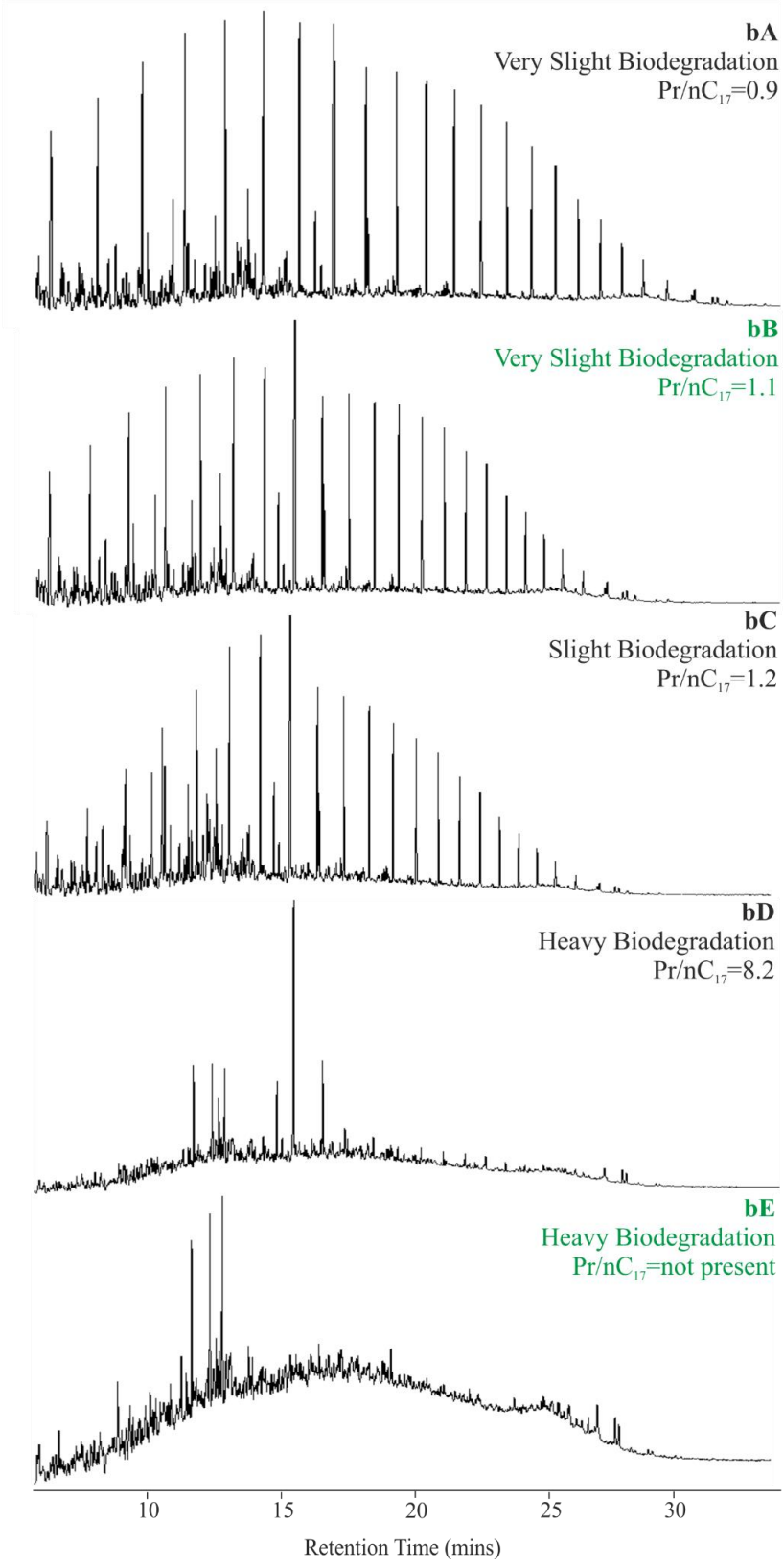

Figure 6-13. GC-MS TICs of the whole oils from the biodegradation suite.

A small number of previous studies have been able to identify changes in the distribution of alkylated nitrogen and oxygen containing PAHs that correlate well with the level of biodegradation (Oldenburg *et al.*, 2002; Huang *et al.*, 2003; Kim *et al.*, 2005). These studies demonstrated the potential of NSO containing compound classes to be employed as markers for the level of biodegradation but it is likely that their resistance to bacterial attack has led to such compound classes being largely dismissed as potential markers. However, this resistance means they are likely present within crude oil samples throughout degradation. As such, they may be capable of providing a quantitative measure of biodegradation across the whole scale. Suggestions for further work pertinent to revealing such changes are discussed in Chapter 7.

6.3.2.2.1. Fraction SAX2

Whilst not suitable for studying the effects of progressive bacterial action, all fractions obtained from SPE separations were nonetheless subjected to analysis by GC-MS in order that any substantial changes in fraction composition could be monitored.

Interestingly, analysis of the SAX2 fraction obtained from sample bB revealed the presence of a highly abundant, late eluting compound series (Figure 6-14). This series was located in a similar chromatographic region to the tocopherols, which were tentatively identified within the SAX2 fraction of the Bonga crude oil (Chapter 5). However, whilst the mass spectra of the present series were similar to those of the tocopherols, they had lower masses (*m/z*) and generated a different mass spectral fragmentation patterns.

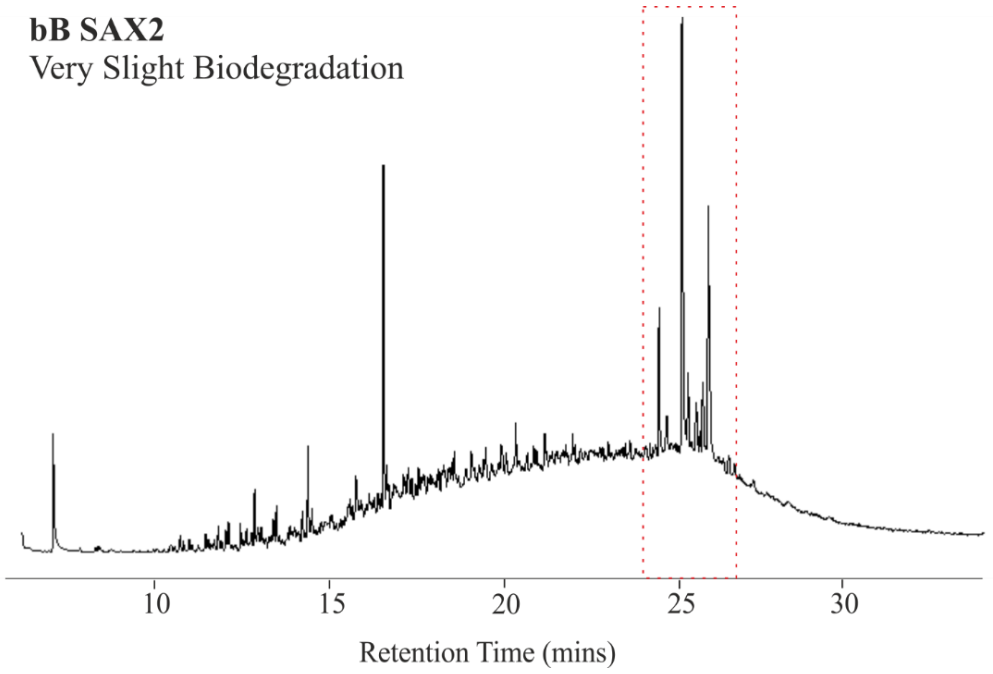

Figure 6-14. GC-MS TIC of the SAX2 fraction obtained from the SPE separation of sample bB of the biodegraded crude oil series with the highlighted compound series highlighted.

Closer inspection of the SAX2 chromatograms revealed the presence of this compound series in all five of the degraded samples. This was confirmed by the generation of EICs using the most abundant ions in each of the peaks (Figure 6-15). Interestingly, the peaks showed a similar distribution in all but the most degraded sample (bE), suggesting the compounds may possess a certain level of bio resistance. The peak distribution was also remarkably similar to that of the tocopherols, suggesting a common origin for both series.

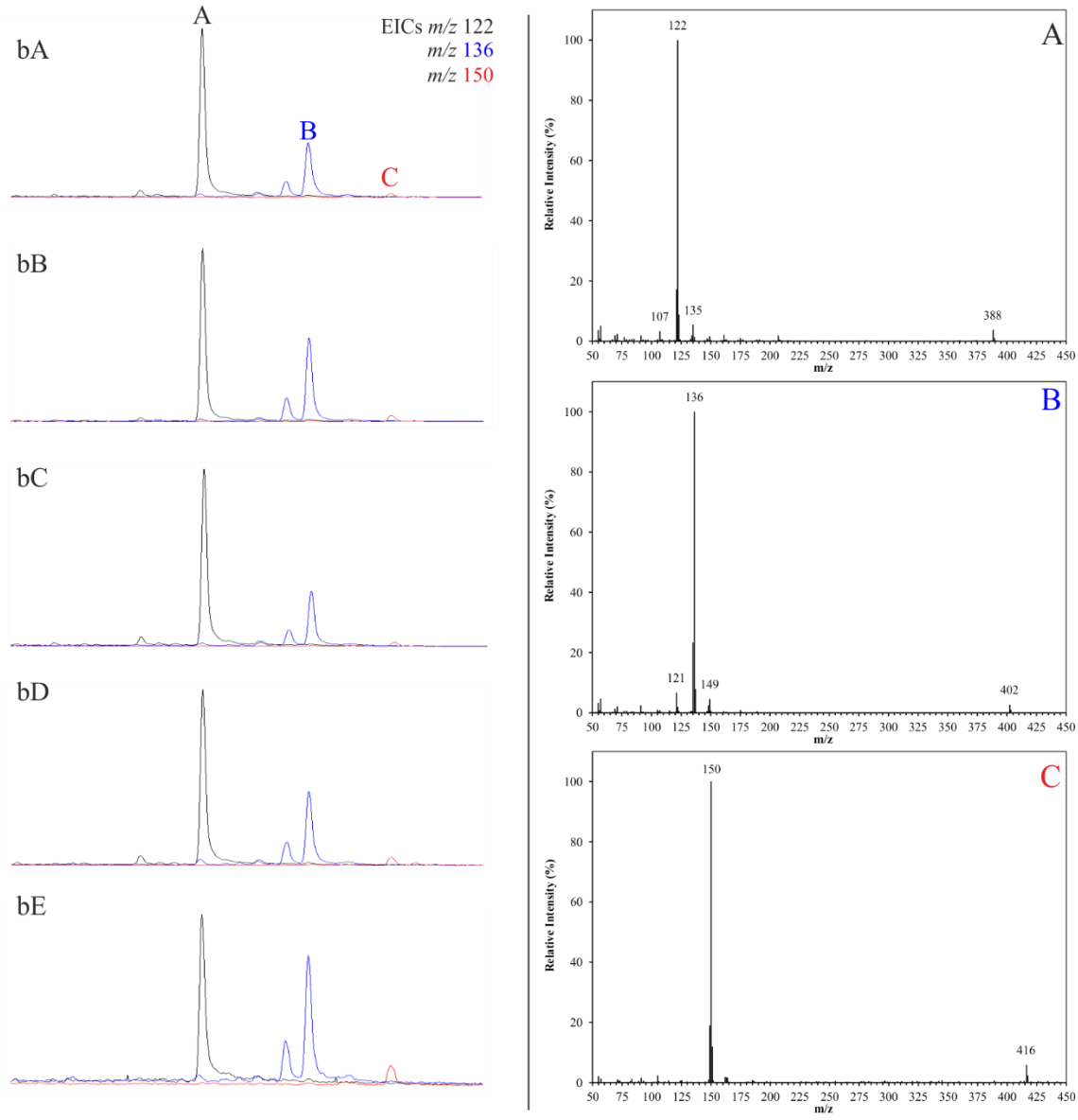

Figure 6-15. GC-MS EICs showing the series of unknowns with adjacent mass spectra for components A, B and C from the analysis of the biodegradation suite.

Mass spectra of the series were characterised by high mass molecular ions (*m/z* 388, 402 and 416) and were dominated by base peak ions at *m/z* 122, 136 and 150 respectively (Figure 6-15 A, B and C). Such mass spectra are consistent with those of highly alkylated benzenes, in which fragmentation induces the loss of the alkyl chains, resulting in base peak ions consistent with that of the benzene nucleus. In this case, the stepwise increase in mass (+14 Da) of both the base peak ions and the molecular ions suggested that the compounds share a side chain of equal length. The common loss of 266 Da observed for each of the compounds would correspond to the loss of a $C_{19}H_{38}$ alkyl chain.

A previous study by Barakat *et al.* (2012) identified a similar series within lacustrine black shales, Southern Germany. The authors tentatively assigned the structures as a series of phytanyl alkylated phenols, however could not discern the positioning of the substitutions. The assignment of these unknowns as phenols fits well with the designation of the SAX2 fraction as the phenol/carbazole fraction. Another similar series was observed in a study of the C_{12}-C_{30} alkylbenzenes in crude oils obtained across the former USSR (Ostroukhov *et al.*, 1983). In conducting this study, the authors identified a series of high abundance C_{26}, C_{27} and C_{28} alkyl benzenes. Further investigation into the structure of these compounds led to the assignment of the side chain attached to the benzene substituent as isoprenoidal and that the increase in carbon number was due to the substitution of additional methyl groups onto the benzene ring. The mass spectra obtained for the synthetic C_{28} compound compared extremely well to that of Peak A (Figure 6-15A). However, the observed ions were some 2 Da less (i.e. molecular ion: 386 and base peak ion: 120). In this instance, the compounds of interest are found within a phenol/pyrrole type fraction. Thus, the difference in mass between the two datasets could be explained if the benzene ring observed previously (Ostroukhov *et al.*, 1983) was due to a phenol group.

Assignment of the compounds as a series of alkylated phenols was supported further by a detailed examination of their mass spectra. The loss of the tentatively assigned isoprenoidal side-chain is suggested to result in the formation of the base peak ions at *m/z* 122, 136 and 150. These fragments generate molecular formulae consistent with the structures of alkylated phenols (*m/z* 122, $C_8H_{10}O$; *m/z* 136, $C_9H_{12}O$; *m/z* 150, $C_{10}H_{14}O$) and additional lower abundance fragments (*e.g.*, *m/z* 107) are then consistent with the fragmentation of phenolic structures (McLafferty and Turecek, 1993).

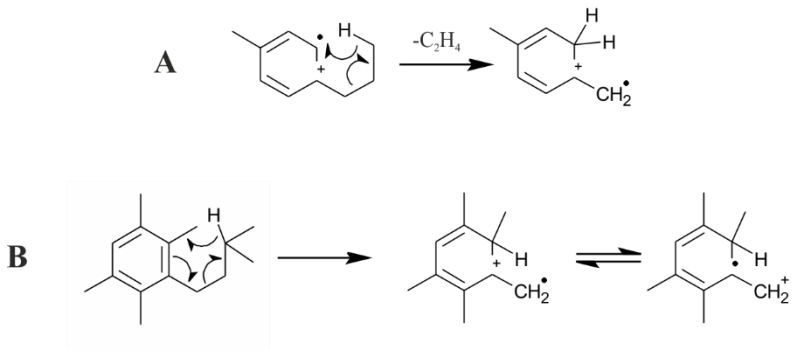

Figure 6-16. γ-Hydrogen rearrangements undergone by di- (A) and tetra- (B) substituted benzene rings leading to the formation of even fragment ions (redrawn from McLafferty (1993) and Kingston *et al.* (1988)).

Interestingly, the production of even fragment ions from the fragmentation of benzene rings exhibiting multiple substitutions can only occur when these substitutions are in specific orientations. These γ-hydrogen rearrangements require at least a C_3 substituted chain (shown in Figure 6-16) and are typically enhanced when the ortho- positions are vacant (Ji-Zhou *et al.*, 1993). However, Kingston *et al.*(1988) showed that these rearrangements also occurred in tetra- substituted rings (Figure 6-16B). It could be considered likely that these rules also would apply to substituted phenols and, by applying them in this instance, structures were tentatively assigned herein. (However, it is also possible that the inherent electronegativity of the O atom would increase the likelihood of H retention within the fragment regardless of the position of the alkyl substituents).

Nonetheless, structures were assigned by application of rules determining alkylbenzene fragmentation, which also allowed the structure of the base peak ion fragments to be postulated (Figure 6-17).

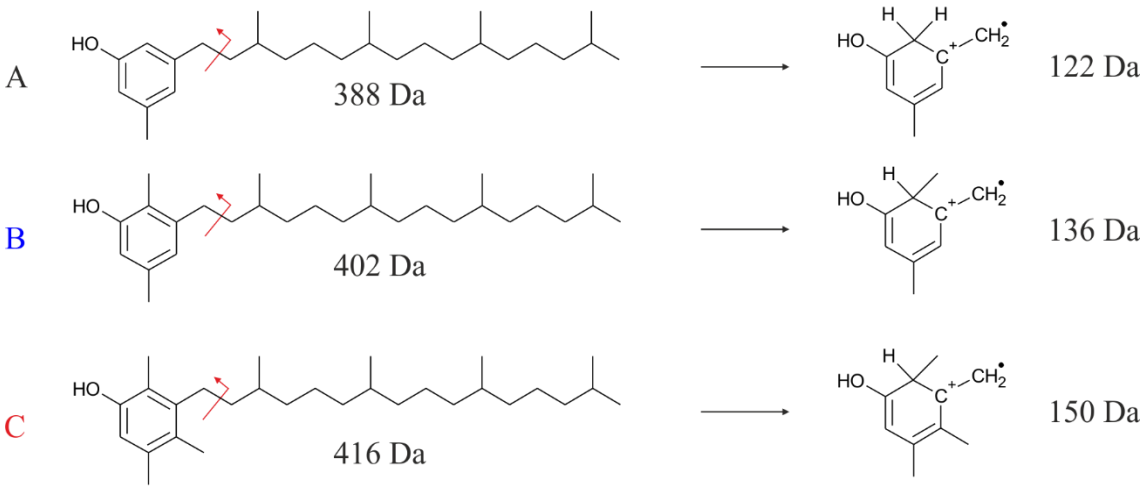

Figure 6-17. Structures assigned to peaks A, B and C based on the observations of (Ostroukhov *et al.*, 1983) and postulated structures of the fragments responsible for the base peak ions.

6.4 Conclusion

The results of the separation of the maturity and biodegradation crude oil 'series' presented herein, have demonstrated the potential for use of the developed SPE to investigate the effects of geochemical processes on crude oil composition. The separation of crude oils into fractions of differing molecular composition provided easy access to fractions containing poorly studied compounds, allowing investigations into their alteration by changing geochemical parameters. Once again, crude oils were efficiently separated with only minor loss of sample to irreversible adsorption occurring.

Analysis of gravimetric data obtained from the separations, identified close correlations between the relative abundance of many of the fractions and changes in both maturity and biodegradation. In the case of the maturity 'series', markedly close correlations were seen between the masses of the SCX2 (sulfoxide), SCX4 (quinoline), SAX2 (phenol/carbazole), S0 (saturated hydrocarbons) and S3 (xanthones) fractions. Correlations in the biodegradation 'series' were not as apparent. However, relationships could be observed in the relative abundance of the SCX4, SAX2, SAX3 (acids), S0 and S3 fractions and the estimated level of biodegradation (nC_{17}/Pr).

Investigations into the composition of fractions obtained from the maturity 'series', led to the identification of a number of potential molecular maturity markers. The relative abundance of specific carbazole, fluorenone and xanthone were observed to respond to changes in thermal maturation, often correlating with previously reported data. Additionally, the identification of series of phytyl-substituted phenols in a number of the SAX2 fractions, further demonstrated the benefits of performing the separation procedure to aid in sample characterisations.

The power of LC-HRAM-MS to characterise crude oil mixtures has been further demonstrated by the analysis of cationic fractions obtained from the maturity oil 'series'.

Separation of benzoquinoline isomers led to the identification of a close correlation between the abundance of several C_2 and C_3 alkylated benzoquinolines and the degree to which oils had undergone thermal alteration. Subject to confirmation by further field studies, the ability to monitor the degree of thermal maturation by the study of alkyl benzoquinoline ratios would find many applications in petroleum geoscience.

Chapter 7. Conclusions

7.1 Conclusions

The present study focused on the development of methods to aid in the characterisation of the NSO-containing constituents of petroleum.

The first stage of these works was the adoption of a previously reported method for the wide scale fractionation for crude oils. The selected method employed both ion exchange and adsorption chromatography to facilitate isolation of nitrogen and oxygen containing compounds from crude oils (Snyder and Buell, 1968). A number of modifications were made to the original method in order to address practical and safety concerns. The most significant modification to the method was the implementation of an SPE procedure utilising pre-manufactured, disposable cartridges. Further changes were also made in an attempt to improve reproducibility and reduce the time and resources required to conduct separations.

To evaluate the selectivity of this modified fractionation scheme towards compound classes of interest, a series of 'model' compounds, chosen to represent these classes were applied to the scheme. 'Model' compounds were separated both alone and when spiked into a crude oil (Alaska North Slope) in order to compensate for the solvent effects of crude oils. Following this, two crude oils were separated by the developed scheme to investigate method selectivity and reproducibility for crude oil separations.

Whilst enabling the identification (using multidimensional gas chromatography; GC×GC-MS) of a number of commonly reported non-hydrocarbon classes (carbazoles, sulfides, carboxylic acids), results from fraction analysis highlighted a number of shortcomings in the modified procedure. The most significant of these was the poor selectivity the method afforded to the compound classes of interest, with seven of the nineteen model compounds eluting within just one fraction. Additional deficiencies

included the low recovery obtained from crude oil separations (72.3 and 69.2% for the ANS and Kuwait blend respectively), thought to be due to the irreversible adsorption of materials to during separation on alumina and the insufficient solvent strength employed to remove ionic components.

The inability of the modified Snyder method to provide suitably discrete fractions, led to the development of a novel separation procedure for the separation of whole crude oils into fractions based on component functionality. Development of the multistep separation procedure involved the 'rearrangement' of the separation steps employed in the Snyder methodology (Snyder and Buell, 1968). The result of these developments yielded a procedure in which crude oil was separated sequentially by cation exchange chromatography, anion exchange chromatography and adsorption chromatography on silica and resulted in the collection of twelve fractions. By performing ion exchange separations prior to adsorption chromatography, losses to irreversible adsorption were minimised allowing near 100% recoveries of non-volatile crude oil components.

Separation of the nineteen 'model' compounds demonstrated method selectivity, with only three instances of the overlap of compound classes (nitro- and acid compounds; SAX3, furans, thiophenes and aromatics; S0, and the carbazoles and phenols; SAX2). Triplicate fractionation of ANS showed the method to have a high reproducibility (average of 4.6% RSD for significant fractions). The method development and results from preliminary fraction analysis were published in *Analytical Chemistry* (Robson *et al.*, 2017).

Following the development of the separation procedure, five crude oils of varying chemical and physical properties were applied to the method to investigate its potential for wider ranging use. Results from the separation of the Brent Blend, Kuwait Blend, ANS, Bonga and TJP crude oils (API gravity range 12.1 to 38.3°) showed changing crude

oil properties to have an insignificant effect on fraction ‘quality’. Furthermore, recoveries of the separated oils were high (77.4 - 97.6%), with the majority of losses being attributable to the loss of volatile components occurring during separation under reduced pressure and solvent removal.

Analysis of the resultant fractions by appropriate gas and liquid chromatographic techniques established that the method is capable of providing well-defined fractions of various compound classes. Analysis of the fractions using gas chromatography- mass spectrometry (GC-MS) showed to the ‘model’ compound predictions of the broader fraction compositions to be largely accurate. Further analysis of the fractions using multidimensional gas chromatography (GC×GC)-MS established that the method was capable of providing quite well defined fractions of various compound classes, allowing rapid identification of common and rarely reported heteroatom-containing crude oil compounds. Common crude oils compound classes identified within individual fractions using GC-MS and GC×GC-MS analysis included polycyclic aromatic hydrocarbons (PAHs), carbazoles, dibenzothiophenes, xanthones, phenols and carboxylic acids and their alkylated homologues.

Mass spectral characterisations of the fractions also resulted in the identification of compound series that, to this authors’ knowledge, have not previously been reported in crude oils. For example, series of tocopherols (E vitamins) were positively identified in the SAX2 fraction of the Bonga crude oil and thioxanthone and its alkylated homologues in the S2 fractions. Also tentatively identified in the S2 fractions were homologues series of alkanals and alkanones, which were well resolved using GC×GC-MS. Additionally, analysis of the sulfoxide fraction (SCX2) of the ANS crude oil led to the tentative identification of rarely reported bicyclic and tetracyclic terpenoidal sulfoxides. The identifications resulting from the analysis of crude oil fractions demonstrated the potential for use of the method in future characterisation studies.

Analysis of the cationic fractions (SCX4) by liquid chromatography-high resolution accurate mass-mass spectrometry (LC-HRAM-MS) showed promise as a technique for the separation and characterisation of such fractions. The coupling of LC to high-resolution mass spectrometers allows additional confidence in MS assignments based on elution retention times. Additionally, accurate mass measurements allow the assignment of elemental formula and provide an insight into the structural complexity of individual molecular formulas. Development of optimised chromatographic LC methods for the separation of the SCX4 fraction led to tentative identification of series of alkylated benzoquinolines. The application of a number of model alkyl benzoquinoline and alkyl phenylquinolines allowed for the confident identification of structures in the SCX4 fractions. Further MS/MS experiments using both the model compounds and fraction components added confidence to their assignment as quinoline derivatives.

Following the successful separation of the initial series of five crude oils, the fractionation procedure was deployed to investigate the change in composition of the various NSO-functionalised fractions in oils at different stages of thermal maturation and biodegradation. Analysis of gravimetric data obtained from the separations, identified, markedly close correlations between the masses of the certain NSO fractions and thermal maturity and biodegradation.

Compositional investigations into the fractions obtained from the maturity 'series', led to the identification of a number of potential molecular maturity markers. The relative abundance of specific carbazole, fluorenone and xanthone were observed to respond to changes in thermal maturation, often correlating with previously reported data. Separation of benzoquinoline isomers led to the identification of a close correlation between the abundance of several C_2 and C_3 alkylated benzoquinolines and the degree of crude oil thermal maturity.

7.2 Future Work

The work presented herein has documented the development of a novel procedure for the separation of crude oils and demonstrated the potential of this procedure to aid in the characterisation of the NSO-containing compounds (so-called 'polars'). Use of the procedure to support the study of the effects of changing geochemical parameters on the composition of these 'polar' compounds yielded promising results. Considering these conclusions, plans for future work should include both strategies to address the limitations of the present investigation as well as for further use of the methodology as a tool aiding the characterisation of crude oils.

7.2.1 Geochemical investigations

Oil and gas prospectivity in geological formations heavily depends on the molecular compositional characteristics of the hydrocarbons present. These characteristics significantly influence the economic viability of an exploration, development or production opportunity. Indeed, the concentrations of certain compound classes directly affect the value of the produced crude, as well as the cost of facility development. Consequently, detailed molecular characterisations of potential oil plays are routinely conducted to aid in the development of potential new oil and gas fields.

To this end, application of the methodologies developed herein to aid in such characterisations could provide invaluable new insights into composition of crude oils. The presented SPE procedure could be easily employed to evaluate potential production opportunities, providing rapid information on compound classes that are known to decrease the value of crudes/increase refining costs (e.g. naphthenic acids and sulphur containing compounds). The widespread adoption of such a method could allow for the creation of large data sets enabling the profiling of new crude oil finds and allow potential production issues to be identified prior to the development of a new well. Furthermore,

the isolation of polar compound classes would enable comprehensive characterisation studies to be conducted, potentially leading to the identification of compounds responsible for specific production issues, potentially aiding in the development of mitigating technologies.

Molecular organic geochemistry is also used routinely within the oil and gas industry to understand the origin and transformation of sedimentary organic matter in the subsurface. As discussed herein, the vast majority of previous investigations have focused solely on saturated and aromatic hydrocarbons to study the source, alteration and migration pathways of oils and gas. However, these represent only a portion of the organic components of petroleum fluids and their integrity as markers can be compromised in many commonly encountered geological settings.

Investigations into the effects of in-reservoir biodegradation on crude oil composition have also been largely limited to only saturated and aromatic fractions. As a result, the majority of molecular indicators are based on compounds found within these classes and many of these markers are only suitable over a limited range. NSO compounds are often dismissed as potential markers of the extent of biodegradation due to an inherent resistance to bacterial attack. However, it is likely that this resistance means they are present throughout the degradation process and have the potential to provide a quantitative measure of biodegradation across the entire range. Consequently, there has been a shift within the oil industry, with research being directed towards the development of new geochemical tools to allow a more comprehensive understanding of geochemical processes.

Application of the herein developed methods would provide a unique opportunity to study the effects of changing geochemistry on the molecular composition of crude oil ‘polars’. Work conducted in Chapter 6 has demonstrated the potential of the method to aid in such

investigations, identifying a number of promising trends and isomeric ratios that appeared to be closely related to geochemical changes. Therefore, future work in this area should first focus on the validation of these trends. Access to similar geochemical series would enable further data on the relationship between benzoquinoline, xanthone and fluorenone compounds and the geochemistry to be studied. Additionally, the effects of factors such as source origin and secondary migration on the composition of these compounds should also be studied with the use of appropriate sample sets. This would ensure changes to composition are specific to thermal alteration and not dramatically effected by other changes in sample geochemistry.

In addition to further validating these trends, work should also focus on the continued use of multidimensional chromatographic and high resolution mass spectrometric techniques to characterise polar fractions. The methods developed herein enable the collection of fractions of specific compounds class allowing instrumental conditions to be better-optimised, thus enabling greater sensitivity to the target analytes. Therefore, continued compositional studies should result in the identification of significant numbers of novel polar compounds. Following their identification, these compounds could be studied for geochemical significance.

7.2.2 Reference compounds

Access to a more comprehensive library of reference compounds would have aided both the development of the SPE procedure and better identification of fraction components. Investigations into the composition of many of the obtained fractions highlighted that the higher alkylated homologues of many of the studied compound classes (*e.g.* thiophenes, carbazoles, xanthones, *etc*.) were often significantly more abundant that of the parent compound. As such, synthesis of reference compounds representing the higher carbon number homologues of many of these groups would aid a better understanding of their

retention behaviour and likely provide a better representation of compound class behaviour. Furthermore, application of model asphaltene compounds (such as those used in Nordgård and Sjöblom, 2008; Pinkston *et al.*, 2009; Schulze *et al.*, 2016) could potentially allow for the behaviour of crude oil asphaltenes within the scheme to be better modelled. Such reference compounds would also be of use during investigations in fraction composition, allowing the confident identification of higher carbon number homologues. Additionally, procurement or synthesis of authentic tocopherols, thioxanthones and terpenoidal sulfoxides and ketones would allow confirmation of the tentative assignments made in Chapter 5.

7.2.3 LC-HRAM-MS

The large volumes of data obtained within a single multidimensional chromatogram or high resolution-LC-MS chromatogram are such that further processing of data would likely enable significantly more identifications to be made. Furthermore, by employing a 'metabolomics' approach to the large datasets obtained from the analysis of the SCX4 fractions obtained from geochemical series, a number of trends may be identified. In order to conduct such a study, the appropriate software would need to be purchased/developed to enable trends within the LC and MS data to be revealed.

The application of LC with orbitrap mass spectrometry has shown great potential as a tool to aid in the characterisation of petroleum. Future work should be focused on the development and optimisation of chromatographic and mass spectral methods for the analysis of other fractions obtained by the scheme. Experimentation with different ionisation sources (e.g. APPI, atmospheric pressure chemical ionisation; APCI and atmospheric pressure laser ionisation; APLI), chromatographic phases and mobile phases would enable molecular and structural characterisation of crude oil fractions.

7.2.4 FT-ICR-MS

The wider application of FT-ICR-MS to the generated fractions would allow for a more comprehensive understanding of fraction composition. Certainly, with the exception of SCX4, the analyses conducted herein were only suitable for those compounds amenable to GC techniques (*m/z* 50-550). Analysis of fractions by FT-ICR-MS would provide information on the entire mass range and accurate mass measurements would allow molecular formula to be assigned, facilitating the identification of all compound classes within fractions. Additionally, the application of different techniques to those employed herein, could enable the characterisation of fractions for which no compositional information could be obtained. For example, the broader molecular composition of fractions SCX1 and SCX3 could likely be investigated using FT-ICR-MS with atmospheric pressure photoionisation (APPI) and the relationship between fractions SCX1 and traditionally isolated asphaltenes studied.

7.2.5 Environmental investigations

The devised SPE methodology could also be employed to aid in pollution investigations. In order to identify the source of crude oil pollution, biomarkers profiles (e.g. terpanes, steranes, etc.) are often used to fingerprint samples against the spilled oil. However, many of these biomarkers are susceptible to chemical and biological weathering and the profile is often altered by these processes. As previously discussed, NSO compounds are typically more resistant to such processes and as a result, could present an alternative means to identify the source of crude oil pollution.

7.2.6 Toxicity

Another potential use of fractions generated by the SPE procedure is in the study of crude oil toxicity. Generation of fractions in which the broader composition is already somewhat understood would enable the toxicity of certain compound classes of to be

investigated. Furthermore, identification of novel NSO structures in crude oils could lead to their synthesis allowing the toxicity of individual structure to be studied. Indeed, preliminary work conducted by collaborators at IMR (unpublished data) exposing basic nitrogen (SCX4) fractions and associated mixtures of reference quinoline compounds to Haddock embryos returned positive results. In addition to this work, the polar crude oil fractions could also be tested for antimicrobial and anticancer activities.

Appendix

Appendix 1. Recovery of model compounds on separation by the modified method of Snyder and Buell (1968).

Model Compound	**Mean (**±rsd)	**Model Compound**	**Mean (**±rsd)
Dibenzofuran Carboxylic Acid	98.6 (±2.4%)	Dibenzothiophene	86.83 (±1.5%)
Adamantane Carboxylic Acid	84.9 (±7.4%)	Fluorenone	72.65(±5.6%)
Benzoquinoline	35.0 (±6.5%)	Phenanthrene	78.88 (±0.8%)
4-pentylbicylco[2,2,2] octane 1- carboxylic acid	101.5 (±0.9%)	Carbazole	75.94 (±2.3%)
Fluoranthene	68.8 (±1.1%)	Xanthone	76.49 (±1.8%)
Dibenzothiophene Carboxylic Acid	105.9 (±8.5%)	Nitroindole	71.23 (±1.3%)
Cholanic Acid	90.4 (±7.0%)	Benzyl Disulfide	32.55 (±1.0%)
Dibenzyl sulfoxide	79.9 (±11.2%)	Dibenzothiophene Sulfone	87.45 (±1.6%)
Phenyl Phenol	68.3 (±2.8%)	Benzo[a]pyrene	88.01 (±1.6%)

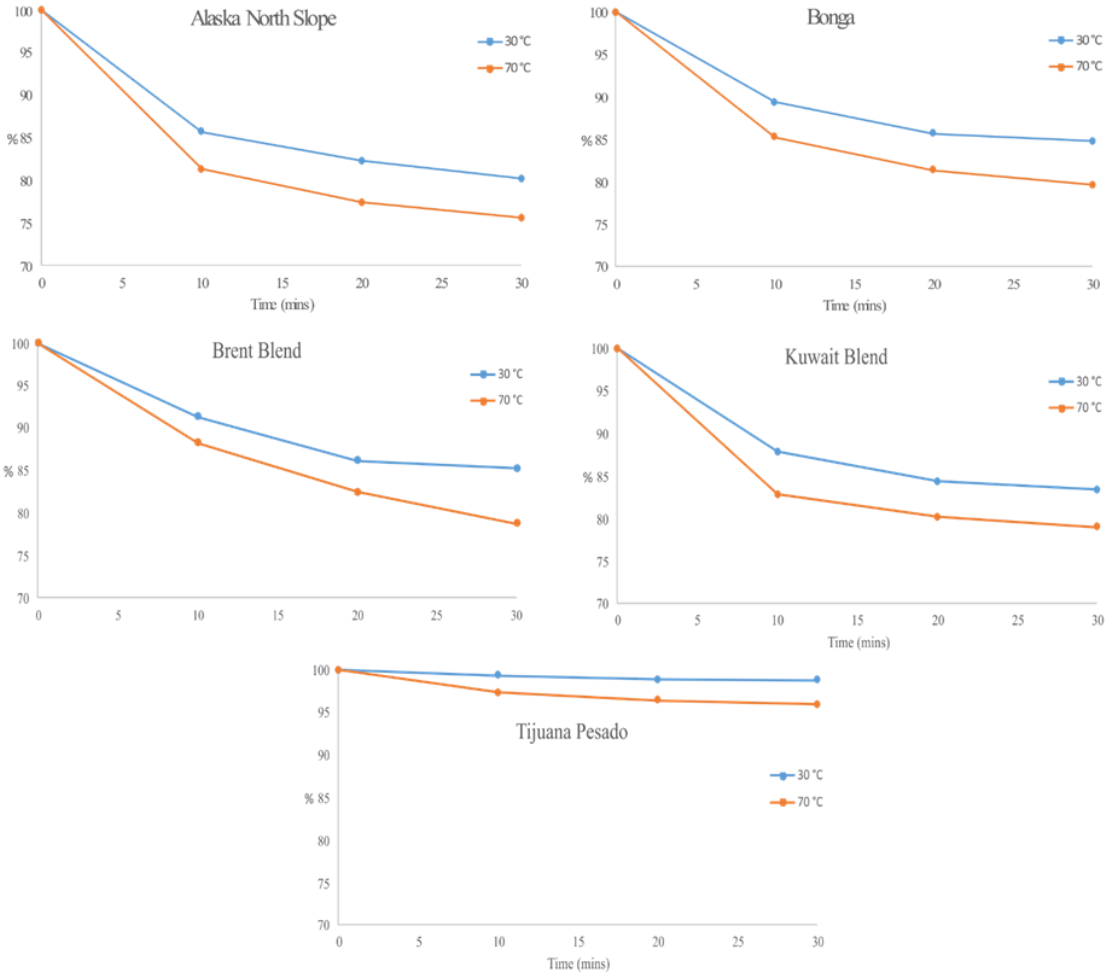

Appendix 2. Reduction in mass (%) of crude oils when ~0.5 g of crude oil was blown down under N_2 at 30 °C and 70 °C.

Appendix 3. Recovery of model compounds on separation by developed SPE procedure.

Model Compound	**Mean (**±rsd)	**Model Compound**	**Mean (**±rsd)
Dibenzofuran Carboxylic Acid	86.9 (±8.4%)	Dibenzothiophene	85.9 (±0.6%)
Adamantane Carboxylic Acid	102.1 (±1.0%)	Fluorenone	89.5 (±1.6%)
Benzoquinoline	97.8 (±81.6%)	Phenanthrene	95.8 (±0.9%)
4-pentylbicylco[2,2,2] octane 1- carboxylic acid	91.1 (±1.0%)	Carbazole	96.1 (±1.4%)
Fluoranthene	98.2 (±1.1%)	Xanthone	93.7(±1.3%)
Dibenzothiophene Carboxylic Acid	93.8 (±1.5%)	Nitroindole	72.2 (±3.6%)
Cholanic Acid	79.3 (±3.0%)	Benzyl Disulfide	108.9 (±7.3%)
Dibenzyl sulfoxide	79.9 (±11.2%)	Dibenzothiophene Sulfone	94.7 (±1.9%)
Phenyl Phenol	95.0 (±0.6%)	Benzo[a]pyrene	91.3(±0.5%)

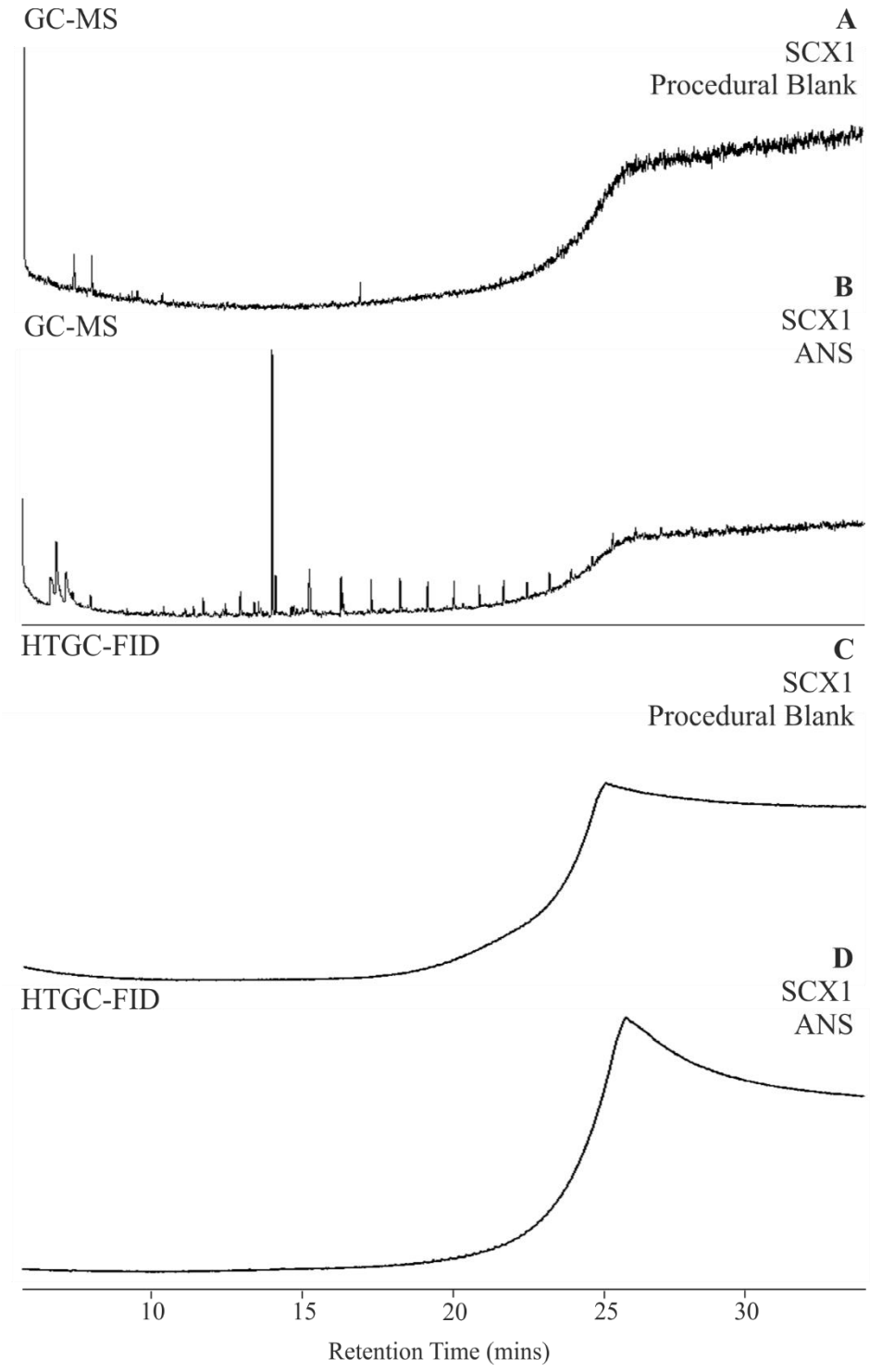

Appendix 4. GC-MS TICs and HTGC-FID chromatograms of the procedural blanks and analysis of SCX1 fractions from the SPE separation procedure.

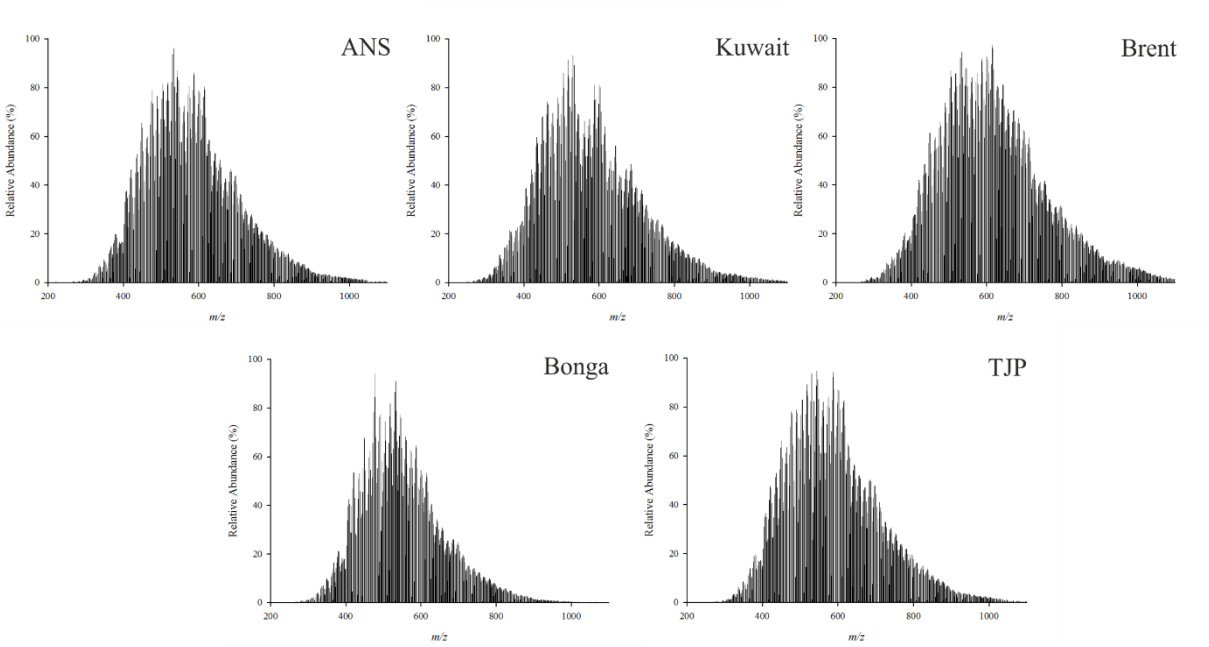

Appendix 5. FT-ICR-MS mass spectra obtained from the analysis of the SCX4 fractions of the ANS, Kuwait, Brent, Bonga and TJP crude oils.

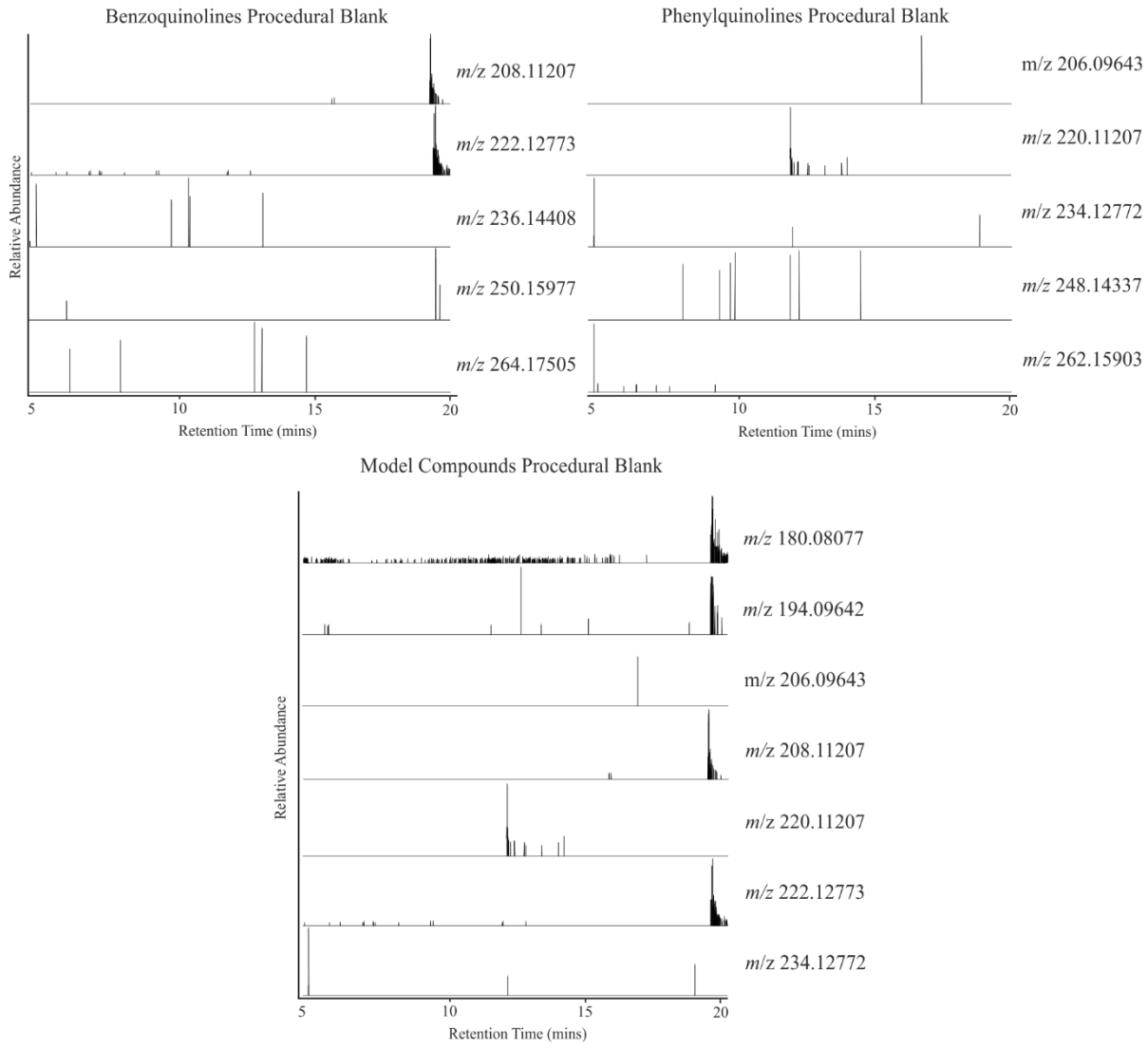

Appendix 6. LC-HRAM-MS EICs of the protonated adducts ($[M+H]^+$) of $C_{2\text{-}6}$ alkyl benzoquinoline homologues, of phenylquinoline and its $C_{1\text{-}4}$ alkylated homologues and the model quinoline compounds, from the analysis of the SCX4 procedural blank.

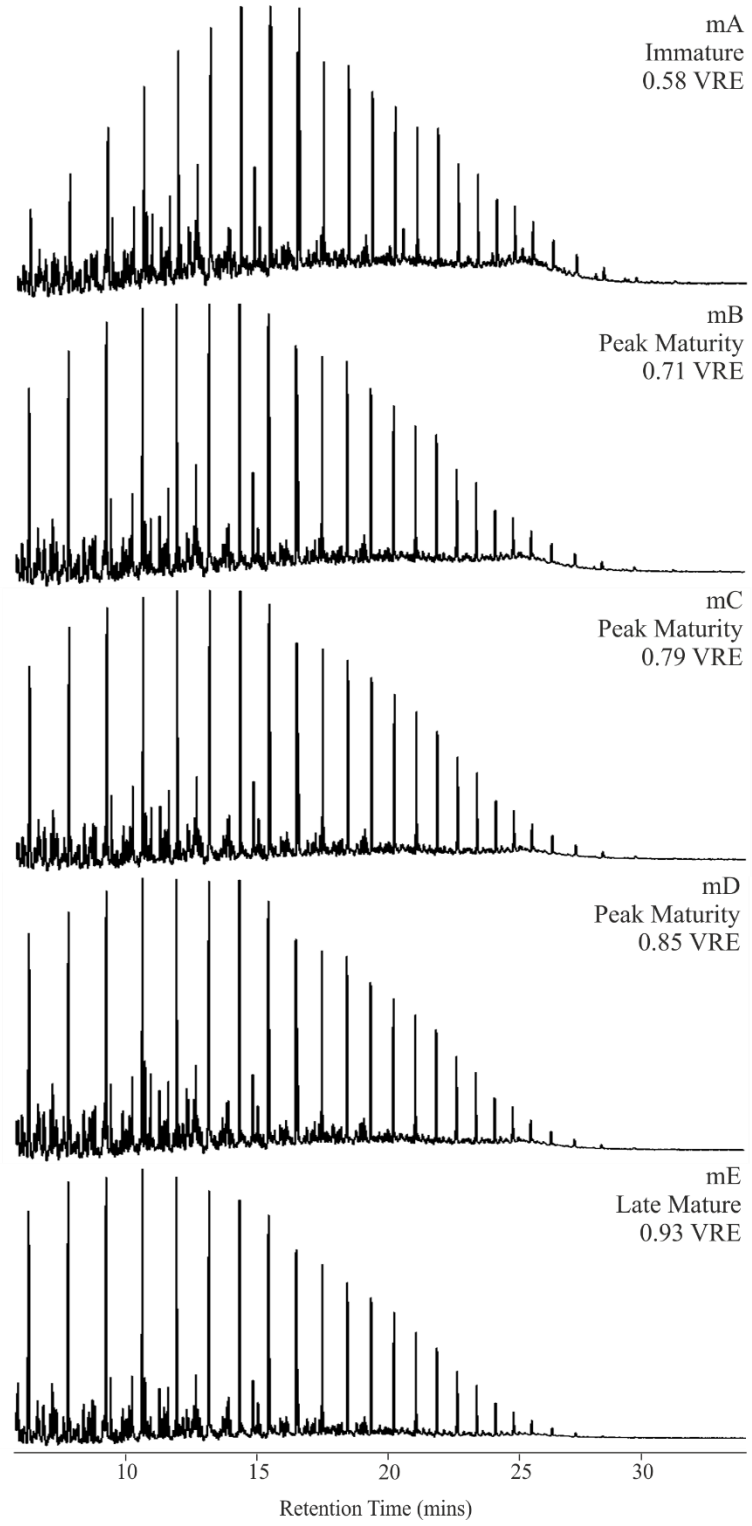

Appendix 7. GC-MS TICs of the whole oils of the maturity crude oil series.

References

Adam, F., Bertoncini, F., Brodusch, N., Durand, E., Thiebaut, D., Espinat, D. & Hennion, M. C. 2007. New benchmark for basic and neutral nitrogen compounds speciation in middle distillates using comprehensive two-dimensional gas chromatography. Journal of Chromatography A, 1148**,** 55-64.

Adams, J., Riediger, C., Fowler, M. & Larter, S. 2006. Thermal controls on biodegradation around the Peace River tar sands: Paleo-pasteurization to the west. Journal of Geochemical Exploration, 89**,** 1-4.

Adams, J. J. 2014. Asphaltene Adsorption, a Literature Review. Energy & Fuels, 28**,** 2831-2856.

Adams, J. J., Schabron, J. F. & Boysen, R. 2015. Quantitative Vacuum Distillation of Crude Oils to Give Residues Amenable to the Asphaltene Determinator Coupled with Saturates, Aromatics, and Resins Separation Characterization. Energy & Fuels, 29**,** 2774-2784.

Aitken, C. M., Head, I. M., Jones, D. M., Rowland, S. J., Scarlett, A. G. & West, C. E. 2017. Comprehensive two-dimensional gas chromatography-mass spectrometry of complex mixtures of anaerobic bacterial metabolites of petroleum hydrocarbons. Journal of Chromatography A**,** 96-109.

Aitken, C. M., Jones, D. M. & Larter, S. R. 2004. Anaerobic hydrocarbon biodegradation in deep subsurface oil reservoirs. Nature, 431**,** 291-4.

Akmaz, S., Iscan, O., Gurkaynak, M. A. & Yasar, M. 2011. The Structural Characterization of Saturate, Aromatic, Resin, and Asphaltene Fractions of Batiraman Crude Oil. Petroleum Science and Technology, 29**,** 160-171.

Alboudwarej, H., Felix, J., Taylor, S., Badry, R., Bremner, C., Brough, B., Skeates, C., Baker, A., Palmer, D., Pattison, K., Beshry, M., Krawchuk, P., Brown, G., Calvo, R., Triana, J. A. C., Hathcock, R., Koerner, K., Hughes, T., Kundu, D., de Cardenas, J. L. & West, C. 2006. Highlighting Heavy Oil. Oilfield Review, 18**,** 34-53.

Alexander, R., Kagi, R. I., Rowland, S. J., Sheppard, P. N. & Chirila, T. V. 1985. The effects of thermal maturity on distributions of dimethylnaphthalenes and trimethylnaphthalenes in some Ancient sediments and petroleums. Geochimica et Cosmochimica Acta, 49**,** 385-395.

Alexander, R., Kagi, R. I., Singh, R. K. & Sosrowidjojo, I. B. 1994. The effect of maturity on the relative abundances of cadalene and isocadalene in sediments from the Gippsland Basin, Australia. Organic Geochemistry, 21**,** 115-120.

Alhassan, A. & Andersson, J. T. 2013. Ketones in Fossil Materials—A Mass Spectrometric Analysis of a Crude Oil and a Coal Tar. Energy & Fuels, 27**,** 5770-5778.

Alvisi, P. P. & Lins, V. F. C. 2011. An overview of naphthenic acid corrosion in a vacuum distillation plant. Engineering Failure Analysis, 18**,** 1403-1406.

Andrade-Eiroa, A., Canle, M., Leroy-Cancellieri, V. & Cerdà, V. 2016a. Solid-phase extraction of organic compounds: A critical review (part i). Trends in Analytical Chemistry, 80**,** 641-654.

Andrade-Eiroa, A., Canle, M., Leroy-Cancellieri, V. & Cerdà, V. 2016b. Solid-phase extraction of organic compounds: A critical review (part ii). Trends in Analytical Chemistry, 80**,** 655-667.

API, T. 2011. Crude Oil Category; Category Assessment Document. American Petroleum Institute.

Arboleda, P. H., Dettman, H. D. & Lucy, C. A. 2015. Hydrocarbon Group Type Separation of Gas Oil Resins by High Performance Liquid Chromatography on Hyper-Cross-Linked Polystyrene Stationary Phase. Energy & Fuels, 29**,** 6686-6694.

Arends, P., Helboe, P. & Møller, J. 1973. Mass spectrometry of xanthones-I: The electron-impact-induced fragmentation of xanthone, monohydroxy- and monomethoxyxanthones. Organic Mass Spectrometry, 7**,** 667-681.

Argyle, M. & Bartholomew, C. 2015. Heterogeneous Catalyst Deactivation and Regeneration: A Review. Catalysts, 5**,** 145.

ASTM 2008. D2007-03, Standard Test Method for Characteristic Groups in Rubber Extender and Processing Oils and Other Petroleum-Derived Oils by the Clay-Gel Absorption Chromatographic Method. *ASTM International*.

ASTM 2009. D4124-09, Standard Test Method for Separation of Asphalt into Four Fractions. ASTM International.

Avila, B. M. F., Pereira, V. B., Gomes, A. O. & Azevedo, D. A. 2014. Speciation of organic sulfur compounds using comprehensive two-dimensional gas chromatography coupled to time-of-flight mass spectrometry: A powerful tool for petroleum refining. Fuel, 126**,** 188-193.

Bae, E., Na, J.-G., Chung, S. H., Kim, H. S. & Kim, S. 2010. Identification of about 30 000 Chemical Components in Shale Oils by Electrospray Ionization (ESI) and Atmospheric Pressure Photoionization (APPI) Coupled with 15 T Fourier Transform Ion Cyclotron Resonance Mass Spectrometry (FT-ICR MS) and a Comparison to Conventional Oil. Energy & Fuels, 24**,** 2563-2569.

Baker, E. W. & Louda, J. W. 1986. *Porphyrins in the geological record*, New York, Elsevier.

Bakr, M. M. Y. 2009. Occurance and Geochemical Significance of Carbazoles and Xanthones in Crude Oil from the Western Desert, Egypt. Journal of King Abdulaziz University; Earth Sciences, 20**,** 127-159.

Bao, J. & Zhu, C. 2009. The effects of biodegradation on the compositions of aromatic hydrocarbons and maturity indicators in biodegraded oils from Liaohe Basin. Science in China Series D: Earth Sciences, 52**,** 59-68.

Barakat, A. O., Baumgart, S., Brocks, P., Scholz-Bottcher, B. M. & Rullkotter, J. 2012. Alkylated phenol series in lacustrine black shales from the Nordlinger Ries, southern Germany. Journal of Mass Spectrometry, 47**,** 987-94.

Barakat, A. O. & Yen, T. F. 1990. Distribution of pentacyclic triterpenoids in Green River oil shale kerogen. Organic Geochemistry, 15**,** 299-311.

Barman Skaare, B., Wilkes, H., Vieth, A., Rein, E. & Barth, T. 2007. Alteration of crude oils from the Troll area by biodegradation: Analysis of oil and water samples. Organic Geochemistry, 38**,** 1865-1883.

Bastow, T. P., van Aarssen, B. G. K., Alexander, R. & Kagi, R. I. 2005. Origins of alkylphenols in crude oils: Hydroxylation of alkylbenzenes. Organic Geochemistry, 36**,** 991-1001.

Batts, B. D. & Fathoni, A. Z. 1991. A literature review on fuel stability studies with particular emphasis on diesel oil. Energy & Fuels, 5**,** 2-21.

Bauserman, J. W., Mushrush, G. W. & Hardy, D. R. 2008. Organic Nitrogen Compounds and Fuel Instability in Middle Distillate Fuels. Industrial & Engineering Chemistry Research, 47**,** 2867-2875.

Baxby, M., Patience, R. L. & Bartle, K. D. 1994. The Origin and Diagenesis of Sedimentary Organic Nitrogen. Journal of Petroleum Geology, 17**,** 211-230.

Bennett, B., Adams, J. J., Gray, N. D., Sherry, A., Oldenburg, T. B. P., Huang, H., Larter, S. R. & Head, I. M. 2013. The controls on the composition of biodegraded oils in the deep subsurface – Part 3. The impact of microorganism distribution on petroleum geochemical gradients in biodegraded petroleum reservoirs. Organic Geochemistry, 56**,** 94-105.

Bennett, B., Bowler, B. F. J. & Larter, S. R. 1996. Determination of C0−C3 Alkylphenols in Crude Oils and Waters. Analytical Chemistry, 68**,** 3697-3702.

Bennett, B., Chen, M., Brincat, D., Gelin, F. J. P. & Larter, S. R. 2002. Fractionation of benzocarbazoles between source rocks and petroleums. Organic Geochemistry, 33**,** 545-559.

Bennett, B., Lager, A., Potter, D. K., Buckman, J. O. & Larter, S. R. 2007a. Petroleum geochemical proxies for reservoir engineering parameters. Journal of Petroleum Science and Engineering, 58**,** 355-366.

Bennett, B. & Larter, S. R. 2000. The isolation, occurrence and origin of fluorenones in crude oils and rock extracts. Organic Geochemistry, 31**,** 117-125.

Bennett, B., Noke, K. J., Bowler, B. F. J. & Larter, S. R. 2007b. The accurate determination of C0–C3 alkylphenol concentrations in crude oils. International Journal of Environmental Analytical Chemistry, 87**,** 307-320.

Bester, K. & Theobald, N. 2000. Results of non target screening of lipophilic organic pollutants in the German Bight V: Xanthen-9-one. Water Research, 34**,** 2277-2282.

Beynon, J. H., Lester, G. R. & Williams, A. E. 1959. Some Specific Molecular Rearrangements in the Mass Spectra of Organic Compounds. The Journal of Physical Chemistry, 63**,** 1861-1868.

Bissada, K. K., Tan, J., Szymczyk, E., Darnell, M. & Mei, M. 2016a. Group-type characterization of crude oil and bitumen. Part I: Enhanced separation and quantification of saturates, aromatics, resins and asphaltenes (SARA). Organic Geochemistry, 95**,** 21-28.

Bissada, K. K., Tan, J., Szymezyk, E., Darnell, M. & Mei, M. 2016b. Group-type characterization of crude oil and bitumen. Part II: Efficient separation and quantification of normal-paraffins iso-paraffins and naphthenes (PIN). Fuel, 173**,** 217-221.

Boduszynski, M., Chadha, B. R. & Szkutapochopien, T. 1977. Investigations on Romashkino Asphaltic Bitumen .3. Fractionation of Asphaltenes Using Ion-Exchange Chromatography. Fuel, 56**,** 432-436.

Bollet, C., Escalier, J. C., Souteyrand, C., Caude, M. & Rosset, R. 1981. Rapid separation of heavy petroleum products by high-performance liquid chromatography. Journal of Chromatography A, 206**,** 289-300.

Borgund, A. E., Erstad, K. & Barth, T. 2007. Normal phase high performance liquid chromatography for fractionation of organic acid mixtures extracted from crude oils. Journal of Chromatography A, 1149**,** 189-196.

Bowie, J. H., Donaghue, P. F., Rodda, H. J. & Simons, B. K. 1968. Electron impact studies—XXIX: The C13H9 skeletal-rearrangement fragment in the mass spectra of heterocyclic systems containing diphenyl substituents. A Deuterium labelling study. Tetrahedron, 24**,** 3965-3979.

Bowman, D. T., Slater, G. F., Warren, L. A. & McCarry, B. E. 2014. Identification of individual thiophene-, indane-, tetralin-, cyclohexane-, and adamantane-type carboxylic acids in composite tailings pore water from Alberta oil sands. Rapid Communications in Mass Spectrometry, 28**,** 2075-2083.

Boysen, R. B. & Schabron, J. F. 2013. The Automated Asphaltene Determinator Coupled with Saturates, Aromatics, and Resins Separation for Petroleum Residua Characterization. Energy & Fuels, 27**,** 4654-4661.

Brassell, S. C., Eglinton, G. & Maxwell, J. R. 1983. The geochemistry of terpenoids and steroids. Biochemical Society Transactions, 11**,** 575-586.

Breysse, M., Djega-Mariadassou, G., Pessayre, S., Geantet, C., Vrinat, M., Pérot, G. & Lemaire, M. 2003. Deep desulfurization: reactions, catalysts and technological challenges. Catalysis Today, 84**,** 129-138.

Brooks, P. W. 1986. Unusual biological marker geochemistry of oils and possible source rocks, offshore Beaufort-Mackenzie Delta, Canada. Organic Geochemistry, 10**,** 401-406.

Brown, L. D. & Ulrich, A. C. 2015. Oil sands naphthenic acids: A review of properties, measurement, and treatment. Chemosphere, 127**,** 276-290.

Budzikiewicz, H., Djerassi, C. & Williams, D. H. 1967. *Mass spectrometry of organic compounds*, Holden-Day, 628-629.

Budzikiewicz, H., Wilson, J. M. & Djerassi, C. 1963. Mass Spectrometry in Structural and Stereochemical Problems. XXXII.1 Pentacyclic Triterpenes. Journal of the American Chemical Society, 85**,** 3688-3699.

Cappelli Fontanive, F., Souza-Silva, É. A., Macedo da Silva, J., Bastos Caramão, E. & Alcaraz Zini, C. 2016. Characterization of sulfur and nitrogen compounds in Brazilian petroleum derivatives using ionic liquid capillary columns in comprehensive two-dimensional gas chromatography with time-of-flight mass spectrometric detection. Journal of Chromatography A, 1461**,** 131-143.

Cassani, F., Gallango, O., Talukdar, S., Vallejos, C. & Ehrmann, U. 1988. Methylphenanthrene maturity index of marine source rock extracts and crude oils from the Maracaibo Basin. Organic Geochemistry, 13**,** 73-80.

Chacón-Patiño, M. L., Rowland, S. M. & Rodgers, R. P. 2018. Advances in Asphaltene Petroleomics. Part 2: Selective Separation Method That Reveals Fractions Enriched in Island and Archipelago Structural Motifs by Mass Spectrometry. Energy & Fuels, 32**,** 314-328.

Chapman, R. E. 1983. *Petroleum Geology*, Elsevier, 67-93.

Chen, X., Shen, B., Sun, J., Wang, C., Shan, H., Yang, C. & Li, C. 2012. Characterization and Comparison of Nitrogen Compounds in Hydrotreated and Untreated Shale Oil by Electrospray Ionization (ESI) Fourier Transform Ion Cyclotron Resonance Mass Spectrometry (FT-ICR MS). Energy & Fuels, 26**,** 1707-1714.

Chester, R. 1993. *Marine Geochemistry*, London, Chapman and Hall, 477-480.

Cho, Y. J., Na, J. G., Nho, N. S., Kim, S. & Kim, S. 2012. Application of Saturates, Aromatics, Resins, and Asphaltenes Crude Oil Fractionation for Detailed Chemical Characterization of Heavy Crude Oils by Fourier Transform Ion Cyclotron Resonance Mass Spectrometry Equipped with Atmospheric Pressure Photoionization. Energy & Fuels, 26**,** 2558-2565.

Clegg, H., Wilkes, H., Oldenburg, T., Santamaría-orozco, D. & Horsfield, B. 1998. Influence of maturity on carbazole and benzocarbazole distributions in crude oils and source rocks from the Sonda de Campeche, Gulf of Mexico. Organic Geochemistry, 29**,** 183-194.

Clingenpeel, A. C., Rowland, S. M., Corilo, Y. E., Zito, P. & Rodgers, R. P. 2017. Fractionation of Interfacial Material Reveals a Continuum of Acidic Species That Contribute to Stable Emulsion Formation. Energy & Fuels, 31**,** 5933-5939.

Comisarow, M. B. & Marshall, A. G. 1974. Fourier transform ion cyclotron resonance spectroscopy. Chemical Physics Letters, 25**,** 282-283.

Conceição Oliveira, E., Vaz de Campos, M. C. l., Sant'Ana Lopes, A., Rodrigues Vale, M. G. & Bastos Caramão, E. 2004. Ion-exchange resins in the isolation of nitrogen compounds from petroleum residues. Journal of Chromatography A, 1027**,** 171-177.

Connan, J. 1984. *Biodegradation of Crude Oils in Reservoirs*, 299-335.

da Silveira, G. D., Faccin, H., Claussen, L., Goularte, R. B., Do Nascimento, P. C., Bohrer, D., Cravo, M., Leite, L. F. M. & de Carvalho, L. M. 2016. A liquid chromatography atmospheric pressure photoionization tandem mass spectrometric method for the determination of organosulfur compounds in petroleum asphalt cements. Journal of Chromatography A, 1457**,** 29-40.

Dalmaschio, G. P., Malacarne, M. M., de Almeida, V. M. D. L., Pereira, T. M. C., Gomes, A. O., de Castro, E. V. R., Greco, S. J., Vaz, B. G. & Romao, W. 2014. Characterization of polar compounds in a true boiling point distillation system using electrospray ionization FT-ICR mass spectrometry. Fuel, 115**,** 190-202.

Davies, N. J. & Wolff, G. A. 1990. The Mersey oil spill, August, 1989 A case of sediments contaminating the oil? Marine Pollution Bulletin, 21**,** 481-484.

Deniau, I., Derenne, S., Beaucaire, C., Pitsch, H. & Largeau, C. 2001. Morphological and chemical features of a kerogen from the underground Mol laboratory (Boom Clay Formation, Oligocene, Belgium): structure, source organisms and formation pathways. Organic Geochemistry, 32**,** 1343-1356.

Derungs, W. A. 1956. Naphthenic Acid Corrosion —An Old Enemy Of the Petroleum Industry. Corrosion, 12**,** 41-46.

Dijkmans, T., Djokic, M. R., Van Geem, K. M. & Marin, G. B. 2015. Comprehensive compositional analysis of sulfur and nitrogen containing compounds in shale oil using GC × GC – FID/SCD/NCD/TOF-MS. Fuel, 140**,** 398-406.

Drushel, H. V. & Sommers, A. L. 1967. Isolation and characterization of sulfur compounds in high-boiling petroleum fractions. Analytical Chemistry, 39**,** 1819-1829.

Duan, Y. 2001. Pentacyclic triterpenoid ketones in peat from Gannan Marsh, China. Chinese Science Bulletin, 46**,** 1433-1435.

Dyer, S. J., Graham, G. M. & Arnott, C. 2003. Naphthenate Scale Formation - Examination of Molecular Controls in Idealised Systems. *International Symposium on Oilfield Scale.* Aberdeen: Society of Petroleum Engineers.

Edwards, M., Mostafa, A. & Gorecki, T. 2011. Modulation in comprehensive two-dimensional gas chromatography: 20 years of innovation. Analytical and Bioanalytical Chemistry, 401**,** 2335-2349.

EI 2001. IP 469, Determination of saturated, aromatic and polar compounds in petroleum products by thin layer chromatography and flame ionization detection.

Ensminger, A., Albrecht, P., Ourisson, G. & Tissot, B. P. 1977. Evolution of polycyclic alkanes under the effect of burial (Early Toarcian Shales, Paris Basin). *In:* Campos, R. & Goni, J. (eds.) *Advances in Organic Geochemistry.* Madrid: Enadimsa.

Evdokimov, I. N. 2005. Bifurcated correlations of the properties of crude oils with their asphaltene content. Fuel, 84**,** 13-28.

Faboya, O. L., Sonibare, O. O., Liao, Z., Ekundayo, O. & Tian, Y. 2014. Occurrence and Distribution of Carbazoles and Benzocarbazoles in Tertiary Niger Delta Source Rocks. Petroleum Science and Technology, 32**,** 2938-2952.

Fan, T., Wang, J. & Buckley, J. S. 2002. Evaluating Crude Oils by SARA Analysis. *SPE/DOE Improved Oil Recovery Symposium.* Tulsa: Society of Petroleum Engineers.

Fang, R., Wang, T. G., Li, M., Xiao, Z., Zhang, B., Huang, S., Shi, S., Wang, D. & Deng, W. 2016. Dibenzothiophenes and benzo[b]naphthothiophenes: Molecular markers for tracing oil filling pathways in the carbonate reservoir of the Tarim Basin, NW China. Organic Geochemistry, 91**,** 68-80.

Fernandez, P. & Bayona, J. M. 1992. Use of off-line gel permeation chromatography · normal-phase liquid chromatography for the determination of polycyclic aromatic compounds in environmental samples and standard reference materials (air particulate matter and marine sediment). Journal of Chromatography A, 625**,** 141-149.

Fisher, S. J., Alexander, R. & Kagi, R. I. O., G. A. 1998. Aromatic hydrocarbons as indicators of biodegradation in North Western Australian reservoirs. Petroleum Exploration Society of Australia Journal**,** 185-94.

Flynn, S. A., Butler, E. J. & Vance, I. 1996. Produced Water Composition, Toxicity, and Fate. *In:* Reed, M. & Johnsen, S. (eds.) *Produced Water 2: Environmental Issues and Mitigation Technologies.* Boston, MA: Springer US.

Franchina, F. A., Purcaro, G., Maimone, M., Tranchida, P. Q. & Mondello, L. 2016. Recent evolution of flow-modulation comprehensive gas chromatography within the context of mass spectrometry hyphenation. Chimica Oggi-Chemistry Today, 34**,** 6-10.

Frank, R. A., Kavanagh, R., Burnison, B. K., Headley, J. V., Peru, K. M., Van Der Kraak, G. & Solomon, K. R. 2006. Diethylaminoethyl-cellulose clean-up of a large volume naphthenic acid extract. Chemosphere, 64**,** 1346-1352.

Frolov, E. B. 1997. Liquid chromatography of petroleum carbazoles. Organic Geochemistry, 26**,** 43-47.

Frolov, Y. B., Smirnov, M. B., Vanyukova, N. A. & Sanin, P. I. 1989. Carbazoles of crude oil. Petroleum Chemistry: U.S.S.R, 29**,** 87-102.

Galya, L. G. & Suatoni, J. C. 1980. Rapid Sara Seprations by High Performance Liquid Chromatography. Journal of Liquid Chromatography, 3**,** 229-242.

Gaspar, A., Zellermann, E., Lababidi, S., Reece, J. & Schrader, W. 2012. Characterization of Saturates, Aromatics, Resins, and Asphaltenes Heavy Crude Oil Fractions by Atmospheric Pressure Laser Ionization Fourier Transform Ion Cyclotron Resonance Mass Spectrometry. Energy & Fuels, 26**,** 3481-3487.

George, S. C. & Jardine, D. R. 1994. Ketones in a Proterozoic dolerite sill. Organic Geochemistry, 21**,** 829-839.

Ghaste, M., Mistrik, R. & Shulaev, V. 2016. Applications of Fourier Transform Ion Cyclotron Resonance (FT-ICR) and Orbitrap Based High Resolution Mass Spectrometry in Metabolomics and Lipidomics. International Journal of Molecular Sciences, 17**,** 816-822.

Ghislain, T., Molnárné Guricza, L. & Schrader, W. 2017. Characterization of crude oil asphaltenes by coupling size-exclusion chromatography directly to an ultrahigh-resolution mass spectrometer. Rapid Communications in Mass Spectrometry, 31**,** 495-502.

Gieleciak, R., Hager, D. & Heshka, N. E. 2016. Application of a quantitative structure retention relationship approach for the prediction of the two-dimensional gas chromatography retention times of polycyclic aromatic sulfur heterocycle compounds. Journal of Chromatography A, 1437**,** 191-202.

Giraldo-Davila, D., Chacon-Patino, M. L., Orrego-Ruiz, J. A., Blanco-Tirado, C. & Combariza, M. Y. 2016. Improving compositional space accessibility in (+) APPI FT-ICR mass spectrometric analysis of crude oils by extrography and column chromatography fractionation. Fuel, 185**,** 45-58.

Goff, J. C. 1983. Hydrocarbon generation and migration from Jurassic source rocks in the E Shetland Basin and Viking Graben of the northern North Sea. Journal of the Geological Society, 140**,** 445-474.

Goossens, H., de Leeuw, J. W., Schenck, P. A. & Brassell, S. C. 1984. Tocopherols as likely precursors of pristane in ancient sediments and crude oils. Nature, 312**,** 440-442.

Grizzle, P. L. & Sablotny, D. M. 1986. Automated liquid chromatographic compound class group-type separation of crude oils and bitumens using chemically bonded silica-NH2. Analytical Chemistry, 58**,** 2389-2396.

Gutierrez Sama, S., Desprez, A., Krier, G., Lienemann, C. P., Barbier, J., Lobinski, R., Barrere-Mangote, C., Giusti, P. & Bouyssiere, B. 2016. Study of the Aggregation of Metal Complexes with Asphaltenes Using Gel Permeation Chromatography Inductively Coupled Plasma High-Resolution Mass Spectrometry. Energy and Fuels, 30**,** 6907-6912.

Hayes, P. C. & Anderson, S. D. 1986. Hydrocarbon group type analyzer system for the rapid determination of saturates, olefins, and aromatics in hydrocarbon distillate products. Analytical Chemistry, 58**,** 2384-2388.

Haynes, W. M. 2016. *CRC handbook of chemistry and physics,* Boca Raton, FL, CRC Press.

Head, I. M., Gray, N. D. & Larter, S. R. 2014. Life in the slow lane; biogeochemistry of biodegraded petroleum containing reservoirs and implications for energy recovery and carbon management. Front Microbiol, 5**,** 566.

Head, I. M., Jones, D. M. & Larter, S. R. 2003. Biological activity in the deep subsurface and the origin of heavy oil. Nature, 426**,** 344.

Headley, J. V., Peru, K. M. & Barrow, M. P. 2016. Advances in mass spectrometric characterization of naphthenic acids fraction compounds in oil sands environmental samples and crude oil—A review. Mass Spectrometry Reviews, 35**,** 311-328.

Holowenko, F., Mackinnon, M. D. & Fedorak, P. M. 2002. Characterization of naphthenic acids in oil sands wastewaters by gas chromatography-mass spectrometry. Water Research, 36**,** 2843-2855.

Horsfield, B., Clegg, H., Wilkes, H. & Santamaría-Orozco, D. 1998. Effect of maturity on carbazole distributions in petroleum systems: new insights from the Sonda de Campeche, Mexico, and Hils Syncline, Germany. Naturwissenschaften, 85**,** 233-237.

Horstad, I., Larter, S. R., Dypvik, H., Aagaard, P., Bjornvik, A. M., Johansen, P. E. & Eriksen, S. 1990. Degradation and maturity controls on oil-field petroleum column heterogeneity in the gullfaks field, norwegian north-sea. Organic Geochemistry, 16**,** 497-510.

Horstad, I., Larter, S. R. & Mills, N. 1992. A quantitative model of biological petroleum degradation within the Brent Group reservoir in the Gullfaks Field, Norwegian North Sea. Organic Geochemistry, 19**,** 107-117.

Hu, Q., Noll, R. J., Li, H., Makarov, A., Hardman, M. & Graham Cooks, R. 2005. The Orbitrap: a new mass spectrometer. J Mass Spectrom, 40**,** 430-43.

Huang, H., Bowler, B. F. J., Zhang, Z., Oldenburg, T. B. P. & Larter, S. R. 2003. Influence of biodegradation on carbazole and benzocarbazole distributions in oil columns from the Liaohe basin, NE China. Organic Geochemistry, 34**,** 951-969.

Huba, A. K., Huba, K. & Gardinali, P. R. 2016. Understanding the atmospheric pressure ionization of petroleum components: The effects of size, structure, and presence of heteroatoms. Science of the Total Environment, 568**,** 1018-1025.

Iida, T., Yoshii, E. & Kitatsuji, E. 1966. Identification of Normal Paraffins, Olefins, Ketones, and Nitriles from Colorado Shale Oil. Analytical Chemistry, 38**,** 1224-1227.

Ikonomou, M. G., Blades, A. T. & Kebarle, P. 1990. Investigations of the electrospray interface for liquid chromatography/mass spectrometry. Analytical Chemistry, 62**,** 957-967.

Ingram, L. L., Ellis, J., Crisp, P. T. & Cook, A. C. 1983. Comparative study of oil shales and shale oils from the Mahogany Zone, Green River Formation (U.S.A.) and Kerosene Creek Seam, Rundle Formation (Australia). Chemical Geology, 38**,** 185-212.

Institute, E. 2004. IP 143: Determination of asphaltenes (heptane insolubles) in crude petroleum and petroleum products. *IP Test Methods.* Energy Institute.

Islas-Flores, C. A., Buenrostro-Gonzalez, E. & Lira-Galeana, C. 2005. Comparisons between Open Column Chromatography and HPLC SARA Fractionations in Petroleum. Energy & Fuels, 19**,** 2080-2088.

Jacobs, R. P. W. M., Grant, R. O. H., Kwant, J., Marquenie, J. M. & Mentzer, E. 1992. The Composition of Produced Water from Shell Operated Oil and Gas Production in the North Sea. *In:* Ray, J. P. & Engelhardt, F. R. (eds.) *Produced Water: Technological/Environmental Issues and Solutions.* Boston, MA: Springer US.

James, K. H. 2000a. The venezuelan hydrocarbon habitat, part 1: Tectonics, structure, palaeogeography and source rocks. Journal of Petroleum Geology, 23**,** 5-53.

James, K. H. 2000b. The venezuelan hydrocarbon habitat, part 2: Hydrocarbon occurrences and generated-accumulated volumes. Journal of Petroleum Geology, 23**,** 133-164.

Jehuda, Y. 1988. Mass spectral fragmentation pathways in phthalate esters. A tandem mass spectrometric collision-induced dissociation study. Organic Mass Spectrometry, 23**,** 755-759.

Jenisch-Anton, A., Adam, P., Schaeffer, P. & Albrecht, P. 1999. Oxygen-containing subunits in sulfur-rich nonpolar macromolecules. Geochimica et Cosmochimica Acta, 63**,** 1059-1074.

Jewell, D. M., Albaugh, E. W., Davis, B. E. & Ruberto, R. G. 1974. Integration of Chromatographic and Spectroscopic Techniques for the Characterization of Residual Oils. Industrial & Engineering Chemistry Fundamentals, 13**,** 278-282.

Jewell, D. M., Weber, J. H., Bunger, J. W., Plancher, H. & Latham, D. R. 1972. Ion-Exchange, Coordination, and Adsorption Chromatographic Separation of Heavy-End Petroleum Distillates. Analytical Chemistry, 44**,** 1391-1404.

Ji-Zhou, D., Vorkink, W. P. & Lee, M. L. 1993. Origin of long-chain alkylcyclohexanes and alkylbenzenes in a coal-bed wax. Geochimica et Cosmochimica Acta, 57**,** 837-849.

Jin, P., Nesic, S. & Wolf, H. A. 2015. Analysis of corrosion scales formed on steel at high temperatures in hydrocarbons containing model naphthenic acids and sulfur compounds. Surface and Interface Analysis, 47**,** 454-465.

Jones, D. M., Head, I. M., Gray, N. D., Adams, J. J., Rowan, A. K., Aitken, C. M., Bennett, B., Huang, H., Brown, A., Bowler, B. F. J., Oldenburg, T., Erdmann, M. & Larter, S. R. 2008. Crude-oil biodegradation via methanogenesis in subsurface petroleum reservoirs. Nature, 451**,** 176.

Jones, D. M., Watson, J. S., Meredith, W., Chen, M. & Bennett, B. 2001. Determination of Naphthenic Acids in Crude Oils Using Nonaqueous Ion Exchange Solid-Phase Extraction. Analytical Chemistry, 73**,** 703-707.

Juyal, P., Mapolelo, M. M., Yen, A., Rodgers, R. P. & Allenson, S. J. 2015. Identification of Calcium Naphthenate Deposition in South American Oil Fields. Energy & Fuels, 29**,** 2342-2350.

Juyal, P., Yen, A. T., Rodgers, R. P., Allenson, S., Wang, J. & Creek, J. 2010. Compositional Variations between Precipitated and Organic Solid Deposition Control (OSDC) Asphaltenes and the Effect of Inhibitors on Deposition by Electrospray Ionization Fourier Transform Ion Cyclotron Resonance (FT-ICR) Mass Spectrometry. Energy & Fuels, 24**,** 2320-2326.

Kaminski, M., Kartanowicz, R. & Przyjazny, A. 2004. Application of high-performance liquid chromatography with ultraviolet diode array detection and refractive index detection to the determination of class composition and to the analysis of gasoline. Journal of Chromatography A, 1029**,** 77-85.

Karlsen, D. A. & Larter, S. R. 1991. Analysis of petroleum fractions by TLC-FID: applications to petroleum reservoir description. Organic Geochemistry, 17**,** 603-617.

Kaufman, R. L., Dashti, H., Kabir, C. S., Pederson, J. M., Moon, M. S., Quttainah, R. & Al-Wael, H. 2002. Characterizing the Greater Burgan Field: Use of Geochemistry and Oil Fingerprinting.

Kennicutt, M. C. 1988. The effect of biodegradation on crude oil bulk and molecular composition. Oil and Chemical Pollution, 4**,** 89-112.

Kharrat, A. M., Zacharia, J., Cherian, V. J. & Anyatonwu, A. 2007. Issues with comparing SARA methodologies. Energy & Fuels, 21**,** 3618-3621.

Killops, S. D. & Killops, V. J. 2005. *Introduction to organic geochemistry,* Malden, MA, Blackwell Pub., 30-37.

Kim, E., Cho, E., Moon, S., Park, J.-I. & Kim, S. 2016. Characterization of Petroleum Heavy Oil Fractions Prepared by Preparatory Liquid Chromatography with Thin-Layer

Chromatography, High-Resolution Mass Spectrometry, and Gas Chromatography with an Atomic Emission Detector. Energy & Fuels, 30**,** 2932-2940.

Kim, S., Stanford, L. A., Rodgers, R. P., Marshall, A. G., Walters, C. C., Qian, K., Wenger, L. M. & Mankiewicz, P. 2005. Microbial alteration of the acidic and neutral polar NSO compounds revealed by Fourier transform ion cyclotron resonance mass spectrometry. Organic Geochemistry, 36**,** 1117-1134.

Kingston, E. E., Eichholzer, J. V., Lyndon, P., Macleod, J. K. & Summons, R. E. 1988. An unexpected γ-hydrogen rearrangement in the mass spectra of di-ortho -substituted alkylbenzenes. Organic Mass Spectrometry, 23**,** 42-47.

Kirk, R. H. 1980. Statfjord Field- A North Sea Giant. *In:* Halbouty, M. T. (eds.) *Giant Oil and Gas Fields of the Decade.* American Association of Petroleum Geologists.

Knotnerus, J. 1957. The Chemical Constitution of the higher naphthenic acids. Journal of the Institute of Petrol, 43**,** 307-312.

Kong, J., Wei, X.-Y., Yan, H.-L., Li, Z.-K., Zhao, M.-X., Li, Y. & Zong, Z.-M. 2015. Analysis of extractable basic nitrogen compounds in Buliangou subbituminous coal by positive-ion ESI FT-ICR MS. Fuel, 159**,** 385-391.

Krumholz, L. R. 2000. Microbial communities in the deep subsurface. Hydrogeology Journal, 8**,** 4-10.

Lababidi, S., Panda, S. K., Andersson, J. T. & Schrader, W. 2013. Direct Coupling of Normal-Phase High-Performance Liquid Chromatography to Atmospheric Pressure Laser Ionization Fourier Transform Ion Cyclotron Resonance Mass Spectrometry for the Characterization of Crude Oil. Analytical Chemistry, 85**,** 9478-9485.

Lababidi, S. & Schrader, W. 2014. Online normal-phase high-performance liquid chromatography/Fourier transform ion cyclotron resonance mass spectrometry: Effects of different ionization methods on the characterization of highly complex crude oil mixtures. Rapid Communications in Mass Spectrometry, 28**,** 1345-1352.

Larter, S. R., Bowler, B. F. J., Li, M., Chen, M., Brincat, D., Bennett, B., Noke, K., Donohoe, P., Simmons, D., Kohnen, M., Allan, J., Telnaes, N. & Horstad, I. 1996. Molecular indicators of secondary oil migration distances. Nature, 383**,** 593-597.

Latham, D. R., Ferrin, C. R. & Ball, J. S. 1962. Identification of Fluorenones in Wilmington Petroleum by Gas-Liquid Chromatography and Spectrometry. Analytical Chemistry, 34**,** 311-313.

Leif, R. N. & Simoneit, B. R. T. 1995. Ketones in hydrothermal petroleums and sediment extracts from Guaymas Basin, Gulf of California. Organic Geochemistry, 23**,** 889-904.

Li, C., Fu, L., Stafford, J., Belosevic, M. & El-Din, M. G. 2017. The toxicity of oil sands process-affected water (OSPW): A critical review. Science of the Total Environment, 601**,** 1785-1802.

Li, M. & Ellis, G. S. 2015. Qualitative and Quantitative Analysis of Dibenzofuran, Alkyldibenzofurans, and Benzo[b]naphthofurans in Crude Oils and Source Rock Extracts. Energy & Fuels, 29**,** 1421-1430.

Li, M., Larter, S. R., Stoddart, D. & Bjoroey, M. 1992a. Liquid chromatographic separation schemes for pyrrole and pyridine nitrogen aromatic heterocycle fractions from crude oils suitable for rapid characterization of geochemical samples. Analytical Chemistry, 64**,** 1337-1344.

Li, M., Larter, S. R., Taylor, P., Jones, D. M., Bowler, B. & Bjorøy, M. 1995. Biomarkers or not biomarkers? A new hypothesis for the origin of pristane involving derivation from methyltrimethyltridecylchromans (MTTCs) formed during diagenesis from chlorophyll and alkylphenols. Organic Geochemistry, 23**,** 159-167.

Li, M., Wang, T.-G., Shi, S., Zhu, L. & Fang, R. 2014a. Oil maturity assessment using maturity indicators based on methylated dibenzothiophenes. Petroleum Science, 11**,** 234-246.

Li, M., Wang, T. G., Shi, S., Liu, K. & Ellis, G. S. 2014b. Benzo[b]naphthothiophenes and alkyl dibenzothiophenes: Molecular tracers for oil migration distances. Marine and Petroleum Geology, 57**,** 403-417.

Li, M., Wang, T. G., Simoneit, B. R. T., Shi, S., Zhang, L. & Yang, F. 2012. Qualitative and quantitative analysis of dibenzothiophene, its methylated homologues, and benzonaphthothiophenes in crude oils, coal, and sediment extracts. Journal of Chromatography A, 1233**,** 126-136.

Li, M., Yao, H., Stasiuk, L. D., Fowler, M. G. & Larter, S. R. 1997. Effect of maturity and petroleum expulsion on pyrrolic nitrogen compound yields and distributions in Duvernay Formation petroleum source rocks in central Alberta, Canada. Organic Geochemistry, 26**,** 731-744.

Li, M., Zhong, N., Shi, S., Zhu, L. & Tang, Y. 2013. The origin of trimethyldibenzothiophenes and their application as maturity indicators in sediments from the Liaohe Basin, East China. Fuel, 103**,** 299-307.

Li, M. W., Larter, S. R., Stoddart, D. & Bjoroy, M. 1992b. Liquid-Chromatographic Separation Schemes for Pyrrole and Pyridine Nitrogen Aromatic Heterocycle Fractions from Crude Oils Suitable for Rapid Characterization of Geochemical Samples. Analytical Chemistry, 64**,** 1337-1344.

Li, N., Ma, X. L., Zha, Q. F. & Song, C. S. 2010. Analysis and Comparison of Nitrogen Compounds in Different Liquid Hydrocarbon Streams Derived from Petroleum and Coal. Energy & Fuels, 24**,** 5539-5547.

Liao, Y., Geng, A. & Huang, H. 2009. The influence of biodegradation on resins and asphaltenes in the Liaohe Basin. Organic Geochemistry, 40**,** 312-320.

Lillis, P. G., King, J. D., Waden, A. & Pribil, M. J. 2002. Oil-Source Rock Correlation Studies, Central Brooks Range Foothills and National Petroleum Reserve, Alaska (NPRA). American Association of Petroleum Geologists Bulletin, 86**,** 1150.

Lillis, P. G., Peters, K. E. & Magoon, L. B. 2006. Oil Types of the Alaskan North Slope- A Progress Report. Geological Society of America Abstracts with Programs, 38**,** 86.

Liu, P., Shi, Q. A., Chung, K. H., Zhang, Y. H., Pan, N., Zhao, S. Q. & Xu, C. M. 2010a. Molecular Characterization of Sulfur Compounds in Venezuela Crude Oil and Its SARA Fractions by Electrospray Ionization Fourier Transform Ion Cyclotron Resonance Mass Spectrometry. Energy & Fuels, 24**,** 5089-5096.

Liu, P., Xu, C. M., Shi, Q. A., Pan, N., Zhang, Y. H., Zhao, S. Q. & Chung, K. H. 2010b. Characterization of Sulfide Compounds in Petroleum: Selective Oxidation Followed by Positive-Ion Electrospray Fourier Transform Ion Cyclotron Resonance Mass Spectrometry. Analytical Chemistry, 82**,** 6601-6606.

Lobodin, V. V., Robbins, W. K., Lu, J. & Rodgers, R. P. 2015. Separation and Characterization of Reactive and Non-Reactive Sulfur in Petroleum and Its Fractions. Energy & Fuels, 29**,** 6177-6186.

Lochte, H. L. & Littman, E. R. 1955. The Petroleum Acids and Bases.

López-Linares, F., Carbognani, L., González, M. F., Sosa-Stull, C., Figueras, M. & Pereira-Almao, P. 2006. Quinolin-65 and Violanthrone-79 as Model Molecules for the Kinetics of the Adsorption of C7 Athabasca Asphaltene on Macroporous Solid Surfaces. Energy & Fuels, 20**,** 2748-2750.

Lundanes, E. & Greibrokk, T. 1994. Separation of fuels, heavy fractions, and crude oils into compound classes: A review. Journal of High Resolution Chromatography, 17**,** 197-202.

Lutnaes, B. F., Brandal, O., Sjoblom, J. & Krane, J. 2006. Archaeal C80 isoprenoid tetraacids responsible for naphthenate deposition in crude oil processing. Organic Biomolecular Chemistry, 4**,** 616-20.

Lutnaes, B. F., Krane, J., Smith, B. E. & Rowland, S. J. 2007. Structure elucidation of C80, C81 and C82 isoprenoid tetraacids responsible for naphthenate deposition in crude oil production. Organic Biomolecular Chemistry, 5**,** 1873-7.

MacCrehan, W. A. & Brown-Thomas, J. M. 1987. Determination of phenols in petroleum crude oils using liquid chromatography with electrochemical detection. Analytical Chemistry, 59**,** 477-479.

MacGowan, D. B. & Surdam, R. C. 1988. Difunctional carboxylic acid anions in oilfield waters. Organic Geochemistry, 12**,** 245-259.

Machado, M. E., Bregles, L. P., de Menezes, E. W., Caramao, E. B., Benvenutti, E. V. & Zini, C. A. 2013. Comparison between pre-fractionation and fractionation process of heavy gas oil for determination of sulfur compounds using comprehensive two-dimensional gas chromatography. Journal of Chromatography A, 1274**,** 165-172.

Mackenzie, A. S., Beaumont, C. & McKenzie, D. P. 1984. Estimation of the kinetics of geochemical reactions with geophysical models of sedimentary basins and applications. Organic Geochemistry, 6**,** 875-884.

Makarov, A. 2000. Electrostatic Axially Harmonic Orbital Trapping: A High-Performance Technique of Mass Analysis. Analytical Chemistry, 72**,** 1156-1162.

Makarov, A., Denisov, E., Kholomeev, A., Balschun, W., Lange, O., Strupat, K. & Horning, S. 2006. Performance Evaluation of a Hybrid Linear Ion Trap/Orbitrap Mass Spectrometer. Analytical Chemistry, 78**,** 2113-2120.

Malkin, A. Y., Rodionova, G., Simon, S., Ilyin, S. O., Arinina, M. P., Kulichikhin, V. G. & Sjöblom, J. 2016. Some Compositional Viscosity Correlations for Crude Oils from Russia and Norway. Energy & Fuels, 30**,** 9322-9328.

Marshall, A. G., Hendrickson, C. L. & Jackson, G. S. 1998. Fourier transform ion cyclotron resonance mass spectrometry: A primer. Mass Spectrometry Reviews, 17**,** 1-35.

Marshall, A. G. & Rodgers, R. P. 2004. Petroleomics: The next grand challenge for chemical analysis. Accounts of Chemical Research, 37**,** 53-59.

Mayer, T. J. & Duswalt, J. M. 1973. Preparation and spectra of trimethylnaphthalene isomers. Journal of Chemical & Engineering Data, 18**,** 337-344.

McKay, J. F., Amend, P. J., Harnsberger, P. M., Cogswell, T. E. & Latham, D. R. 1976. Separation and analyses of petroleum residues. Abstracts of Papers of the American Chemical Society, 172**,** 53-53.

McKenna, A. M., Nelson, R. K., Reddy, C. M., Savory, J. J., Kaiser, N. K., Fitzsimmons, J. E., Marshall, A. G. & Rodgers, R. P. 2013. Expansion of the Analytical Window for Oil Spill Characterization by Ultrahigh Resolution Mass Spectrometry: Beyond Gas Chromatography. Environmental Science & Technology, 47**,** 7530-7539.

McLafferty, F. & Turecek, F. 1993. Interpretation of Mass Spectra.

Merdrignac, I., Behar, F., Albrecht, P., Briot, P. & Vandenbroucke, M. 1998. Quantitative Extraction of Nitrogen Compounds in Oils: Atomic Balance and Molecular Composition. Energy & Fuels, 12**,** 1342-1355.

Mills, G. A., Boedeker, E. R. & Oblad, A. G. 1950. Chemical Characterization of Catalysts. I. Poisoning of Cracking Catalysts by Nitrogen Compounds and Potassium Ion*. Journal of the American Chemical Society, 72**,** 1554-1560.

Moldowan, J. M., Sundararaman, P. & Schoell, M. 1986. Sensitivity of biomarker properties to depositional environment and/or source input in the Lower Toarcian of SW-Germany. Organic Geochemistry, 10**,** 915-926.

Molnárné Guricza, L. & Schrader, W. 2015a. Electrospray ionization for determination of non-polar polyaromatic hydrocarbons and polyaromatic heterocycles in heavy crude oil asphaltenes. Journal of Mass Spectrometry, 50**,** 549-557.

Molnárné Guricza, L. & Schrader, W. 2015b. New Separation Approach for Asphaltene Investigation: Argentation Chromatography Coupled with Ultrahigh-Resolution Mass Spectrometry. Energy & Fuels, 29**,** 6224-6230.

Mössner, S. G. & Wise, S. A. 1999. Determination of Polycyclic Aromatic Sulfur Heterocycles in Fossil Fuel-Related Samples. Analytical Chemistry, 71**,** 58-69.

Mullins, O. C. 2010. The Modified Yen Model. Energy & Fuels, 24**,** 2179-2207.

Nagy, B. & Colombo, U. 1967. *Fundamental aspects of petroleum geochemistry,* Amsterdam, London etc. Barking (Ex.), Elsevier, 1-37.

Neff, J., Lee, K. & DeBlois, E. M. 2011. Produced Water: Overview of Composition, Fates, and Effects. *In:* Lee, K. & Neff, J. (eds.) *Produced Water: Environmental Risks and Advances in Mitigation Technologies.* New York, NY: Springer New York.

Nelson, S. D. 2001. Structure Toxicity Relationships - How Useful Are They in Predicting Toxicities of New Drugs? *In:* Dansette, P. M., Snyder, R., Delaforge, M., Gibson, G. G., Greim, H., Jollow, D. J., Monks, T. J. & Sipes, I. G. (eds.) *Biological Reactive Intermediates VI: Chemical and Biological Mechanisms in Susceptibility to and Prevention of Environmental Diseases.* Boston, MA: Springer US.

Netzel, D. A. & Guffey, F. D. 1989. Nmr and gc/ms investigation of the saturate fractions from the cerro negro heavy petroleum crude. Energy & Fuels, 3**,** 455-460.

Nishioka, M. 1988. Aromatic sulfur compounds other than condensed thiophenes in fossil fuels: enrichment and identification. Energy & Fuels, 2**,** 214-219.

Niu, L. N., Liu, Z. L. & Tian, S. B. 2014. Identification and Characterization of Sulfur Compounds in Straight-Run Diesel Using Comprehensive Two-Dimensional GC Coupled with TOF MS. China Petroleum Processing & Petrochemical Technology, 16**,** 10-18.

Nordgård, E. L. k. & Sjöblom, J. 2008. Model Compounds for Asphaltenes and C80 Isoprenoid Tetraacids. Part I: Synthesis and Interfacial Activities. Journal of Dispersion Science and Technology, 29**,** 1114-1122.

Nytoft, H. P., Bojesen-Koefoed, J. A., Christiansen, F. G. & Fowler, M. G. 2002. Oleanane or lupane? Reappraisal of the presence of oleanane in Cretaceous–Tertiary oils and sediments. Organic Geochemistry, 33**,** 1225-1240.

Okuno, I., Latham, D. R. & Haines, W. E. 1967. Separation of sulfoxides from petroleum fractions by cation-exchange resin chromatography. Analytical Chemistry, 39**,** 1830-1833.

Oldenburg, T. B. P., Brown, M., Bennett, B. & Larter, S. R. 2014. The impact of thermal maturity level on the composition of crude oils, assessed using ultra-high resolution mass spectrometry. Organic Geochemistry, 75**,** 151-168.

Oldenburg, T. B. P., Larter, S. R. & Huang, H. 2007. Nitrogen isotope systematics of petroleum fractions of differing polarity - Neutral versus basic compounds. Organic Geochemistry, 38**,** 1789-1794.

Oldenburg, T. B. P., Wilkes, H., Horsfield, B., van Duin, A. C. T., Stoddart, D. & Wilhelms, A. 2002. Xanthones - novel aromatic oxygen-containing compounds in crude oils. Organic Geochemistry, 33**,** 595-609.

Oliveira, E. C., de Campos, M. C. V., Lopes, A. S., Vale, M. G. R. & Caramao, E. B. 2004. Ion-exchange resins in the isolation of nitrogen compounds from petroleum residues. Journal of Chromatography A, 1027**,** 171-177.

Olsen, J. V., Macek, B., Lange, O., Makarov, A., Horning, S. & Mann, M. 2007. Higher-energy C-trap dissociation for peptide modification analysis. Nature Methods, 4**,** 709-12.

Oriuma, V. O. 2015. *Markers of Crude Oil Migration Through Low-Maturity Organic-Rich Pathways.* Newcastle University.

Ostroukhov, S. B., Aref'yev, O. A., Zabrodina, M. N. & Petrov, A. A. 1983. C12−C30 petroleum alkylbenzenes with regular isoprenane chains. Petroleum Chemistry U.S.S.R., 23**,** 217-226.

Padula, L., Balestrin, L. B. d. S., Rocha, N. d. O., de Carvalho, C. H. M., Westfahl, H., Cardoso, M. B., Sabadini, E. & Loh, W. 2016. Role of Asphaltenes and Additives on the Viscosity and Microscopic Structure of Heavy Crude Oils. Energy & Fuels, 30**,** 3644-3651.

Panda, S. K., Schrader, W. & Andersson, J. T. 2008. Fourier transform ion cyclotron resonance mass spectrometry in the speciation of high molecular weight sulfur heterocycles in vacuum gas oils of different boiling ranges. Analytical and Bioanalytical Chemistry, 392**,** 839-848.

Panic, O. & Gorecki, T. 2006. Comprehensive two-dimensional gas chromatography (GCxGC) in environmental analysis and monitoring. Analytical and Bioanalytical Chemistry, 386**,** 1013-1023.

Payzant, J. D., Cyr, T. D., Montgomery, D. S. & Strausz, O. P. 1988. Studies on the Structure of the Terpenoid Sulfide Type Biological Markers in Petroleum. *In:* yen, T. F. & Moldowan, J. M. (eds.) *Geochemical Biomarkers.* Routledge.

Payzant, J. D., Montgomery, D. S. & Strausz, O. P. 1983. Novel Terpenoid Sulfoxides and Sulfides in Petroleum. Tetrahedron Letters, 24**,** 651-654.

Payzant, J. D., Montgomery, D. S. & Strausz, O. P. 1986. Sulfides in Petroleum. Organic Geochemistry, 9**,** 357-369.

Pereira, T. M. C., Vanini, G., Oliveira, E. C. S., Cardoso, F. M. R., Fleming, F. P., Neto, A. C., Lacerda, V., Castro, E. V. R., Vaz, B. G. & Romao, W. 2014a. An evaluation of the aromaticity of asphaltenes using atmospheric pressure photoionization Fourier transform ion cyclotron resonance mass spectrometry - APPI(+/-)FT-ICR MS. Fuel, 118**,** 348-357.

Pereira, T. M. C., Vanini, G., Tose, L. V., Cardoso, F. M. R., Fleming, F. P., Rosa, P. T. V., Thompson, C. J., Castro, E. V. R., Vaz, B. G. & Romao, W. 2014b. FT-ICR MS analysis of asphaltenes: Asphaltenes go in, fullerenes come out. Fuel, 131**,** 49-58.

Peters, K. E. & Moldowan, J. M. 1991. Effects of source, thermal maturity, and biodegradation on the distribution and isomerization of homohopanes in petroleum. Organic Geochemistry, 17**,** 47-61.

Peters, K. E., Moldowan, J. M., McCaffrey, M. A. & Fago, F. J. 1996. Selective biodegradation of extended hopanes to 25-norhopanes in petroleum reservoirs. Insights from molecular mechanics. Organic Geochemistry, 24**,** 765-783.

Peters, K. E., Moldowan, J. M., Schoell, M. & Hempkins, W. B. 1986. Petroleum isotopic and biomarker composition related to source rock organic-matter and depositional environment. Organic Geochemistry, 10**,** 17-27.

Peters, K. E., Walters, C. C. & Modwowan, J., M, 2005. *The Biomarker Guide*, Cambridge, Cambridge.

Philp, R. P., Oung, J. N., Yu, C. P. & Lewis, S. 1990. The determination of biomarker distributions by tandem mass-spectrometry. Organic Geochemistry, 16**,** 1211-1220.

Pinkston, D. S., Duan, P., Gallardo, V. A., Habicht, S. C., Tan, X. L., Qian, K. N., Gray, M., Mullen, K. & Kenttamaa, H. I. 2009. Analysis of Asphaltenes and Asphaltene Model Compounds by Laser-Induced Acoustic Desorption/Fourier Transform Ion Cyclotron Resonance Mass Spectrometry. Energy & Fuels, 23**,** 5564-5570.

Pluskal, T., Castillo, S., Villar-Briones, A. & Orešič, M. 2010. MZmine 2: Modular framework for processing, visualizing, and analyzing mass spectrometry-based molecular profile data. Bioinformatics, 11**,** 395.

Porter, Q. N. & Baldas, J. 1970. *Mass Spectrometry of Heterocyclic Compounds*, John Wiley & Sons.

Purcell, J. M., Juyal, P., Kim, D.-G., Rodgers, R. P., Hendrickson, C. L. & Marshall, A. G. 2007. Sulfur Speciation in Petroleum: Atmospheric Pressure Photoionization or Chemical Derivatization and Electrospray Ionization Fourier Transform Ion Cyclotron Resonance Mass Spectrometry. Energy & Fuels, 21**,** 2869-2874.

Purcell, J. M., Merdrignac, I., Rodgers, R. P., Marshall, A. G., Gauthier, T. & Guibard, I. 2010. Stepwise Structural Characterization of Asphaltenes during Deep Hydroconversion Processes Determined by Atmospheric Pressure Photoionization (APPI) Fourier Transform Ion Cyclotron Resonance (FT-ICR) Mass Spectrometry. Energy & Fuels, 24**,** 2257-2265.

Pursch, M., Sun, K., Winniford, B., Cortes, H., Weber, A., McCabe, T. & Luong, J. 2002. Modulation techniques and applications in comprehensive two-dimensional gas chromatography (GCxGC). Analytical and Bioanalytical Chemistry, 373**,** 356-367.

Qian, K. N., Robbins, W. K., Hughey, C. A., Cooper, H. J., Rodgers, R. P. & Marshall, A. G. 2001. Resolution and identification of elemental compositions for more than 3000 crude acids in heavy petroleum by negative-ion microelectrospray high-field Fourier transform ion cyclotron resonance mass spectrometry. Energy & Fuels, 15**,** 1505-1511.

Radke, M. 1988. Application of aromatic compounds as maturity indicators in source rocks and crude oils. Marine and Petroleum Geology, 5**,** 224-236.

Radke, M. & Welte, D. H. 1983. The methylphenanthrene index (MPI). A maturity parameter based on aromatic hydrocarbons. *In:* Bjoroy, M., Albrecht, P. & Cornford, C. (eds.) *Advances in Organic Geochemistry.* New York: Joohn Wiley & Sons.

Radke, M., Welte, D. H. & Willsch, H. 1982a. Geochemical study on a well in the Western Canada Basin: relation of the aromatic distribution pattern to maturity of organic matter. Geochimica et Cosmochimica Acta, 46**,** 1-10.

Radke, M., Willsch, H., Leythaeuser, D. & Teichmüller, M. 1982b. Aromatic components of coal: relation of distribution pattern to rank. Geochimica et Cosmochimica Acta, 46**,** 1831-1848.

Reid, A. M., Brougham, C. A., Fogarty, A. M. & Roche, J. J. 2007. An investigation into possible sources of phthalate contamination in the environmental analytical laboratory. International Journal of Environmental Analytical Chemistry, 87**,** 125-133.

Riboulleau, A., Derenne, S., Largeau, C. & Baudin, F. 2001. Origin of contrasting features and preservation pathways in kerogens from the Kashpir oil shales (Upper Jurassic, Russian Platform). Organic Geochemistry, 32**,** 647-665.

Riboulleau, A., Derenne, S., Sarret, G., Largeau, C., Baudin, F. & Connan, J. 2000. Pyrolytic and spectroscopic study of a sulphur-rich kerogen from the "Kashpir oil shales" (Upper Jurassic, Russian platform). Organic Geochemistry, 31**,** 1641-1661.

Robson, W. J., Sutton, P. A., McCormack, P., Chilcott, N. P. & Rowland, S. J. 2017. Class Type Separation of the Polar and Apolar Components of Petroleum. Analytical Chemistry, 89**,** 2919-2927.

Roddy, J. W. & Coleman, C. F. 1968. Solubility of water in hydrocarbons as a function of water activity. Talanta, 15**,** 1281-1286.

Rodgers, R. & Marshall, A. 2007. Petroleomics: Advanced Characterization of Petroleum-Derived Materials by Fourier Transform Ion Cyclotron Resonance Mass Spectrometry (FT-ICR MS). *In:* Mullins, O., Sheu, E., Hammami, A. & Marshall, A. (eds.) *Asphaltenes, Heavy Oils, and Petroleomics.* Springer New York.

Rodgers, R. P., White, F. M., Hendrickson, C. L., Marshall, A. G. & Andersen, K. V. 1998. Resolution, Elemental Composition, and Simultaneous Monitoring by Fourier Transform Ion Cyclotron Resonance Mass Spectrometry of Organosulfur Species before and after Diesel Fuel Processing. Analytical Chemistry, 70**,** 4743-4750.

Rowland, S., Scarlett, A. G., Jones, D., West, C. E. & Frank, R. A. 2011a. Diamonds in the Rough: Identification of Individual Naphthenic Acids in Oil Sands Process Water. Envrionmental Science & Technology.

Rowland, S. J., Alexander, R. & Kagi, R. I. 1984. Analysis of trimethylnaphthalenes in petroleum by capillary gas chromatography. Journal of Chromatography A, 294**,** 407-412.

Rowland, S. J., Alexander, R., Kagi, R. I. & Jones, D. M. 1986. Microbial degradation of aromatic components of crude oils: A comparison of laboratory and field observations. Organic Geochemistry, 9**,** 153-161.

Rowland, S. J., West, C. E., Jones, D., Scarlett, A. G., Frank, R. A. & Hewitt, L. M. 2011b. Steroidal aromatic 'naphthenic acids' in oil sands process-affected water: structural comparisons with environmental estrogens. Environmental Science & Technology, 45**,** 9806-15.

Rowland, S. J., West, C. E., Scarlett, A. G. & Jones, D. 2011c. Identification of individual acids in a commercial sample of naphthenic acids from petroleum by two-dimensional comprehensive gas chromatography/mass spectrometry. Rapid communications in mass spectrometry, 25**,** 1741-51.

Rowland, S. J., West, C. E., Scarlett, A. G., Jones, D. & Frank, R. A. 2011d. Identification of individual tetra- and pentacyclic naphthenic acids in oil sands process water by comprehensive two-dimensional gas chromatography/mass spectrometry. Rapid communications in mass spectrometry, 25**,** 1198-204.

Rowland, S. M., Robbins, W. K., Corilo, Y. E., Marshall, A. G. & Rodgers, R. P. 2014. Solid-Phase Extraction Fractionation To Extend the Characterization of Naphthenic Acids in Crude Oil by Electrospray Ionization Fourier Transform Ion Cyclotron Resonance Mass Spectrometry. Energy & Fuels, 28**,** 5043-5048.

Rowley, H. H. & Reed, W. R. 1951. Solubility of Water in Diethyl Ether at 25°. Journal of the American Chemical Society, 73**,** 2960-2960.

Rueter, P., Rabus, R., Wilkest, H., Aeckersberg, F., Rainey, F. A., Jannasch, H. W. & Widdel, F. 1994. Anaerobic oxidation of hydrocarbons in crude oil by new types of sulphate-reducing bacteria. Nature, 372**,** 455.

Ruiz-Guerrero, R., Vendeuvre, C., Thiébaut, D., Bertoncini, F. & Espinat, D. 2006. Comparison of Comprehensive Two-Dimensional Gas Chromatography Coupled with Sulfur-Chemiluminescence Detector to Standard Methods for Speciation of Sulfur-Containing Compounds in Middle Distillates. Journal of Chromatographic Science, 44**,** 566-573.

Rullkötter, J., Mackenzie, A. S., Welte, D. H., Leythaeuser, D. & Radke, M. 1984. Quantitative gas chromatography — mass spectrometry analysis of geological samples. Organic Geochemistry, 6**,** 817-827.

Scherzer, J. & Mcarthur, D. P. 1986. Tests Show Effects of Nitrogen-Compounds on Commercial Fluid Cat Cracking Catalysts. Oil & Gas Journal, 84**,** 76-84.

Schmitter, J. M., Ignatiadis, I., Arpino, P. & Guiochon, G. 1983. Selective isolation of nitrogen bases from petroleum. Analytical Chemistry, 55**,** 1685-1688.

Schulze, M., Scherer, A., Hampel, F., Stryker, J. M. & Tykwinski, R. R. 2016. Synthesis and Aggregation Behavior of Chiral Naphthoquinoline Petroporphyrin Asphaltene Model Compounds. Chemistry, 22**,** 3378-3386.

Sedivy, R. A., Penfield, I. E., Halpern, H. I., Drozd, R. J., Cole, G. A. & Burwood, R. 1987. *Investigation of source rock-crude oil relationships in the northern Alaska hydrocarbon habitat*, Society of Economic Paleontologists and Mineralogists and Alaska Geological Society, 169-179.

Seifert, W. K. & Michael Moldowan, J. 1978. Applications of steranes, terpanes and monoaromatics to the maturation, migration and source of crude oils. Geochimica et Cosmochimica Acta, 42**,** 77-95.

Seifert, W. K., Michael Moldowan, J. & Demaison, G. J. 1984. Source correlation of biodegraded oils. Organic Geochemistry, 6**,** 633-643.

Seifert, W. K. & Moldowan, J. M. 1986. Use of biological markers in petroleum exploration. *In:* Johns, R. B. (eds.) *Methods in Geochemistry and Physics.* Stroudsburg: Dowden, Hutchinson and Ross.

Seizo, T. & Shigeru, O. 1972. Effect of Ring Size on the Mass Spectral Fragmentation of Cyclic Sulfoxides. Bulletin of the Chemical Society of Japan, 45**,** 1767-1772.

Sharipov, A. K. 1988. Production of concentrates of sulphoxides and sulphones from petroleum crude oil (review). Petroleum Chemistry U.S.S.R., 28**,** 213-227.

Shell. 2017. *Brent Field Decomissioning* [Online]. Available: http://www.shell.co.uk/sustainability/decommissioning/brent-field-decommissioning.html [Accessed 10/11/2017].

Silva, R. C., Radović, J. R., Ahmed, F., Ehrmann, U., Brown, M., Carbognani Ortega, L., Larter, S., Pereira-Almao, P. & Oldenburg, T. B. P. 2016. Characterization of Acid-Soluble Oxidized Asphaltenes by Fourier Transform Ion Cyclotron Resonance Mass Spectrometry: Insights on Oxycracking Processes and Asphaltene Structural Features. Energy & Fuels, 30**,** 171-179.

Simon, S., Nenningsland, A. L., Herschbach, E. & Sjöblom, J. 2010. Extraction of Basic Components from Petroleum Crude Oil. Energy & Fuels, 24**,** 1043-1050.

Singh, D., Chopra, A., Patel, M. B. & Sarpal, A. S. 2011. A Comparative Evaluation of Nitrogen Compounds in Petroleum Distillates. Chromatographia, 74**,** 121-126.

Sinninghe Damsté, J. S., Leeuw, J. W. d. & Gelin, F. 1995. Selective preservation of organic matter in the marine environment: where are we? Organic Geochemistry: Developments and Applications to Energy, Climate, Environment and Human History**,** 814-820.

Slavcheva, E., Shone, B. & Turnbull, A. 1999. Review of naphthenic acid corrosion in oil refining. British Corrosion Journal, 34**,** 125-131.

Smith, B. E., Sutton, P. A., Lewis, C. A., Dunsmore, B., Fowler, G., Krane, J., Lutnaes, B. F., Brandal, O., Sjoblom, J. & Rowland, S. J. 2007. Analysis of 'ARN' naphthenic acids by high temperature gas chromatography and high performance liquid chromatography. J Sep Sci, 30**,** 375-80.

Snyder, L. R. 1961a. Applications of Linear Elution Adsorption Chromatography to the Separation and Analysis of Petroleum. I. Compound Class Separations over Alumina and Silica. Analytical Chemistry, 33**,** 1527-1534.

Snyder, L. R. 1961b. Applications of Linear Elution Adsorption Chromatography to the Separation and Analysis of Petroleum. III. Routine Determination of Certain Sulfur Types. Analytical Chemistry, 33**,** 1538-1543.

Snyder, L. R. 1968. *Principles of Adsorption Chromatography: The Separation of Nonionic Organic Compounds*, Marcel Dekker, Inc.

Snyder, L. R. & Buell, B. E. 1968. Nitrogen and oxygen compound types in petroleum. A general separation scheme. Analytical Chemistry, 40**,** 1295-1302.

Snyder, L. R., Buell, B. E. & Howard, H. E. 1968. Nitrogen and oxygen compound types in petroleum. Total analysis of a 700-850.deg.F. distillate from a California crude oil. Analytical Chemistry, 40**,** 1303-1317.

Somogyvari, A., Zanzotto, L., Sieben, D. & Auger, J. 1988. The aliphatic sulphide sulphur content of some Western Canadian crudes, their distillates and residues. Fuel, 67**,** 1269-1272.

Sonibare, O., Alimi, H., Jarvie, D. & Ehinola, O. A. 2008. Origin and occurrence of crude oil in the Niger delta, Nigeria. Journal of Petroleum Science and Engineering, 61**,** 99-107.

Sorensen, L., Silva, M. S., Booth, A. M. & Meier, S. 2016. Optimization and comparison of miniaturized extraction techniques for PAHs from crude oil exposed Atlantic cod and haddock eggs. Analytical and Bioanalytical Chemistry, 408**,** 1023-1032.

Sosrowidjojo, I. B., Murray, A. P., Alexander, R., Kagi, R. I. & Summons, R. E. 1996. Bicadinanes and related compounds as maturity indicators for oils and sediments. Organic Geochemistry, 24**,** 43-55.

Stalling, D. L., Gehrke, C. W. & Zumwalt, R. W. 1968. A new silylation reagent for amino acids bis (trimethylsilyl)trifluoroacetamide (BSTFA). Biochemical and Biophysical Research Communications, 31**,** 616-622.

Strachan, M. G., Alexander, R. & Kagi, R. I. 1988. Trimethylnaphthalenes in crude oils and sediments: Effects of source and maturity. Geochimica et Cosmochimica Acta, 52**,** 1255-1264.

Strandell, M., Zakrisson, S., Alsberg, T., Westerholm, R., Winquist, L. & Rannug, U. 1994. Chemical analysis and biological testing of a polar fraction of ambient air, diesel engine, and gasoline engine particulate extracts. Environ Health Perspect, 102**,** 85-92.

Strausz, O. P., Lown, E. M., Morales-Izquierdo, A., Kazmi, N., Montgomery, D. S., Payzant, J. D. & Murgich, J. 2011. Chemical Composition of Athabasca Bitumen: The Distillable Aromatic Fraction. Energy & Fuels, 25**,** 4552-4579.

Strelnikova, E. B. & Serebrennikova, O. V. 2011. Ketones of western siberian Jurassic oils. Petroleum Chemistry, 51**,** 264.

Strohmenger, C. J., Weber, L. J., Ghani, A., Al-Mehsin, K., Al-Jeelani, O., Al-Mansoori, A., Al-Dayyani, T., Vaughan, L., Khan, S. A. & Mitchell, J. C. 2006. *High-resolution Sequence Stratigraphy and Reservoir Charactersiation of Upper Thamama (Lower Cretaceous) Reservoirs of a Giant Abu Dhabi Oil Field, United Arab Emirates*, Association of American Petroleum Geologists.

Suatoni, J. C. & Swab, R. E. 1975. Rapid Hydrocarbon Group-Type Analysis by High Performance Liquid Chromatography. Journal of Chromatographic Science, 13**,** 361-366.

Subramanian, S., Simon, S. & Sjöblom, J. 2016. Asphaltene Precipitation Models: A Review. Journal of Dispersion Science and Technology, 37**,** 1027-1049.

Sundararaman, P., Biggs, W. R., Reynolds, J. G. & Fetzer, J. C. 1988. Vanadylporphyrins, indicators of kerogen breakdown and generation of petroleum. Geochimica et Cosmochimica Acta, 52**,** 2337-2341.

Sutton, P. A. & Rowland, S. J. 2014. Determination of the Content of C80 Tetraacids in Petroleum. Energy & Fuels, 28**,** 5657-5669.

Sutton, P. A., Smith, B. E. & Rowland, S. J. 2010. Mass spectrometry of polycyclic tetracarboxylic ('ARN') acids and tetramethyl esters. Rapid Communications in Mass Spectrometry, 24**,** 3195-3204.

Svalova, A., Parker, N. G., Povey, M. J. W. & Abbott, G. D. 2017. Determination of Asphaltene Critical Nanoaggregate Concentration Region Using Ultrasound Velocity Measurements. Scientific Reports, 7**,** 16125.

Taylor, P., Bennett, B., Jones, M. & Larter, S. 2001. The effect of biodegradation and water washing on the occurrence of alkylphenols in crude oils. Organic Geochemistry, 32**,** 341-358.

Terken, J. M. J., Frewin, N. L. & Indrelid, S. L. 2001. Petroleum systems of Oman: Charge timing and risks American Association of Petroleum Geologists Bulletin, 85**,** 1817-45.

Theobald, N. 1988. Rapid preliminary separation of petroleum hydrocarbons by solid-phase extraction cartridges. Analytica Chimica Acta, 204**,** 135-144.

Thiäner, J. B. & Achten, C. 2017. Liquid chromatography–atmospheric pressure laser ionization–mass spectrometry (LC-APLI-MS) analysis of polycyclic aromatic hydrocarbons with 6–8 rings in the environment. Analytical and Bioanalytical Chemistry, 409**,** 1737-1747.

Thomson, J. S., Green, J. B. & McWilliams, T. B. 1997. Determination of Sulfides and Thiols in Petroleum Distillates Using Solid-Phase Extraction and Derivatization with Pentafluorobenzoyl Chloride. Energy & Fuels, 11**,** 909-914.

Thorn, K. A. & Aiken, G. R. 1998. Biodegradation of crude oil into nonvolatile organic acids in a contaminated aquifer near Bemidji, Minnesota. Organic Geochemistry, 29**,** 909-931.

Tissot, B. P. & Welte, D. H. 1984. Petroleum Formation and Occurrence. 3-13, 69-73, 382-403.

Tomasek, P. H. & Crawford, R. L. 1986. Initial reactions of xanthone biodegradation by an Arthrobacter sp. J Bacteriol, 167**,** 818-27.

Trolio, R., Grice, K., Fisher, S. J., Alexander, R. & Kagi, R. I. 1999. Alkylbiphenyls and alkyldiphenylmethanes as indicators of petroleum biodegradation. Organic Geochemistry, 30**,** 1241-1253.

Turnbull, A., Slavcheva, E. & Shone, B. 1998. Factors controlling naphthenic acid corrosion. Corrosion, 54**,** 922-930.

Tuttle, M. L. W., Charpentier, R. R. & Brownfield, M. E. 1999. The Niger Delta Petroleum System: Niger Delta Province, Nigeria, Cameroon, and Equatorial Guinea, Africa.

Ugochukwu, U. C., Jones, M. D., Head, I. M., Manning, D. A. C. & Fialips, C. I. 2013. Compositional changes of crude oil SARA fractions due to biodegradation and adsorption on colloidal support such as clays using Iatroscan. Environmental Science and Pollution Research, 20**,** 6445-6454.

van Aarssen, B. G. K., Bastow, T. P., Alexander, R. & Kagi, R. I. 1999. Distributions of methylated naphthalenes in crude oils: indicators of maturity, biodegradation and mixing. Organic Geochemistry, 30**,** 1213-1227.

Vargas, V., Castillo, J., Torres, R. O., Bouyssiere, B. & Lienemann, C. P. 2017. Development of a chromatographic methodology for the separation and quantification of V, Ni and S compounds in petroleum products. Fuel Processing Technology, 162**,** 37-44.

Vasconcelos, G. A., Pereira, R. C. L., Santos, C. D., Carvalho, V. V., Tose, L. V., Romao, W. & Vaz, B. G. 2017. Extraction and fractionation of basic nitrogen compounds in vacuum residue by solid-phase extraction and characterization by ultra-high resolution mass spectrometry. International Journal of Mass Spectrometry, 418**,** 67-72.

Vassoevich, N. B. 1957. *Terminology for designating stages and steps of lithogenisis*, Gostoptekhizdat, Chapters 1-7.

Volkman, J. K., Alexander, R., Kagi, R. I., Rowland, S. J. & Sheppard, P. N. 1984. Biodegradation of aromatic hydrocarbons in crude oils from the Barrow Sub-basin of Western Australia. Organic Geochemistry, 6**,** 619-632.

von Mühlen, C., de Oliveira, E. C., Morrison, P. D., Zini, C. A., Caramão, E. B. & Marriott, P. J. 2007. Qualitative and quantitative study of nitrogen-containing compounds in heavy gas oil using comprehensive two-dimensional gas chromatography with nitrogen phosphorus detection. Journal of Separation Science, 30**,** 3223-3232.

Wang, Z., Li, K., Lambert, P. & Yang, C. 2007. Identification, characterization and quantitation of pyrogenic polycylic aromatic hydrocarbons and other organic compounds in tire fire products. Journal of Chromatography A, 1139**,** 14-26.

Wei, H. & Songnian, L. 1990. A new maturity parameter based on monoaromatic hopanoids. Organic Geochemistry, 16**,** 1007-1013.

Wells, J. M. & McLuckey, S. A. 2005. Collision-Induced Dissociation (CID) of Peptides and Proteins. Methods in Enzymology, 402**,** 148-185.

Wenger, L. M. & Isaksen, G. H. 2002. Control of hydrocarbon seepage intensity on level of biodegradation in sea bottom sediments. Organic Geochemistry, 33**,** 1277-1292.

West, C. E., Scarlett, A. G., Tonkin, A., O'Carroll-Fitzpatrick, D., Pureveen, J., Tegelaar, E., Gieleciak, R., Hager, D., Petersen, K., Tollefsen, K.-E. & Rowland, S. J. 2013. Diaromatic sulphur-containing 'naphthenic' acids in process waters. Water research, 51**,** 206-215.

Whitehead, E. V. Molecular evidence for the biogenesis of petroleum and natural gas. Symposium on Hydrogeochemistryand Biogeochemistry, 1973. Clarke Co.

Wilde, M. J. 2015. *On the bicyclic acids of petroleum.* Plymouth University.

Wilde, M. J. & Rowland, S. J. 2015. Structural Identification of Petroleum Acids by Conversion to Hydrocarbons and Multidimensional Gas Chromatography-Mass Spectrometry. Analytical Chemistry, 87**,** 8457-8465.

Wilde, M. J., West, C. E., Scarlett, A. G., Jones, D., Frank, R. A., Hewitt, L. M. & Rowland, S. J. 2015. Bicyclic naphthenic acids in oil sands process water: Identification by comprehensive multidimensional gas chromatography–mass spectrometry. Journal of Chromatography A, 1378**,** 74-87.

Wilhelms, A., Larter, S. R., Head, I., Farrimond, P., di-Primio, R. & Zwach, C. 2001. Biodegradation of oil in uplifted basins prevented by deep-burial sterilization. Nature, 411**,** 1034.

Wilkes, H., Clegg, H., Disko, U., Willsch, H. & Horsfield, B. 1998a. Fluoren-9-ones and carbazoles in the Posidonia Shale, Hils Syncline, northwest Germany. Fuel, 77**,** 657-668.

Wilkes, H., Disko, U. & Horsfield, B. 1998b. Aromatic aldehydes and ketones in the Posidonia Shale, Hils Syncline, Germany. Organic Geochemistry, 29**,** 107-117.

Willsch, H., Clegg, H., Horsfield, B., Radke, M. & Wilkes, H. 1997. Liquid chromatographic separation of sediment, rock, and coal extracts and crude oil into compound classes. Analytical Chemistry, 69**,** 4203-4209.

Witt, M., Godejohann, M., Oltmanns, S., Moir, M. & Rogel, E. 2018. Characterization of Asphaltenes Precipitated at Different Solvent Power Conditions Using Atmospheric Pressure Photoionization (APPI) and Laser Desorption Ionization (LDI) Coupled to Fourier Transform Ion Cyclotron Resonance Mass Spectrometry (FT-ICR MS). Energy & Fuels, 32**,** 2653-2660.

Worstell, J. H., Daniel, S. R. & Frauenhoff, G. 1981. Deposit formation in liquid fuels. 3. The effect of selected nitrogen compounds on diesel fuel. Fuel, 60**,** 485-487.

Xiaobo, C., Yibin, L., Jin, W., Honghong, S., Chaohe, Y. & Chunyi, L. 2014. Characterization of nitrogen compounds in coker gas oil by electrospray ionization Fourier transform ion cyclotron resonance mass spectrometry and Fourier transform infrared spectroscopy. Applied Petrochemical Research, 4**,** 417-422.

Yamamoto, M., Taguchi, K. & Sasaki, K. 1991. Basic nitrogen compounds in bitumen and crude oils. Chemical Geology, 93**,** 193-206.

Yang, B., Xu, C., Zhao, S., Hsu, C. S., Chung, K. H. & Shi, Q. 2013a. Thermal transformation of acid compounds in high TAN crude oil. Science China Chemistry, 56**,** 848-855.

Yang, B. J., Hou, W., Zhang, K. Y. & Wang, X. R. 2013b. Application of solid-phase microextraction to the determination of polycyclic aromatic sulfur heterocycles in Bohai Sea crude oils. Journal of Separation Science, 36**,** 2646-2655.

Yang, L., Li, M., Wang, T. G., Liu, X., Jiang, W., Fang, R. & Lai, H. 2017. Phenyldibenzofurans and Methyldibenzofurans in Source Rocks and Crude Oils, and Their Implications for Maturity and Depositional Environment. Energy & Fuels, 31**,** 2513-2523.

Yang, Z. Y., Yang, C., Wang, Z. D., Hollebone, B., Landriault, M. & Brown, C. E. 2011. Oil fingerprinting analysis using commercial solid phase extraction (SPE) cartridge and gas chromatography-mass spectrometry (GC-MS). Analytical Methods, 3**,** 628-635.

Yin, P., Chen, H., Liu, X., Wang, Q., Jiang, Y. & Pan, R. 2014. Mass Spectral Fragmentation Pathways of Phthalate Esters by Gas Chromatography–Tandem Mass Spectrometry. Analytical Letters, 47**,** 1579-1588.

Zengler, K., Richnow, H. H., Rossello-Mora, R., Michaelis, W. & Widdel, F. 1999. Methane formation from long-chain alkanes by anaerobic microorganisms. Nature, 401**,** 266-9.

Zhang, C., Zhang, Y. & Cai, C. 2011. Maturity effect on carbazole distributions in source rocks from the saline lacustrine settings, the western Qaidam Basin, NW China. Journal of Asian Earth Sciences, 42**,** 1288-1296.

Zhang, L. L., Yang, G. H., Wang, J. Q., Li, Y., Li, L. & Yang, C. H. 2014. Study on the polarity, solubility, and stacking characteristics of asphaltenes. Fuel, 128**,** 366-372.

Zhang, X. Y., Lu, H., Liao, J., Tang, C. M., Sheng, G. Y. & Peng, P. A. 2017. Two new oxygen-containing biomarkers isolated from the Chinese Maoming oil shale by silica gel column chromatography and preparative gas chromatography. Journal of Separation Science, 40**,** 813-818.